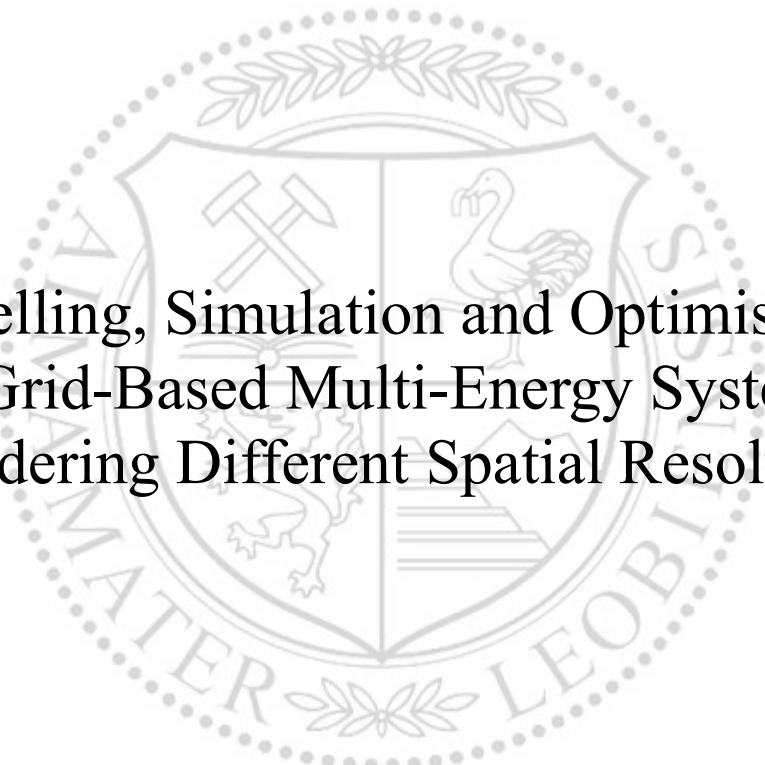




Chair of Energy Network Technology

Doctoral Thesis



Modelling, Simulation and Optimisation
of Grid-Based Multi-Energy Systems
Considering Different Spatial Resolutions

Dipl.-Ing. Matthias Greiml, BSc

June 2022



MONTANUNIVERSITÄT LEOBEN

www.unileoben.ac.at

AFFIDAVIT

I declare on oath that I wrote this thesis independently, did not use other than the specified sources and aids, and did not otherwise use any unauthorized aids.

I declare that I have read, understood, and complied with the guidelines of the senate of the Montanuniversität Leoben for "Good Scientific Practice".

Furthermore, I declare that the electronic and printed version of the submitted thesis are identical, both, formally and with regard to content.

Date 29.06.2022

Signature Author
Matthias Greiml

ACKNOWLEDGEMENTS

I want to open the acknowledgements of my doctoral thesis with a quotation from one personal role model since it describes the opportunity I was offered.

“Opportunities come infrequently. When it rains gold, put out the bucket, not the thimble.”

Warren E. Buffet

In this context, I'd like to thank my doctoral thesis supervisor Prof. Thomas Kienberger. You offered me the chance to catch some of the “raining gold” in the form of knowledge and enable me to continue working on the subject of my master thesis at your chair. Throughout the years you entrusted me with numerous exciting projects together with various partners, where I could gather immense knowledge and experiences about the present and future challenges in our energy system and work on potential solutions. Thank you for your unconditional, professional support and all the intense scientific discussions we had during various PhD-talks throughout my time at your chair. I would also like to thank my mentor Prof. Helmut Zsifkovits for his support and for exciting me for logistical topics since my first semester. Many things I learned from you and your chair's staff were particularly helpful to address research questions throughout my doctoral thesis.

At the same time, I'd like to thank Benjamin Böckl, who entrusted me as a future Industrial Logistics graduate with a complex energy network technology related master thesis together with Lukas Leitner. The results and experiences of our mutual work paved the way for my doctoral thesis since I really enjoyed working on this topic.

During my time at the Chair of Energy Network Technology, many new colleagues joined the team or graduated. Thank you, Andreas, Anna, Benjamin, Bernd, Christoph, Christopher, David, Elisabeth, Günther, Jasmin, Johannes, Josef, Julia, Kerstin, Lisa, Lukas, Maedeh, Nouman, Peter, Rebecca, Roberta, Thomas, Thomas & Vanessa for your cooperation and countless discussions about our researches. A special thanks to our office management team Jasmin and Rebecca for your excellent cooperation and support no matter what. Johannes Dock, we both share the passion for drinking coffee from time to time, so unconsciously we often ran head-to-head for the chair's highest coffee consumption count in each accounting period. Thank you for your companionship and the countless scientific and private discussions during our mutual coffee breaks.

I also owe a great debt to all my project-, bachelor- and master thesis students, as well as interns that worked together with me on numerous topics. Florian Fritz, Josef Steinegger and Theresa Schlömicher thank you for all your efforts and hard work. Your work contributed a significant share to my doctoral thesis. Nicolas Wolf-Williams and Negar Zaghi, I had the pleasure of working together with you throughout your internship at our chair. Like the

Acknowledgements

students, you contributed a great share to my doctoral thesis. Since you both came from Canada, thank you for brushing up my English skills, all the personal exchange and intercultural experiences throughout your stay in Austria.

Almost exactly ten years ago, I started as a so-called “Schwammerl” (EN: freshman) at the University of Leoben. Since then, many friendships have developed and remain until today. Daniel Ginter, I met you basically at the first minute when I moved to Leoben. Thank you for the great times together in our shared flat and your support throughout the years. During my first pure Industrial Logistics semester, I was fortunate to meet Thomas Kurz. Thank you Thomas for the great friendship that evolved throughout the years, in addition to all the numerous sports challenges and leisure activities we have encountered together. David Paczona, although you joined our chair during Covid-19, where personal contacts were rather limited, we quickly got along nicely. Thank you and your fiancée, Natalia, for the countless outdoor activities we have spent together and mutual evenings, challenging each other with board games.

I also would like to acknowledge friends from outside the university. Dieter, Gerhard, Johannes and Mario, basically we know each other for two decades or even longer. Thank you for everything we experienced together ever since and for always having an open ear, no matter how busy you are.

Last but not least, I would like to thank my parents Herta and Karl-Heinz and my brother Philipp Greiml. I guess you were quite relieved hearing that I want to start studying in Leoben rather than continuing to travel for work purposes to Iran, China or Russia. Thank you for supporting every decision throughout my life - no matter how questionable you deemed it, encouraging me to pursue my way and always having advice on hand when I was in need. Although we don't always share the same opinion, I can't imagine any other/better family than you.

By finishing this doctoral thesis, another period of life ends for me. However,

“The future is exciting. Ready?”

Vodafone Group

Ready! and looking forward to it.

Matthias Greiml

Leoben, June 2022

CONTENTS

Nomenclature	I
List of figures	III
List of tables	IV
1 Introduction	1
2 Context	4
2.1 Energy System in Austria	4
2.1.1 <i>Energy Consumption in Austria</i>	4
2.1.2 <i>Grid-bound Energy Transmission in Austria</i>	5
2.2 Multi-Energy System Assessment Frameworks.....	8
2.2.1 <i>Definition Multi-Sector / Energy System</i>	8
2.2.2 Types of MES Frameworks	10
3 Research Objective and Methodology	17
3.1 Research Objective	17
3.2 Methodology.....	19
3.3 Contribution to Scientific Knowledge	23
4 Results, Discussion and Conclusion	25
4.1 HyFlow MES Simulation Framework [29, 65–67]	25
4.2 MES model of Austria [29]	28
4.3 RES Expansion at Different Spatial Resolution	30
5 Summary & Outlook	38
6 Bibliography	43
Appendix A: Peer-Reviewed Scientific Publications	50
Appendix B: Further Scientific Publications	53

NOMENCLATURE

Abbreviation

ADC	Advanced Case
AGGM	Austrian Gas Grid Management
APG	Austrian Power Grid AG
BC	Base Case
BS	Battery Storage
DG	Distribution Grid
DRESE	Degree of RES Expansion
DSS	Degree of Self-Sufficiency
ENTSO-E	European Network of Transmission System Operators for Electricity
ENTSO-G	European Network of Transmission System Operators for Gas
EU	European Union
EV	Electric Vehicle
FLH	Full-Load Hours
GCV	Gross Caloric Value
GtH	Gas to Heat
HAG	Hungary Austria Gasleitung (EN: Hungary Austria Gas Pipeline)
KIP	Kittsee Petrzalka Gasleitung (EN: Kittsee Petrzalka Gas Pipeline)
KPI	Key Performance Indicator
MAB	March Baumgarten Gasleitung (EN: March Baumgarten Gas Pipeline)
MES	Multi Energy System
NEP	Netzentwicklungsplan (EN: Network Development Plan)
NGP	Natural Gas Pipeline
PtG	Power to Gas
PtH	Power to Heat

Nomenclature

PV	Photovoltaics
RES	Renewable Energy Source
RL	Residual Load
RLO	Power Line Overloads
SNG	Synthetic Natural Gas
SLP	Standardised Load Profile
SOL	Süd-Ost Leitung (EN: South-East Pipeline)
SS	Substation
SSD	Substation District
TAG	Trans Austria Gasleitung (EN: Trans Austria Gas Pipeline)
TG	Transmission Grid
TYNDP	Ten Year Network Development Plan
WAG	West Austria Gasleitung (EN: West Austria Gas Pipeline)

LIST OF FIGURES

Figure 1: Overview of RES potentials in Austria at the district level [8]	2
Figure 2: Gross domestic energy consumption of Austria, divided by energy carrier, 2020 [6]4	
Figure 3: Final Energy Consumption of Austria, divided by energy carrier, 2020 [6]	5
Figure 4: Power transmission grid in Austria [19].....	5
Figure 5: Austria's natural gas grid in market area East [23, 26, 28]	7
Figure 6: District heat grids in Austria [28, 30]	8
Figure 7: Structure and technological details [32]	9
Figure 8: Purpose, methodology and assessment criteria [32]	9
Figure 9: Basic principle of an energy hub	13
Figure 10: Example of grid-based MES [18, 49]	15
Figure 11: Considered spatial resolutions of assessed MES	18
Figure 12: Structure of doctoral thesis and research questions.....	18
Figure 13: Covered area for local RES expansion MES.....	20
Figure 14: Overview of investigated federal states' natural gas grid	21
Figure 15: Example of a node.....	25
Figure 16: Derivation of node-edge model based on MES depiction	26
Figure 17: Calculation process for enhanced gas load flow calculation	27
Figure 18: Example of Austria's MES model, one SSD exemplarily highlighted yellow [28]....	28
Figure 19: Austria's Power and Natural Gas Energy Grids [28].....	29
Figure 20: Technical limitations and achievable PV integration for each scenario	31
Figure 21: Comparison of RES power generation in summer and winter week.....	32
Figure 22: Overview of investigated federal state's natural gas grid	34
Figure 23: Spatial and temporal resolved GCV fluctuations in winter.....	34
Figure 24: Spatial and temporal resolved GCV fluctuations in summer	35
Figure 25: Average power grid line overloads for Scenario 2 (worst case)	37

LIST OF TABLES

Table 1: Electricity generation from RES in 2018 and additions until 2030 [4, 7]	1
Table 2: Criteria used for MES framework comparison	11
Table 3: Distinct MES planning framework criteria [37–42]	12
Table 4: Distinct energy hub criteria [44–46].....	14
Table 5: Distinct grid-bound MES framework criteria [49, 50, 53–55, 57]	15
Table 6: Scenario Parameters	22
Table 7: Comparison of the electrolysis' achievable full-load hours, depending on operating strategy	30
Table 8: Cost comparison for an electrolysis power of 52,5 MW	31
Table 9: Comparison of KPIs for different RES expansion scenarios	33
Table 10: Comparison of power grid results of each scenario.....	36
Table A 1: Author statement to the first journal article.	50
Table A 2: Author statement to the second journal article.	51
Table A 3: Author statement to the third journal article.	52

1 INTRODUCTION

According to the European Commission, 93 per cent of Europeans consider climate change a severe problem. The same percentage of Europeans has taken at least one action to tackle this problem. An overwhelming majority of 79 per cent of Europeans agree that action on climate change will lead to innovation. Beside others, this broad support encouraged the European Commission to aim for the European Green Deal. The Green Deal aims to achieve a climate-neutral European Union (EU) by 2050 and addresses each economic sector (energy, buildings, industry, mobility). Clean products and technologies, as well as a reduction of pollution and social support to ensure a just transition should improve the well-being of European people [1, 2]. As an interim target toward a climate-neutral EU, the European Commission published the “Fit for 55” target to strengthen the EU’s global leadership by action and example. “Fit for 55” aims to reduce net emissions by at least 55 per cent by 2030, based on emissions from the year 1990 [3].

As a member of the European Union, the current Austrian government has set an even more ambitious target than the European Green Deal, aiming to achieve climate neutrality by 2040. This should be achieved by e.g. efficiency measures, phase-out of fossil energy sources and expansion of renewable energy sources (RES). By 2030, RES should be expanded by 27 TWh to achieve a 100 per cent electricity generation from RES, net balanced over one year. The scheduled addition of each RES is displayed in Table 1. The year 2018 is selected as the reference year since the Austrian climate and energy strategy #mission2030 was implemented this year [4, 5]. In the EU, Austria achieves a RES share of 73 per cent of Austria’s gross electricity consumption already today, compared to 32 per cent of the EU’s average. In contrast, RES cover 33 per cent of Austria’s gross final energy consumption. Therefore, aside from achieving #mission2030 targets, further measures such as energy system restructuring, energy efficiency or saving measures are essential to achieve climate neutrality by 2040 [6].

Table 1: Electricity generation from RES in 2018 and additions until 2030 [4, 7]

RES	Generation 2018	RES expansion until 2030
Hydro	37.6 TWh	+ 5 TWh
Wind	6.0 TWh	+ 10 TWh
Photovoltaics	1.5 TWh	+ 11 TWh
Biomass	4.9 TWh	+ 1 TWh
Total	50 TWh	+ 27 TWh

Several studies, such as [8–12], deal with Austria’s technical, reduced technical and economic-technical RES potential. A wide range of individual RES potentials is determined depending on the methodology, considered technology, and potential competition between technologies (e.g. solar thermal vs photovoltaics vs biomass for currently unused land). Sejkora et al.

provide an overview of Austria’s technical RES potentials, spatially resolved for each district, displayed in Figure 1. It can be seen that RES potentials vary in both quantity and composition across Austria. For example, significant wind potentials are found in the north-eastern part with offshoots into the centre of Austria. Hydroelectric potentials accrue mainly in the western part of Austria and along major rivers such as Danube, Inn, Enns and Drau. Photovoltaics (PV) and Biomass potentials are available throughout Austria. The high share of PV potentials in the alpine western and central Austria is caused by the consideration of fallow land according to [8]. Compared to a current annual gross domestic energy consumption of approximately 400 TWh, a total RES potential of roughly 266 TWh per year is available [7, 8]. The gap between gross domestic energy consumption and RES potentials can be closed by either imports, energy savings or efficiency measures. A formerly stable and reliable energy import source can suddenly become questionable for the future. Austria experienced this development after the war outbreak of Russia against Ukraine in the winter of 2022, since 80 per cent of Austria’s natural gas imports depend on supplies from Russia [13].

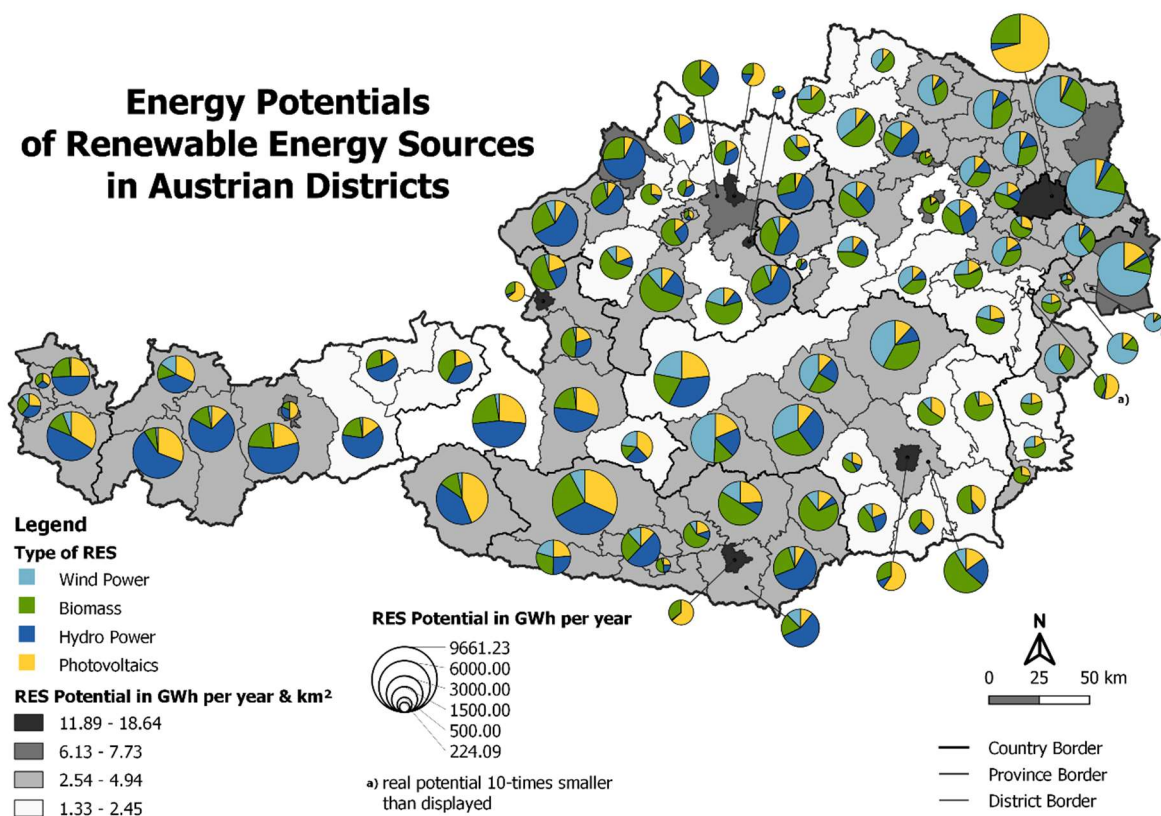


Figure 1: Overview of RES potentials in Austria at the district level [8]

A wide range of challenges must be addressed to convert the current energy system. These challenges are both economic and technical, mainly resulting from volatility effects accruing in the electricity sector. Some examples are given as follows: [14–16]

- Absorb seasonal RES generation mismatch – implement suitable and feasible storage technologies.

- Match supply and demand over multiple timescales.
- Balance supply and demand economically.
- New inverter designs and grid operations, depending on the mix of RES to cope with instantaneous penetration of RES.
- Curtailment of RES at periods with high RES supply.

Since 2010, research regarding 100 per cent RES has been gaining traction. To address the previously mentioned challenges, current research does not only consider the power sector but focuses on the entire energy system. The whole energy system may contain different energy carriers (e.g. electricity, natural gas, district heat), storage and sector-coupling options [17]. A depiction of an entire energy system is defined as a multi-energy system (MES), providing significant technical, economic and environmental advantages compared to single energy carrier considerations such as: [18]

- Increase the energy systems flexibility.
- Optimal deployment of both centralised and decentralised resources.
- Increase efficiency of conversion and utilisation of primary energy sources.
- Additional potentials for long-term storage (e.g. seasonal).

2 CONTEXT

As described in the introduction, present energy systems are challenged by RES expansion to achieve emissions reduction goals. Suitable assessment frameworks are necessary to assess the potential effects of RES expansion on existing MESs. This chapter displays and compares state-of-the-art MES assessment frameworks and their corresponding capabilities. Furthermore, an overview of energy consumption / usage and grid-bound energy transmission in Austria is given.

2.1 Energy System in Austria

In this section, an overview of Austria's energy system is presented. Both energy usage and energy transmission are covered.

2.1.1 Energy Consumption in Austria

In 2020, Austria's gross domestic consumption of energy was 374 TWh. About one-third of the gross domestic consumption was produced in Austria, resulting in import needs of two-thirds. The coverage of Austria's gross domestic consumption by energy carriers is displayed in Figure 2. On the right side, renewable energy sources are shown. It can be seen that the main RESs today are biomass and hydropower. Wind and PV show the strongest, most substantial growth rates of Austria's gross domestic energy consumption coverage. The share of fossil fuels (oil, natural gas and coal) shows a slightly long-term decline in its share of the gross domestic energy consumption. In the long term, Austria's gross domestic energy consumption is stagnant, despite a growing gross domestic product [6, 7]

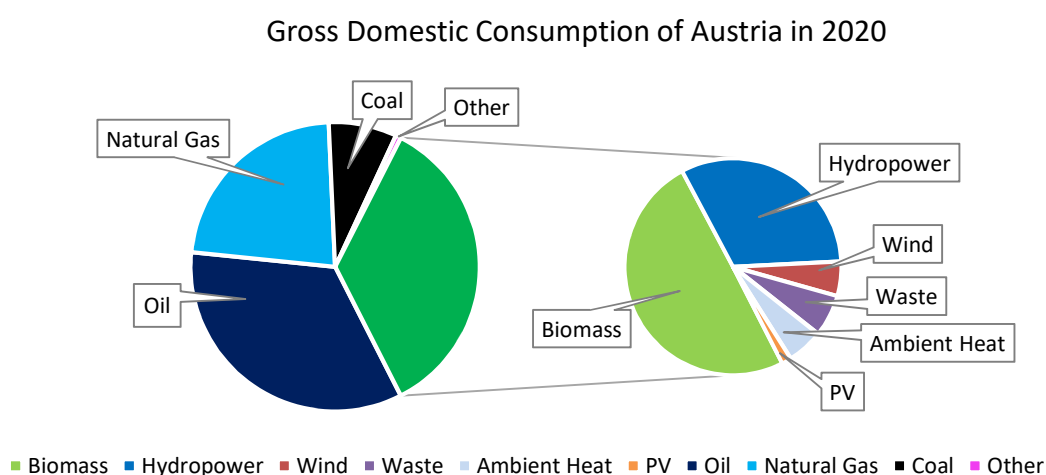


Figure 2: Gross domestic energy consumption of Austria, divided by energy carrier, 2020 [6]

The coverage of Austria's final energy consumption by energy carrier is displayed in Figure 3. Being the second-largest share after oil, electricity accounts for about 20 per cent of Austria's

final energy consumption of about 305 TWh per year. According to #mission2030, the electricity share should be fully decarbonised by 2030 [5, 6]. Therefore, further efforts are necessary to substitute fossil energy sources and achieve climate neutrality in Austria by 2040 [4]. Electricity, natural gas and district heat represent grid-bound energy carriers transported via power grids or pipelines.

Final Energy Consumption of Austria in 2020

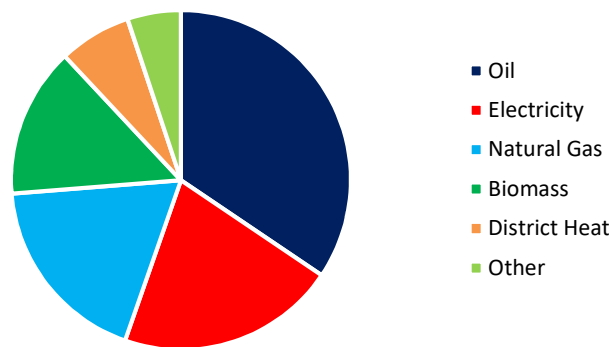


Figure 3: Final Energy Consumption of Austria, by energy carrier, 2020 [6]

2.1.2 Grid-bound Energy Transmission in Austria

This chapter discusses Austria’s grid-bound energy grids (power, natural gas, district heat).

Power Grid

In Figure 4, the Austrian power transmission grid is shown. It can be seen that a 380 kV transmission grid almost encircles the central and eastern parts of Austria.

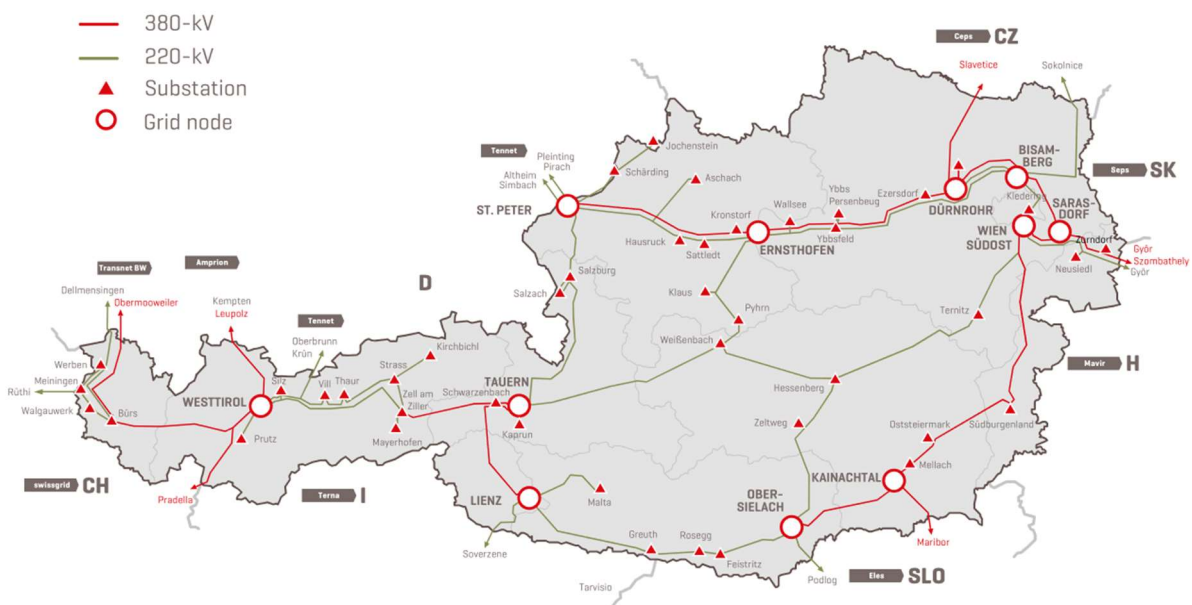


Figure 4: Power transmission grid in Austria [19]

The two missing sections between St. Peter – Tauern and Lienz – Obersielach are currently under construction and in the planning stage, respectively. Aside from before mentioned expansion projects, several other transmission grid projects are presently under construction or in the planning stage to further enhance Austria's power transmission grid and enable the integration of additional renewable energy sources [20]. In the western part of Austria, the transmission grid mainly follows the densely populated Inn and Rhine valley. Due to its location in central Europe, Austria's power transmission grid is connected to transmission grids of neighbouring countries. In particular, multiple transmission grid interconnections are established between Austria and Germany. Network development plans can be found at both international (ENTSO-E: Ten Year Network Development Plan – TYNDP) and national (APG: Netzentwicklungsplan – NEP) level [20, 21].

Natural Gas Grid

The Austrian natural gas grid comprises of three market areas: Vorarlberg, Tyrol and East. The market areas Vorarlberg and Tyrol are supplied with natural gas from Germany. Market area East covers the remaining area of Austria. In the northeast of Austria, a central European natural gas hub is located in Baumgarten, where about ten per cent of the European Union's natural gas demand is imported from Russia and further distributed. Several international transmission pipelines enable natural gas transportation from Austria to neighbouring countries, starting from Baumgarten. Main transmission pipelines for international exchange run from Baumgarten westwards to Germany (West Austria Gasleitung – WAG), southwest to Italy (Trans Austria Gasleitung – TAG) with a branch to Slovenia (Süd-Ost Leitung – SOL), southeast to Hungary (Hungaria Austria Gasleitung – HAG) and Slovakia (Kittsee Petrzalka Gasleitung - KIP) and east so Slovakia (March Baumgarten Gasleitung – MAB). Approximately 75 per cent of the imported natural gas is transferred to neighbouring countries, mainly towards Italy [22–26]. In Figure 5, international and national transmission and national distribution pipelines are displayed for the market area East. It can be roughly seen that areas without an alpine environment (Upper Austria, Lower Austria, Vienna, Burgenland) have comprehensive spatial coverage of high-level natural gas infrastructure. In contrast to regions with an alpine environment (Salzburg, Styria, Carinthia), the natural gas infrastructure is concentrated along densely populated valleys (e.g. Drava, Mur, Mürz, Salzach valley). The current focus in the natural gas transmission is to ensure a reliable supply with upgrades of the existing grid rather than grid expansion. In the future, existing natural gas transmission pipelines could be converted for hydrogen transportation (e.g. European Hydrogen Backbone considering TAG and WAG) [22, 26]. Network development plans can be found at both international (ENTSOG: TYNDP) and national (AGGM: NEP) levels [22, 27].

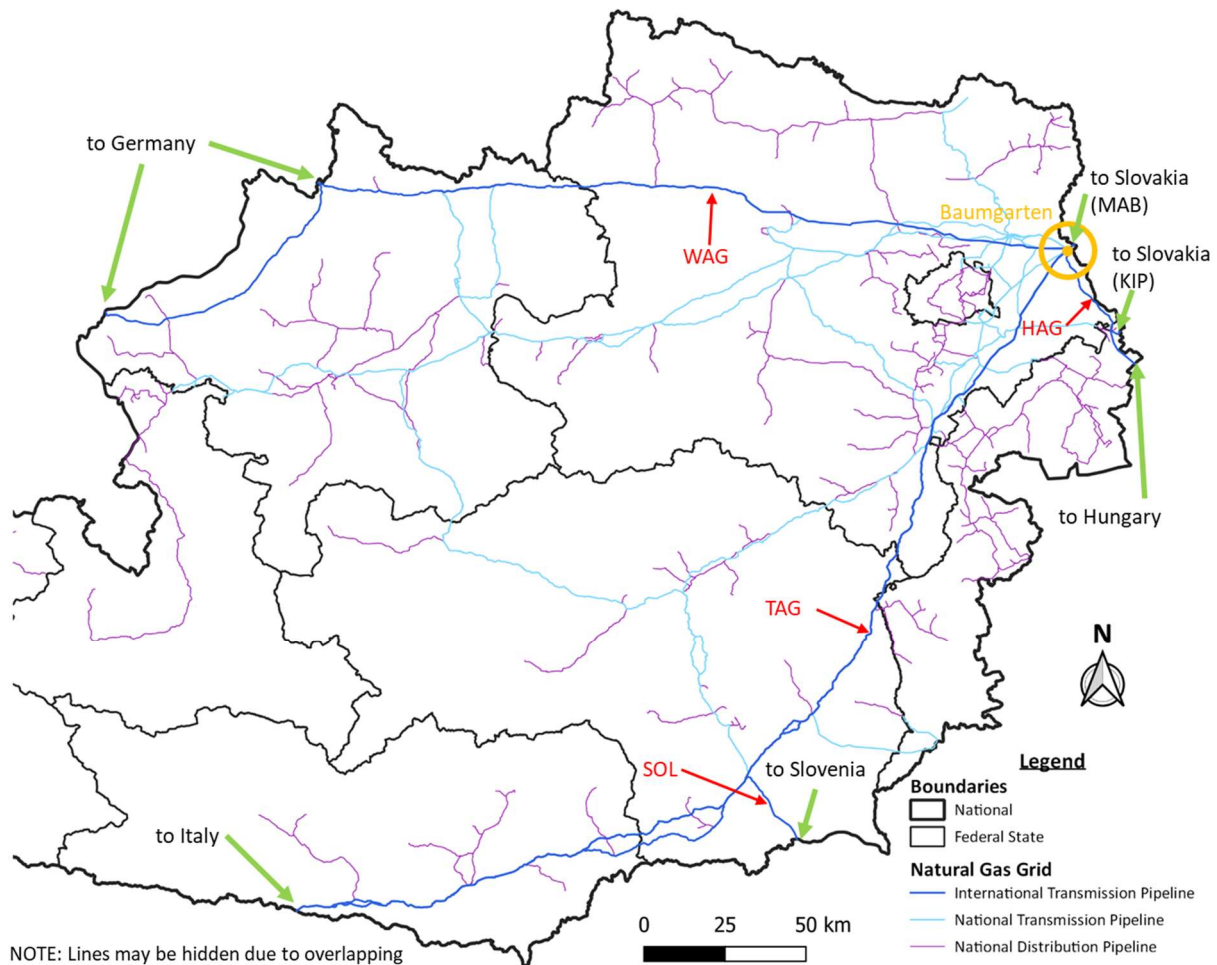


Figure 5: Austria's natural gas grid in the market area East [23, 26, 28] ¹

District Heat Grids

According to the Austrian Heat Map [30], a total of 1842 district heating grids exist in Austria. In Figure 6, all district heat grids with ten or more supplied residential units are displayed. These district heat grids are spread all over Austria, while a vast majority of supplied residential units is less than 100 per district heat grid. Although district heat grids are often within proximity, no interconnections are established between district heating grids. Municipalities containing one or more district heat grid are coloured grey in Figure 6 [30, 31].

¹ This map is an excerpt of Austria's natural gas infrastructure. A full depiction of Austria's natural gas and power grid infrastructure, including the methodology how the map is created can be found in [29].

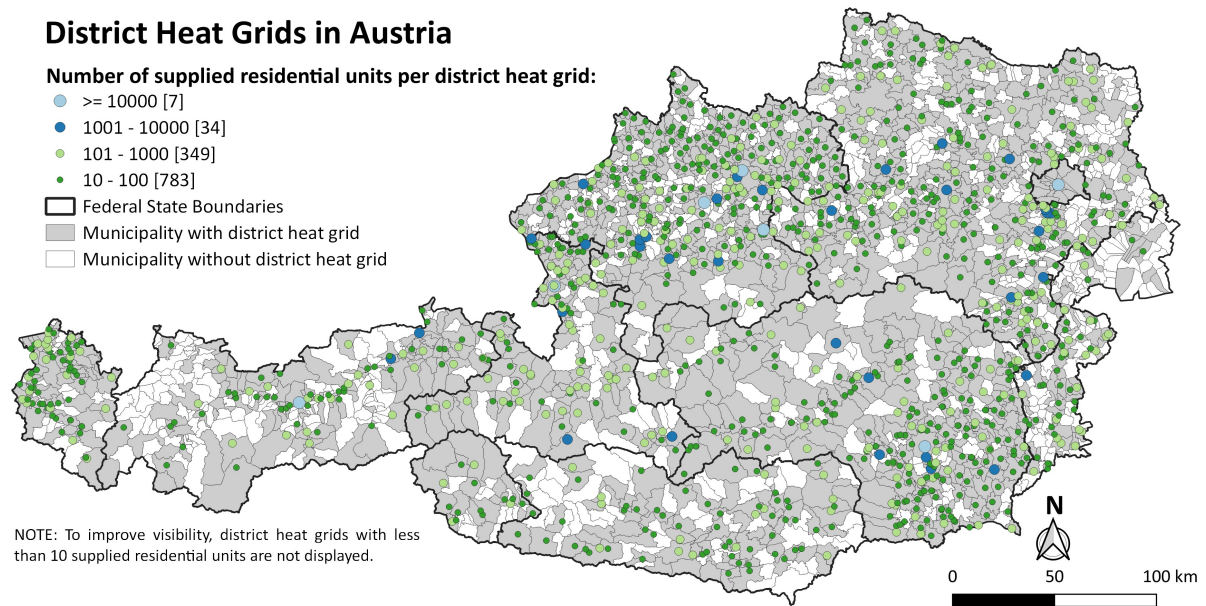


Figure 6: District heat grids in Austria [28, 30]

2.2 Multi-Energy System Assessment Frameworks

An increasing number of research activities consider not only the power sector but include a multi-sector approach [17]. This section defines the commonly used term multi-sector or multi-energy system approach based on literature and displays various examples of assessment frameworks, including their distinct characteristics.

2.2.1 Definition Multi-Sector / Energy System

The term multi-sector or multi-energy system is very broad. Therefore, no distinct or unique definition is available. Generally, all energy systems can be considered multi-energy based on a physical perspective. This includes the generation and demand of various energy carriers or sectors interacting at different levels, including energy grids. Mancarella defines the concept of multi-energy as a whole system approach to optimise and evaluate a specific case study. Characteristic criteria for MES are presented as follows: [18]

- **Spatial perspective:** The spatial perspective depends on the capability of a MES framework to depict individual objects. It ranges from a single entity (e.g. household) via community-, district- or federal state- to national- or even international level. Depending on the MES framework, it can be tailored towards specific problems or address various spatial resolutions.
- **Multi-service perspective:** Multiple services (energy outputs) can be provided based on different inputs. For example, a combined heat and power plant can transform natural gas into heat and power. Multi-service is focused on the output side of a MES, e.g. transportation, electricity, heat, cooling or chemicals.

- Multi-fuel perspective: Compared to the multi-service perspective, multi-fuel focuses on the interaction of the MES with its environment on the input side. Inputs are for example electricity, hydrogen, waste, natural gas or RES.
- Network perspective: Interconnections can consider connections between single components of a MES or between single MESs. Various energy grids such as electricity, natural gas, water or CO₂ can be considered.

Furthermore, time resolution and scale, assessment criteria and general type of the MES framework are discussed. Time relates to the length of a single time step (e.g. one hour) the MES can be resolved for a specific time scale period (e.g. one year). A wide range of assessment criteria, such as environmental, economic or energetic, can be considered in a MES framework. The type of MES framework can be generally distinguished between optimisation and simulation. Simulation frameworks can be further divided into operational and planning analysis [18].

Klemm and Vennemann suggest that energy system models can be categorised according to two different groups of properties. The first group includes structural and technological details (refer to Figure 7), and the second includes purpose methodology and assessment criteria (refer to Figure 8) [32].

geographic coverage	spatial resolution	temporal resolution	time horizon	sectoral coverage	demand sectors	technical coverage	demand side management	change of properties
<ul style="list-style-type: none"> • global • international • national • regional • local • single object 	<ul style="list-style-type: none"> • consumer • house • district • nation 	<ul style="list-style-type: none"> • fixed • input data dependent • milli seconds to years 	<ul style="list-style-type: none"> • day to years • lifespan of technology 	<ul style="list-style-type: none"> • electricity • heat • cooling • fossil sources 	<ul style="list-style-type: none"> • residential • industrial • transport 	<ul style="list-style-type: none"> • renewable generation • conventional generation • storage 	<ul style="list-style-type: none"> • renovation • demand response 	<ul style="list-style-type: none"> • costs • used technology • demand

Figure 7: Structure and technological details [32]

methodology	assessment criteria	analytical approach	mathematical approach	reusability	challenges
<ul style="list-style-type: none"> • optimisation • forecasting or simulation • back-casting 	<ul style="list-style-type: none"> • financial • energy efficiency • environmental • technical • social / economic 	<ul style="list-style-type: none"> • bottom-up • top-down • hybrid 	<ul style="list-style-type: none"> • linear programming • mixed-integer programming • artificial intelligence • stochastic programming 	<ul style="list-style-type: none"> • open • closed 	<ul style="list-style-type: none"> • closed models and modeling frameworks • data quality and transparency • assumptions • complexity • conflicting interests • need of coding

Figure 8: Purpose, methodology and assessment criteria [32]

Comparing Klemm and Vennemann’s MES distinguishing criteria to Mancarella, there is predominantly agreement in the field of structure and technological details. However, the purpose, methodology, and assessment criteria of Klemm and Vennemann provide additional criteria to characterise a MES. The methodology can be considered an essential distinguishing

criterion since it indicates the main concept of a MES framework. Therefore, it is important to know the characteristic properties and capabilities of the concepts of optimisation (an optimal scenario), forecasting/simulation (a most likely scenario) and back-casting (a path to an envisaged scenario), all three of which will be explained in the following paragraphs [32].

A forecasting or simulation model is based on future user-defined conditions and assumptions. Based on the defined conditions, the system's behaviour can be determined [32]. This means the user must make suitable and realistic assumptions to gain satisfactory results. The usage of "forecasting" and "simulation" differs from the literature. Klemm and Vennemann [32] argue that simulation can also be included in optimisation problems. Therefore, the term simulation is misleading, and forecasting should be used instead [32]. In contrast, Lund et al. define simulation as an umbrella term for both forecasting and back-casting, distinguishing only between simulation and optimisation [33].

A back-casting model determines the path towards an envisioned future state or set of properties, defined by the applier. Back-casting models are especially relevant for models with extensive geographic coverage, such as national or international MES. The envisioned future state can be defined, for example, by political goals [32].

Depending on the optimisation target (e.g. refer to "assessment criteria" in Figure 8), given as the target function to be minimised or maximised (e.g. equation (2-1)), an optimisation model determines an optimum solution based on a given set of conditions. Compared to forecasting or simulation, the user defines specific constraints, allowing the optimisation to vary certain parameters as long as constraints are not violated [33]. The following equations (2-1) to (2-3) show a generic optimisation problem with constraints. Equation (2-1) represents the target function, to be minimised, based on the variation of variables x within constraints. The constraints are defined as either inequality (refer to equation (2-2)) or equality (refer to equation (2-3)) constraints. The variables m and p represent the optimisation's problem number of inequality and equality constraints [34].

$$\min f(\vec{x}) \tag{2-1}$$

$$g_i(\vec{x}) \leq 0 \quad \text{for } i = 1, 2, \dots, m \tag{2-2}$$

$$h_j(\vec{x}) = 0 \quad \text{for } j = 1, 2, \dots, p \tag{2-3}$$

2.2.2 Types of MES Frameworks

This chapter describes the capabilities of various MES frameworks such as MES planning frameworks, node optimisation and grid-bound MES frameworks based on the following

defined criteria in this subchapter. The chapter is concluded by comparing the advantages and disadvantages of each MES framework.

Based on previously disclosed criteria to categorise MES, the following criteria, displayed in Table 2, will be used to demonstrate the capabilities and enable a comparison of different MES frameworks.

Table 2: Criteria used for MES framework comparison

Criterion	Description
Methodology	The methodology describes the basic principle of the MES framework. It can be either an optimisation or simulation framework. If the MES framework is based on simulation, further differentiation can be made between back-casting and forecasting.
Assessment criterion	The main assessment criterion of the MES framework can be: <ul style="list-style-type: none"> • Economic • Technical • Environmental
Spatial resolution	Depending on the individual MES framework, spatial resolution might consider two different criteria: <ul style="list-style-type: none"> • The spatial resolution of the whole depicted area (generally multiple points). • The spatial resolution of the smallest entity within the depicted area (single point). For example, the MES framework might consider a whole country (first bullet point), spatially resolved at the district level (second bullet point).
Temporal resolution	Depending on the individual MES framework, temporal resolution might consider two different criteria: <ul style="list-style-type: none"> • The temporal resolution of total considered time. • Duration of single time steps as a share of total considered time. For example, a MES framework might consider a full year (first bullet point) divided into 15 minutes time steps (second bullet point).
Energy carrier considered	This criterion considers both input and output parameters. In case a parameter is only available as input or output, it is declared. Otherwise, the energy carrier can be considered as an input and output parameter.
Energy grids considered	Some MES frameworks consider grid properties of e.g. power, gas and heat grids with different degrees of consideration.
Technical coverage	The technical coverage of MES describes if additional energy system components such as e.g. storage, sector-coupling and individual power stations can be considered or implemented.

MES Planning Frameworks

Generally, the two research fields polygeneration and energy system planning can be distinguished. Polygeneration planning frameworks aim to e.g. reduce primary energy usage or emissions by determining an optimised composition of the energy systems generation technologies. Two or more energy outputs should be achieved from one or more natural sources per definition of polygeneration [35]. Simulation and optimisation frameworks are available for energy system planning, allowing goals and technologies to be user-defined. The planning framework determines if and when a technology will be used to achieve the defined goal [36]. An example of a simulation MES planning framework is EnergyPLAN. The basic layout is comparable to an energy hub (refer to Figure 9) since the depicted energy system is aggregated into one single node but implements further energy carrier, conversion and storage technologies to meet various demands. The operation of energy storage and conversion can be set to different strategies for a simulation. As a result, technical, economic and environmental outputs can be assessed as a consequence of the user's choices and investments. A full year divided into one-hour time steps can be simulated [37, 38]. Multi-energy system planning frameworks such as Markal can be used to determine a cost-optimal energy system considering user-defined constraints. The optimisation considers a spatial resolution of a single node multi-energy system and allows for an optimisation period of several decades, divided into user-defined time steps [39]. Optimisation can be focused on multiple energy carriers (e.g. partially EnergyPLAN [37], Markal [39]) or single energy carrier (e.g. OSeMOSYS [40], Dispa-Set [41]).

Table 3: Distinct MES planning framework criteria [37–42]

Criterion	Description
Methodology	Simulation (EnergyPLAN), Optimisation (e.g. Markal, OSeMOSYS). Depending on the framework, investment/operation decision support or scenarios can be addressed.
Assessment criterion	Economic, ecologic, technical.
Spatial resolution	Flexible, usually ranging from urban spatial resolution up to international spatial resolution.
Temporal resolution	Depending on the planning framework and user, one year or more is commonly divided hourly, daily or monthly.
Energy carrier considered	Framework dependent, e.g. Fuel, electricity, heat, hydrogen, steam, CO ₂ , transportation, water and cooling. Multi-energy carrier considerations e.g. EnergyPLAN, Markal. Single energy carrier consideration: OSeMOSYS, Dispa-SET.

Criterion	Description
Energy grids considered	Planning framework dependent, e.g. not considered in the case of EnergyPLAN, considered with capacity constraints on lines in Dispa-SET.
Technical coverage	Depends on the framework. Single energy carrier frameworks such as Dispa-SET include various types of power plants, pumped-hydro storage, combined heat and power, power to heat and demand-side management. Multi-energy carrier frameworks such as EnergyPLAN can implement further technologies such as electrolysis, vehicles, boiler and storage.

Node Optimisation

The concept of node optimisation is defined by different names in literature, such as micro energy system [43], energy hub [44] or hybrid energy hub [45]. Although different names are used, the concepts are rather similar. In Figure 9 a basic energy hub is depicted. It consists of various input and output energy carriers. The energy hub can be composed of multiple components such as RES, storage, and converters (sector-coupling). The fundamental relation between inputs (I) and outputs (O) via the internal connection and conversion components of an energy hub (C) can be seen in Equation (2-4). If additional components such as storage are to be considered, Equation (2-4) must be extended accordingly [44, 45].

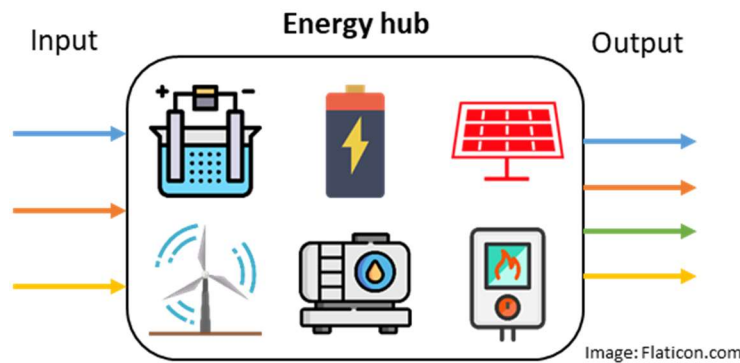


Figure 9: Basic principle of an energy hub

$$\begin{bmatrix} I_1 \\ I_2 \\ \vdots \\ I_n \end{bmatrix} \begin{bmatrix} C_{11} & C_{12} & \dots & C_{1n} \\ C_{21} & C_{22} & \dots & C_{2n} \\ \vdots & \vdots & \ddots & \vdots \\ C_{m1} & C_{m2} & \dots & C_{mn} \end{bmatrix} = \begin{bmatrix} O_1 \\ O_2 \\ \vdots \\ O_m \end{bmatrix} \quad (2-4)$$

An optimal dispatch of energy hub components might consider price and demand forecasts. This enables a time shift of energy consumption based on e.g. electricity prices [43]. Table 4 shows the vast bandwidth of criteria an energy hub can address.

Table 4: Distinct energy hub criteria [44–46]

Criterion	Description
Methodology	Optimisation
Assessment criterion	Single or multiple objectives can be considered, such as economic, exergetic, energetic and environmental objectives.
Spatial resolution	An energy hub depicts a particular object or area. If several energy hubs are interconnected, spatial resolution and detail level can be increased. As an alternative, one energy hub can supply two regions, as described in [43].
Temporal resolution	Similar to spatial resolution, temporal resolution is very flexible as well. It reaches from single time step optimisation up to more extended periods with flexible time step duration.
Energy carrier considered	Electricity and natural gas are most common. Solar, wind, district heat and biomass are used to a lesser extent.
Energy grids considered	An energy hub usually does not consider grid properties. However, if several energy hubs are interconnected, energy grid properties can be considered (e.g.: [35, 47, 48] – refer to chapter “Grid-Bound MES Frameworks”).
Technical coverage	A wide range of components is considered in energy hubs such as sector-coupling, storage or renewable generation.

Concluding this section, due to its flexibility of application, the energy hub can be applied to a wide range of individual single node research questions, covering various spatial and temporal resolutions as well as an energy carrier and assessment criteria.

Grid-Bound MES Frameworks

An example of grid-bound MES, representing an initial development of the HyFlow MES simulation framework, is displayed in Figure 10. The MES can be depicted as a node-edge model. Each node (the black circle in Figure 10) can be composed of demand or generation for various energy carriers as well as sector-coupling or storage options. Nodes can be interconnected via various edges (lines between nodes in Figure 10), representing the energy grid consideration of different energy carriers. The proposed framework has limited and inflexible energy grid depiction capabilities and limitations in adding further objects (e.g. storage, sector-coupling) [49].

A comprehensive overview of grid-bound MES modelling and assessment frameworks can be found in [50]. The authors conclude that Calliope [51], oemof [48] and urbs [52] are the most suitable grid-bound MES modelling frameworks since they are open source, support user-defined time resolution & horizons, energy grids and various energy sectors. All three aforementioned frameworks are optimisation frameworks, whereas an economic optimum is the primary assessment criteria [50].

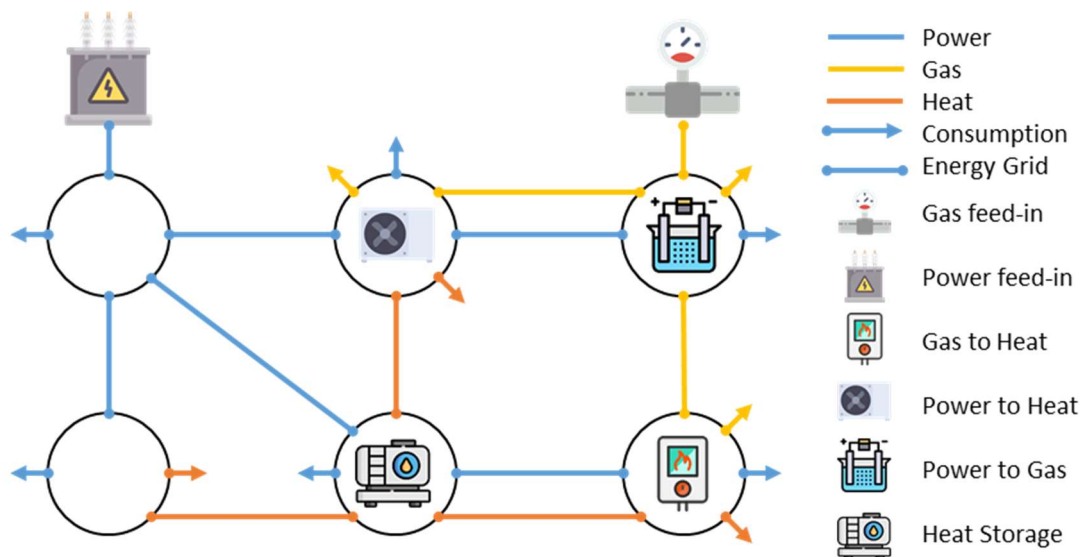


Figure 10: Example of grid-based MES [18, 49]

Lohmeier et al. [53] propose a combination of Pandapower, Pandapipes and multi-energy controller to set up a MES simulation framework. Pandapower and Pandapipes are used for detailed grid-bound load-flow calculations. The multi-energy controller allows for the implementation of sector-coupling and storage options with distinct operation strategies. The proposed framework can be considered a grid-bound MES simulation framework [53, 54]. The scenario analysis interface for energy systems (SAInt) enables detailed natural gas and power grid depiction to simulate power-gas grid interdependencies and their impact on the security of supply [55]. TransiEnt includes energy carriers power, natural gas and heat, as well as storage and sector-coupling technologies. Using dynamic simulation, non-linear behaviour, control strategies and system stability can be investigated [56].

Table 5: Distinct grid-bound MES framework criteria [49, 50, 53–55, 57]

Criterion	Description
Methodology	Optimisation and simulation models are most common.
Assessment criterion	Economic, technical, security of supply.
Spatial resolution	The user can individually set the spatial resolution. Specific grid-bound MES frameworks can consider more than one network level (e.g. [49]).
Temporal resolution	Similar to spatial resolution, temporal resolution is very flexible as well. It reaches from single time step consideration up to more extended periods with flexible time step duration.
Energy carrier considered	Electricity, gas and heat are standard. Other sectors might also be considered, such as transportation [48]. Certain frameworks are only suitable for single energy carrier consideration (e.g. [57]).

Criterion	Description
Energy grids considered	Energy grids and their properties are considered. However, the level of detail depends on the individual model. Load flows can be calculated via iteration (power flow) or optimisation (optimal power flow).
Technical coverage	Model-dependent may include sector-coupling, storage, various generation sources, or residual loads.

Conclusion & Lessons Learned

In previous chapters, the different MES frameworks: MES planning, node optimisation and grid-bound MES frameworks are described. The majority of the frameworks rely on an optimisation approach. However, an optimisation approach has its limitations since a trade-off between model complexity (= accuracy) and computation time / hardware requirements must be found to solve the optimisation problem. The complexity of an optimisation problem can be influenced by the temporal and spatial resolution as well as the number of model components such as energy carriers, storage and sector-coupling options. A further simplification of the optimisation problem can be achieved by converting non-linear, non-continuous or multi-dimensional functions into linear functions [58]. A high aggregation of both spatial and time-resolved data can be seen as the main disadvantage of MES optimisation frameworks since it doesn't allow for a detailed infrastructure depiction and time-resolved residual load profiles. As an example in [59–61], the spatial depiction of Italy (20 regions, 6 electricity market bidding zones), the United Kingdom (20 zones, 550 time steps with hourly or daily temporal resolution) and Europe (497 regions, temporal resolution of three hours) applying Calliope MES optimisation can be seen. It can be concluded that both spatial and temporal resolution is highly aggregated to achieve a solvable optimisation problem [59–61]. This problem can be solved by using a simulation framework instead. However, a simulation framework requires operational decisions to be made by the user. Therefore, the results likely do not represent an optimal solution.

In concluding this chapter, it should be noted that both optimisation and simulation have opposite advantages and disadvantages. The selection of either simulation or optimisation must be aligned with the problem to be addressed.

3 RESEARCH OBJECTIVE AND METHODOLOGY

Many scientific works address the modelling and assessment of multi-energy systems covering a wide range of different, individual frameworks. As discussed in the previous chapter 2.2.2, optimisation frameworks lack detailed temporal and spatial resolution due to computational time and hardware limitations, and simulation frameworks require user's decisions regarding scenario assumptions but can cope with high temporal and spatial resolution. Based on the literature review following research gaps or lack of capabilities could be identified in existing MES frameworks that should be addressed in a new multi-energy system framework:

- The framework should be flexible in terms of infrastructure depiction to be applied to various research questions. This should enable the framework to be adaptable to research questions rather than only suitable for specific research questions. Energy infrastructure depiction should include a high degree of its existing technical properties.
- Many multi-energy system frameworks are based on optimisation. To avoid limitations in the field of infrastructure depiction and spatial as well as temporal resolution, the proposed framework should be a simulation tool but also consider and implement optimisation capabilities, to take advantage of both simulation and optimisation capabilities.
- The modelling structure should be easily expandable to implement further objects or object operating strategies into the framework. This facilitates expandability of the framework.
- The grid-bound energy carrier power, gas and heat should be considered, including suitable load-flow calculation algorithms.

To demonstrate the capabilities of the proposed multi-energy system framework HyFlow, it is applied to assess various research questions. The research questions of this doctoral thesis are defined in the following chapter.

3.1 Research Objective

The foundation of this doctoral thesis is to further develop the multi-energy system simulation framework HyFlow, based on the previously identified scientific gaps in existing frameworks. Based on the foundation, the overall addressed research question focuses on the effects of renewable energy sources expansion on multi-energy systems considering different spatial resolutions. This general research question is divided into three sub-research question pillars, each contributing to answering the overall research question. Each of the three sub-research question pillars addresses a different spatial resolution of the assessed multi-energy system,

considering different distinctive challenges. The spatial resolutions are displayed in Figure 11 and range from the local level (green) via the Austrian federal state level (yellow) to the national level (red), on the example of Austria. The work focuses on individual challenges and solution strategies for each examined spatial level.

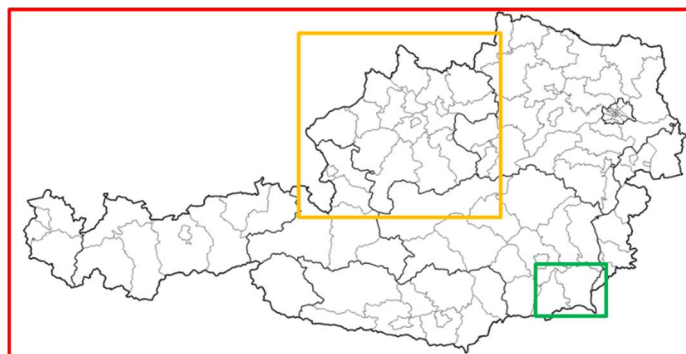


Figure 11: Considered spatial resolutions of assessed MES

In following Figure 12, this doctoral thesis’ research structure and addressed research questions are depicted. The icons indicate where research results were published (peer-reviewed journal articles and/or presented at conferences including proceedings).

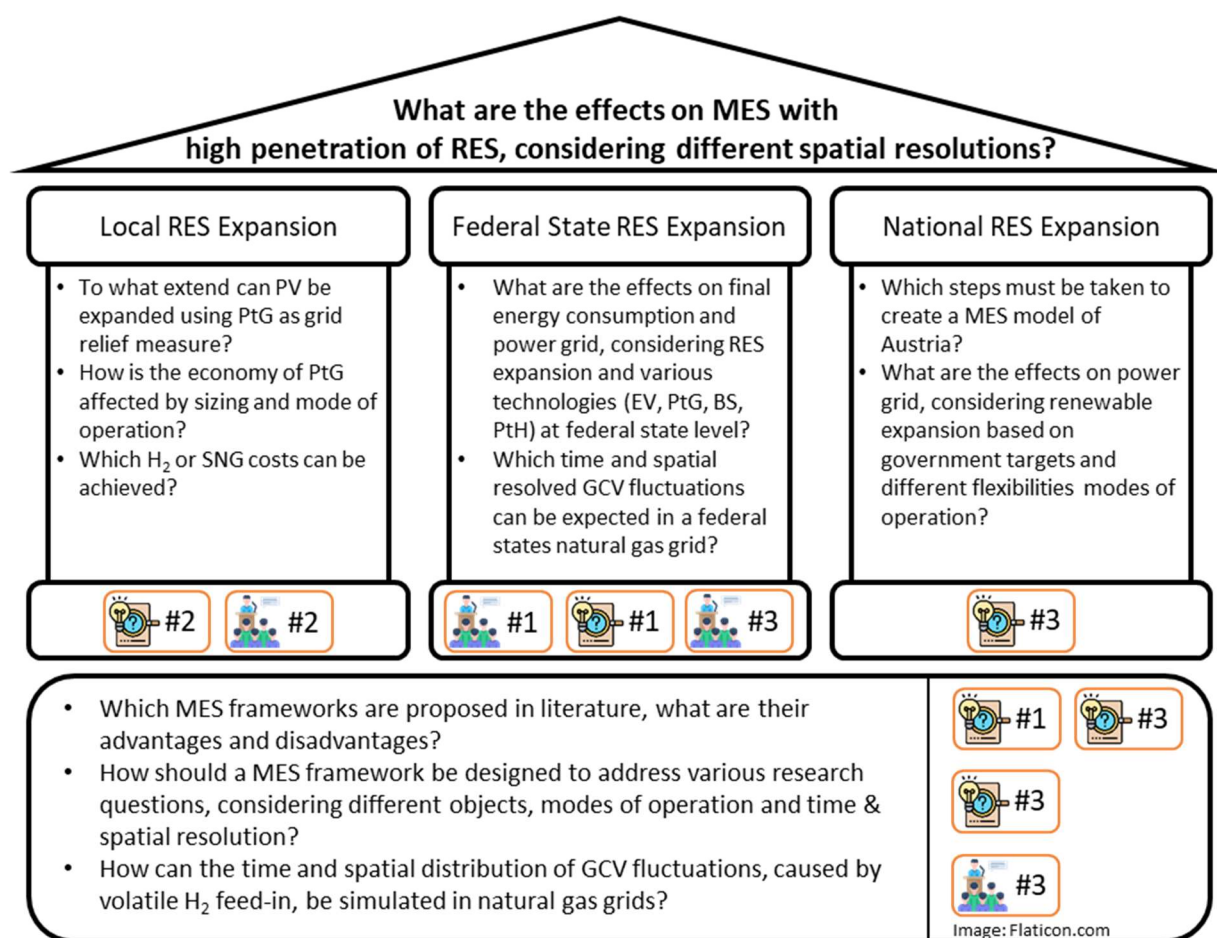


Figure 12: Structure of doctoral thesis and research questions

The roof over the building's structure defines the overall research question addressed in this doctoral thesis. Three sub-research question pillars, including their specific addressed research questions, can be seen in each pillar. The foundation of the building covers methodological research questions with a focus on the multi-energy system simulation framework HyFlow.

3.2 Methodology

This doctoral thesis is based on peer-reviewed journal articles and conference contributions. The research questions in Figure 12 are addressed in peer-reviewed journal articles and conference proceedings. Further details regarding the journal articles and conference contributions can be found in Appendix A and Appendix B.

Research Structure - Foundation

Throughout this doctoral thesis and serving as the methodological foundation for each journal paper, the multi-energy system simulation framework HyFlow is continuously improved, and its capabilities expanded based on the stage of development described in [49]. Several comprehensive literature reviews ensure that HyFlow development efforts contribute to scientific gaps or serve as ideas for potential new capabilities. Identified and addressed fields of improvement are described at the beginning of Chapter 3. Furthermore, a new methodology is introduced to determine the time and spatial distribution of gross caloric value (GCV) fluctuations in natural gas grids originating from hydrogen feed-in. An existing steady-state natural gas load-flow calculation methodology [62] is extended by a batch tracking, tracing concept to determine temporal and spatial GCV fluctuations via semi-dynamic gas load-flow calculation.

Research Structure - Pillar 1 & 2

The first and second research question pillars, assessing RES expansion at a local and federal states MES (refer to Figure 12), are independently assessed in close cooperation with two utility. This enables the usage of measured demand and generation data as well as the consideration of real energy grid properties, ensuring high input data quality. Furthermore, potential future developments at each multi-energy system level are based on a combination of scientific research and utility expert knowledge. This ensures that the assessed multi-energy system's simulated future states are based on realistic data and scenario assumptions.

The local level RES expansion MES investigates how much PV can be installed in a local 110 kV distribution grid section if power-to-gas (PtG) is installed as a grid relief measure. The feed-in of hydrogen into natural gas transmission pipelines and synthetic natural gas (SNG) in the local natural gas distribution grid are investigated. For SNG production, local fermentation plants

are considered as a potential CO₂ source. Based on the PtG facility’s calculated operation, the generation costs for hydrogen and SNG are calculated. The electrolysis is operated if either the power residual load (RL) of substation (SS) South and Rhine or all except North, Drava and West turns negative. The local area and available infrastructure are depicted in Figure 13. The following scenarios are considered:

- Scenario 1: Electrolysis at „SS South“ and hydrogen feed-in into “Natural Gas Pipeline (NGP) 2”.
- Scenario 2: Electrolysis at „SS North“ and hydrogen feed-in into „NGP 1“.
- Scenario 3: Electrolysis at „SS South“ and using biogas from local fermentation plants as carbon dioxide source to feed SNG into „Local grid“. To cope with different generation profiles (steady fermentation plants, volatile PV), storage and electricity purchase options are considered additionally.

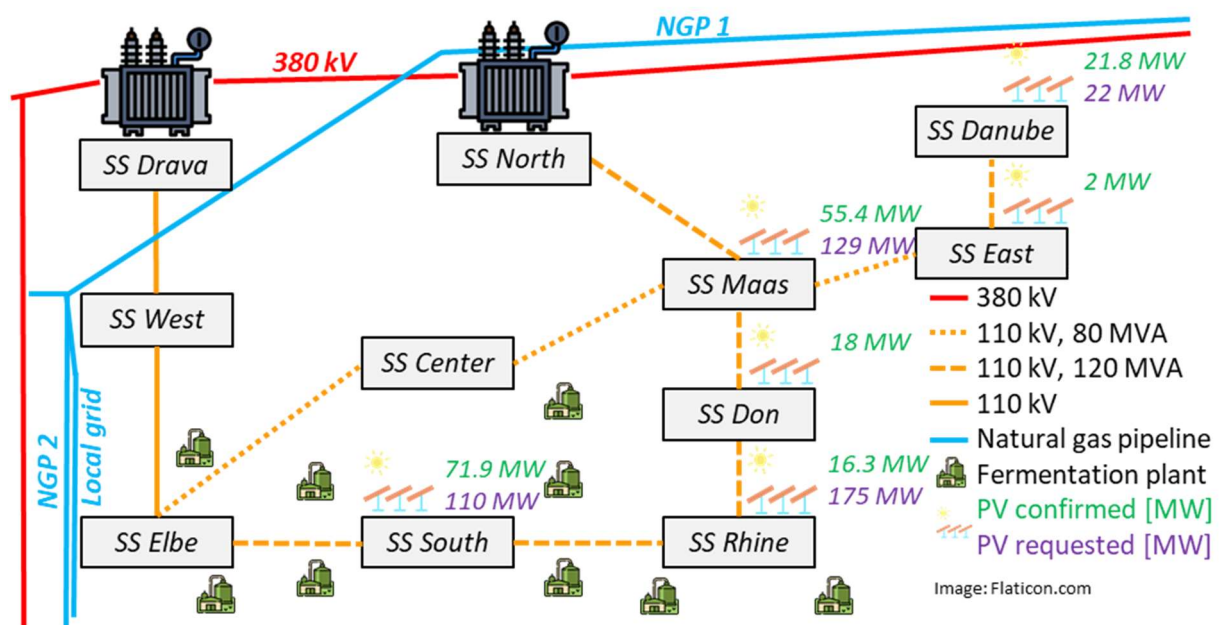


Figure 13: Covered area for local RES expansion MES

The federal state’s case investigates two independent research questions on the MES of two federal states.

Firstly, the MES of a federal state, considering different scenarios regarding energy consumption developments (stable –Scenario 1 and decline – Scenario 2), is investigated. The RES expansion is based on federal states’ targets and available potentials depicted in two RES expansion scenarios (#mission2030 – Scenario 1 and full exploitation of technical RES potentials – Scenario 2). Each scenario is further divided into two case studies: base case and advanced case. Compared to the base case, the advanced case considers heat pumps instead of gas for heating purposes, battery storage (BS), electric vehicles (EV) and a central PtG facility. The base case doesn’t consider previously mentioned technologies. Different technical

key performance indicators such as degree of self-sufficiency, the share of RES, primary energy demand and relative electricity line overload are used to compare the scenarios.

Secondly, the developed methodology to simulate GCV fluctuations from hydrogen feed-in to natural gas grids, is applied to a federal state's natural gas grid, displayed in Figure 14. The GCV fluctuations at each node to be investigated are caused by hydrogen, produced via electrolysis that is operated based on RES generation profiles and fed into the federal state's natural gas grid at different locations. A hydrogen admixture of up to 50 per cent into the natural gas grid is investigated.

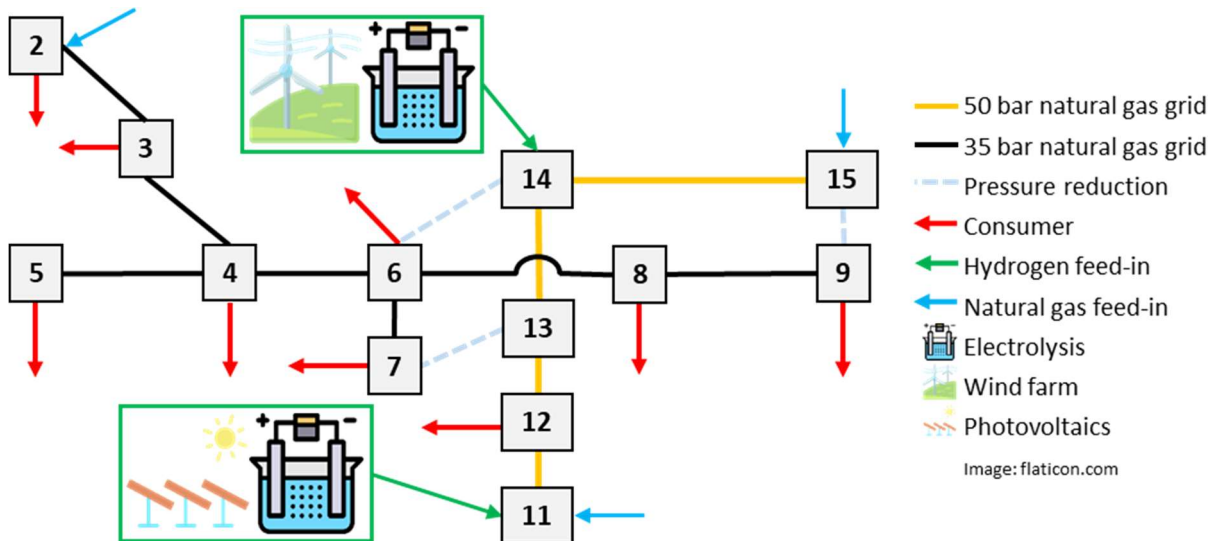


Figure 14: Overview of investigated federal states' natural gas grid

Research Structure – Pillar 3

For the third research questions pillar, assessing Austria's national MES (refer to Figure 12), a different approach than for research question pillars number one and two is carried out. Investigating the national MES of Austria as a whole is crucial to assess the national effects of RES expansion since research pillars one and two only investigate specific parts of Austria. To depict a national MES system following points must be addressed to create a comprehensive MES model for Austria:

- Energy grids (power, heat, gas) must be modelled, considering their technical grid properties.
- The area of Austria must be spatially divided into suitable sub-areas, here so-called substation districts (SSD). For each SSD, energy-related consumption and generation must be determined and temporally resolved.
- Technical properties of objects such as e.g. (pumped)-storage hydropower plants, heat pumps, CHP, fermentation plants, and power plants (PV, wind, run-off hydro, natural gas) must be determined and assigned to the object's corresponding SSD.

- Expansion of RESs must be carried out, considering the SSD’s RESs potentials, already installed RESs, and federal government targets.

To address before mentioned bullet points, a combination of the following sources is used to create a national multi-energy system model for Austria:

- Experiences and data from previously carried out research at the Chair of Energy Network Technology (e.g. [8, 49]) such as technical grid and power plant properties.
- Publicly available data from various utilities or regulators such as grid and power plant properties.
- Publications from regulators, public institutions, lobbies and stakeholder representatives (e.g. Umweltbundesamt, Statistik Austria, Österreichs Energie) about properties of the past, current or future energy system composition.
- Experiences, methodologies, data and results published in scientific journals such as energy consumption data or RES potentials.
- Governmental targets for a future composition of Austria’s multi-energy system (e.g. #mission2030 or current government program (from 2020 to 2024) [4, 5]).

Based on the created MES model of Austria, a total of three simulations are carried out to investigate potential future challenges in the power grid, based on #mission2030 RES expansion in 2030. Each scenario considers different modes of operation of flexible elements (e.g. electric vehicles, heat pumps, battery storage) and different power load-flow determination approaches (power flow and optimal power flow). Flexibilities are operated based on actual RL profiles (ENTSO-E), resulting RLs based on algorithms (greedy, load following), results of optimisation or standardised load profiles (SLP). An overview of each scenario is provided in Table 6. For further details, refer to [29].

Table 6: Scenario Parameters

Flexibility	Scenario 1	Scenario 2	Scenario 3
Thermal generation and (pumped)-hydropower storage	ENTSO-E	ENTSO-E	Flexibility
Electric vehicle	SLP	Optimised	Optimised
Battery storage	Greedy algorithm	Optimised	Optimised
Heat Pump	Load following	Optimised with storage	Optimised with storage
Power grid calculation	PF	PF	OPF

Research Structure – Roof

Results from both the research structures foundation and pillars contribute to answering the all-inclusive and overall research question defined in the research structures roof. Based on the results of each research pillar as an overall summary, it should be discussed if each pillar's results are corresponding or contradictory (e.g. do national results comply with local or federal state results?).

3.3 Contribution to Scientific Knowledge

Generally, questions covered in this doctoral thesis contribute to MES framework development & application, improvements in gas load-flow calculation and the effects of RES expansion on various MESs with different spatial resolutions. The following bullet points are considered as main fields of contribution to the scientific community and are further discussed in this section:

- A fully flexible, expandable and innovative MES simulation framework HyFlow with optimisation capabilities. Improved gas load-flow calculation, considering temporal and spatial gross caloric value fluctuations.
- Exemplary procedure to depict a national MES with a high degree of both spatial and temporal resolution.
- Implications of RES expansion and potential solution strategies in multi-energy systems with various spatial coverage.

MES Simulation Framework HyFlow

Several different concepts to assess various MES research topics are currently available (refer to chapter 2.2.2). However, significant gaps could be identified, leading to the development of a unique MES simulation framework with optimisation capabilities, HyFlow. The scientific novelty of HyFlow is that it offers the user to address a wide range of multi-energy systems with minimal adoption efforts. The wide range of applications refers to flexible temporal and spatial resolution as well as additional elements that can be integrated into MES, such as e.g. storage, sector-coupling and power stations, depending on the user's individual needs. A detailed infrastructure consideration allows for considering technical power, gas and heat grid properties. The detailed infrastructure depiction further allows for the usage of detailed load-flow calculations for each energy carrier.

Current natural gas load-flow calculation approaches fail to consider fluctuations of temporal and spatial gross caloric values. The current state of research can be described as a steady-state approach, considering every calculated time step independently. This means results from previous time steps are not considered, although it is necessary to do so to consider

fluctuating GCVs [62]. To determine the temporal and spatial GCV fluctuations, caused for instance by hydrogen feed-in to natural gas grids, the existing steady-state approach must be further developed towards a semi-dynamic or dynamic load-flow calculation approach. The enhancement is implemented by expanding the steady-state load-flow calculation by a batch tracking, tracing concept to enable semi-dynamic load-flow calculations. This upgraded load-flow calculation presents a novel approach that can be used to assess temporal and spatial GCV fluctuations in gas grids caused by e.g. hydrogen feed-in, originating e.g. from electrolysis fed by fluctuating RES.

Model of Austria's National MES

To the best of my knowledge, two research papers address Austria's national MES. However, both studies are based on an optimisation approach. Therefore, temporal and especially spatial resolution is implemented to a highly simplified degree (single node [63], 19 regions [64]). This current work considers a detailed energy grid infrastructure depiction, allowing for detecting potential infrastructure bottlenecks in Austria's MES. Furthermore, individual generation profiles for RES (wind, hydropower, PV) are assigned to each depicted SSD of Austria. This offers both a detailed and wide range of various fluctuating generation profiles. The methodology to model Austria's MES relies mainly on public data and research results. It can serve as a reference guideline to set up a MES model for other regions or countries. Further research questions in the context of Austria's MES can be addressed using the created MES model.

Implications of RES Expansion and Solution Strategies

The effects of RES are assessed on three different spatial MES levels (regional, federal state, and national). For each spatial level, RESs are expanded according to available technical potentials and governmental strategies, that might limit certain RES potentials exploitation. For each spatial level, individual scenarios are discussed to investigate the grid relief capabilities of a MES. Solution strategies may include different objects (e.g. electric vehicle, storage, sector-coupling) added to a MES, providing different types of flexibility. Each spatial level assessed deals with real MES issues to be resolved. The main scientific novelty lies in the consideration of detailed energy infrastructure properties, detailed temporal resolved demand & generation profiles and the proposed individual solution strategies. Additionally, the GCV fluctuations assessment shows how different natural gas grid sections are affected by GCV fluctuations, depending on fluctuating hydrogen feed-in.

4 RESULTS, DISCUSSION AND CONCLUSION

This section presents and discusses methodological and scenario-based RES expansion results from research questions defined in Chapter 3.1.

4.1 HyFlow MES Simulation Framework [29, 65–67]

The already existing HyFlow framework was further developed within this doctoral thesis to implement new capabilities. This includes a more flexible network depiction, improved load-flow calculations and further options to add individual objects with distinct operation strategies. If all components of a MES are known (e.g. like in Figure 18), a HyFlow compatible node-edge model can be derived. Nodes represent a specific area covered (e.g. refer to the yellow SSD in Figure 18), including particular objects within this area and their corresponding RL profile (e.g. fermentation power plants inside the yellow area in Figure 18). For example, the yellow SSD in Figure 18 can be transferred into a node displayed in Figure 15. The node comprises energy carrier-related IDs and a RL collection that contains all objects within the SSD. Since the highlighted SSD in Figure 18 has no district heat connection to neighbouring SSDs, Heat ID isn't necessary to be used. The exemplary node in Figure 15 contains several objects in its RL collection, such as residential consumers, fermentation power plant (aggregated), electric vehicles, PV, gas to heat and power to heat. Generally available sector-coupling technologies (e.g. PtH and GtH in Figure 15) at nodes enable the conversion from energy carrier to other energy carriers. For each object, a characteristic RL profile is necessary. It can be based on fixed or standardised load profiles, determined by a distinct operation strategy or flexibly in combination with optimisation.

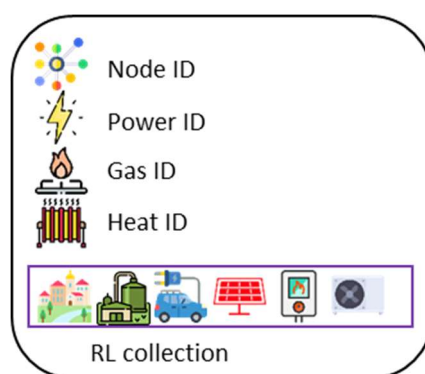


Figure 15: Example of a node

Edges represent the depiction of the energy grid infrastructure. Depending on the usage of power, gas and heat IDs, each node can be interconnected to one or more other nodes considering real energy grid properties. As an example of the node-edge representation, the yellow SSD and its surrounding SSDs in Figure 18, as well as objects in these SSDs, are displayed

in Figure 16. Here, all nodes / SSDs are interconnected by power and natural gas grids. No heat connections exist between the depicted nodes in this case. Objects in the SSDs such as fermentation power plants and run-off hydropower are displayed inside the corresponding node.

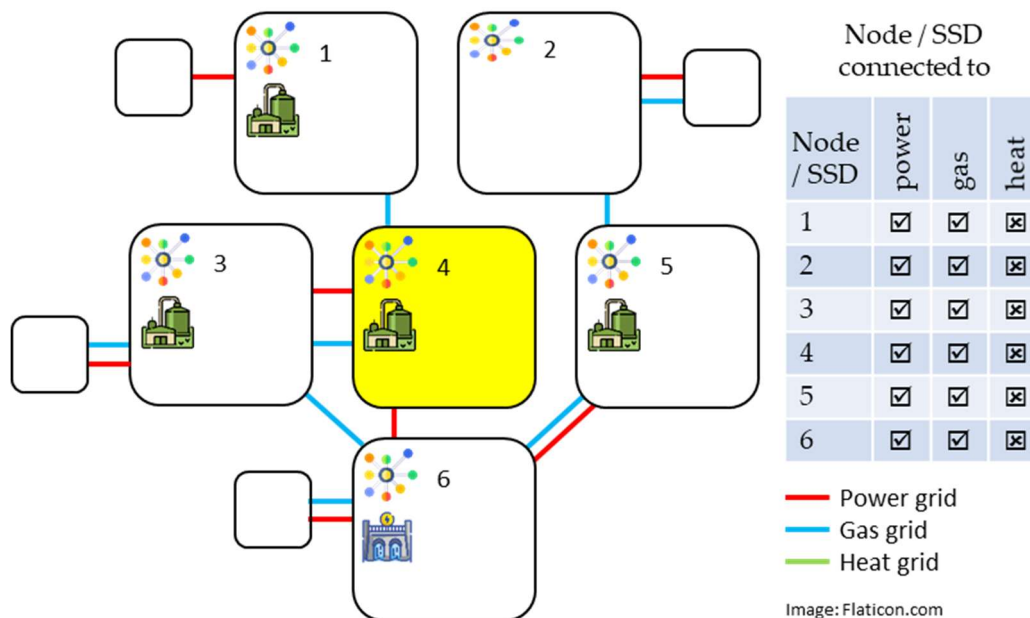


Figure 16: Derivation of node-edge model based on MES depiction

A time step loop ensures that each time step of a simulation period is simulated. Simulations of load-flows in HyFlow are carried out based on all previously described data (grid data, object properties and RL profiles). To determine power, gas and heat load-flows between nodes, adequate load flow calculation methodologies are implemented in HyFlow. Power grid load flows can be determined via either MATPOWER power flow or optimal power flow [68]. Natural gas and district heat load flow calculations rely on a steady-state load flow consideration based on an iterative Newton-Raphson solver and the Darcy-Weisbach equation. Both node- and edge-related results of the load-flow calculation are stored and can be further evaluated. Node-related results are node voltage, angle, pressure and temperature levels. Edge-related results are load-flow, loss and flow velocity. Both node and edge results may be used for further assessments such as:

- Check if a node’s voltage, angle, pressure or temperature is within a defined allowed range.
- Check if edge load-flows or flow velocity is above a maximum allowed limit.
- Further assessment of some geographic areas.

The actual RL is stored for each node’s object after determining its operating strategy or optimisation. The corresponding RL timeline can be used for further assessment after the simulation is finished, such as:

- Analysis of temporally resolved dispatch.
- Calculation of annual full-load hours or generated/consumed energy.
- Economic key performance indicators based on full-load hours and/or dispatch.

Both previously described assessments are partially used to evaluate three specific scenarios in the following chapter 4.3.

Based on the Darcy-Weisbach equation, an existing steady-state natural gas load-flow calculation is enhanced to cope with GCV fluctuations from injected hydrogen into natural gas grids. The basic calculation of the semi-dynamic process is presented in Figure 17. The position of each hydrogen, natural gas, or mixture batch and its distinct GCV is updated within several iterations during one time step. GCVs can be determined for each node depending on the position of individual batches. If the average GCV change of all nodes between two iterations is below a user-defined limit, the calculation is considered accurate, and the GCVs of each node and the final position of all batches are determined.

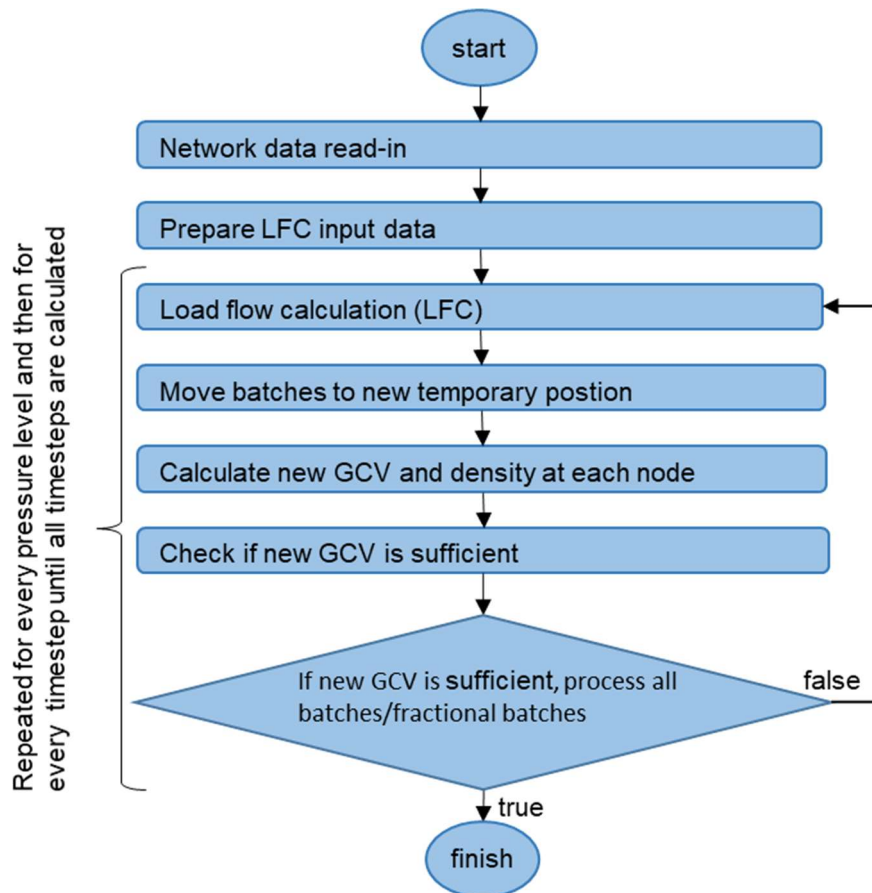


Figure 17: Calculation process for enhanced gas load flow calculation

Further information regarding the mathematical and methodological concept of the developed batch tracking, tracing approach can be found in [67].

4.2 MES model of Austria [29]

To create a national MES model with high spatial resolution, Austria is divided into 398 so-called substation districts. Each SSD represents the smallest spatially covered area in the model and is fed with various data. This includes power, heat and natural gas energy consumption data which are temporally resolved, considering multiple load profiles.

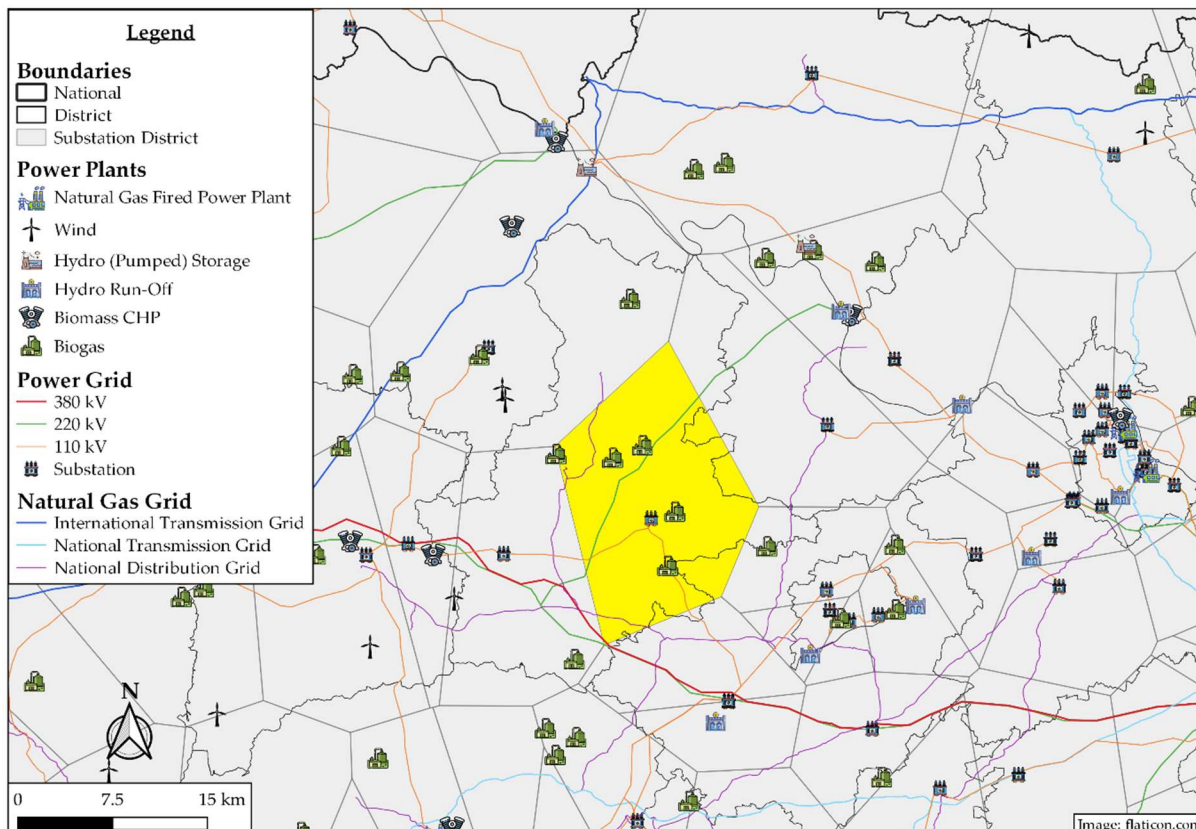


Figure 18: Example of Austria's MES model, one SSD exemplarily highlighted yellow [28]

Furthermore, technical data of flexible and inflexible objects were determined for each SSD. This includes power plants (e.g. hydro, PV, wind, biomass, fermentation, natural gas-fired), storage (pumped-hydro) and sector-coupling technologies (e.g. GtH, PtH). The scenario-dependent mode of operation of an object defines if the object serves as flexibility or not. For each power plant, individual generation profiles were determined based on e.g. water flow rate, wind speed or solar radiation. As an example, a SSD is highlighted in yellow in Figure 18. The SSD includes a total of four fermentation plants as well as both power and natural gas grids.

Energy grids represent another vital component of Austria's MES since they enable the energy transfer between SSDs. Both the modelled natural gas and power grids of Austria are displayed in Figure 19. The model can easily be expanded and updated. Newly constructed or projected energy grids can be easily implemented into the model to keep Austria's MES model up to

date. For the usage of the MES model in far distant years, it's crucial to consider changes in generation and energy grids for accurate simulations.

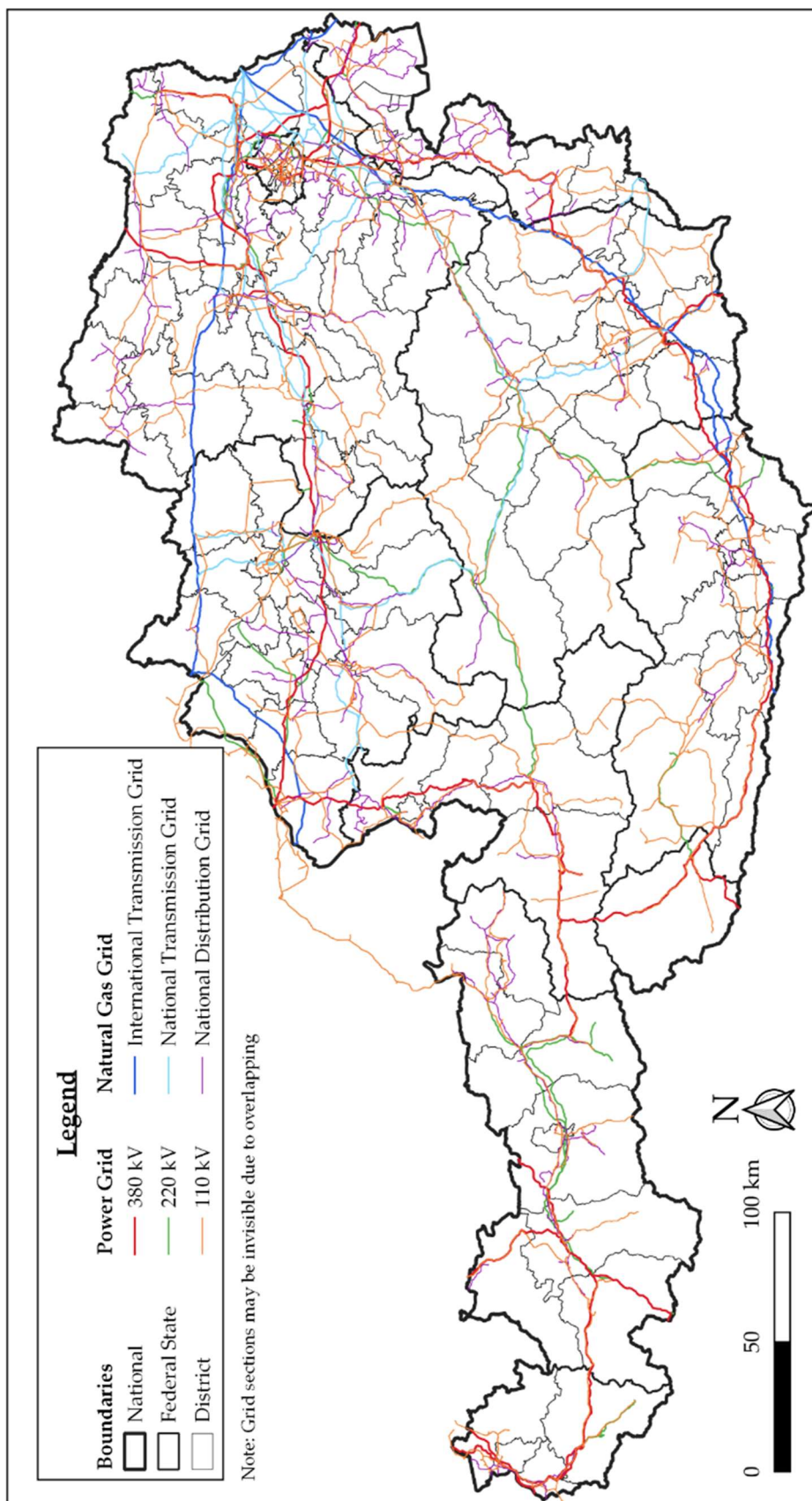


Figure 19: Austria's Power and Natural Gas Energy Grids [28]

4.3 RES Expansion at Different Spatial Resolution

This section discusses results from individual studies at different spatial resolutions.

Regional RES Expansion [65]

The local RES expansion study investigates potential problems of a region with high renewable potential and a lack of both consumer and transmission capacity. The effect of electrolysis on a regional distribution grid section to maximise the locally installable PV power is techno-economically investigated. Hydrogen or synthetic natural gas generation costs are calculated based on each scenario's technical results.

Firstly, technical results such as the influence of operating strategies on achievable full-load hours and realisable PV power in connection to the electrolysis power are discussed. Two operating strategies are assessed to investigate the influence of the mode of operation on the electrolysis' achievable full-load hours (FLH). The first operating strategy is based on the residual load of two substations with high PV potentials. In contrast, the second operating strategy considers the RL of almost the whole investigated area. In Table 7 the achieved FLH for different electrolysis powers are displayed for Scenario 1. It can be seen that achievable FLHs are highly dependent on the electrolysis operating strategy. Furthermore, operating strategy #1 is always favourable in terms of FLH compared to operating strategy #2. Therefore, electrolysis operation should depend on the RL of substations with high PV potentials.

Table 7: Comparison of the electrolysis' achievable full-load hours, depending on operating strategy

Operating Strategy	17.5 MW Electrolysis	87.5 MW Electrolysis	227.5 MW Electrolysis
# 1	3,008 FLH	2,355 FLH	1,659 FLH
# 2	1,570 FLH	1,474 FLH	1,125 FLH

In Figure 20 the maximum installable PV power in dependence on electrolysis power and limitations are displayed. It can be seen that the lowest PV integration is achieved in Scenario 2. The location of the electrolysis explains this since significant PV potentials are located at different locations. Therefore, power must be transferred via the power grid towards the electrolysis. In comparison, the electrolysis location is different in Scenario 1 and Scenario 3 compared to Scenario 2. Scenario 1 considers hydrogen feed-in, whereas Scenario 3 uses hydrogen originating from electrolysis in combination with biogas from local fermentation plants to feed-in bio-methane and synthetic natural gas (SNG). As can be seen in Figure 20 one limitation in each Scenario (NGP 2 feed-in limit in Scenario 1 and CO₂ availability in Scenario 3) must be overcome before the grid limitations take effect. The addable PV power can approximately be expanded proportionally to the electrolysis power.

P Electrolysis	Scenario 1	Scenario 2	Scenario 3
0 MW		110 kV grid PV: 279 MW	
50 MW	NGP 2 feed-in limit PV: 337 MW		
100 MW			CO ₂ availability PV: 411 MW
150 MW			
200 MW			
250 MW	110 kV grid PV: 500 MW		110 kV grid PV: 500 MW

Figure 20: Technical limitations and achievable PV integration for each scenario

Technically it can be concluded that the location and electrolysis operation is highly relevant for its efficiency. A location close to excess RES generation allows for the direct usage of power, reducing the need for grid-bound energy transfer. Limitations such as feed-in capacity or CO₂ availability must be overcome to tap an even higher share of RES potentials. The surrounding environment is highly relevant for the electrolysis and the potential need for auxiliary units such as storage, alternative transportation solutions or CO₂ sources. Since natural gas and power infrastructure are relevant, a multi-energy system consideration is beneficial. If an electrolysis waste heat is to be used, district heat infrastructure might be considered additionally.

Secondly, the economic efficiency is determined, based on technical results. Three main cost drivers can be differentiated. Firstly, the electrolysis, secondly auxiliary units such as storage, pipeline, compressor and methanation and thirdly power purchasing costs. In Table 8 a cost comparison for all investigated scenarios and an electrolysis power of 52,5 MW is displayed.

Table 8: Cost comparison for an electrolysis power of 52,5 MW

Key Performance Indicator	Scenario 1	Scenario 2	Scenario 3 cheapest	Scenario 3 most expensive
Gas injected	Hydrogen	Hydrogen	SNG	SNG
Specific CapEx [€Cent/kWh]	5.3	6.8	5.1	7.4
Specific OpEx [€Cent/kWh]	1.3	1.7	1.9h	3.6
Specific Electricity Costs [€Cent/kWh]	5.5	5.5	7.0	5.4
Installed PV Power [MW]	357 MW	279 MW	357 MW	357 MW
Electrolysis FLH [h]	2,610 h	1,931 h	4,265 h	2,610 h

The electrolysis costs are only dependent on the electrolysis sizing across all scenarios, whereas the costs for auxiliary units and power purchases depend on the scenario. The annual depreciation for methanation and auxiliary units is usage-independent and not dependent on e.g. FLHs. Therefore, the specific capital expenditure costs decrease, if more FLHs are achieved. Operational expenditures and power purchases depend on both the scenario and necessary auxiliary units. As pointed out in the technical assessment, higher FLHs are achieved if the electrolysis sizing is smaller, leading to reduced PV power integration. A compromise

between the necessary electrolysis power and economic efficiency must be found to overcome this conflict of objectives. Generally, it can be stated that feed-in of hydrogen is more economical than SNG since fewer auxiliary units are necessary.

Further information and results can be found in the second journal article [65].

Federal State RES Expansion [66, 67]

This section is divided into two parts, firstly addressing RES expansion at federal state level ([66]) and secondly discussing GCV fluctuations from hydrogen injection in a federal state's natural gas grid ([67]).

For the RES expansion study, the RES potentials and RES expansion strategy of an Austrian federal state are applied. Since hydropower and biomass potentials are already exploited to a high degree and no wind expansion is allowed by the federal state's energy policy, most RES expansion must be covered by PV. The expectable effects of RES expansion (mainly PV) can be seen in Figure 21 on the example of a summer and winter week.

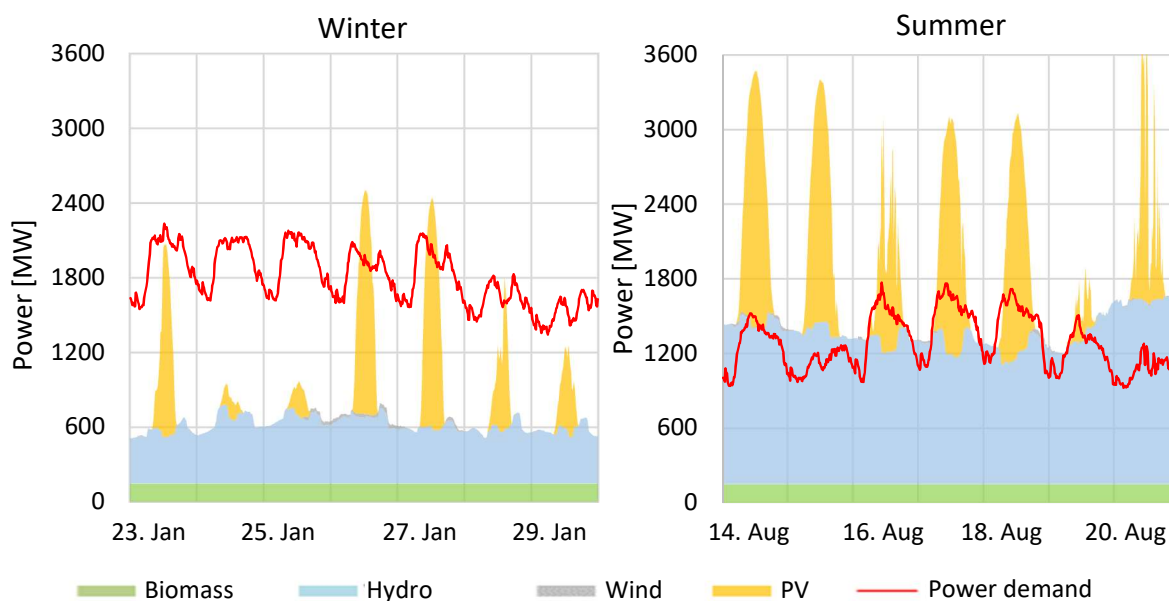


Figure 21: Comparison of RES power generation in summer and winter week

In the displayed winter week additional power plants (e.g. gas-fired), storage or power imports are necessary to cover the power demand. In summer, during PV peak generation, excess power is generated at a magnitude of the federal state's power demand. As an alternative to power exports or generation curtailment flexibility options can be applied. This study uses a central PtG facility to convert excess power into natural gas. Table 9 displays key performance indicators (KPI) for both renewable expansion scenarios and corresponding sub-scenarios (advanced and base case – ADC, BC). KPIs include the degree of self-sufficiency (DSS), share of RES compared to federal state's power demand, degree of RES expansion (DRESE) based on technical RES potential, relative power line overload (PLO) and primary energy demand.

Table 9: Comparison of KPIs for different RES expansion scenarios

KPI	Scenario 1		Scenario 2	
	BC	ADC	BC	ADC
DSS power	58 %	81 %	75 %	93 %
DSS natural gas	0 %	1.1 %	0 %	4.4 %
Share of RES	97 %		125 %	
DRESE	84 %		100 %	
Rel. PLO	0.41 %	1.49 %	1.25 %	3.90 %
Primary energy demand	36.6 TWh	32.1 TWh	35.9 TWh	29.4 TWh

For both Scenario 1 and 2 it can be seen that the usage of heat pumps, electric vehicles and PtG increases the electric DSS and reduces primary energy demand. However, the additional power consumption increases the relative PLO. The power grid overloads are mainly caused by the PtG facility since it must cope with excess power in the magnitude of the federal state's power demand. Several decentralised PtG facilities or strengthening of certain grid sections, mainly around the PtG facility, might reduce relative PLO significantly. Although the share of RES is increased to 125 per cent of the federal state's power demand in Scenario 2, a power DSS of only 93 per cent is achieved. This indicates that power imports or further (fossil) power plants are still necessary in the future to cover shortfalls of available power, as can be seen for example in the displayed winter week in Figure 21.

Concluding, the federal state's MES study demonstrates what effects can be caused by a federal state's RESs expansion strategy. The high addition of one specific RES (PV) causes large peaks of excess power, especially but not solely in summer. Although technical RES potentials are exploited in line with the federal state's policy to 100 per cent and should be able to cover 125 per cent of the federal state's power demand, a power DSS of only 93 per cent is achieved over one year. This leads to the conclusion that power exchange with adjacent regions, further power storage options or (fossil) power plants are necessary.

Further information and results can be found in the first journal article [66].

The following section discusses GCV simulation results, applying the developed batch tracking, tracing methodology on a federal state's natural gas grid. The spatial and temporal resolved GCV fluctuations in the investigated federal state are assessed for both a summer and winter case. This separation is necessary since about twice as much hydrogen can be fed into the natural gas grid in winter compared to summer, due to higher gas demand for heating. To gain better results insights, the investigated federal state's natural gas grid is again displayed in Figure 22.

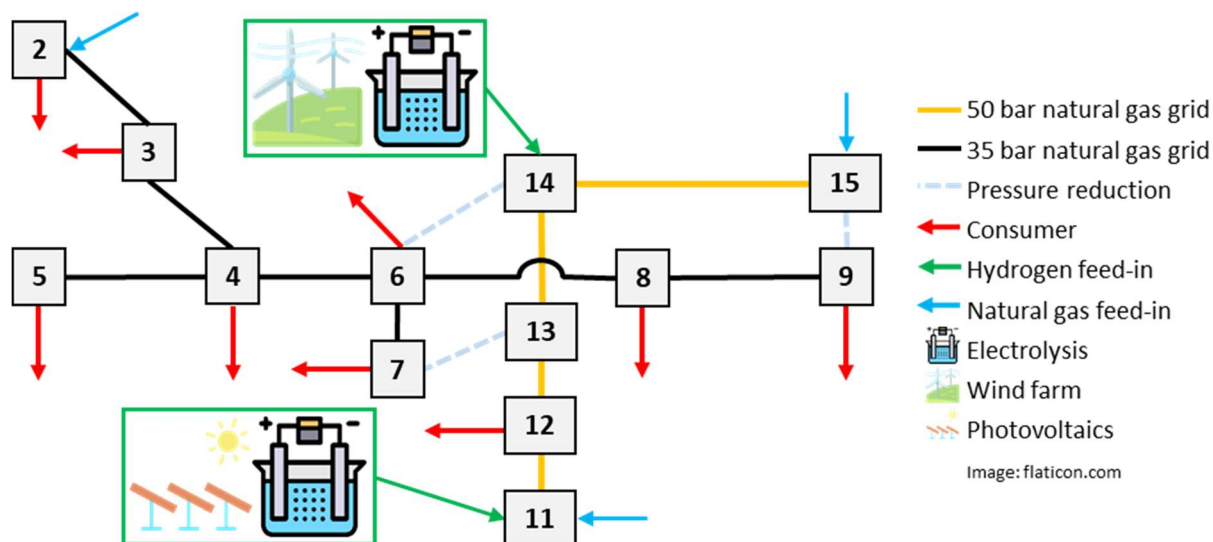


Figure 22: Overview of investigated federal state's natural gas grid

The GCV fluctuations for two characteristic winter and summer days are displayed in the following Figure 23 and Figure 24. One single time step represents a 15-minute time interval.

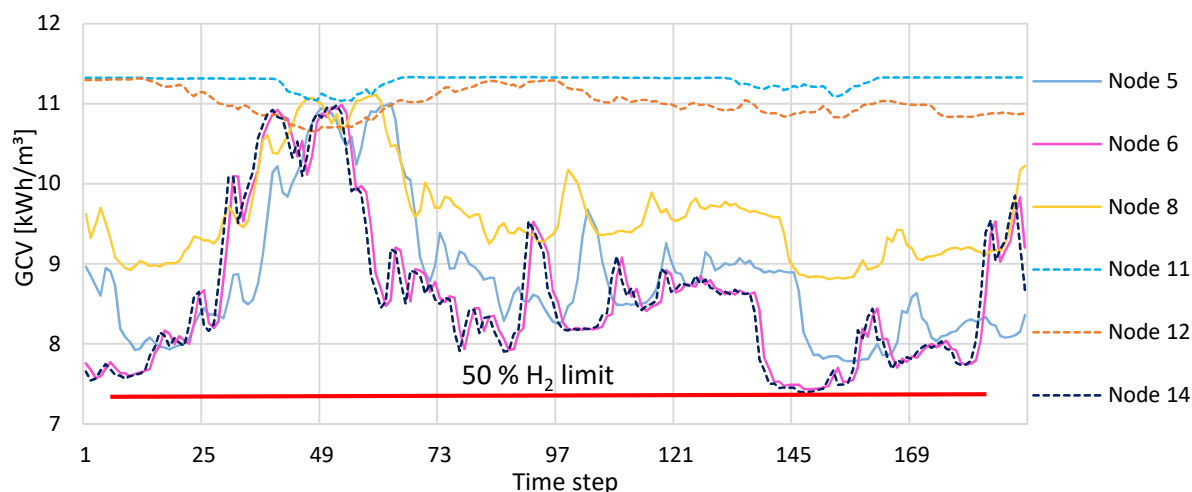


Figure 23: Spatial and temporal resolved GCV fluctuations in winter

The displayed results in Figure 23 represent two winter days. Therefore, PV generation is relatively low (see high GCV at nodes 11 and 12). In contrast, the wind farm driven electrolysis at node 14 shows strong fluctuation in its generation, resulting in GCV fluctuations at node 14 and surrounding. It can be seen that the GCV fluctuations of node 6 follow the fluctuations of node 14 closely. In comparison, node 5 is geographically further away from node 14 than node 6. Therefore, it takes several time steps until the hydrogen-natural gas mixture reaches this node and causes GCV fluctuations. Node 8 is influenced by gas flows from both node 6 (hydrogen, natural gas mixture) and 9 (pure natural gas), resulting in a lower fluctuation than node 6. Due to the gas flows in the grid, certain nodes such as 2, 3, 9 and 15 (not displayed in Figure 23) are not affected by GCV fluctuation since no hydrogen – natural gas mixture reaches these specific nodes. These nodes are always supplied with 100 percent natural gas.

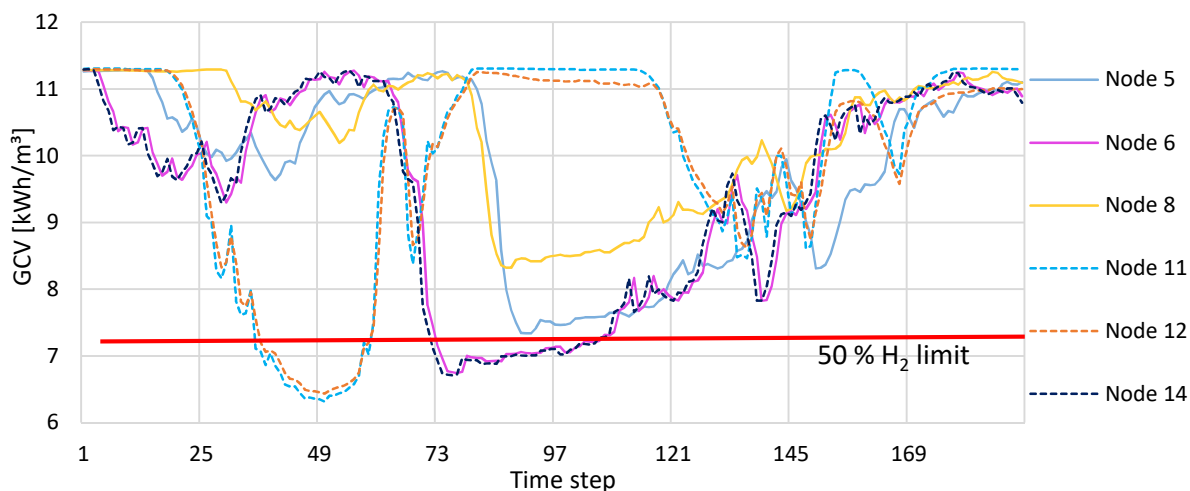


Figure 24: Spatial and temporal resolved GCV fluctuations in summer

To complement Figure 23, in Figure 24 results from summer are displayed. Here, the amount of hydrogen generated from PV is significantly higher, resulting in lower GCV at nodes 11 and 12 near the hydrogen injection node. Generally, the natural gas flows are similar in terms of flow directions compared to winter. However, lower demands result in slower flow velocities. This leads to an increased number of time steps it takes a node to react to GCV fluctuations, as can be seen for example at node 5. Between time steps 37 to 60 and 72 and 108, the 50 % hydrogen limit is violated. This issue could be addressed either via smaller electrolysis or temporary storage.

Generally, it can be concluded that each node is affected to a different degree in terms of GCV fluctuations. This depends on the node's location and the distribution of gas flows in the gas grid. Furthermore, hydrogen originating from wind or PV-operated electrolysis shows seasonal fluctuations. Hydrogen originating from wind power operated electrolysis is mainly fed-in in winter, whereas hydrogen originating from PV-operated electrolysis is mainly fed-in in summer. Due to the higher natural gas demand in winter, about twice as much hydrogen can be feed-in in natural gas grids during winter compared to summer months.

Further information can be found in the third conference contribution [67].

National RES Expansion [29]

For this study, RESs in Austria are expanded according to #mission2030 government target. We assume that RESs are expanded proportionally in relation to their technical potentials. Furthermore, the effects of different modes of operation of flexibilities such as electric vehicles, battery storage, heat pump, (pumped)-storage hydropower and natural gas-fired power plants are investigated. In all three discussed MES scenarios, power grids are evaluated to be the most critical. In following Table 10, a comparison of overloaded distribution power grid (DG) and transmission power grid (TG) lines is displayed (please refer to Table 6 in section

3.2 for flexibility's mode of operation and load flow calculation approach). It can be seen that in Scenario 2 the number of time steps, as well as affected electricity grid lines, increases compared to Scenario 1. This can be explained by the price optimised mode of operation, since demand increases disproportionately in time steps with cheaper electricity, leading to RL peaks. Scenario 3 reduces the count of overloaded DG and TG lines significantly compared to Scenario 1 and 2 due to the flexible power generation from (pumped)-storage hydropower and natural gas-fired power plants in combination with optimal power flow.

Table 10: Comparison of power grid results of each scenario

Flexibility	Scenario 1	Scenario 2	Scenario 3
Overload time DG	182,000 time steps	207,000 time steps	82,000 time steps
Count of overloaded DG lines	39 / 480	57 / 480	40 / 480
Overload time TG	3,900 time steps	8,100 time steps	140 time steps
Count of overloaded TG lines	5 / 104	7 / 104	6 / 104

As an example of power grid overloads, the results for Scenario 2 (worst case) are displayed in Figure 25. It can be seen that the maximum overloads of power grid sections are relatively small (refer to yellow to light orange grid sections in Figure 25). Generally, three distinct fields of power grid overloads can be differentiated:

- Grid sections with low transmission capacity, e.g. only one three-wire system is available and/or the transmission capacity is generally low.
- Overloads occur in urban areas.
- Large areas with high potential of RESs expansion, sometimes in combination with low transmission capacity to/from the area.

It can be concluded that Austria's power grid is generally able to handle a RES expansion proportionally in relation to its technical RES potentials with relatively few power grid overloads. Energy transmission to or from neighbouring countries is barely affected by grid overloads, indicating that power imports or exports are possible to balance Austria's power supply. However, trans-national power flows were not investigated in detail. Implementing flexibilities into the energy system is advantageous to minimise power grid overloads and the need for grid strengthening. A market-oriented approach such as the price optimised power demand and generation should be coupled with a grid-oriented approach that considers the power grid's current state (= power load flows and transmission capacities). Combining market- and grid-oriented approaches like in Scenario 3 results in the lowest count of overloaded power lines and overload hours.

Further information and results can be found in the third journal article [29].

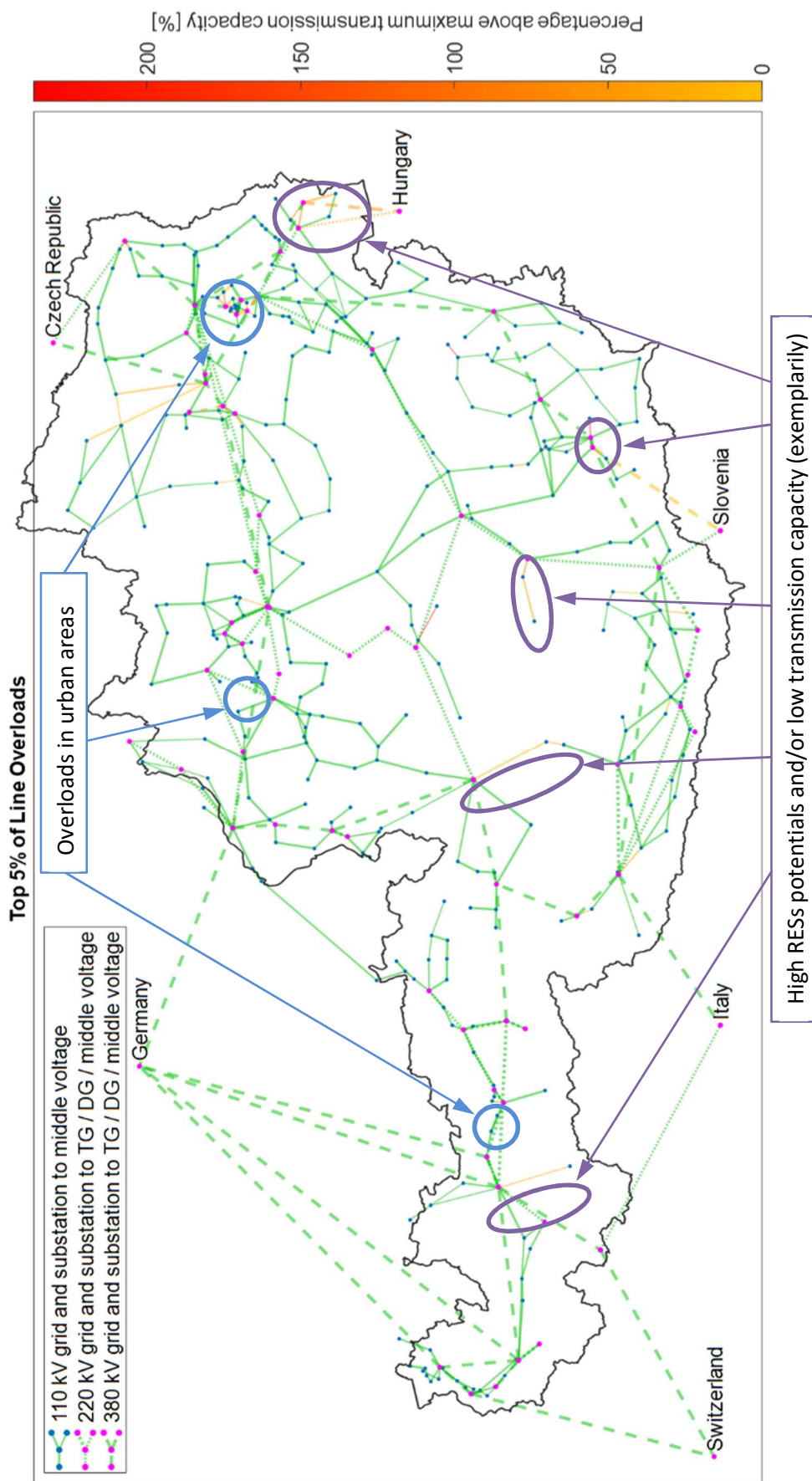


Figure 25: Average power grid line overloads for Scenario 2 (worst case)

5 SUMMARY & OUTLOOK

This doctoral thesis addresses the effects of expanding renewable energy sources on multi-energy systems under various spatial resolutions. This includes suitable simulation methodologies, an approach to depict a national multi-energy system, and assessing various multi-energy systems with different spatial resolutions and scenarios.

HyFlow Framework

The basis for this doctoral thesis and all MES studies is the MES simulation and optimisation framework HyFlow. It can depict the grid-bound energy carriers power, natural gas and district heat, including energy grids, power plants, storage and sector-coupling options. A previous stage of HyFlow's development can be found in [49]. However, the application of the previously developed HyFlow in various projects and literature reviews disclosed specific potential fields of improvements. These considered improvements include a fully flexible energy grid depiction, capabilities to add further objects into the MES and operate them based on a variety of different approaches and advanced load-flow calculation capabilities. The energy grid depiction is improved so that an individual count of different energy grid levels (e.g. pressure level) can be defined. The advanced HyFlow framework can implement an individual number of additional MES objects (e.g. power stations, storage, sector-coupling) at any user-defined location in the MES, compared to one sector-coupling object and one storage per energy carrier in the previous stage of development. Load flow calculations were improved for power and district heat. To determine power load-flows, the MATPOWER framework is integrated into HyFlow, allowing for both alternating and direct current power and optimal power flow load-flow calculations [68]. District heat load flow calculation is improved to cope with meshed grid topology instead of a tree topology without meshes. Future potential fields of HyFlow development can be the addition of further objects and corresponding operating strategies into HyFlow.

The developed semi-dynamic gas load-flow calculation with batch tracking, tracing capability allows for determining timely and spatially resolved GCV fluctuations. The presented gas load-flow calculation approach can be used to derive a similar concept for heat load-flow calculations by tracking water batches and their distinct temperatures instead of gas batches and their GCV.

The presented methodologies can be applied to any other MES simulation research question to be addressed.

MES Model of Austria

The MES model of Austria has been developed based on publicly available data, previous research projects and experiences from previous projects. The model divides Austria into 398 so-called substation districts. For each substation district, distinct generation and consumption profiles are determined. The consumption side considers several sectors such as household, agriculture, service and industrial and the energy carriers power, natural gas and heat. Annual consumption data are temporally resolved using a combination of standardised load profiles and research results. To determine SSD specific generation profiles, all power plants (hydro run-off, (pumped)- storage hydro, PV, wind, biogas, biomass, natural gas) within a substation district are determined. A temporal resolved generation profile is calculated using water flow rates, standardised load profiles or generation timelines based on solar radiation or wind speed measurements. A detailed model of Austria's power and natural gas energy infrastructure is established to consider energy grid properties between substation districts.

The MES model of Austria can further be adapted to meet the demands of different scenarios to be investigated. Potential improvements can be implemented in both substation district-related data and energy grids. The energy consumption and generation within a substation district can further be adjusted by considering for example a change of population between substation districts, open / closure of new industrial plants, the retirement of power plants or expansion of RESs. Furthermore, the effects of political decisions such as phasing out of gas boilers, the number of electric vehicles, or an increase in heat pump usage can be considered to a scenario-dependent degree. Considering future grid expansion or closure of grid sections, the energy grid infrastructure depiction can be updated accordingly.

Effects of RES Expansion on MES

The effects of RES expansion on MES with different spatial resolutions are mainly affected by the underlying scenario and its distinct RESs expansion strategy. As demonstrated in the case of Austria's MES, a few grid strengthening measures would enable the integration of RESs in accordance with #mission2030 RES expansion targets. However, as demonstrated in the federal state and local use case, political decisions and local circumstances might lead to different RESs expansion scenarios, affecting especially power grids to a significantly different degree. To cope with these circumstances, alternative solution strategies should be considered. In the federal state use case, biomass and hydropower potentials are already exploited to a high degree. No wind expansion is allowed, leaving PV as the only RES to expand. This leads to temporary excess generation peaks, mainly in summer at a magnitude of the federal state's power consumption. The excess power has to be either stored, exported or consumed. The local use case demonstrates both positive and negative effects of PtG as a power grid relief measure. If the grid relief measure is misplaced, hardly any RES expansion

can be integrated without having to avoid power grid overloads. If the PtG is positioned close to RES, the generated hydrogen or SNG can be fed into nearby natural gas grids and the installed RES generation can be expanded significantly. Especially hydrogen feed-in into natural gas grids can cause both temporal and spatial resolved GCV fluctuations in natural gas grids. Fluctuations must remain within defined boundaries to guarantee a predictable gas quality. Furthermore, the potential hydrogen amount that can be fed into the natural gas grid differs between summer and winter, due to varying natural gas demand for e.g. heating.

The created models and methodologies may serve as a basis for further investigations. This may include improved or updated generation and demand data, different RES expansion strategies or deviating scenario parameters. The proposed solution strategies can be used or further adapted and investigated in any region or country with similar characteristics.

Following key results can be concluded, assessing RES expansion at different spatial resolutions:

- An equal distribution of RESs across Austria (e.g. realising a certain, equivalent percentage of potentials) according to RESs potentials is beneficial to implement RES in line with government targets. A purely market-oriented operation of flexibilities such as heat pumps, battery storage or electric vehicles results in demand peaks when electricity prices are low. To take advantage of cheap electricity and avoid energy grid overloads, the power grid's status should be considered in addition – as a market oriented approach combined with grid oriented approach. Power distribution grid overloads can be more than halved and transmission grid overloads almost reduced to zero if market and grid oriented approaches are combined. Due to their flexibility, (pumped)-storage hydropower and natural gas-fired power plants can provide the necessary flexibility to ease and minimise power grid congestion.
- Political decisions might limit or increase both potential solution strategies or challenges. This includes for example the favourable development of single RES or hydrogen concentration levels in natural gas grids. Heavy reliance on a single RES induces higher fluctuations in the power grid. If a federal state relies almost solely on PV to meet its renewable power generation target, excess power at the magnitude of a federal states power demand can be expected. Furthermore, seasonal and daily generation (e.g. winter-summer or day-night) might show stronger fluctuations compared to a more balanced RES expansion. The implementation of e.g. EV and PtH can reduce primary energy consumption by about 20 percent.
- A PtG facility can enable the integration of further PV into a power grid. However, the PtG facility's location must be carefully selected. If it is misplaced, no additional PV integration can be achieved at all. A location close to high potential PV generation is

favourable to achieve a maximum grid relief. Further considerations such as hydrogen feed-in limit and capacity or availability of CO₂ for methanation should be considered additionally to enable the maximum possible grid relief.

- When PtG is implemented into the MES to achieve a power grid relief, the feed-in of hydrogen into natural gas grids causes temporal and spatial GCV fluctuations with a high degree of volatility. Within few hours the gas supplied to a node might change from 100 per cent natural gas to a 50/50 per cent mixture of hydrogen and natural gas. The amount of hydrogen that can be fed into the natural gas grid varies over one year. Due to gas demand for heating in winter, about twice as much hydrogen can be fed into the natural gas transmission grid without violating hydrogen concentration levels compared to summer. It must be ensured that defined hydrogen concentration levels are not exceeded for consumers.
- For electrolysis, achievable FLHs depend on both electrolysis sizing and mode of operation. A smaller electrolysis can achieve more FLHs compared to bigger ones. In our example, a 17.5 MW electrolysis achieves 3008 FLH, whereas an 87.5 MW electrolysis achieves about 20 per cent less FLHs. Suppose the electrolysis is operated based on the RL of substations with high PV generation and low demand only, more FLHs can be achieved compared to the consideration of further additional substations with different characteristics (e.g. high demand, few PV generation). An increasing number of FLHs benefit the economic efficiency, since fixed costs such as electrolysis depreciation can be allocated towards a larger amount of produced hydrogen.
- Assuming a 52,5 MW electrolysis, hydrogen and SNG generation costs range between 12.1 to 16.4 €/Cent/kWh hydrogen or SNG. The generation of hydrogen is favourable over SNG, since fewer auxiliary units are necessary, reducing capital and operational expenditures. However, SNG feed-in enables an increased potential electrolysis sizing, since no hydrogen feed-in limitations have to be considered.

It should be noted that an equal rate of increase of RESs potentials can be handled with minimum grid overloads. However, if at certain locations more RESs potentials are realised or political decisions only allow for certain RESs to be expanded, further measures are necessary. A power grid relief can be achieved via deployment of PtG or combining marked and grid oriented approach. However, if PtG is implemented, further factors such as location, mode of operation, hydrogen feed-in limits and capacities or availability of CO₂ for methanation must be considered.

This doctoral thesis displays potential future challenges arising with an increase of RESs expansion to transform the current energy system towards climate neutrality. It is demonstrated that the consideration of the total multi energy system is highly relevant and

advantageous to cope with potential challenges in the future energy system and to enable a smooth energy transition.

6 BIBLIOGRAPHY

- [1] EUROPEAN COMMISSION (Ed.): *What is the European Green Deal?* Brussels, 12/2019
- [2] EUROPEAN COMMISSION (Ed.): *The European Green Deal*. Brussels, 11.12.2019
- [3] EUROPEAN COMMISSION (Ed.): *Fit for 55 : Delivering the EU's 2030 Climate Target on the way to climate neutrality*. Brussels, 14.7.2021
- [4] BUNDESKANZLERAMT: *Aus Verantwortung für Österreich : Regierungsprogramm 2020 - 2024*. Wien, 2020
- [5] BUNDESMINISTERIUM NACHHALTIGKEIT UND TOURISMUS ; BUNDESMINISTERIUM VERKEHR INNOVATION UND TECHNOLOGIE: *#mission2030 : Die österreichische Klima- und Energiestrategie*. Wien, 2018
- [6] BUNDESMINISTERIUM KLIMASCHUTZ, UMWELT, ENERGIE, MOBILITÄT, INNOVATION UND TECHNOLOGIE: *Energie in Österreich : Zahlen, Daten, Fakten*. Wien, 2021
- [7] STATISTIK AUSTRIA: *Energiebilanzen*. URL http://www.statistik.at/web_de/statistiken/energie_umwelt_innovation_mobilitaet/energie_und_umwelt/energie/energiebilanzen/index.html – Überprüfungsdatum 2021-11-20
- [8] SEJKORA, Christoph ; KÜHBERGER, Lisa ; RADNER, Fabian ; TRATTNER, Alexander ; KIENBERGER, Thomas: *Exergy as Criteria for Efficient Energy Systems—A Spatially Resolved Comparison of the Current Exergy Consumption, the Current Useful Exergy Demand and Renewable Exergy Potential*. In: *Energies* 13 (2020), Nr. 4, S. 843. URL 10.3390/en13040843
- [9] PÖYRY: *Wasserkraftpotenzialstudie Österreich*. 2018
- [10] BRAUNER, Günther: *Energiesysteme: regenerativ und dezentral : Strategien für die Energiewende*. [1. Auflage]. Wiesbaden : Springer Vieweg, 2016
- [11] STANZER, Gregori ; NOVAK, Stefanie ; DUMKE, Hartmut ; PLHA, Stefan ; SCHAFFER, Hannes ; BREINESBERGER, Josef ; KIRTZ, Manfred ; BIERMAYER, Peter ; SPANRING, Christian: *REGIO Energy : Regionale Szenarien erneuerbarer Energiepotentiale in den Jahren 2021/2020*. Wien / St. Pölten, Dezember 2010
- [12] KALTSCHMITT, Martin ; STREICHER, Wolfgang: *Regenerative Energien in Österreich : Grundlagen, Systemtechnik, Umweltaspekte, Kostenanalysen, Potenziale, Nutzung*. 1. Aufl. Wiesbaden : Vieweg + Teubner, 2009 (Praxis)

- [13] ÖSTERREICHISCHE ENERGIEAGENTUR: *Strategische Handlungsoptionen für eine österreichische Gasversorgung ohne Importe aus Russland : Eine Analyse im Auftrag des BMK*. Wien, 2022
- [14] DENHOLM, Paul ; ARENT, Douglas J. ; BALDWIN, Samuel F. ; BILELLO, Daniel E. ; BRINKMAN, Gregory L. ; COCHRAN, Jaquelin M. ; COLE, Wesley J. ; FREW, Bethany ; GEVORGIAN, Vahan ; HEETER, Jenny ; HODGE, Bri-Mathias S. ; KROPOSKI, Benjamin ; MAI, Trieu ; O'MALLEY, Mark J. ; PALMINTIER, Bryan ; STEINBERG, Daniel ; ZHANG, Yingchen: *The challenges of achieving a 100% renewable electricity system in the United States*. In: *Joule* 5 (2021), Nr. 6, S. 1331–1352. URL 10.1016/j.joule.2021.03.028
- [15] KROPOSKI, Benjamin ; JOHNSON, Brian ; ZHANG, Yingchen ; GEVORGIAN, Vahan ; DENHOLM, Paul ; HODGE, Bri-Mathias ; HANNEGAN, Bryan: *Achieving a 100% Renewable Grid: Operating Electric Power Systems with Extremely High Levels of Variable Renewable Energy*. In: *IEEE Power and Energy Magazine* 15 (2017), Nr. 2, S. 61–73. URL 10.1109/MPE.2016.2637122
- [16] TRAINER, Ted: *Some problems in storing renewable energy* 110 (2017), S. 386–393
- [17] HANSEN, Kenneth ; BREYER, Christian ; LUND, Henrik: *Status and perspectives on 100% renewable energy systems*. In: *Energy* 175 (2019), S. 471–480. URL 10.1016/j.energy.2019.03.092
- [18] MANCARELLA, Pierluigi: *MES (multi-energy systems): An overview of concepts and evaluation models*. In: *Energy* 65 (2014), S. 1–17. URL 10.1016/j.energy.2013.10.041
- [19] AUSTRIAN POWER GRID AG: *Austrian Transmission Grid*. URL <https://www.apg.at/en/Power-grid/APG-Netz> – Überprüfungsdatum 2022-01-28
- [20] AUSTRIAN POWER GRID AG: *Netzentwicklungsplan 2020 : für das Übertragungsnetz der Austrian Power Grid AG (APG)*. Wien, 2020
- [21] ENTSO-E (Ed.); VOVK, Andriy (Cont.); POWELL, Dante (Cont.); MEYRUEY, Etienne (Cont.); AREOSA BÄUML, Guillermo (Cont.); BORGHI, Ilyes (Cont.); PAQUEL, Jean-Baptiste (Cont.); DUBOIS, Jérémy (Cont.); MOREIRA, Joao (Cont.); DEHAUDT, Léa (Cont.); LO, Mamadou (Cont.); SAWADOGO, Nestor (Cont.); LABRA FRANCOS, Patricia (Cont.); VRÁBEL, Radek (Cont.) : *Ten-Year Network Development Plan 2020 : Completing the map Power system needs in 2030 and 2040*. Brussels, 2021
- [22] AGGM, GAS CONNECT AUSTRIA, TAG: *Koordinierter Netzentwicklungsplan 2020 : für die Gas-Fernleitungsinfrastruktur in Österreich für den Zeitraum 2021 - 2030*. 2021
- [23] STAPLES, Mark: *Erdgasinfrastruktur - Marktgebiet Ost : Georeferenzierte Darstellung nach Netzebenen*. 3.5. Aufl. Vienna : AGGM - Austrian Gas Grid Management AG, 2021

- [24] STAPLES, Mark: *Erdgasinfrastruktur - Marktgebiet Tirol : Georeferenzierte Darstellung nach Netzebenen*. 1.5. Aufl. Vienna : AGGM - Austrian Gas Grid Management AG, 2021
- [25] STAPLES, Mark: *Erdgasinfrastruktur - Marktgebiet Vorarlberg : Georeferenzierte Darstellung nach Netzebenen*. 1.6. Aufl. Vienna : AGGM - Austrian Gas Grid Management AG, 2021
- [26] GAS CONNECT AUSTRIA GMBH: *Factsheet : Gas Connect Austria - Fit für die Zukunft*. ENERGIE für Österreich und Europa. Wien, 06/2021
- [27] WATINE, Louis: *Ten Year Network Development Plan*. URL <https://entsog.eu/tyndp> – Überprüfungsdatum 2022-05-11
- [28] BUNDESAMT FÜR EICH- UND VERMESSUNGSWESEN: *Katalog Verwaltungsgrenzen (VGD) - Stichtagsdaten 1:50 000* : Bundesamt für Eich- und Vermessungswesen
- [29] GREIML, Matthias ; FRITZ, Florian ; STEINEGGER, Josef ; SCHLÖMICH, Theresa ; WOLF WILLIAMS, Nicholas ; ZAGHI, Negar ; KIENBERGER, Thomas: *Modelling and Simulation/Optimization of Austria's National Multi-Energy System with a High Degree of Spatial and Temporal Resolution*. In: *Energies* 15 (2022), Nr. 10, S. 3581
- [30] AUSTRIAN HEAT MAP: *Fernwärme und Kraft-Wärme-Kopplung in Österreich : Tabellarische Daten*. CSV für Microsoft Excel (ISO-8859-15, Strichpunkt als Trennzeichen). URL <https://austrian-heatmap.gv.at/ergebnisse/>. – Aktualisierungsdatum: 2022-02-15
- [31] BÜCHELE, Richard ; FALLAHNEJAD, Mostafa ; FELBER, Bernhard ; HASANI, Jeton ; KRANZL, Lukas ; THEMEBL, Niko ; HABIGER, Jul ; HUMMEL, Marcus ; MÜLLER, Andreas ; SCHMIDINGER, David: *Potential für eine effiziente Wärme- und Kälteversorgung*. 02.2021
- [32] KLEMM, Christian ; VENNEMANN, Peter: *Modeling and optimization of multi-energy systems in mixed-use districts: A review of existing methods and approaches* 135 (2021), S. 110206
- [33] LUND, Henrik ; ARLER, Finn ; ØSTERGAARD, Poul ; HVELPLUND, Frede ; CONNOLLY, David ; MATHIESEN, Brian ; KARNØE, Peter: *Simulation versus Optimisation: Theoretical Positions in Energy System Modelling*. In: *Energies* 10 (2017), Nr. 7, S. 840
- [34] PIEPER, Martin: *Mathematische Optimierung : Eine Einführung in die kontinuierliche Optimierung mit Beispielen*. Wiesbaden, Heidelberg : Springer Fachmedien Wiesbaden GmbH, 2017 (essentials)
- [35] GOPISETTY, Satya ; TREFFINGER, Peter ; REINDL, Leonhard Michael: *Open-source energy planning tool with easy-to-parameterize components for the conception of polygeneration systems*. In: *Energy* 126 (2017), S. 756–765

- [36] HERC, Luka ; PFEIFER, Antun ; FEIJOO, Felipe ; DUIĆ, Neven: *Energy system transitions pathways with the new H2RES model: A comparison with existing planning tool*. In: *e-Prime - Advances in Electrical Engineering, Electronics and Energy 1* (2021), S. 100024. URL <https://www.sciencedirect.com/science/article/pii/S2772671121000231>
- [37] LUND, Henrik ; THELLUFSEN, Jakob Zinck ; ØSTERGAARD, Poul Alberg ; SORKNÆS, Peter ; SKOV, Iva Ridjan ; MATHIESEN, Brian Vad: *EnergyPLAN – Advanced analysis of smart energy systems*. In: *Smart Energy 1* (2021), S. 100007
- [38] LUND, Henrik ; THELLUFSEN, Jakob Zinck: *EnergyPLAN - Advanced Energy Systems Analysis Computer Model*. 2020
- [39] KRZEMIEŃ, Joanna: *Application of Markal Model Generator in Optimizing Energy Systems*. In: *Journal of Sustainable Mining 12* (2013), Nr. 2, S. 35–39
- [40] NIET, T. ; SHIVAKUMAR, A. ; GARDUMI, F. ; USHER, W. ; WILLIAMS, E. ; HOWELLS, M.: *Developing a community of practice around an open source energy modelling tool*. In: *Energy Strategy Reviews 35* (2021), S. 100650
- [41] EUROPEAN COMMISSION. JOINT RESEARCH CENTRE.; QUOILIN, Sylvain (Cont.); HIDALGO, Ignacio (Cont.); ZUCKER, Andreas (Cont.) : *Modelling future EU power systems under high shares of renewables: the Dispa SET 2.1 open source model* : Publications Office, 2017
- [42] FERRARI, Simone ; ZAGARELLA, Federica ; CAPUTO, Paola ; BONOMOLO, Marina: *Assessment of tools for urban energy planning*. In: *Energy 176* (2019), S. 544–551
- [43] CHEN, Zexing ; ZHANG, Yongjun ; TANG, Wenhui ; LIN, Xiaoming ; LI, Qifeng: *Generic modelling and optimal day-ahead dispatch of micro-energy system considering the price-based integrated demand response*. In: *Energy 176* (2019), S. 171–183
- [44] MOHAMMADI, Mohammad ; NOOROLLAHI, Younes ; MOHAMMADI-IVATLOO, Behnam ; YOUSEFI, Hossein: *Energy hub: From a model to a concept – A review*. In: *Renewable and Sustainable Energy Reviews 80* (2017), S. 1512–1527
- [45] GEIDL, Martin: *Integrated Modeling and Optimization of Multi-Carrier Energy Systems*. ETH Zurich. 2007
- [46] NOZARI, Mohammad Hossein ; YAGHOUBI, Mahmoud ; JAFARPUR, Khosrow ; MANSOORI, G. Ali: *Development of dynamic energy storage hub concept: A comprehensive literature review of multi storage systems*. In: *Journal of Energy Storage 48* (2022), S. 103972
- [47] BOTTECCHIA, Luigi ; LUBELLO, Pietro ; ZAMBELLI, Pietro ; CARCASI, Carlo ; KRANZL, Lukas: *The Potential of Simulating Energy Systems: The Multi Energy Systems Simulator Model*. In: *Energies 14* (2021), Nr. 18, S. 5724

- [48] HILPERT, Simon ; GÜNTHER, Stephan ; KALDEMEYER, Cord ; KRIEN, Uwe ; PLESSMANN, Guido ; WIESE, Frauke ; WINGENBACH, Clemens: *Addressing Energy System Modelling Challenges: The Contribution of the Open Energy Modelling Framework (oemof)*, 2017
- [49] BÖCKL, Benjamin ; GREIML, Matthias ; LEITNER, Lukas ; PICHLER, Patrick ; KRIECHBAUM, Lukas ; KIENBERGER, Thomas: *HyFlow—A Hybrid Load Flow-Modelling Framework to Evaluate the Effects of Energy Storage and Sector Coupling on the Electrical Load Flows*. In: *Energies* 12 (2019), Nr. 5, S. 956
- [50] KRIECHBAUM, Lukas ; SCHEIBER, Gerhild ; KIENBERGER, Thomas: *Grid-based multi-energy systems—modelling, assessment, open source modelling frameworks and challenges*. In: *Energy, Sustainability and Society* 8 (2018), Nr. 1
- [51] PFENNINGER, Stefan ; HAWKES, Adam ; KEIRSTEAD, James: *Energy systems modeling for twenty-first century energy challenges*. In: *Renewable and Sustainable Energy Reviews* 33 (2014), S. 74–86
- [52] JOHANNES DORFNER ; KONRAD SCHÖNLEBER ; MAGDALENA DORFNER ; SONERCANDAS ; FROEHLIE ; SMUELLR ; DOGAUZREK ; WYAUDI ; LEONHARD-B ; LODERSKY ; YUNUSOZSAHIN ; ADEELSID ; THOMAS ZIPPERLE ; SIMON HERZOG ; KAIS-SIALA ; OKAN AKCA: *tum-ens/urbs: urbs v1.0.1* : Zenodo, 2019
- [53] LOHMEIER, Daniel ; CRONBACH, Dennis ; DRAUZ, Simon Ruben ; BRAUN, Martin ; KNEISKE, Tanja Manuela: *Pandapipes: An Open-Source Piping Grid Calculation Package for Multi-Energy Grid Simulations*. In: *Sustainability* 12 (2020), Nr. 23, S. 9899
- [54] THURNER, Leon ; SCHEIDLER, Alexander ; SCHAFER, Florian ; MENKE, Jan-Hendrik ; DOLLICHON, Julian ; MEIER, Friederike ; MEINECKE, Steffen ; BRAUN, Martin: *Pandapower—An Open-Source Python Tool for Convenient Modeling, Analysis, and Optimization of Electric Power Systems*. In: *IEEE Transactions on Power Systems* 33 (2018), Nr. 6, S. 6510–6521
- [55] PAMBOUR, Kwabena Addo ; ÇAKIR ERDENER, Burcin ; BOLADO-LAVIN, Ricardo ; DIKEMA, Gerard P.J.: *SANt – A novel quasi-dynamic model for assessing security of supply in coupled gas and electricity transmission networks*. In: *Applied Energy* 203 (2017), S. 829–857
- [56] HECKEL, Jan-Peter ; BECKER, Christian: *Advanced Modeling of Electric Components in Integrated Energy Systems with the TransiEnt Library*. In: *Proceedings of the 13th International Modelica Conference, Regensburg, Germany, March 4–6, 2019* : Linköping University Electronic Press, 2019 (Linköping Electronic Conference Proceedings), S. 759–768
- [57] BUSSAR, C. ; STÖCKER, P. ; MORAES, L. ; JACQUÉ, Kevin ; AXELSEN, Hendrik ; SAUER, D. U.: *The Long-Term Power System Evolution – First Optimisation Results*. In: *Energy Procedia* 135 (2017), S. 347–357

- [58] KOTZUR, Leander ; NOLTING, Lars ; HOFFMANN, Maximilian ; GROß, Theresa ; SMOLENKO, Andreas ; PRIESMANN, Jan ; BÜSING, Henrik ; BEER, Robin ; KULLMANN, Felix ; SINGH, Bismark ; PRAKTIKNJO, Aaron ; STOLTEN, Detlef ; ROBINIUS, Martin: *A modeler's guide to handle complexity in energy systems optimization*. In: *Advances in Applied Energy* 4 (2021), S. 100063
- [59] PFENNINGER, Stefan: *Dealing with multiple decades of hourly wind and PV time series in energy models: A comparison of methods to reduce time resolution and the planning implications of inter-annual variability*. In: *Applied Energy* 197 (2017), S. 1–13
- [60] LOMBARDI, Francesco ; PICKERING, Bryn ; COLOMBO, Emanuela ; PFENNINGER, Stefan: *Policy Decision Support for Renewables Deployment through Spatially Explicit Practically Optimal Alternatives*. In: *Joule* 4 (2020), Nr. 10, S. 2185–2207
- [61] TRÖNDLE, Tim ; LILLIESTAM, Johan ; MARELLI, Stefano ; PFENNINGER, Stefan: *Trade-Offs between Geographic Scale, Cost, and Infrastructure Requirements for Fully Renewable Electricity in Europe*. In: *Joule* 4 (2020), Nr. 9, S. 1929–1948
- [62] RÜDIGER, Jens: *Enhancements of the numerical simulation algorithm for natural gas networks based on node potential analysis*. In: *IFAC-PapersOnLine* 53 (2020), Nr. 2, S. 13119–13124
- [63] SEJKORA, Christoph ; KÜHBERGER, Lisa ; RADNER, Fabian ; TRATTNER, Alexander ; KIENBERGER, Thomas: *Exergy as criteria for efficient energy systems – Maximising energy efficiency from resource to energy service, an Austrian case study*. In: *Energy* 239 (2022), S. 122173
- [64] WAGNER & ELBLING GMBH: *ONE100 : Österreichs nachhaltiges Energiesystem - 100% dekarbonisiert*. Wien, 2021
- [65] GREIML, Matthias ; FRITZ, Florian ; KIENBERGER, Thomas: *Increasing installable photovoltaic power by implementing power-to-gas as electricity grid relief – A techno-economic assessment*. In: *Energy* 235 (2021), S. 121307
- [66] KIENBERGER, Thomas ; TRAUPMANN, Anna ; SEJKORA, Christoph ; KRIECHBAUM, Lukas ; GREIML, Matthias ; BÖCKL, Benjamin: *Modelling, designing and operation of grid-based multi-energy systems*. 7-24 Pages / *International Journal of Sustainable Energy Planning and Management*, Vol. 29 (2020) (2020)
- [67] GREIML, Matthias ; WOLF WILLIAMS, Nicolas ; KIENBERGER, Thomas: *Timely resolved natural gas grid simulation considering hydrogen feed-in from volatile renewable energy sources*. In: *Institut für Elektrizitätswirtschaft und Energieinnovation (Hrsg.): EnInnov*

2022 : 17. *Symposium Energieinnovation*. Graz : Institut für Elektrizitätswirtschaft und Energieinnovation, 2022

- [68] ZIMMERMAN, Ray Daniel ; MURILLO-SANCHEZ, Carlos Edmundo ; THOMAS, Robert John:
MATPOWER: Steady-State Operations, Planning, and Analysis Tools for Power Systems Research and Education. In: *IEEE Transactions on Power Systems* 26 (2011), Nr. 1, S. 12–19

APPENDIX A: PEER-REVIEWED SCIENTIFIC PUBLICATIONS

First Journal Article

Greiml, Matthias ; Traupmann, Anna ; Sejkora, Christoph ; Kriechbaum, Lukas ; Böckl, Benjamin ; Pichler, Patrick ; Kienberger, Thomas : *Modelling, designing and operation of grid-based multi-energy systems*. 7-24 Pages / International Journal of Sustainable Energy Planning and Management, Vol. 29 (2020)

DOI: 10.5278/ijsepm.3598

Published on: 28th of September 2020

Table A 1: Author statement to the first journal article.

Activity	Contributing authors
Conceptualisation	Greiml M., Kienberger T.
Methodology	Greiml M., Böckl B., Traupmann A., Sejkora C., Kriechbaum L.
Data curation	Greiml M.
Software development and validation	Greiml M., Böckl B., Pichler P.
Modelling	Pichler P., Greiml M.
Investigation and analysis	Greiml M., Pichler P., Kienberger T.
Visualization	Greiml M.
Writing (original draft)	Greiml M.
Writing (review and editing)	Greiml M., Kienberger T.

Second Journal Article

Greiml, Matthias ; Fritz, Florian ; Kienberger, Thomas: Increasing installable photovoltaic power by implementing power-to-gas as electricity grid relief - A techno-economic assessment. In: Energy 235 (2021), S. 121307

DOI: 10.1016/j.energy.2021.121307

Published on: 22nd of Juni 2021

Table A 2: Author statement to the second journal article.

Activity	Contributing authors
Conceptualisation	Greiml M., Kienberger T.
Methodology	Greiml M., Fritz F.
Data curation	Greiml M., Fritz F.
Software development and validation	Greiml M., Fritz F.
Modelling	Greiml M., Fritz F.
Investigation and analysis	Greiml M., Fritz F., Kienberger T.
Visualization	Greiml M.
Writing (original draft)	Greiml M.
Writing (review and editing)	Greiml M., Kienberger T.

Third Journal Article

Greiml, Matthias ; Fritz, Florian ; Steinegger, Josef ; Schlömicher, Theresa ; Wolf Williams, Nicholas ; Zaghi, Negar ; Kienberger, Thomas: Modelling and Simulation/Optimization of Austria's National Multi-Energy System with a High Degree of Spatial and Temporal Resolution. In: Energies 15 (2022), Nr. 10, S. 3581

DOI: doi.org/10.3390/en15103581

Published on: 13th of May 2022

Table A 3: Author statement to the third journal article.

Activity	Contributing authors
Conceptualisation	Greiml M., Kienberger T.
Methodology	Greiml M., Steinegger J, Wolf Williams N., Zaghi N..
Data curation	Greiml M., Steinegger J., Schlömicher T., Wolf Williams N.
Software development and validation	Greiml M., Fritz F., Steinegger J., Zaghi N., Wolf Williams N
Modelling	Greiml M., Steinegger J., Wolf Williams N., Schlömicher T.
Investigation and analysis	Greiml M., Wolf Williams N., Kienberger T.
Visualization	Greiml M., Wolf Williams N.
Writing (original draft)	Greiml M.
Writing (review and editing)	Greiml M., Wolf Williams N, Kienberger T.

APPENDIX B: FURTHER SCIENTIFIC PUBLICATIONS

Co-Authorship in Publications

Böckl, Benjamin ; Greiml, Matthias ; Leitner, Lukas ; Pichler, Patrick ; Kriechbaum, Lukas ; Kienberger, Thomas : *HyFlow-A Hybrid Load Flow-Modelling Framework to Evaluate the Effects of Energy Storage and Sector Coupling on the Electrical Load Flows*. In: *Energies* 12 (2019), Nr. 5, P. 956

DOI: 10.1016/j.energy.2021.121307

Traupmann, Anna ; Greiml, Matthias ; Kienberger, Thomas: Reduction method for planning cross-energy carrier networks in the cellular approach applicable for stability assessment in low-voltage networks. In: *e & i Elektrotechnik und Informationstechnik* 137 (2020), Nr. 8, P. 509-514

DOI: 10.1007/s00502-020-00851-4

Traupmann, Anna ; Greiml, Matthias ; Kienberger, Thomas: Equivalent cellular-based electrical network models for voltage regulation using hybrid conversion technologies at the medium-voltage level. In: *CIREN 2021 - The 26th International Conference and Exhibition on Electricity Distribution : Institution of Engineering and Technology, 2021*, P. 1874-1878

DOI: 10.1049/icp.2021.2014

Kienberger, Thomas ; Greiml, Matthias ; Braunstein, René.: Is Power to Hydrogen an appropriate approach to mitigate PV-induced strain on 110 kV high-voltage grids? In: *CIREN 2021 - The 26th International Conference and Exhibition on Electricity Distribution : Institution of Engineering and Technology, 2021*, S. 2512-2517

DOI: 10.1049/icp.2021.2089

Braunstein, René ; Greiml, Matthias ; Fritz, Florian ; Wisiak, Johannes ; Pachernegg, Manfred ; Streppl, Franz ; Kienberger, Thomas: Sektorenkopplung als Alternative zur 110-kV-Netzverstärkung am Beispiel der Region Oststeiermark. In: *e & i Elektrotechnik und Informationstechnik* 138 (2021), Nr. 8, S. 636–638

DOI: <https://doi.org/10.1007/s00502-021-00956-4>

Steinegger, Josef ; Greiml, Matthias ; Kienberger, Thomas: A New Quasi-Dynamic Load Flow Calculation for District Heating Networks. In: Energy (2022) – At the time of the doctoral thesis writing under submission.

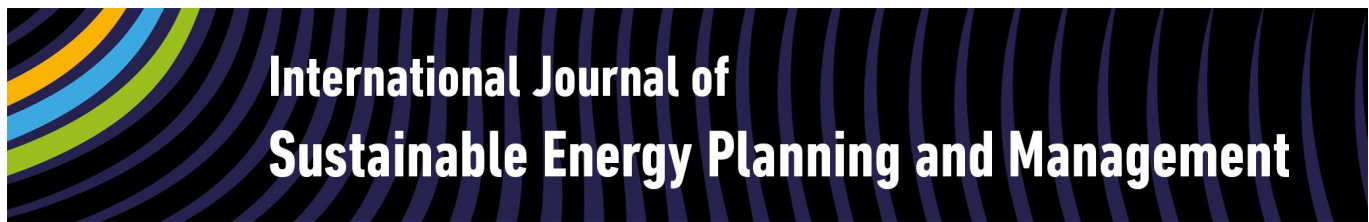
Traupmann, Anna ; Greiml, Matthias ; Steinegger, Josef ; Kühberger, Lisa ; Kienberger, Thomas: Impact of Sector Coupling Technologies as Re-purposing Options of Coal-Fired Power Plant Sites on the Austrian Grids - A MES Approach. In: Sustainable Energy Technologies and Assessments (2022) – At the time of the doctoral thesis writing under submission.

Conference Contributions

Greiml, Matthias ; Böckl, Benjamin ; Traupmann, Anna ; Kienberger, Thomas: HyFlow - A Modelling and Simulation Tool for Hybrid Grids. In: 14th Conference on Sustainable Development of Energy, Water and Environment Systems : Book of Abstracts. Zagreb : Faculty of Mechanical Engineering and Naval Architecture, 2019, P. 372

Greiml, Matthias; Fritz, Florian; Kienberger, Thomas : Assessing usage of power-to-gas as an alternative to electricity grid expansion to increase photovoltaic generation in south-east Austria. In: Lund, Henrik; Mathiesen, Brian Vad; Østergaard, Poul Alberg; Brodersen, Hans Jørgen (Pub.): Book of Abstracts: 6th International Conference on Smart Energy Systems, 2020, P. 112

Greiml, Matthias ; Wolf Williams, Nicolas ; Kienberger, Thomas: Timely resolved natural gas grid simulation considering hydrogen feed-in from volatile renewable energy sources. In: Institut für Elektrizitätswirtschaft und Energieinnovation (Pub.): EnInnov 2022 : 17. Symposium Energieinnovation. Graz : Institut für Elektrizitätswirtschaft und Energieinnovation, 2022



Modelling and model assessment of grid based Multi-Energy Systems

Matthias Greiml*, Anna Traupmann, Christoph Sejkora, Lukas Kriechbaum, Benjamin Böckl, Patrick Pichler, Thomas Kienberger

Chair of Energy Network Technology, Montanuniversity of Leoben, Franz Josef Straße 18, 8700 Leoben, Austria

ABSTRACT

Strategies to decarbonise energy sectors by substituting fossil fuels with renewable energy sources (RES) pose challenges for today's energy system. RES are mainly decentralised, not always predictable and introduce a high degree of volatility into energy grids. To cope with this challenges, flexible multi-energy-systems (MES) may be beneficial. To assess impacts of high degree of RES on energy grids and derive suitable countermeasures, simulation tools are necessary. In this article we propose a modelling framework suitable to perform a detailed technical assessment of MES. This framework (HyFlow) allows for MES simulation and includes depiction of spatial area and simplification of electricity grids without neglecting its properties. Additionally, we demonstrate the application of HyFlow to assess the impacts of the Austrian energy strategy #mission2030 on the energy grids of an Austrian federal state. We present and analyse two scenarios with various degrees of future generation and demand developments, including sector-coupling technologies, energy storages and electric vehicles. Both scenarios demonstrate that a high degree of renewable electricity generation can be realised with few improvements of the current energy infrastructure. Hybrid technologies such as heat pumps and power-to-gas turned out to be crucial in terms of both, energy efficiency as well as flexibility.

Keywords

Multi-energy-system modelling and simulation;
Energy systems;
Renewable energy integration;
Load flow calculation;

URL: <https://doi.org/10.5278/ijsepm.3598>

1. Introduction

In order to meet the binding goals agreed to at the COP 21 in Paris, two major strategies should be implemented: substituting fossil fuels with RES and increasing system efficiency [1]. These strategies present challenges for current energy systems and their operators, since RES are mainly decentralised, not always predictable, and introduce volatility into grids. Therefore, energy systems must be effectively designed and operated to provide temporal and spatial flexibility. MES, which incorporate multiple energy sectors, allow additional flexibility to be used across energy carriers and thus further increase system flexibility. Moreover, these MES can improve overall energy efficiency and allow for seasonal storage of different energy carriers [2].

In general, energy system models which may determine optimal system design- and operation strategies,

are tools for suggesting appropriate energy system improvement measures to grid operators or political decision makers [3]. There already exist a number of widely used modelling tools for representing energy grids and infrastructure, but they only consider single-energy carrier networks. However, comprehensive modelling frameworks for MES, which link single-energy networks by using coupling technologies, are to the best of our knowledge not yet available [4], but may further advance the transition to RES.

Making reliable statements with regard to holistic approaches for integrating RES in future energy systems and grid infrastructure requires adequate consideration of network interactions and dependencies by using complex models. [5, 6] In the context of effectively designing and operating grid-based MES, modelling frameworks must take into account multiple aspects of energy

*Corresponding author - e-mail: matthias.greiml@unileoben.ac.at

Abbreviations

BEV	Battery electric vehicle;
DRE	Degree of renewable expansion;
DSS	Degree of self-sufficiency;
ELO	Electricity line overload;
GtPH	Gas-to-power-and-heat;
GtH	Gas-to-heat;
KPI	Key performance indicator
LP	Linear programming;
MES	Multi-energy-system;
MI(N)LP	Mixed-integer-(non)-linear-programming;
PHEV	Plug-in hybrid vehicle;
PtG(H)	Power-to-gas(-and-heat);
PtH	Power-to-heat;
RES	Renewable energy sources;

systems modelling. This includes energy network infrastructures across different energy carriers and flexibility options like storage facilities. Three aspects are relevant for characterizing them:

Firstly (1), the degree of detail determines the model accuracy. A decreased degree of detail reduces model complexity and hence, computational effort. The accuracy specifies how well the original behaviour of the system is preserved. In this work, the cellular approach addresses the issues of detail as a method that supports spatial resolution reduction and thus simplifies physical properties of energy grids. The second aspect (2) is the definition and consideration of boundary conditions which represent all assumptions as well as technical details for all relevant units within the system [1]. Finally, (3), the operation scheduling for flexible system units and utilities must be addressed. This can be done either by mathematical optimisation methods like linear programming or by heuristic approach, considering specific operation algorithms.

As shown in Figure 1, the development of the modelling objective directly influences a model's level of detail (1). In turn, this affects the overall system design (2) and consequently the way the system is operated (3) [4].

2. Motivation

Substituting fossil fuels with RES brings major changes into our energy systems, since RES, firstly introduce high volatility into the grid and, secondly, are spatially spread. This is shown on the example of Austria in Figure 2: Most of Austria's RES potentials are highly volatile solar- and wind-power or moderately volatile hydro-power. The only RES that can be deployed demand-orientated is biomass. This leads to power surpluses – so called negative residual-load (Eq. (1)) during the summer months, mainly occurring in the electrical grid. In contrast, the winter months tend to show temporal shortfalls, while positive residual-loads, according to Eq. (1), occur.

$$P_{Res,i}[t] = P_{Load,i}[t] - P_{Gen,i}[t] \quad (1)$$

Besides their temporal volatility, the Austrian RES-potential is not sufficient to cover the country's primary-energy demand, which accounted to approximately 381 TWh/a [7] in 2017. With RES potentials of around 265 TWh/a [7], a shortfall of around 116 TWh/a [7] is left to be covered. In order to cover this gap, RES imports and/or measures to increase the primary energy efficiency have to be applied in the future.

As we show in Figure 2, besides this general shortfall of RES potentials, there is a strong spatial component as well: Especially the highly industrialised regions of Austria as well as the urban centres are strongly under-supplied in the energy net-balance over a year (indicated in green). Besides the questions related to the RES volatility and the systems energy-efficiency, this leads to

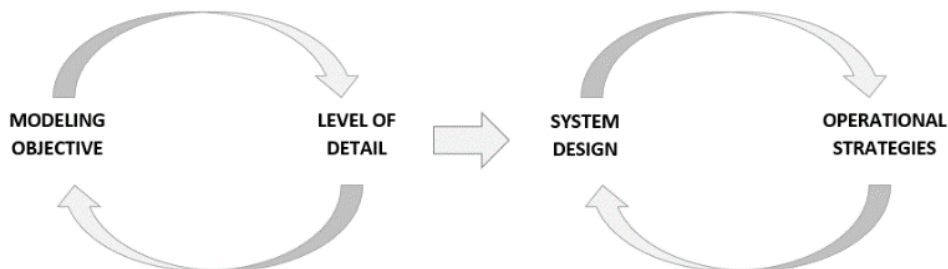


Figure 1: Interactions of the areas in energy system modelling

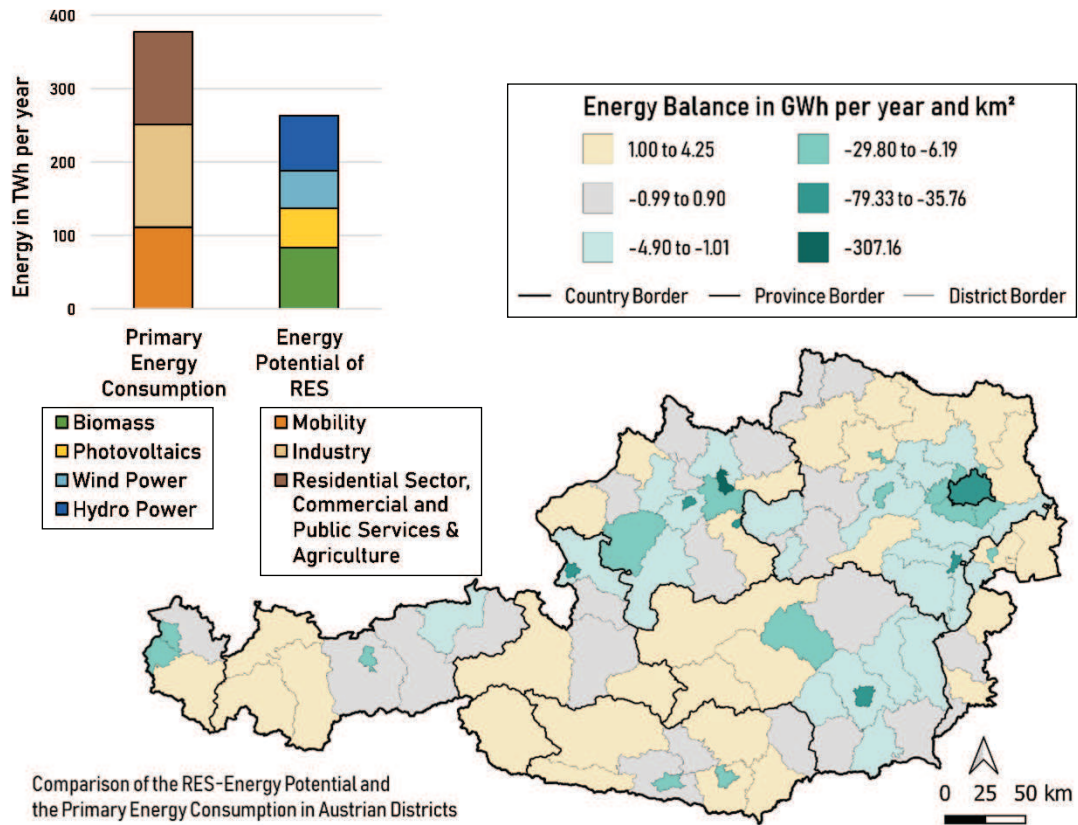


Figure 2: Energy balance in Austrian districts

questions with regard to the energy grids, covering the distances between RES production and demand. Sejkora et al. provide a comprehensive overview on the spatially resolved energy and exergy system of Austria [7].

In order to address the challenges mentioned above, energy system simulations, considering more than one energy carrier, may act as a helpful tool in order to evaluate various solution strategies.

The aim of this work is to show the correlation between the three major aspects of grid based MES as described above. How they are addressed today and how they can be combined in one novel system modelling framework. Further, we show the application and assessment of this modelling framework on a case-study of an Austrian federal state. Therefore, we analyse future impacts of the Austrian Climate and Energy strategy #mission2030, which aims for 100 % renewable electricity production net-balanced over one year, until the year 2030 [8]. We also discuss a solution strategy, in order to enhance the system's primary energy efficiency and to overcome congestions related to the #mission2030 RES expansion.

3. State of research

Current literature in energy system modelling covers distinct perspectives, approaches, and types of models based on different levels of detail. Different types of models (i.e. scenario models, planning models, operating models and optimisations), allow complex energy systems to be considered on several temporal and spatial levels [9]. Either energy-based or power-based perspectives are applied, depending on the type of model. Energy-based perspectives use highly aggregated data such as annual energy demand and supply values, while power-based perspectives calculate models using time-resolved power values [1]. When integrating distributed and volatile RES, it is necessary to ensure the finest possible temporal resolution, since there must be a balance between energy generation and demand at all times [10].

Energy system modelling approaches are either based on one of two principles: top-down or bottom-up, both offering specific advantages as well as limitations [11]. While the top-down-approach pursues macroeconomic

considerations – simplifying and aggregating the energy sector by the underlying economic theory – the bottom-up approach presents a techno-economic view. The bottom-up principle includes technological details which are evaluated using an economically-oriented concept corresponding to the investigated technologies, and therefore requires a comprehensive database [10, 11].

Simulation models and optimisation models are the most commonly applied models using a bottom-up approach. Simulation models are used for describing, explaining and predicting the behaviour of energy systems. Attaining a specific goal, such as optimal unit scheduling or optimal dispatch, requires the application of optimisation models in order to define an optimal set of technology options. This goal should be achieved by minimising operating costs under certain constraints, while at the same time, energy quantity and prices should remain unchanged [11].

The model formulation requires mathematical equations describing the energy system appropriately. Linear programming (LP), mixed-integer linear programming (MILP) and mixed-integer non-linear programming (MINLP) are most commonly used in this context. Almost all optimisation models used in energy system planning are LP models as they are fully linearised. They are therefore easy to use and deliver fast results. For the same reason, they tend to deviate for non-linear conditions [9]. MILP models extend LP models as they offer greater detail in terms of technical properties. MINLP models tend to better approximate the real energy system as they also map non-linear conditions, but they require more calculation time [9, 12].

The models can also be categorised according to their modelling scope. While planning models are used to assess long-term developments of energy-systems, operating models are used to assess the reliability of scenarios in terms of their operating conditions. They differ mainly with regards to the time horizon: planning models must consider long periods of time, whereas operating models range from one day to one year. Additionally, planning models usually use an energy-based-perspective, while operational models use power-based-perspectives [1].

For this work, MES operational models turn out to be relevant. To gain an overview about existing models, we compared listings from various databases [13–15]. Following filter criteria were applied on all previously described MES listings:

- MES must be open source and accessible to enable further development.

- Energy carriers electricity, gas and heat must be included to depict MES.
- MES must be an operational model, that allows scenario based simulations.

Three open-source MES modelling tools Calliope, OEMOF and URBS could be identified meeting the criteria mentioned above. However, they focus on economic tasks such as optimal dispatch based on minimal costs not on technical questions.

Commercial software such as DiGSilent PowerFactory, NEPLAN and PSS Sincal provide highly accurate grid depiction and load flow calculation. However, they don't provide any interconnection between different energy carriers, therefore they are unsuitable for the assessment of MES [16–18].

In comparison to MES planning tools like EnergyPLAN or TIMES, HyFlow aims not to determine an optimised MES. The main motivation for HyFlow is to assess technical infrastructure impacts by scenario based changes of consumer and producer behaviour as well as impacts of sector coupling and storage technologies. Therefore, MES planning tools such as EnergyPLAN or TIMES can be a valuable supplement for HyFlow, providing input data for further detailed technical assessment [19, 20].

To conclude, the literature analysis shows that multiple MES assessment tools are available. However, as shown in Figure 3 existing grid based MES models cannot be used as scenario based operational models, commercial software cannot implement sector-coupling technologies and future MES development assessment tools lag detailed energy grid depiction.

Our self-developed hybrid MES simulation tool HyFlow aims to address before mentioned issues: a scenario based operational model with implementable sector-coupling and storage technologies in combination with detailed energy grid depiction.

4. Methodology

The following section explains the methodology for each relevant part of MES modelling. The first subsection, “Cellular approach – level of detail”, explains the relevance of degree of detail when using the cellular approach which supports spatial-resolution reduction. Based on the cellular approach, network design of energy networks is described in the second subsection “Energy network modelling”. In subchapter three “MES modelling and simulation tool” we describe how we apply before mentioned methodologies in the mentioned grid-based MES modelling framework HyFlow.

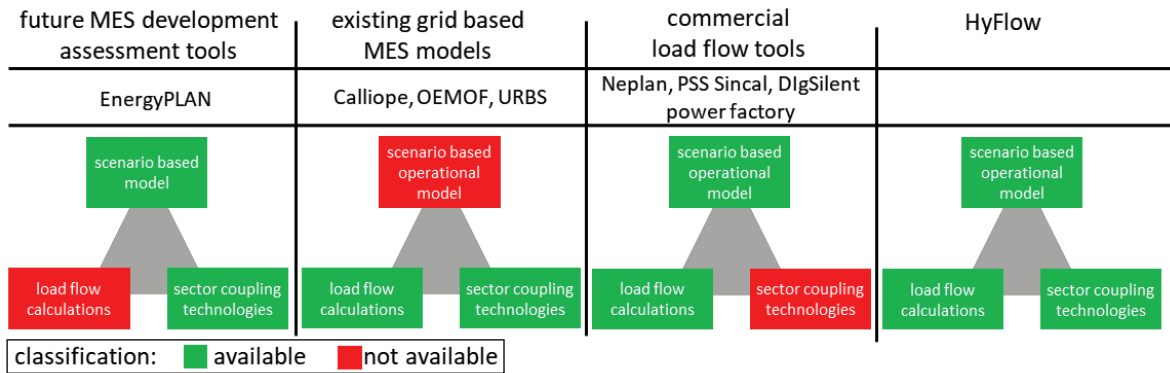


Figure 3: Research gap between commercial software and existing grid-based MES models.

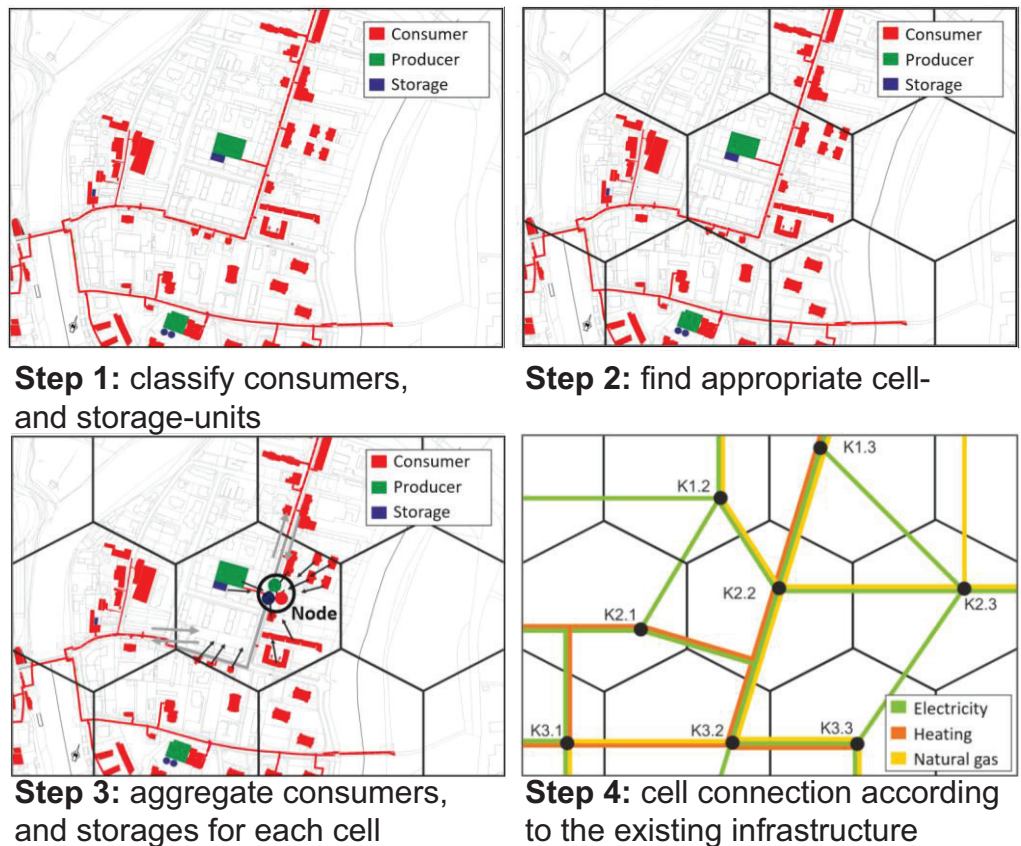


Figure 4: Visualisation of process steps within the cellular approach

4.1 Cellular approach – level of detail

The main objective of this approach is to balance supply and demand at the lowest possible level to prevent high load flows over network connections. The cellular approach also is a means of aggregating users (e.g. consumers, producers and storages) in nodes to reduce computational time. Additionally, aggregating the users within one cell allows for standard load profiles [21] and

synthetic load profiles [22] to be used, even if the data of the modelled region is incomplete.

The cellular approach is designed to be as modular and generic as possible. The process of applying the cellular approach is visualised in Figure 4. All energy consumers, generation and storage units are aggregated to a single node within a defined cell or system boundary. This procedure is followed for each energy carrier.

It is important to choose cells according to the geographical distribution of users, the number of aggregated users, and the grid routes. A more detailed explanation on cell design and recommendations within the cellular approach can be found in [23, 24].

The energy generation $P_{Gen,i}(t)$ and the demand $P_{Load,i}(t)$ for each time-step and each energy carrier are combined in the residual load $P_{Res,i}(t)$ as defined in Eq. (1). The resulting nodes containing the residual loads of each cell are now linked via intercellular connections, if a real grid connection exists between the cells. Importantly, the interconnecting lines are modelled to fit the original grid as accurately as possible. This includes network reduction measures such as appropriate compensation lines instead of multiple lines from one cell to another.

Cells of the same level (e.g. households) can be further aggregated to a superior cell level (e.g. city quarter) in order to allow the spatial flexibility needed. Cells can represent a wide variety of sizes. They may be city quarters as depicted in Figure 4, but may also represent a single household or any other unit. The size of the smallest cell level is important because intracellular load flows within the smallest cell levels are neglected.

4.2 Energy network modelling

Electrical grid: Currently, the greatest challenge when implementing volatile renewables into an energy system, is the lack of transport and storage possibilities within the electrical grid [25]. Therefore, electric networks need to be accurately modelled in order to make reliable statements regarding infrastructural planning of future network structures. When modelling electrical grids, DC- and AC-load flow models are used. While

DC-models are simplified, or rather linearised, by taking into account only active power flows, AC-models also consider reactive power flows. This allows for electrical grid transmission characteristics to be described more precisely [26]. Reactive power is required for building up electromagnetic fields which facilitate energy transmission. Analysing reactive power in electrical networks allows additional network aspects to be assessed. This includes overloads of network elements, voltage stability, network losses, network capacity calculations and determining the grids behaviour in case of failure. Network elements, non-linear loads, fluctuating power consumption and asymmetrical network loadings also introduce reactive power into the grid. Additionally, reactive power conditions within network structures depend on voltage levels and degrees of loading [27].

Modelling reactive power flows in aggregated network models according to the cellular approach is therefore a complex process. Since each cell is represented by a single node, changes in the network structure occur. This requires the implementation of compensation elements. Therefore, we apply serial RLC-elements and adapt with them the changed nodal conditions after aggregation in order to correctly model active and reactive power flows within the connecting lines between cells. This process and the structure of one compensation element are shown in Figure 5.

These serial RLC-elements are parameterised using electrical line parameters of the neglected lines (dotted lines in Figure 5, left) within one cell. Thereby, these elements represent complex electrical impedances allowing variable active and reactive power correction with changing operating states of the network. The active and reactive power produced by them compen-

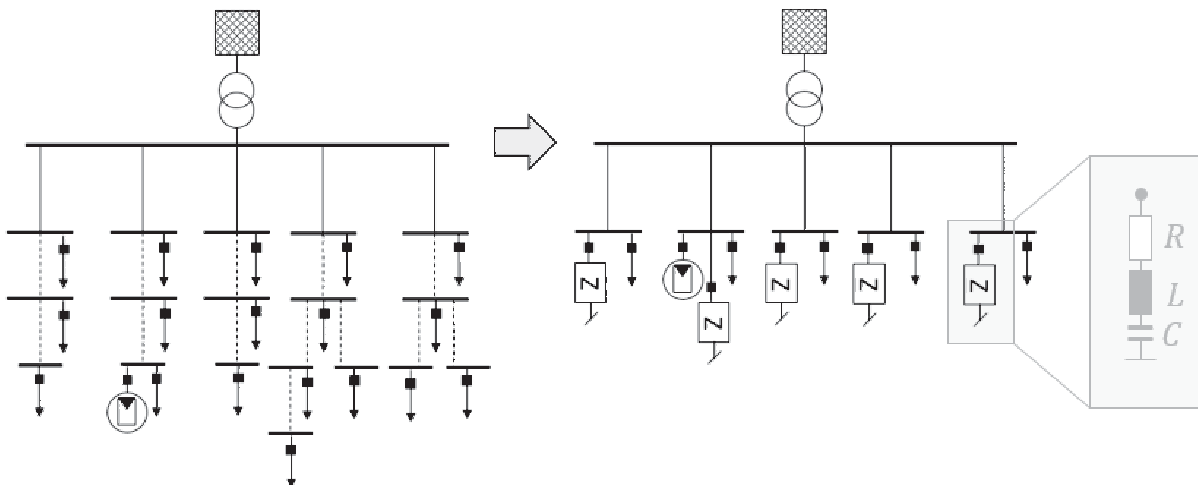


Figure 5: Grid reduction and compensation of losses by means of RLC-elements

sates for the neglected line losses and, therefore, also corrects the overall network losses, the load flow via the slack-node as well as the load flows between the cells. Traupmann et al. [28] give a detailed explanation of grid reduction and compensation procedure.

Pipeline grids – heat and gas grid: Enabling cross energy carrier load flows in MES, mainly for extending storage and transport possibilities available for covering both, positive and negative electrical residual loads, requires an optimised and coordinated use of existing infrastructures. Therefore, pipeline grids for heat and gas also need to be considered using correspondingly created models.

Pipeline network load flow calculations can be used to evaluate various gas- and heat network parameters such as average flow rates V , pressure drops Δp , pressure distributions and temperatures. The mathematical formulation of the load flow equations for pipeline networks is significantly different compared to the electrical grid. The correlation describing the behaviour of pipeline grids shows quadratic dependency according to Darcy’s law - Eq. (4), taking into account the Darcy friction factor λ , the pipe length l and diameter d as well as the fluid density ρ . [29] The following equations Eq. (2) to (4) show similarities between both electrical and pipeline networks:

$$\Delta p \hat{=} \Delta U \tag{2}$$

$$\dot{V} \hat{=} I \tag{3}$$

$$\Delta U = R \cdot I \hat{=} \Delta p \frac{\lambda \cdot l \cdot \rho \cdot 8}{d^5 \cdot \pi^2} \cdot \dot{V}^2 \tag{4}$$

Practical pipeline models use a static approach that solves the quadratic Darcy equation by using linearization methods or non-linear solution methods [30, 31]. Compared to electrical networks, additional input variables are necessary to characterise a pipeline network. For example, input variables such as medium density, medium and ambient temperatures, pipe diameter, length, roughness, and thermal conductivity are considered. In district heating networks heat losses occur. They are decoupled from average flow rates and the corresponding pressure drop. Therefore, they only depend on variable fluid and ambient temperatures [32]. Pressure losses are considered in both heat and gas networks. Heat losses over a pipe section are based on different inlet and calculated outlet temperature which considers pipe parameters such as thermal conductivity, pipe

length and diameter. Boeckl et al. [33] give a detailed explanation of the grid procedure, depicted here briefly.

4.3 MES modelling and simulation

The temporal and spatial challenges, explained in the previous sections, require for tools allowing the consideration of various RES expansion scenarios, the determination of resulting grid constrains, as well as for the design of flexibility options needed for their mitigation. In this work we introduce a MES modelling framework - HyFlow - that addresses these points. In order to allow the consideration of a broad range of energy system case-studies, HyFlow works on three cell levels with a different spatial depth of detail, individually selectable by the user. Level 1 cells can for instance represent low-voltage grid areas and level 2 cells the medium voltage area supplying them. Consequently, in this example level 3 would be the high-voltage grid area, supplying the lower grid-levels. A level 3 cell is also concerned with the energy exchange to the superior energy system. So called slack-nodes allow energy to be transferred between network levels. This concept is shown in Figure 6.

In addition to the network structure of all considered energy carriers, information regarding physical network properties, timely resolved customer demands, timely resolved generation profiles as well as parameters for describing flexibility options like storages and sector-coupling technologies (= hybrid element) must be defined. Demand and generation data are represented by using residual loads according to Eq. (1). Flexibility options are integrated via technology-independent parameters in order to allow the implementation of various technologies, as shown in Table 1.

In HyFlow, for the operation of flexibility options we apply a rule-based approach instead of mathematical optimisation. Thereby we distinguish between cell- and overall system serving operation. The cell serving

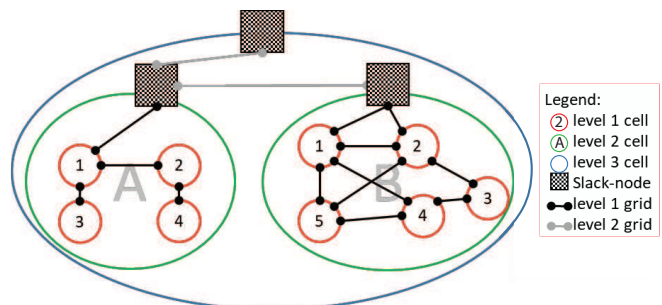


Figure 6: Various network levels in combination with the cellular approach

approach aims to reduce the residual load of the corresponding level 1 cell to a maximum extent. The overall system serving approach aims to reduce the electrical residual load of the highest level being considered (level 3 cell). The electrical residual load is chosen since electricity grids are considered as most critical of congestions. An overview about which hybrid elements are implementable in HyFlow is given in Figure 7. Four main categories (GtPH, PtGH, PtH, GtH) of hybrid elements are shown, each category considering various subtypes of hybrid element technologies.

The computation-steps for considering the interactions between the calculation of multi energy carrier load flows and the operation of cell- and system serving flexibility options, are shown in Figure 8 for one time-

step. Dark arrows indicate the first computation loop, whereas light arrows indicate an additional calculation loop in case system serving hybrid elements are activated.

In the first step, each level 1 cell and its corresponding flexibility options, both, in cell as well as system serving operation mode, are fully used to minimise the residual load of the corresponding level 1 cell. Any energy storage capacity of system serving elements, still available after balancing cell-level 1, is used as described in step 3 and 4 to minimise the system’s residual load.

After energy storages were used to minimise a level 1 cell’s residual load, cell-serving hybrid elements such as PtH, GtPH and GtH are used. The detailed mode of operation for each hybrid element depends on various factors such as storage levels and residual loads. For example, if a PtH hybrid element is to be used, the electrical residual load of the corresponding level 1 cell must be negative (generation), the heat residual load positive (demand) and/or free storage capacity in thermal energy storages available. In this case, the generated electricity would be used to produce heat, and if heat demand is met and there is still electricity left, it would be used to

Table 1: Necessary data for storage and hybrid elements

Storage	Hybrid element
storage capacity	power
charge / discharge power	conversion efficiency for each
charge / discharge efficiency	energy carrier
self-discharge	ramp rate up & down
operation strategy	operation strategy

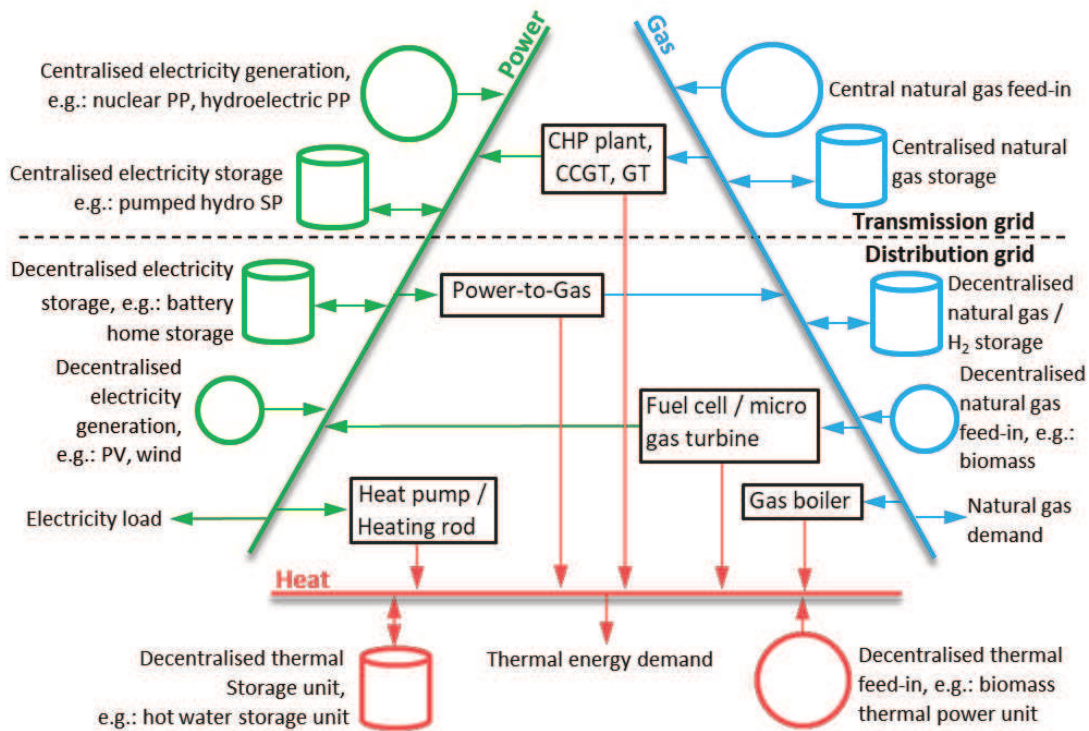


Figure 7: Cross energy carrier and storage flexibility options in HyFlow

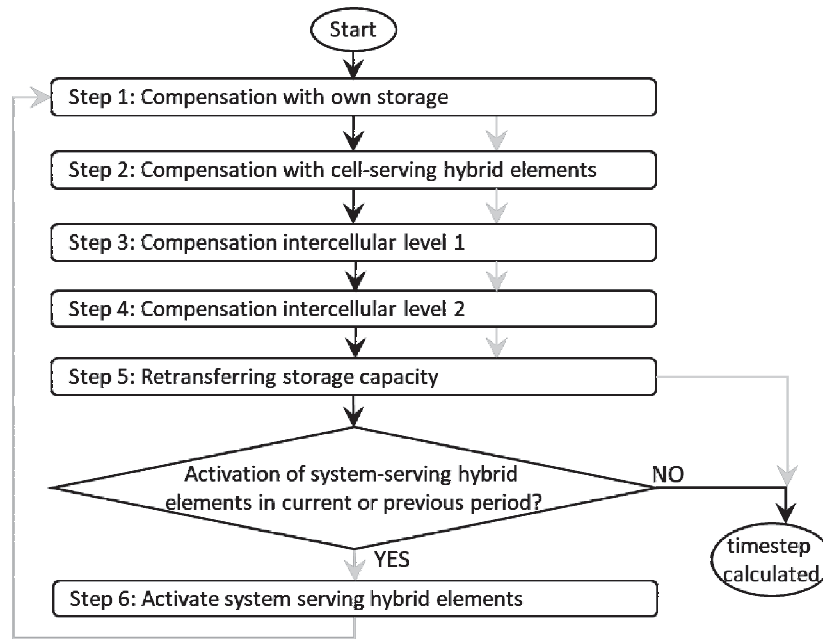


Figure 8: Calculation steps in *HyFlow*

charge the thermal energy storage, if the maximum power of the PtH hybrid element is not exceeded.

In step three, each level 2 cell, with its corresponding and already balanced level 1 cells, is balanced. In Figure 6 two level 2 cells, A and B, and their four respectively five corresponding level 1 cells are displayed. To calculate load flows within each level 2 cell, load flow calculations (see section 4.2) are performed. Leftover capacities from system serving storages located in cell-level 1 are used in order to minimise residual loads of a single level 2 cell by transferring energy to or from energy storages in the corresponding level 1 cells containing the storages. The remaining residual load is balanced via slack node.

Step four is similar to previously described step three. Just as in step three, load flow calculations are carried out in order to calculate load flows between level 2 cells. The remaining residual loads are balanced via slack node, per definition to or from outside the systems boundaries. Since storages are defined in level 1 cells only, virtual storage capacities between level 2 cells are used. The virtual storage capacity of each level 2 cell is the sum of all system serving storage capacities of the corresponding level 1 cells. If any system serving storages were used in step 4, the virtual storages' charging levels change and have to be retransferred to the corresponding level 1 cells of each level 2 cell. This procedure

is carried out in step 5, using an iterative process. However, the iterative process affects the residual loads of level 1 cells, where the system serving storage is physically located. Therefore, load flow calculations, similar to step 3 and 4 have to be executed again, to recalculate load flows and grid losses between both level 1 and level 2 cells.

Afterwards, the need for usage of system serving hybrid elements is evaluated. In case hybrid elements were active in the previous time-step or used in the current time-step, calculation steps one to five have to be repeated (see Figure 8 – grey arrows). The usage of system serving hybrid elements depends on the electricity residual load. In case of a negative electricity residual load, excess power is used within the system by system serving hybrid elements such as PtH and PtGH. If the electricity residual load is positive, additional electricity is generated inside the system. Prerequisite conditions for both cases are the availability of suitable hybrid elements within the system.

As a result, time resolved residual loads for each energy carrier as well as the usage of storages and hybrid elements are displayed for all calculated time-steps. Further information such as line loads, node voltage, pressure or temperature levels as well as information regarding the usage of each energy storage and hybrid element can be assessed.

5. Model assessment on the case-study of an Austrian federal state's MES

In order to demonstrate and assess the capabilities of HyFlow, the effects of the national Austrian climate and energy strategy #mission2030 on federal state level, are examined. With regards to the expansion of RES, the specific energy policy of the considered federal state doesn't allow additional wind power [34–36]. Therefore, hydroelectric, photovoltaic and biomass expansion are the only RES options to be exploited in the future. In Table 2 technical- as well as exploitable renewable electricity potentials for the federal state are displayed.

To take possible development-pathways of the federal state's energy consumption until the year 2030 into consideration, two different scenarios are presented:

Scenario 1 represents the climate and energy policy based scenario, where total energy demand is expected to be stable throughout the year 2030. Renewable electricity potentials are almost exploited up to a degree to meet the expected demand. In comparison to the climate and energy policy scenario a further, more ambitious scenario 2 is presented.

In the second scenario the total energy demand is expected to decline, whereas the renewable technical potentials are fully exploited. Scenario 2 aims to show upcoming challenges from an increase of volatile electricity producers, especially in the federal state's electricity grid. Both scenarios were developed in cooperation with the federal state's regional utility, providing both, energy residual load and grid data. Based on grid data the federal state's energy network is depicted in

96 energy cells, with distinctive residual load characteristics.

5.1 Scenario 1: Climate & Energy Strategy Scenario

In the study "Empowering Austria" from Oesterreichs Energie [41], several studies regarding future energy consumption development in Austria are compared. The final energy demand forecasted for the year 2030 ranges from a decrease of minus 9,5 to plus 1,7 percent, based on the final energy demand of year 2012. For this scenario a conservative approach is selected, therefore the total final energy demand until the year 2030 is expected to be stable. Table 3 shows the expected final energy demand in the year 2030. Considering the trend of further electrification and population growth, an increase in electricity demand and mobility can be expected. In the scenario, those increases are countered with savings in heat and natural gas sector.

To cope with an increasing electricity demand and to fulfil the federal state's energy strategy for 2030, RES have to be expanded up to a level to produce 14.874 GWh of electricity per year [42]. Figure 9 shows the amounts of each renewable source to be expanded until the year 2030. It can be seen that hydropower and biomass potentials have almost been fully exploited today, therefore photovoltaic is the only real option to be expanded.

Scenario 1 is further divided into two cases to examine the influence of technologies such as heat pumps, electric vehicles, home electricity battery storage and a central power-to-gas facility on the federal states energy grids. In the base-case none of the mentioned technolo-

Table 2: Technical and exploitable renewable potential

Source	Production 2017 [GWh]	Technical potential [GWh]	Exploitable potential [GWh]
Hydropower	9.909 [37]	11.158 [37, 38]	10.784 [38]
Biomass	963 [37]	2.470 [39]	1.370 [40]
Wind	90 [37]	812 [39]	90 [37]
Photovoltaic	252 [37]	3.344 [39]	---

Table 3: Demand development in climate & energy strategy scenario

Sector	Final energy demand 2017 [GWh]	Final energy demand 2030 [GWh]
Electricity	14.604 [37]	15.334
Natural gas	14.404 [37]	12.734
Heat	21.259 [37]	20.621
Mobility	17.921 [37]	18.548

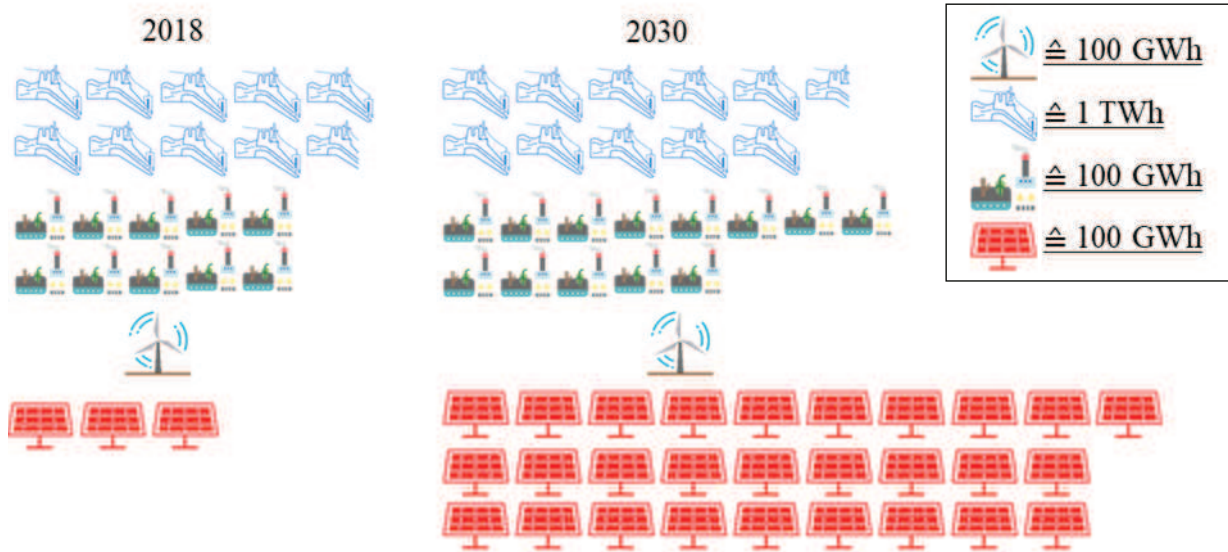


Figure 9: Expansion of renewable generation to fulfil energy strategy goal

gies is implemented. In the advanced case, all technologies mentioned above are implemented. The degree of implementation of each technology follows the assumptions explained in the following:

- We replace natural gas for heating purpose by heat pumps in combination with thermal storages. To determine the spatially resolved consumption of natural gas for heating purpose, the total natural gas consumption is separated in natural gas demand for heating and industrial process demand. The individual heating- and industrial process demand for each cell is calculated considering available consumption data from both, utilities and industrial companies as well as from the study Renewables4Industries [39].
- A study from Pötscher [44] expects all newly registered vehicles in the year 2030 to be a mixture of 70% plug-in and 30% battery electric vehicles (PHEV, BEV). The Austrian Automobile Association ÖAMTC expects the share of newly registered petrol or diesel only powered vehicles to be almost zero in the year 2030. The ramp-up curve of BEV in the ÖAMTC study is almost linear from today's market share until the year 2030, therefore a linear ramp up curve is selected for this work [45]. Based on the trend of past vehicle registration statistics, the annual vehicle registration number is assumed to be stable with 60.000 vehicles per year until the year 2030 [46]. The described statistics and ramp-up curve result

in 130.000 BEV and 302.000 PHEV in the federal state in the year 2030. The charging behaviour of two PHEV is assumed to be like one BEV, therefore a total number of 281.000 electric vehicles is considered in the scenarios with a time resolved arrival characteristic from the project Move2grid [47]. The number of electric vehicles per cell is calculated based on the share of population per cell, compared to the federal state's total population.

- For every household we apply a home electricity battery storage, with a storage capacity of 10 kWh and charge / discharge power of 4,8 kW.
- We implement a central PtG facility in the centre of the federal state with unlimited capacity to convert excess electricity generation into natural gas instead of exporting. The centralised location was selected according to the existing infrastructure of high pressure natural gas as well as the high voltage electricity transmission grid.

5.2 Scenario 2: Ambitious Scenario

This scenario aims to demonstrate the occurring effects if renewables are exploited up to their exploitable potential (see Table 2). This results in a significant increase of volatile renewable electricity generation. The final energy demand in scenario 2 is reduced by 7,5 percent in each sector, compared to scenario 1, resulting in a final energy consumption as shown in Table 4. Scenario 2

is divided in a base- and advanced case, analogously to scenario 1.

6 Results of federal state’s scenarios

In this chapter results from both scenarios are presented, discussed and compared. Additionally, we compare our results with other research in this field.

6.1 Scenario 1: Climate & Energy Strategy Scenario

Figure 10 shows the electricity demand and renewable generation in a summer- and a winter week for scenario 1 in the year 2030. Negative electricity residual loads can appear even during winter months, rising significantly in both, count and excess during summer months. The overproduction of electricity in summer reaches similar levels compared to the electricity demand.

Table 4: Demand development in ambitious scenario

Sector	Final energy 2017 [GWh]	Final energy 2030 [GWh]
Electricity	14.604 [37]	14.239
Natural gas	14.404 [37]	11.728
Heat	21.259 [37]	19.027
Mobility	17.921 [37]	17.204

A comparison of electricity load flows in the federal state’s transmission grid (transmission grid voltage: 110 kV) to or from the superior electricity system grid for the base- and advanced case scenario is displayed in Figure 11 and Figure 12. In the advanced case, far less electricity is exported over the system boundaries, compared to the base case. Instead of being exported, excess electricity is used within the system, feeding battery storages, heat pumps and a central PtG facility. Especially during days with high photovoltaic generation, the PtG facility is able to supply the federal state’s whole natural gas demand. From April until October electricity imports are hardly necessary, compared to winter months with excessive electricity imports.

The federal state’s primary energy demand can be reduced from 37.600 GWh by approximately 15 % in the base case to 32.100 GWh in the advanced case. Electric vehicles and sector-coupling technologies such as PtH and PtG are the main drivers for primary energy savings.

By examining the electricity grid in detail, line-overloads can be analysed. In the base case scenario, the total overload time is 3.500 hours (relative overload time: 0,41 %), whereas in the advanced case, a total overload time of 12.800 hours (relative overload time: 1,49 %) occurs across the federal state’s electricity

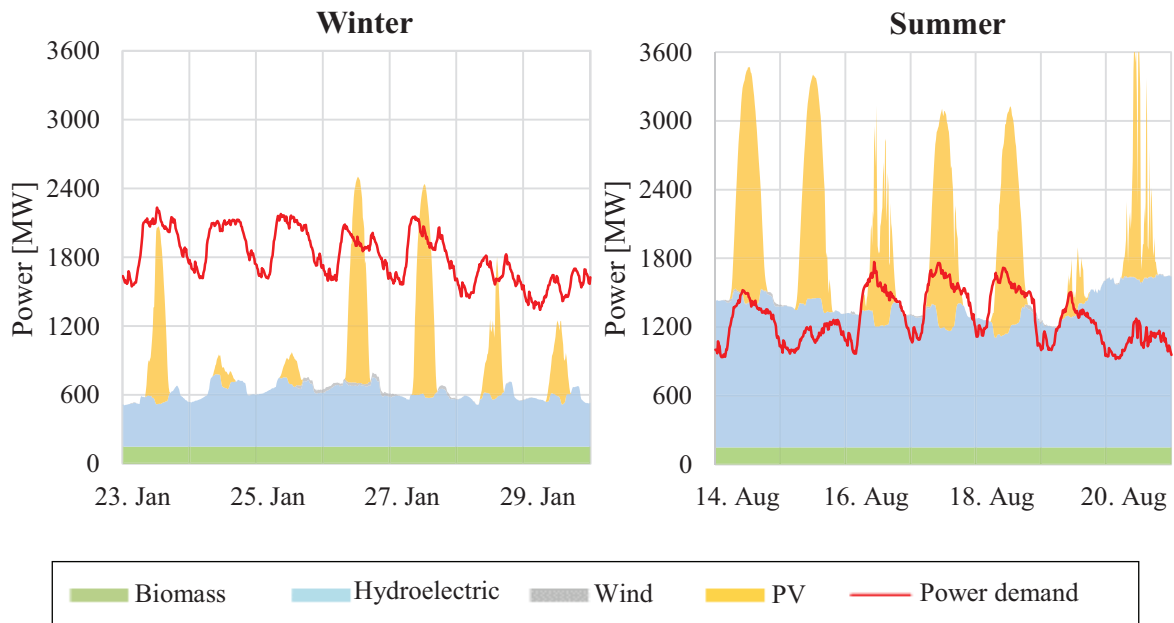


Figure 10: Scenario 1 - Electricity generation and demand in summer and winter

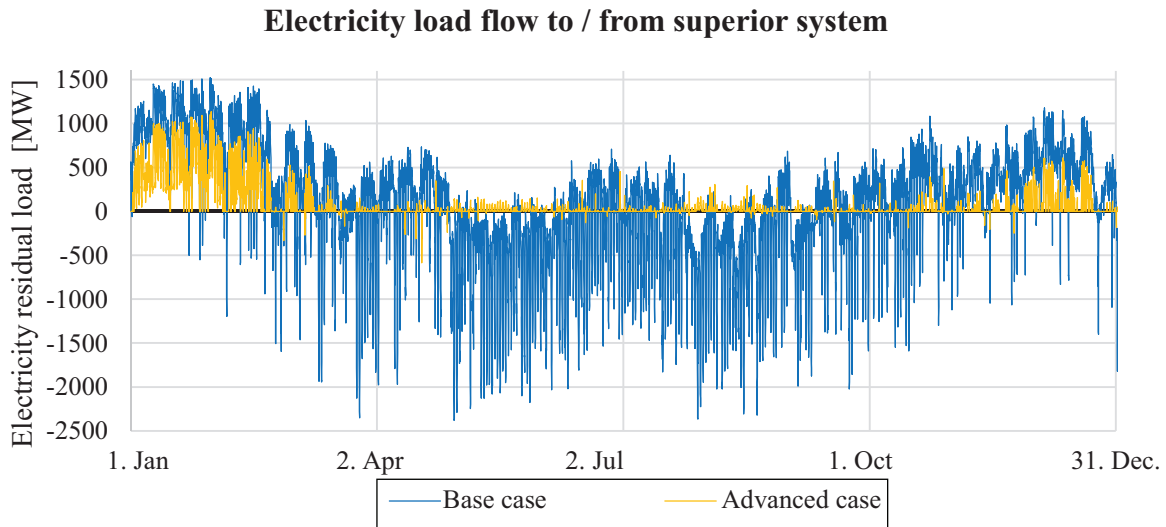


Figure 11: Comparison of electricity load flow in base and advanced case

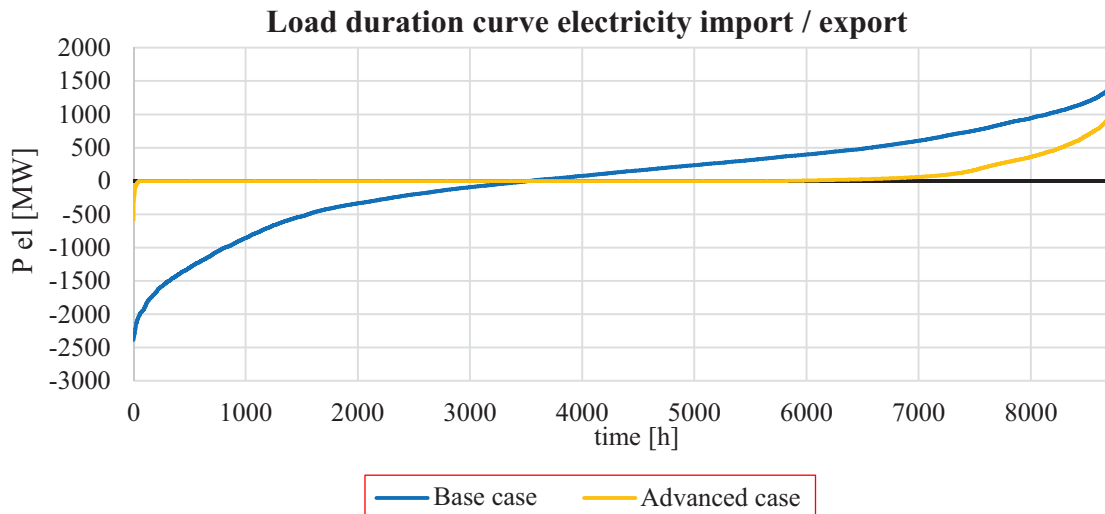


Figure 12: Comparison of load duration in base and advanced case

grid. The electricity grid examination shows that many overloads occur due to operation of the central PtG facility. Since no grid expansion is considered, the number of overload hours can be reduced significantly by expanding certain electricity lines, especially around the central PtG facility or considering several decentralised PtG facilities.

6.2 Scenario 2: Ambitious Scenario

Compared to the previously presented scenario 1, the federal state’s electricity demand decreases slightly, whereas renewable generation increases significantly. This results in even more excess electricity generation,

reaching up to more than twice the federal state’s peak electricity demand, shown in Figure 13.

Due to the higher overproduction of electricity in scenario 2 compared to scenario 1, the central PtG facility converts even more excess electricity into natural gas. The increase in electricity to natural gas conversion leads to occasionally negative residual loads in the federal state’s natural gas grid during summer. Negative natural gas residual loads can be stored temporary in the federal state’s natural gas storages. The amount of natural gas being imported can be reduced by about 25 percent in the base case and 45 percent in the advanced case compared to the year 2017.

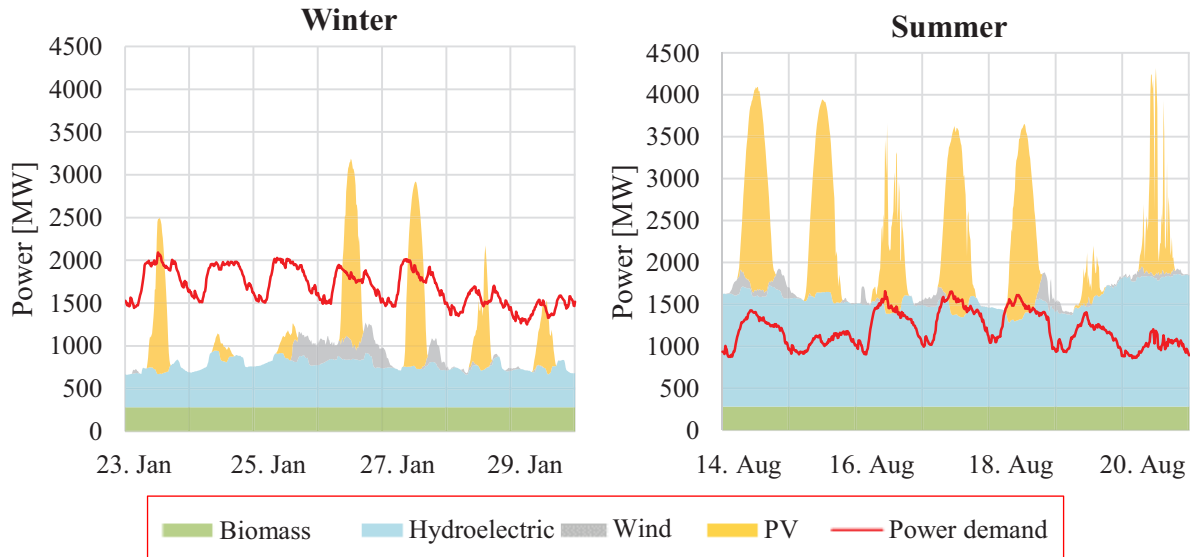


Figure 13: Scenario 2 - Electricity generation and demand in summer and winter

Heat pumps in combination with thermal storages can significantly reduce negative electricity residual loads during winter months. However, heat demand is low during summer months therefore, heat pumps hardly contribute to residual load reduction during summer. The federal state's primary energy demand can be reduced from 35.900 GWh by approximately 18 percent in the base case to 29.400 GWh in the advanced case.

In the base case scenario, the total overload time is 10.696 hours (relative overload time: 1,25 %), whereas in the advanced case a total overload time of 33.496 hours (relative overload time: 3,90 %) occurs across the federal state's electricity grid. Like in scenario 1, no line expansion has been considered and overloads appear mainly in certain grid sections close to the central PtG facility.

6.3 Comparison and discussion of scenarios

The following Table 5 displays key performance indicators (KPI) for both scenarios such as degree of self-sufficiency (DSS), share of RES in the electricity sector, degree of renewable expansion (DRE), relative electricity line overload (ELO) time and primary energy demand.

A high RES penetration correlates positively with DSS, ELO and negatively with primary energy demand. For both scenarios, the advanced case is capable of increasing electricity DSS compared to base case. Comparing relative ELO in each sub scenario a high degree of RES seems unfavourable in terms of relative

ELO. However, a detailed overload analysis has shown that in both advanced cases line overloads occur mainly on a few transmission grid sections around the PtG facility. If these particular grid sections are strengthened the KPI relative ELO can be improved significantly.

6.4 Comparison of results with other research

Kroposki et al. [48] concludes that 100 % renewable grids require significant curtailment of renewables. The scenario simulations on Austrian federal state level presented here clearly show that curtailment of renewable generation can be avoided by strengthening only a few transmission lines.

A PtG deployment scenario review by Eveloy and Gebreegziabher [49] shows that research regarding PtG deployment is mainly attached to excessive renewable energy generation. PtG facilities contribute positively to avoid curtailment of renewable generation, grid stabilization and improvement of energy supply security [49]. Schwarz et al. [50], discuss the positive systematic effects of PtG in energy systems with high degree of renewable penetration.

Our Simulations also show, similar to their results, positive impacts of flexibilities such as PtG on electricity grids.

7 Conclusions

Within this work we discuss general aspects on modelling, designing and operating of MES, coupling the grid

Table 5: Comparison of KPIs for both scenarios

KPI	Scenario 1		Scenario 2	
	Base case	Advanced case	Base case	Advanced case
DSS electricity	58 %	81 %	75 %	93 %
DSS natural gas	0 %	1,1 %	0 %	4,4 %
share of RES		97 %		125 %
DRE		84 %		100 %
Rel. ELO	0,41 %	1,49 %	1,25 %	3,90 %
Primary energy demand	36.600 GWh	32.100 GWh	35.900 GWh	29.400 GWh

bound energy carrier electricity, gas, and heat. Such systems allow for a better integration of volatile renewables and provide the opportunity for an enhanced primary energy efficiency, compared to current energy systems with decoupled energy carriers.

When modelling such MES, beside the volatile behaviour of future generation and demand, also their spatial distribution has to be considered. Therefore, we introduce a cellular approach which facilitates balancing energy production and demand on the lowest cell level being implemented. In order to investigate grid congestions, resulting mainly from RES expansion, exact load flow calculations of all energy carriers have been applied. A measure for mitigating such congestions is the appropriate design- and operation of flexibility options. MES-flexibility options are particularly interesting, since they enable cross energy carrier seasonal storages.

All these mentioned aspects are integrated in our MES modelling framework HyFlow. The framework is a unique MES simulation tool that allows scenario based analysis of future MES with a technical focus on infrastructure and flexibility options. Results from the investigated scenarios can provide decision support, especially for grid operators and political decision makers.

The capabilities of HyFlow are presented on the example of two scenarios. In both we demonstrate, that an expansion of RES can be realised with few improvements of the current energy infrastructure. The implementation of energy storages and MES elements, as for instance PtG, facilitate grid relief. However, the location of flexibility options has to be selected carefully. If misplaced or oversized, flexibility options can benefit overloads at certain grid sections, as both scenarios display. Overloads can be avoided by either strengthening particular grid sections, or several decentralised facilities instead of a central one.

The HyFlow framework can be further improved in areas such as load flow calculation, grid depiction and operational strategies of both storage and hybrid technologies. We continuously aim to improve HyFlow based on feedback from its application in research projects.

Acknowledgement

This paper was prepared for the IJSEPM special issue of the 14th SDEWES conference 2019 in Dubrovnik [51].

This paper belongs to an IJSEPM special issue on *Sustainable Development using Renewable Energy Systems*[51].”

References

- [1] COLLINS, Seán; DEANE, John Paul; PONCELET, Kris; Panos, Evangelos; PIETZCKER, Robert C.; DELARUE, Erik; Ó GALLACHÓIR, Brian Pádraig: *Integrating short term variations of the power system into integrated energy system models: A methodological review*. In: *Renewable and Sustainable Energy Reviews* 76 (2017), S. 839–856. <http://doi.org/10.1016/j.rser.2017.03.090>
- [2] MANCARELLA, Pierluigi: *MES (multi-energy systems): An overview of concepts and evaluation models*. In: *Energy* 65 (2014), S. 1–17. <http://doi.org/10.1016/j.energy.2013.10.041>
- [3] STRACHAN, Neil ; Fais, Birgit ; DALY, Hannah: *Reinventing the energy modelling -policy interface*. In: *Nature Energy* 1 (2016), Nr. 3, S. 16012. <http://doi.org/10.1038/nenergy.2016.12>
- [4] KRIECHBAUM, Lukas; SCHEIBER, Gerhild; KIENBERGER, Thomas: *Grid-based multi-energy systems —modelling, assessment, open source modelling frameworks and challenges*. In: *Energy, Sustainability and Society* 8 (2018), Nr. 1, S. 244. <http://doi.org/10.1186/s13705-018-0176-x>
- [5] LUND, Henrik; ØSTERGAARD, Poul Alberg; CONNOLLY, David; MATHIESEN, Brian Vad: *Smart energy and smart energy systems*.

- In: *Energy* 137 (2017), S. 556–565. <http://doi.org/10.1016/j.energy.2017.05.123>
- [6] LUND, Henrik; ANDERSEN, Anders N.; ØSTERGAARD, Poul Alberg; MATHIESEN, Brian Vad; CONNOLLY, David: *From electricity smart grids to smart energy systems – A market operation based approach and understanding*. In: *Energy* 42 (2012), Nr. 1, S. 96–102. <http://doi.org/10.1016/j.energy.2012.04.003>
- [7] SEJKORA, Christoph; KÜHBERGER, Lisa; RADNER, Fabian; TRATTNER, Alexander; KIENBERGER, Thomas: *Exergy as Criteria for Efficient Energy: Systems A Spatially Resolved Comparison of the Current Exergy Consumption, the Current Useful Exergy Demand and Renewable Exergy Potential*. In: *Energies* 13 (2020), Nr. 4, S. 843. <http://doi.org/10.3390/en13040843>
- [8] FEDERAL MINISTRY FOR SUSTAINABILITY AND TOURISM IN COOPERATION WITH FEDERAL MINISTRY OF TRANSPORT INNOVATION AND TECHNOLOGY (Hrsg.): *#mission2030 Austrian Climate and Energy Strategy*. Vienna, September 2018
- [9] VAN BEECK, N.M.J.P.: *Classification of Energy Models*. Tilburg, 1999 (FEW Research Memorandum Vol. 777). <https://research.tilburguniversity.edu/en/publications/classification-of-energy-models>
- [10] PFENNINGER, Stefan; HAWKES, Adam; KEIRSTEAD, James: *Energy systems modeling for twenty-first century energy challenges*. In: *Renewable and Sustainable Energy Reviews* 33 (2014), S. 74–86. <http://doi.org/10.1016/j.rser.2014.02.003>
- [11] HERBST, Andrea; TORO, Felipe; REITZE, Felix; JOCHEM, Eberhard: *Introduction to Energy Systems Modelling*. In: *Swiss Journal of Economics and Statistics* 148 (2012), Nr. 2, S. 111–135. <http://doi.org/10.1007/BF03399363>
- [12] OMMEN, Torben; MARKUSSEN, Wiebke Brix; ELMEGAARD, Brian: *Comparison of linear, mixed integer and non-linear programming methods in energy system dispatch modelling*. In: *Energy* 74 (2014), S. 109–118. <http://doi.org/10.1016/j.energy.2014.04.023>
- [13] ENERGYPLAN.EU: *Links to Energy System Analysis Models*. <https://www.energyplan.eu/othertools/> – Überprüfungsdatum 2019-12-05
- [14] OPENMOD: *Open Models*. https://wiki.openmod-initiative.org/wiki/Open_Models#List_of_models – Überprüfungsdatum 2019-12-05
- [15] WIKIPEDIA: *Open energy system models*. https://en.wikipedia.org/wiki/Open_energy_system_models. – Aktualisierungsdatum: 2019-11-12 – Überprüfungsdatum 2019-12-05
- [16] DIGSILENT.DE: *DIGSILENT | PowerFactory*. <https://www.digsilent.de/en/powerfactory.html> – Überprüfungsdatum 2019-12-05
- [17] NEPLAN: *NEPLAN | Products*. <https://www.neplan.ch/en-products/> – Überprüfungsdatum 2019-12-05
- [18] SIEMENS.COM: *PSS®SINCAL – simulation software for analysis and planning of all network types*. <https://new.siemens.com/global/en/products/energy/services/transmission-distribution-smart-grid/consulting-and-planning/pss-software/pss-sincal.html> – Überprüfungsdatum 2019-12-05
- [19] LUND, Henrik: *Chapter 4 - Tool: The EnergyPLAN Energy System Analysis Model*. 2014. <http://doi.org/10.1016/B978-0-12-410423-5.00004-3>
- [20] BALK, Olexandr; ANDERSEN, Kristoffer S.; DOCKWEILER, Steffen; GARGIULO, Maurizio; KARLSSON, Kenneth; NÆRAA, Rikke; PETROVIĆ, Stefan; TATTINI, Jacopo; TERMANSEN, Lars B.; VENTURINI, Giada: *TIMES-DK: Technology-rich multi-sectoral optimisation model of the Danish energy system*. In: *Energy Strategy Reviews* 23 (2019), S. 13–22. <http://doi.org/10.1016/j.esr.2018.11.003>
- [21] E-CONTROL: *Sonstige Marktregeln Strom : Kapitel 6: Zählwerte, Datenformate und standardisierte Lastprofile*. Wien, 2012
- [22] BDEW, VKU, GEODE: *Abwicklung von Standardlastprofilen Gas*. Berlin, 30.6.2015. https://www.bdew.de/media/documents/20200331_KoV_XI_LF_SLP_Gas_clean_final.pdf
- [23] BÖCKL, Benjamin; KRIECHBAUM, Lukas; KIENBERGER, Thomas: *Analysemethoden für kommunale Energiesysteme unter Anwendung des zellularen Ansatzes*. In: *Institut für Elektrizitätswirtschaft und Energieinnovation (Hg.) 2016 - 14. Symposium Energieinnovation*.
- [24] KIENBERGER, Thomas; BÖCKL, Benjamin; KRIECHBAUM, Lukas: *Hybrid approaches for municipal future energy-grids*. In:
- [25] HEIMBERGER, Markus; KAUFMANN, Thomas; MAIER, Christoph; NEMEC-BEGLUK, Sabina; WINTER, Alexander; GAWLIK, Wolfgang: *Energieträgerübergreifende Planung und Analyse von Energiesystemen*. In: *e & i Elektrotechnik und Informationstechnik* 134 (2017), Nr. 3, S. 229–237. <http://doi.org/10.1007/s00502-017-0504-4>
- [26] KILE, Hakon; UHLEN, Kjetil; WARLAND, Leif; KJOLLE, Gerd: *A comparison of AC and DC power flow models for contingency and reliability analysis*. In: *2014 Power Systems Computation Conference : IEEE, 2014 - 2014*, S. 1–7. <http://doi.org/10.1109/PSCC.2014.7038459>
- [27] INA - INSTITUT FÜR NETZ- UND ANWENDUNGSTECHNIK GMBH: *Beitrag industrieller Blindleistungs-Kompensationsanlagen und -Verbraucher für ein innovatives Blindleistungs-Management in der Stromversorgung Deutschlands*. 2013. <https://www.b-w.at/upload-bw/Blindkompensation.pdf>
- [28] TRAUHMANN, Anna; KIENBERGER, Thomas: *Modeling of electrical networks in the cellular approach with regard to influencing variables on active and reactive power accuracy at different voltage levels*. In: *2019 54th International Universities Power Engineering Conference (UPEC) : IEEE, 2019 - 2019*, S. 1–6. <http://doi.org/10.1109/UPEC.2019.8893482>

- [29] RÜDIGER, J.: *Gasnetzsimulation durch Potentialanalyse*. Hamburg, Helmut-Schmidt-Universität/ Universität der Bundeswehr Hamburg. Dissertation. 2009
- [30] ALMASSALKHI, Mads; HISKENS, Ian: Cascade mitigation in energy hub networks. In: *2011 50th IEEE Conference on Decision and Control and European Control Conference*, 2011, S. 2181–2188. <http://doi.org/10.1109/CDC.2011.6161484>
- [31] GEIDL, Martin; ANDERSSON, Goran: *Optimal Power Flow of Multiple Energy Carriers*. In: *IEEE Transactions on Power Systems* 22 (2007), Nr. 1, S. 145–155. <http://doi.org/10.1109/TPWRS.2006.888988>
- [32] HAMMER, Andreas; SEJKORA, Christoph; KIENBERGER, Thomas: *Increasing district heating networks efficiency by means of temperature-flexible operation*. In: *Sustainable Energy, Grids and Networks* 16 (2018), S. 393–404. <http://doi.org/10.1016/j.segan.2018.11.001>
- [33] BÖCKL, Benjamin; GREIML, Matthias; LEITNER, Lukas; PICHLER, Patrick; KRIECHBAUM, Lukas; KIENBERGER, Thomas: *HyFlow—A Hybrid Load Flow-Modelling Framework to Evaluate the Effects of Energy Storage and Sector Coupling on the Electrical Load Flows*. In: *Energies* 12 (2019), Nr. 5, S. 2–3. <http://doi.org/10.3390/en12050956>
- [34] LAND OBERÖSTERREICH: *Windkraft - Masterplan 2017 Ausschluss*. Linz, 2017. https://www.land-oberoesterreich.gv.at/Mediendateien/Formulare/Dokumente%20UWD%20Abt_US/us_en_Ausschlusszonen_Windmasterplan2017.pdf
- [35] LAND OBERÖSTERREICH: *Richtlinie Oö. Windkraft-Masterplan 2017 : Kriterienkatalog*. Linz, 2017. https://www.land-oberoesterreich.gv.at/Mediendateien/Formulare/Dokumente%20UWD%20Abt_US/us_en_Windkraftmasterplan_2017_Kriterienkatalog.pdf
- [36] IG WINDKRAFT: *Windkraft-Ausschlusszone Oberösterreich?* 13.2.2017. https://www.igwindkraft.at/?mdoc_id=1034436
- [37] STATISTIK AUSTRIA: *Energiebilanzen*. https://www.statistik.at/web_de/statistiken/energie_umwelt_innovation_mobilitaet/energie_und_umwelt/energie/energiebilanzen/index.html – Überprüfungsdatum 2019-12-06
- [38] RATSCHAN, Clemens ; ZAUNER, Gerald ; SCHEDER, Christian ; GUMPINGER, Clemens ; MIELACH, Carina ; SCHMUTZ, Stefan ; TICHLER, Robert ; SCHWARZ, Markus ; STEINMÜLLER, Horst: *Oö. Wasserkraftpotentialanalyse 2012/13 : Abschätzung und Evaluierung des energetischen Revitalisierungs- und Ausbaupotentials an umweltgerechten Standorten an mittleren und größeren Gewässern in Oberösterreich*. 2015. https://www.land-oberoesterreich.gv.at/files/publikationen/AUWR_Wasserkraftpotentialanalyse.pdf
- [39] MOSER, Simon; GOERS, Sebastian; DE BRUYN, Kathrin; STEINMÜLLER, Horst; HOFMANN, Rene; PANUSCHKA, Sophie; KIENBERGER, Thomas; SEJKORA, Christoph; HAIDER, Markus; WERNER, Andres; BRUNNER, Christoph; FLUCH, Jürgen; GRUBBAUER, Anna: *Renewables4Industry: Abstimmung des Energiebedarfs von industriellen Anlagen und der Energieversorgung aus fluktuierenden Erneuerbaren*. Diskussionspapier (Endberichtsteil 2 von 3). 2018. <http://www.energieinstitut-linz.at/v2/wp-content/uploads/2018/04/Renewables4Industry-Diskussionspapier.pdf>
- [40] LAND OBERÖSTERREICH: *Energiezukunft 2030 : Die oberösterreichische Energiestrategie*. Linz, 2009. https://www.energiesparverband.at/fileadmin/redakteure/ESV/Info_und_Service/Publikationen/Broschuere_Energiezukunft_2030_fin.pdf
- [41] OESTERREICHS ENERGIE: *Empowering Austria : Die Stromstrategie von Oesterreichs Energie bis zum Jahr 2030*. Wien, 2015. https://oesterreichsenergie.at/files/Stromstrategie/Stromstrategie_Broschuere_kl.pdf
- [42] LAND OBERÖSTERREICH: *Energieleitregion OÖ 2050 : Die Energiestrategie Oberösterreichs*. 2017. https://www.land-oberoesterreich.gv.at/files/publikationen/esv_Energiestrategie_Leitregion.pdf
- [43] #MISSION2030: *#mission2030 : Austrian Climate and Energy Strategy*. Vienna, September 2018. https://mission2030.info/wp-content/uploads/2018/10/Klima-Energiestrategie_en.pdf
- [44] PÖTSCHER, Friedrich: *Szenarien zur Entwicklung der Elektromobilität in Österreich : Bis 2020 und Vorschau 2030*. Wien, 2015
- [45] ÖAMTC: *Expertenbericht Mobilität & Klimaschutz 2030*. In: *auto touring extra* 2018 (2018), September 2018. <https://www.oeamtc.at/Kompaktversion+-+%C3%96AMTC+Expertenbericht+Mobilit%C3%A4t+%26+Klimaschutz+2030.pdf/28.401.248>
- [46] AMT DER OÖ. LANDESREGIERUNG - ABTEILUNG STATISTIK: *Bundesländervergleiche - Kraftfahrzeuge : Neu- und Gebrauchtzulassungen*. <https://www2.land-oberoesterreich.gv.at/internetstatistik/Start.jsp?SessionID=SID-525C3A8C-A0C01F07&xmliid=Seiten%2F129552.htm&kategorie=kfzbundesl> – Überprüfungsdatum 2019-12-06
- [47] VOPAVA, Julia; KIENBERGER, Thomas; HAMMER, Andreas; THORMANN, Bernd; KRIECHBAUM, Lukas; SEJKORA, Christoph; HERMANN, Robert; WATSCHKA, Karin; BERGMANN, Ulrich; KOß, Janina; FREWEIN, Markus; BRANDL, Hannes; VOGEL, Julia; MOSER, Simon; BARESCH, Martin; DE BRUYN, Kathrin; BRAUNSTEIN, René; FREITAG, Christina; PEYREDER, Markus: *MOVE2GRID: Umsetzung regionaler Elektromobilitätsversorgung durch hybride Kopplung*. Wien, 2019. https://nachhaltigwirtschaften.at/resources/sdz_pdf/berichte/schriftenreihe-2019-57-move2grid.pdf
- [48] KROPOSKI, Benjamin ; JOHNSON, Brian ; ZHANG, Yingchen ; GEVORGIAN, Vahan ; DENHOLM, Paul ; HODGE, Bri-

- Mathias ; HANNEGAN, Bryan: *Achieving a 100% Renewable Grid: Operating Electric Power Systems with Extremely High Levels of Variable Renewable Energy*. In: *IEEE Power and Energy Magazine* 15 (2017), Nr. 2, S. 61 -73. <http://doi.org/10.1109/MPE.2016.2637122>
- [49] EVELOY, Valerie ; GEBREEGZIABHER, Tesfaldet: *A Review of Projected Power-to-Gas Deployment Scenarios*. In: *Energies* 11 (2018), Nr. 7, S. 1824. <http://doi.org/10.3390/en11071824>
- [50] SCHWARZ, Simon ; METZGER, Jochen ; JACHMANN, Henning: *„P2G-Netze“ : Potenziale der Vernetzung von Strom-und Gassektor zur Stärkung der Systemstabilität und der Versorgungssicherheit in Baden-Württemberg durch Power-to-Gas(-to-Power)*. Stuttgart. <https://www.transnetbw.de/uploads/2019-01-17-16-25-07-98-1.pdf>
- [51] ØSTERGAARD, PA ; JOHANNSEN, RM ; DUIC, N: *Sustainable Development using Renewable Energy Systems*. *Int J Sustain Energy Plan Manag.* <https://doi.org/10.5278/ijsepm.4302>



Increasing installable photovoltaic power by implementing power-to-gas as electricity grid relief – A techno-economic assessment



Matthias Greiml*, Florian Fritz, Thomas Kienberger

Chair of Energy Network Technology, Montanuniversitaet of Leoben, Franz-Josef Straße 18, 8700, Leoben, Austria

ARTICLE INFO

Article history:

Received 4 March 2021

Received in revised form

19 May 2021

Accepted 19 June 2021

Available online 22 June 2021

Keywords:

100 % RES

Electricity grid congestion relief

Levelised costs of gas

High degree of renewable penetration

Multi energy system modelling and simulation

ABSTRACT

The integration of renewable electricity generation poses challenges for today's energy system. Since renewable potentials are geographically unevenly distributed, solutions to overcome bottlenecks such as grid congestion are necessary to raise as much renewable potentials as possible. In specific, a part of Austria is characterised with high photovoltaic installation inquiries and low electricity demand. Electricity grids are designed to cope with today's loads, therefore the integration of inquired photovoltaic would overstrain the built infrastructure. In this paper we investigate how power-to-gas can ease this photovoltaic related grid strain. The feed-in of hydrogen into natural gas transmission pipelines and the usage of hydrogen and biogas from local fermentation plants for methanation feeding synthetic natural gas (SNG) into local distribution grid is assessed in various scenarios. Based on the technical assessment results, an economic evaluation of each scenario is performed to determine generation costs of hydrogen or SNG. Depending on the electrolyser location in the electricity grid, the installable photovoltaic power can be increased significantly without causing electricity grid congestion. Costs for hydrogen and SNG vary across each scenario, mainly influenced by CapEx for electrolyser and methanation as well as electricity purchasing costs.

© 2021 Elsevier Ltd. All rights reserved.

1. Introduction

To meet the binding goals agreed to at the COP 21 in Paris, two major strategies should be implemented: substituting fossil fuels with renewable energy sources (RES) and increasing system efficiency [1]. Research regarding the pathway to 100% renewable energy systems has been gaining traction throughout the last 15 years. An increasing share of research is focusing on a cross-sectoral approach, considering the full energy system, depicting e.g. electricity, natural gas, district heating grids, hydrogen or carbon-dioxide grids in combination with storage and sector-coupling options [2]. An enhanced use of RES in multi-energy-systems presents challenges for current energy systems and their operators, since RES are mainly decentralised, not always predictable, and introduce volatility into grids [3]. Kroposki et al. [4], concludes his research on 100% volatile renewable energy by stating that achieving 100% renewable energy will require [4]:

- New solutions matching supply and demand over multiple timescales.
- Significant curtailment of variable renewable energy sources.
- Operation capable to cope with high instantaneous penetration of variable renewable energy sources.

Austria's climate and energy strategy #mission2030 aims to achieve 100% renewable electricity generation net balanced over one year [5]. Since hydroelectric and biomass potentials are already exploited to a high degree, an expansion of wind and photovoltaic (PV) is the only feasible option to reach this goal. Therefore, the currently installed wind generation capacity has to be tripled, whereas the current photovoltaic installation has to be increased elevenfold by the year 2030 [6].

Sejkora et al. [7] provide a comprehensive study regarding technical exergy potentials of renewable energy sources for each Austrian district. The RES exergy potential can be directly converted into RES energy potential. As shown in Fig. 1, technical renewable energy potentials differ in both spatial composition and quantity. However, the availability of certain technical potentials doesn't allow for inference of the developability of RES [7].

Bottlenecks in exploiting renewable energy potentials can be a

* Corresponding author.

E-mail address: matthias.greiml@unileoben.ac.at (M. Greiml).

Abbreviation	
AEL	Alkaline water electrolysis
AF	Annuity factor
BGS	Biogas storage
CO ₂ sep	CO ₂ separation
EP	Electricity purchase
HS	Hydrogen storage
LCOG	Levelised costs of gas
NGP	Natural gas pipeline
PEM	Proton exchange membrane
PV	Photovoltaic
RES	Renewable energy sources
SNG	Synthetic natural gas
SS	Substation

lack of local consumers followed by possible transmission or distribution grid restrictions if a spatial balance of renewable generation is necessary. To avoid grid congestion, renewable energy sources must be curtailed as ultima-ratio-measure to avoid supply outages [4,8]. Other solution options as an alternative to curtailment due to grid restrictions are: grid expansion, sector-coupling or energy storage.

In order to address the challenges mentioned above, we aim to

demonstrate the positive effects of power-to-gas sector coupling in a region with large photovoltaic potentials with a target to integrate as much photovoltaic power as possible into the existing electricity distribution grid.

1.1. Literature overview & research need

Studies such as [9–15] demonstrate the advantages of power-to-gas sector coupling in regions with a high degree of renewable penetration. To provide an overview of current fields of research for the application of power-to-gas, literature sources are categorised into two groups: The first group focuses on a macro perspective of power-to-gas applications, investigating certain regions or a national power-to-gas potential. While the second group focuses on certain single power-to-gas facilities. Depending on the scope of the presented research, a technological and or economic potential is investigated.

1.1.1. Single power-to-gas facility research

Using excess wind energy for a single power-to-gas facility, Simonis and Newborough [10] investigate a power-to-gas deployment scenario in the region of Emden, Germany. The authors provide a detailed technical power-to-gas deployment plan, keeping pace with local renewable energies expansion. Hydrogen is either fed into the local natural gas grid or used for methanation by utilising carbon dioxide from a local fermentation plant. The authors' research also shows that electrolyser utilization increases

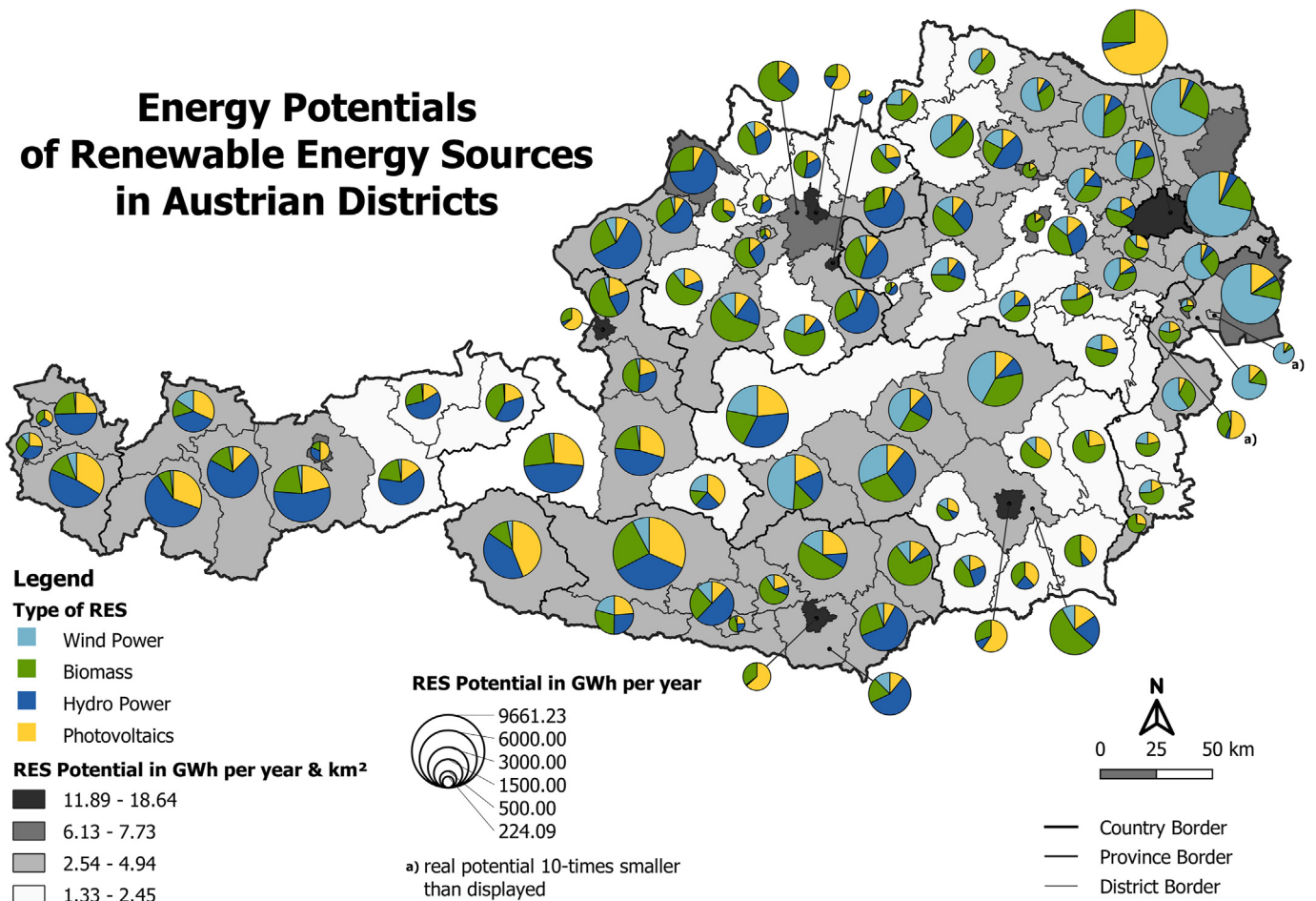


Fig. 1. Technical energy potential of RES per Austrian district, derived from Ref. [7]

significantly within five years due to an increased availability of renewable energy [10].

Kopp et al. [16] provide a technical and economic evaluation of the already operational 6 MW electrolyser, located in “Energiepark Mainz”. The technical evaluation investigates the power-to-gas process efficiency. The economic analysis focuses on various strategies for electricity procurement, showing that participation in the German secondary control reserve market can significantly improve the facility’s economic efficiency [16].

The influence of electricity prices and the usage of produced hydrogen is assessed by Walker et al. [17]. The authors use various electricity price limits to activate and deactivate the power-to-gas facility and analyse corresponding operating costs for various scenarios. Furthermore, they assess potential revenue sources such as replacing hydrogen from steam methane reformation, using hydrogen for renewable ethanol production, and participating in cap and trade carbon dioxide emission trading [17].

A framework for locating and modelling the flexibility potentials considering temporal and spatial resolution as well as load and generation in middle voltage distribution systems is introduced by Henni et al. [15]. The authors demonstrate their approach by assessing a potential future single power-to-gas facility. The facilities locations are selected based on the developed framework. Local middle voltage electricity and natural gas grids are considered. However, the capacity of the grids has to be estimated. Considering avoiding reimbursements or grid expansion, profitability could be achieved in the future [15].

1.1.2. Macro perspective research of power-to-gas

Estermann et al. [9] investigate the feasibility of power-to-gas to absorb surplus power from electricity distribution networks grids in southern Germany. Furthermore, they include biomass potentials as a carbon dioxide source for the production of synthetic natural gas. Their focus is on low-voltage distribution grid relief, however, no real-life grids are considered. A total installed power-to-gas capacity of 370 MW could capture 20% of excess solar in 2025 [9].

A techno-economic assessment of the future role of power-to-gas on both regional and local levels in Baden-Württemberg is assessed by McKenna et al. [18]. A detailed assessment of potential carbon dioxide sources, local renewable generation, as well as power-to-gas potentials are presented. The authors expect a cost-covering operation of power-to-gas in 2030. Any grid restrictions are sparsely considered [18].

Guandalini et al. [19] investigated the long term power-to-gas potential on the national Italian scale if the whole Italian renewable potentials are exploited. Five percent of Italy’s natural gas consumption or seven percent of Italy’s national fuel consumption could be replaced [19]. Similar research is carried out by Bailera et al. [20] in Spain, stating a power-to-gas potential between 7 and 19,5 GW, depending on excess renewable energy in 2050 [20]. However, to decarbonise the Spanish electricity sector and industrial combined heat and power units, a power-to-gas capacity between 80 and 90 GW is necessary [21].

Greiml et al. [22] demonstrate the positive systemic effects of power-to-gas taking a federal state’s energy infrastructure into account. However, the work didn’t focus on the power-to-gas facilities location in detail, its economics, and the influence of renewable potentials tap ability [22].

Clegg and Mancarella [23] identified a lack of research focusing on both network implications and benefits of power-to-gas on both electricity and natural gas grids. To overcome before mentioned gap, the authors introduce a new methodology that has been applied on a simplified energy grid of Great Britain to investigate the impact of power-to-gas on both electricity and gas grids. The

electricity grid consists of a 29 busbar model and the natural gas grid of 79 nodes. Providing an alternative to curtailment, excess wind can be used in power-to-gas units feeding hydrogen or synthetic natural gas into gas grids [23].

Similar to the research described above, Jentsch and Trost [24] investigate the role of power-to-gas with different degrees of renewable energy generation in Germany. They use a simplified spatially and time resolved energy model for Germany, depicting 18 defined regions in Germany, to determine an optimized dispatch of sector coupling and storage options [24].

To the best of our knowledge, the effect of power-to-gas on energy transmission or distribution infrastructure is hardly investigated. Since they concentrate their research on power-to-gas implementation on national state level, Clegg and Mancarella as well as Jentsch and Trost include a very simplified depiction of national energy infrastructure in their research. Their generic infrastructure depiction doesn’t allow for any deep analysis of effects caused by power-to-gas facilities on the built energy infrastructure or on the implementation of RES potentials.

In this paper, we aim to close previously described scientific gap by investigating the effects of power-to-gas on a rural distribution grid section in Austria, with a high degree of potential future renewable penetration. Furthermore, we aim to bridge between both before mentioned scientific fields by combining technical macro results with an economic assessment of potentially deployable power-to-gas facilities. Following research questions are to be investigated in this paper:

- To what extent can photovoltaic be expanded at certain substations, using variable power-to-gas power at different locations within a certain electricity- and natural gas grid section?
- What are the generation costs for hydrogen and synthetic natural gas?
- What are the effects of power-to-gas sizing and mode of operation on the economics of the power-to-gas facility?

To answer above described research question we have structured our paper as followed: The following subchapter describes upcoming challenges in the examined area. In Section 2 the methodology is described. Potential solution scenarios and their corresponding technical and economic results are disclosed in Section 3 and 4 respectively. Technical and economic results are discussed in Section 5, followed by a conclusion and an outlook for potential further research in Section 6.

1.2. Problem description

The examined part of Austria is sparsely populated without large industrial energy consumers but has significant photovoltaic potentials as can be seen in Fig. 2. Presently, the distribution grid operator is faced with requests for photovoltaic installations that are more than double the power of the current 110 kV distribution grid capacity (refer to orange lines in Fig. 2). In Fig. 2, the examined area including its infrastructure is depicted. Due to anonymization reasons, each substation is named with a synonym.

It can be seen that substations (SS) with high photovoltaic requests such as SS South and Rhine are connected to less powerful distribution grid lines compared to other substations. At SS Drava and SS North, the 110 kV distribution grid is connected to the 380 kV transmission grid (refer to red lines in Fig. 2). Adjacent to the north and west, major natural gas pipelines (NGP) are tangential to the examined area (refer to blue lines in Fig. 2). Near SS Elbe, South and Rhine several fermentation plants are available as potential carbon dioxide sources. In order to realise as much requested photovoltaic power as possible solutions to overcome

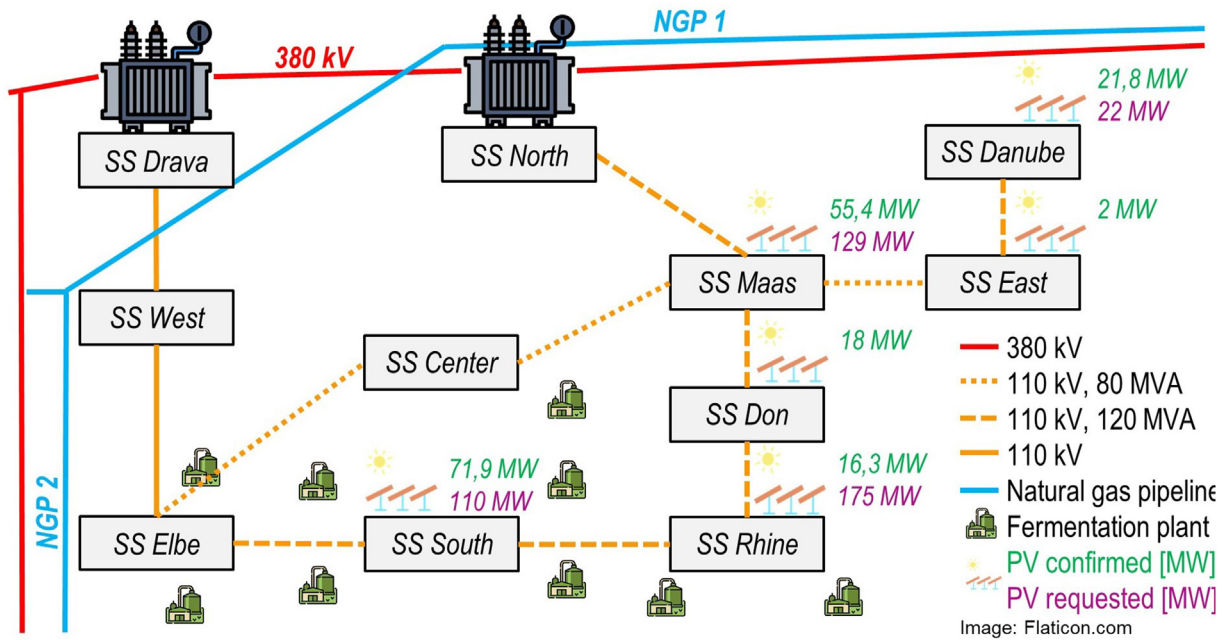


Fig. 2. Overview of examined area.

grid congestions are necessary. Following solution scenarios are investigated in this paper:

- Installation of power-to-gas electrolyser at SS South with hydrogen feed-in into NGP 2.
- Installation of power-to-gas electrolyser at SS North with hydrogen feed-in into NGP 1.
- Installation of power-to-gas electrolyser at SS South. Produced hydrogen as well as biogas as carbon dioxide source from local fermentation plants is used for methanation. Produced methane is being feed into local natural gas distribution grid.

For each scenario, we investigate to what extend the requested photovoltaic power can be implemented into the electricity grid at each substation without causing any grid congestion using power-to-gas at the substations mentioned above. Based on the technical assessment, the levelised costs of gas (LCOG) are to be calculated.

Currently, the guideline G31 issued by Österreichische Vereinigung für das Gas-und Wasserfach allows a maximum hydrogen content of four percent of the volume in natural gas grids [25]. However, an increase of the hydrogen content to ten percent of the volume and further can be expected in the future [26–28]. Therefore, for this paper, the maximum amount of hydrogen in NGP 1 and 2 is defined at ten percent of the volume.

2. Methodology

For the load flow calculations within this work, we use the self-developed software framework HyFlow [22,29]. HyFlow aims for load flow based design and operation simulation of flexibility options such as storage, sector-coupling or demand responsive processes, in multi-energy-systems. In order to allow the consideration of a broad range of energy system case studies, HyFlow depicts three cell levels with various depths of detail for each energy carrier considered. For example, level 1 cells can represent a 110 kV distribution grid, level 2 cells a 220 kV transmission grid, and one level 3 cell a 380 kV transmission grid. Slack nodes allow energy to be transferred between network levels (Fig. 3 right image). If available,

energy can be transferred across energy carriers via sector coupling options at each node (Fig. 3 left image). Sector coupling options therefore influence cross sectoral energy carriers.

In the current version of HyFlow, the direct current power load flow calculation has been upgraded with an alternating power load flow calculation tool (Matpower). Matpower allows for the calculation of nodal prices as well as optimal power flow calculations [30].

The control of hybrid elements depends on the electrical residual load ($RL_{Control, Power}(t)$ - Eqs. (2) and (1)) of a user-defined subsection of the whole depicted area (see Fig. 4 and Eqs. (2-1)–(2-3)). The described calculation is valid for $P_{electrolyser}$ smaller than $RL_{Control, Power}$. If $RL_{Control, Power}$ exceeds $P_{Electrolyser}$, the electrolyser is operated at its maximum rated power. This approach is similar to other approaches described in Ref. [9] or [10] to absorb excess renewable generation.

$$RL_{Control, Power}(t) = \sum P_{Res,Power,i}(t) \tag{2-1}$$

$$\{ (RL_{Control, Power}(t) \leq 0) \wedge (|RL_{Control, Power}(t)| \leq P_{maxelectr.}) \} \tag{2-2}$$

$$P_{Electrolysis} = RL_{Control, Power}(t) \tag{2-3}$$

2.1. Technical assessment

For each scenario, the process depicted in Fig. 5 is manually performed to determine the maximum installable photovoltaic and corresponding electrolyser power. Photovoltaic power iteration starts from confirmed photovoltaic power (current maximum) and is increased incrementally up to the confirmed, plus requested photovoltaic power (refer to “no” path at green diamond in Fig. 5). In case of grid overloads (refer to “yes” path at green diamond in Fig. 5), it is evaluated if the electrolyser’s power was increased before the current simulation. If it has been increased (refer to “yes” path at blue diamond in Fig. 5), the electrolyser doesn’t avoid any

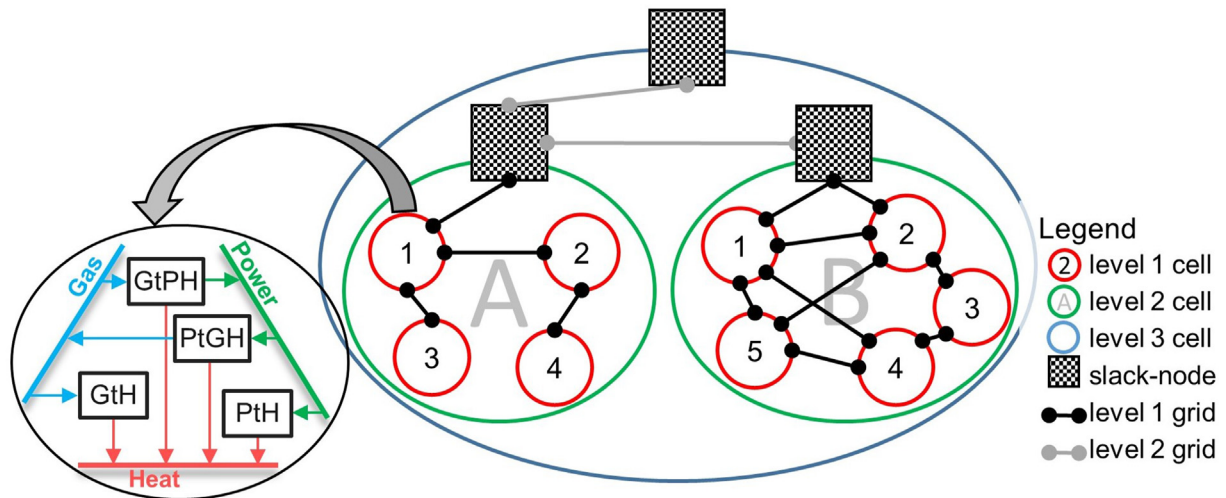


Fig. 3. Various network levels in combination with cellular approach.

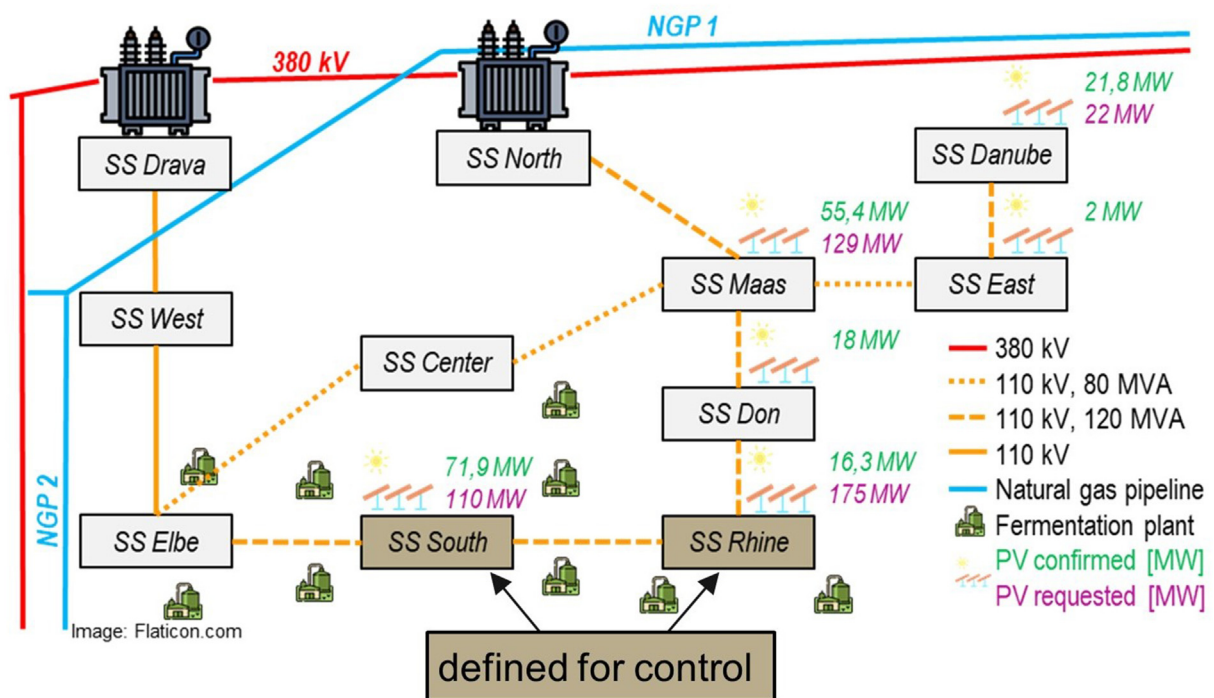


Fig. 4. Example for selected control substations.

grid overloads, therefore, a maximum PV power has been determined in the previous HyFlow simulation. If the electrolyser's power wasn't increased (refer to "no" path at blue diamond in Fig. 5) before the current simulation, the electrolyser's power is increased and a HyFlow simulation determines if grid overloads still occur.

As a result, various electrolyser and photovoltaic powers are determined. For each of the investigated scenarios, further examinations are performed on how produced hydrogen could be used and if limitations occur.

The local distribution grid operator provided us residual loads of each substation and photovoltaic generation profile both for one year in 15 min resolved time-steps as well as technical data to model power and gas grids.

2.2. Economic assessment

To enable a simplified economic comparison between scenarios, the levelised costs of gas are calculated based on technical and economic parameters for each scenario. To transform one-time capital expenditure (CapEx) into annual payments, the annuity method, according to Eqs. (2)–(4) is used [31]. For the calculation of specific CapEx, two annuity factors are calculated. One considers a 12-year period (AF_{12}) for an electrolyser and related planning and construction expenses and the second annuity factor considers a 30-year period (AF_{30}) for pipeline infrastructure, storage, compressor, CO₂ separation, and methanation. For both discounting factors an interest rate of four percent is considered. Costs for

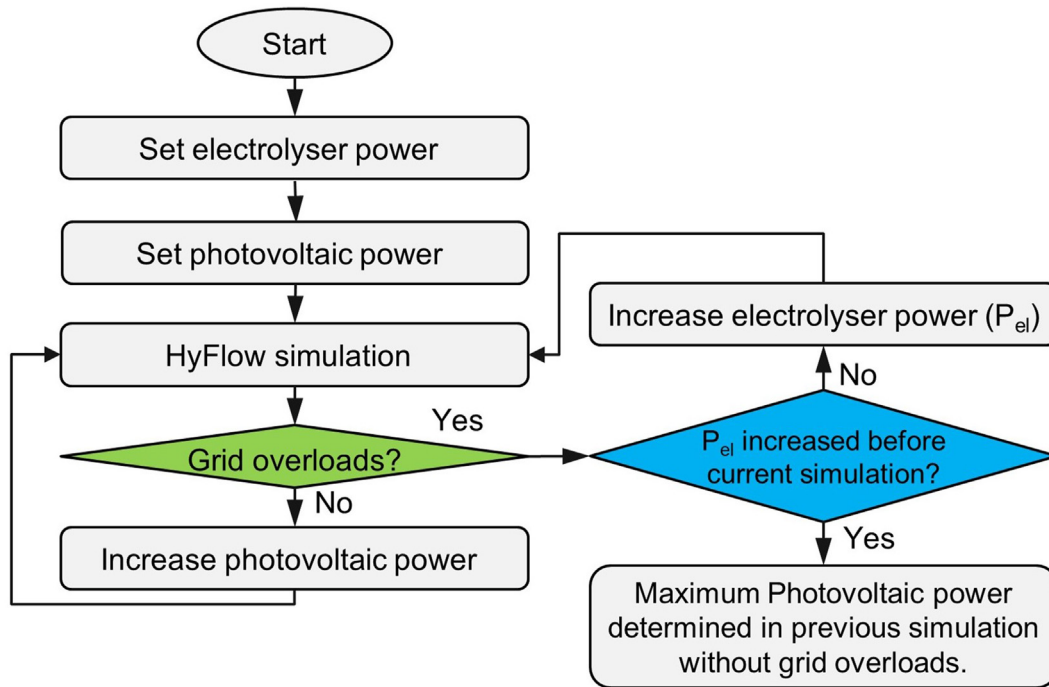


Fig. 5. Determination of maximum photovoltaic and electrolyser power.

operational expenditure (OpEx) and electricity purchases can hardly be predicted for a 12- or 30-year period, therefore no discounting is applied. The simplified LCOG are calculated taking specific CapEx, OpEx as well as costs for electricity, as displayed in Fig. 6 and Eqs. (2-5)–(2-7) derived from Ref. [32] into account.

$$AF = \frac{q^n * (q - 1)}{q^n - 1} \quad (2 - 4)$$

AF annuity factor
q discounting factor
n number of years

$$specific\ CapEx = \frac{CapEx\ AF_{12} * AF_{12} + CapEx\ AF_{30} * AF_{30}}{feedin\ Energy} \quad (2 - 5)$$

$$specific\ OpEx = \frac{Annual\ OpEx}{feedin\ Energy} \quad (2 - 6)$$

$$specific\ electricity\ costs = \frac{Purchased\ electricity}{feedin\ Energy} \quad (2 - 7)$$

In the following section, we discuss costs for necessary infrastructure components. Costs are determined based on expected costs in the year 2025.

2.3. Electrolyser

Within this work we investigate proton exchange membrane (PEM) electrolyser for hydrogen production. A review of power-to-gas projects in Europe by Wulf et al. shows that the majority of

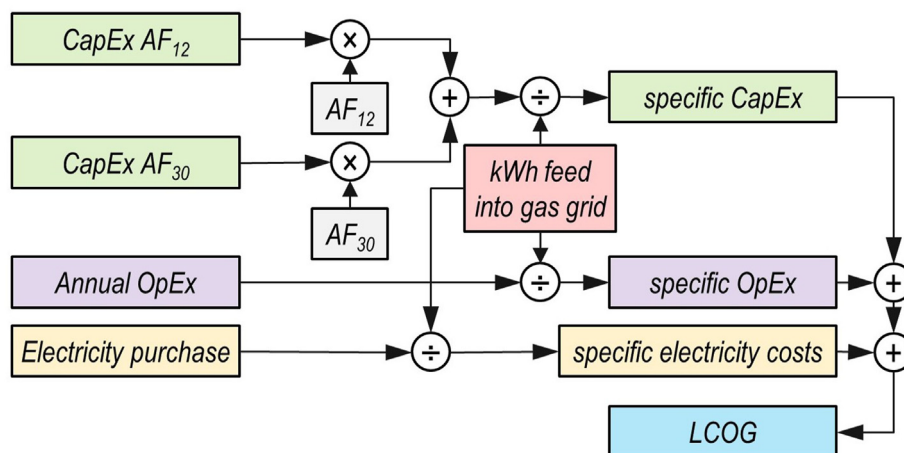


Fig. 6. Calculation of LCOG.

recently realised power-to-gas projects in Europe rely on PEM technology [33]. Therefore, PEM CapEx and OpEx are considered.

Bertuccioli et al. [34] expect PEM electrolyzers specific CapEx in a range between 480 and 1270 €/kW, whereas Butler and Spliethoff [35] expect CapEx within a range between 500 and 1400 €/kW in 2025. Both expect OpEx excluding electricity within a range between two and five percent of CapEx per year [34,35]. Tremel [36] includes several studies in PEM CapEx cross-down curves, ranging from 400 to 900 €/kW in 2025. Thema et al. [37] expect PEM electrolyser OpEx to be at about 900 €/kW in 2025. The electrolyser efficiency of current projects is up to 77% [37]. Schiebahn et al. [38] expect a potential future PEM electrolyser efficiency up to 74%. Manufacturers of PEM electrolyzers such as H-TEC and Siemens Energy specify the plant efficiency of their products between 74 and 75,5% [39,40].

2.4. Methanation

Gorre et al. [41] expects CapEx of 295–375 €/kW_{SNG} and fixed OpEx of five percent of CapEx as well as a variable OpEx of 0.63 €/(MW_{el} × h) in 2030 [41]. A study from Frontier Economics expect CapEx of 432–756 €/kW_{CH4} in 2030 and annual OpEx of four percent of CapEx. The methanations efficiency is, based on several other studies defined in a range between 78 and 83% [42]. To convert €/kW_{SNG} and €/kW_{CH4} into €/kW_{Electrolyser} CapEx they have to be multiplied with electrolyser and methanation efficiency. Based on selected efficiencies of an electrolyser (75%) and methanation (79%), CapEx ranges between 175 and 445 €/kW_{el} [42].

2.5. CO₂ separation

Döhler [43] provides CapEx as well as fixed and variable OpEx for various CO₂ separation technologies such as pressure water scrubbing, amine gas treating, and pressure swing adsorption. Based on costs for the mentioned technologies, each cost category is averaged. For several processing capacities, a cost function is determined via regression (result see Table 3) [43].

2.6. Natural gas and hydrogen pipeline

Average costs for both natural gas and hydrogen transmission and distribution pipelines are provided by van Leuween et al. [44]. The authors provide different cost estimates based on various studies depending on the pipeline surroundings, as displayed in Table 1. Hydrogen pipelines require advanced technology compared to natural gas pipelines, resulting in higher CapEx [44].

OpEx are defined as 2% of CapEx [44]. In Ref. [26] costs for natural gas pipelines were defined as shown in Table 2.

2.7. Hydrogen and biogas storage

Costs for storage of hydrogen and biogas are widely spread depending on pressure, size, and technology. Gorre et al. [41] expect hydrogen storage (HS) costs of 75 €/Nm³ in the year 2030 [41]. Van Leuween et al. [44] define the following costs for steel tanks based on several literature sources: CapEx range between 23 and 195 €/m³, and OpEx between 0,5 and 2,5% of CapEx [44]. CapEx

Table 1
Pipeline costs according to van Leuween [44].

	Rural	Medium	Urban
CapEx methane pipeline [€/m]	100	300	500
CapEx hydrogen pipeline [€/m]	350	450	550

Table 2
Pipeline costs according to Ref. [26].

	CapEx	OpEx
DN 150 PN 70	300 €/m	1 €/(m × a)
DN 150 PN 6	150 €/m	1 €/(m × a)

for low pressure biogas storage (BGS) range between 12 and 53 €/m³, according to Döhler [43].

2.8. Compressor

Costs for hydrogen compressors vary within a wide range, according to van Leuween et al. [44]. CapEx range between 144 and 18,500 €/kW, indicating that costs for compressors depend highly on their application. Most values spread around 1500 €/kW for compression up to 70 bar. OpEx range between 1,5 and 4% of CapEx [44]. Costs for methane and biogas compressors were defined as shown in Table 3 according to Refs. [26,44].

2.9. Planning and construction

For planning and construction of electrolyser and methanation Gorre et al. [41] consider planning costs of 100–160 t€. For construction, 10% of CapEx are considered [41].

2.10. Electricity purchase

A study from Kost et al. [45] regarding electricity generation costs provides cross-down curves for various renewable energies until the year 2035. For the year 2025, electricity generation costs for open space photovoltaic in Germany are forecasted to range between 3 and 5,5 €cent/kWh [45]. Considering higher solar radiation in the south of Austria compared to Germany, electricity generation costs can be assumed to be at the lower end or below the described range [46]. The International Renewable Energy Agency [47] expects the global levelised costs of electricity for photovoltaics to drop to a range of 0,02 to 0,08 US\$/kWh until the year 2030. For this study, costs for electricity purchases of 30 €/MWh are considered. Network fees for electricity grid are considered amounting to 1,15 €Cent/kWh excluding value-added tax [48,49]. Electricity purchasing prices are defined considering near term future PV generation costs. If electricity is purchased from open market, the price might fluctuate depending on addressed market and season.

2.11. Selected costs for economic assessment

In Table 3, the costs for necessary facilities based on literature overview for the economic assessment of each scenario are displayed.

3. Scenarios

In this section the three investigated scenarios are explained. The local distribution grid operator provided us residual loads of each substation and photovoltaic generation profile both for one year in 15 min resolved time-steps as well as technical data to model power and gas grids.

3.1. Scenario 1: hydrogen feed into NGP 2

As displayed in Fig. 7, an electrolyser is placed at SS South. Produced hydrogen is fed into NGP 2. Two modes of operation for

Table 3
Defined costs for economic assessment.

	CapEx	OpEx _{fix}	OpEx _{variable}
Electrolyser	800 €/kW _{EI}	3%/a CapEx	–
Methanation	200 €/kW _{EI}	5%/a CapEx	0,63*P _{MW} *h _{oper}
CO₂ separator	1528*V _{Biogas} + 872004	141*V _{Biogas} + 82654	0,042*V _{Biogas} + 8,71
Hydrogen pipeline	500 €/m	1 €/(m × a)	–
Natural gas or biogas pipeline PN70	300 €/m	1 €/(m × a)	–
Natural gas or biogas pipeline PN6	150 €/m	1 €/(m × a)	–
Hydrogen storage	50 €/m ³	1,5%/a CapEx	–
Biogas storage	50 €/m ³	1,5%/a CapEx	–
Hydrogen compressor	1500 €/kW _{EI}	2,5%/a CapEx	–
Biomethan/Biogas compressor	389802 + 996*V _{Biogas}	2,5%/a CapEx	7e ⁻³ *P _{Comp} *h _{oper}

the electrolyser are investigated to determine a suitable mode of operation to increase electrolyser utilization:

- Electrolyser is activated once residual load of substations South and Rhine turns negative (refer to Fig. 4).
- Electrolyser is activated once the residual load of all substations except Drava, North and West turns negative.

3.2. Scenario 2: hydrogen feed into NGP 1

In scenario 2, an electrolyser is placed at substation North and produced hydrogen is fed into NGP 1. The electrolyser is operated like in scenario 1 with the addition of SS Maas in operating strategy 1.

3.3. Scenario 3: Methane/SNG feed into local natural gas distribution grid

This scenario takes into consideration local fermentation plants in proximity to substations Elbe, South, and Rhine. The total amount of raw gas (60% CH₄, 40% CO₂) available for methanation is

approximately 3400 Nm³/h. A central electrolyser is placed at substation South, operated like scenario 1 (see Fig. 9) (see Fig. 8).

This scenario is divided into sub-scenarios, as displayed in Fig. 10.

To overcome different production profiles between volatile photovoltaic powered electrolyser and steady fermentation plants, storage options are investigated for both hydrogen and biogas in technical terms such as storage capacity as well as economic terms. In Fig. 11 different production profiles for both hydrogen and biogas are displayed, displaying a need for storage solutions.

To avoid biogas flaring or curtailment of fermentation plants in case no hydrogen is available from storage or photovoltaic generation, two further cases for each sub-scenario are considered. These include CO₂ separation (CO₂ sep) from biogas to produce methane, to be fed into the local distribution grid, or electricity purchase (EP) to operate the electrolyser with purchased electricity and provide hydrogen for methanation.

4. Results

In this section we present technical as well as economical results for each scenario.

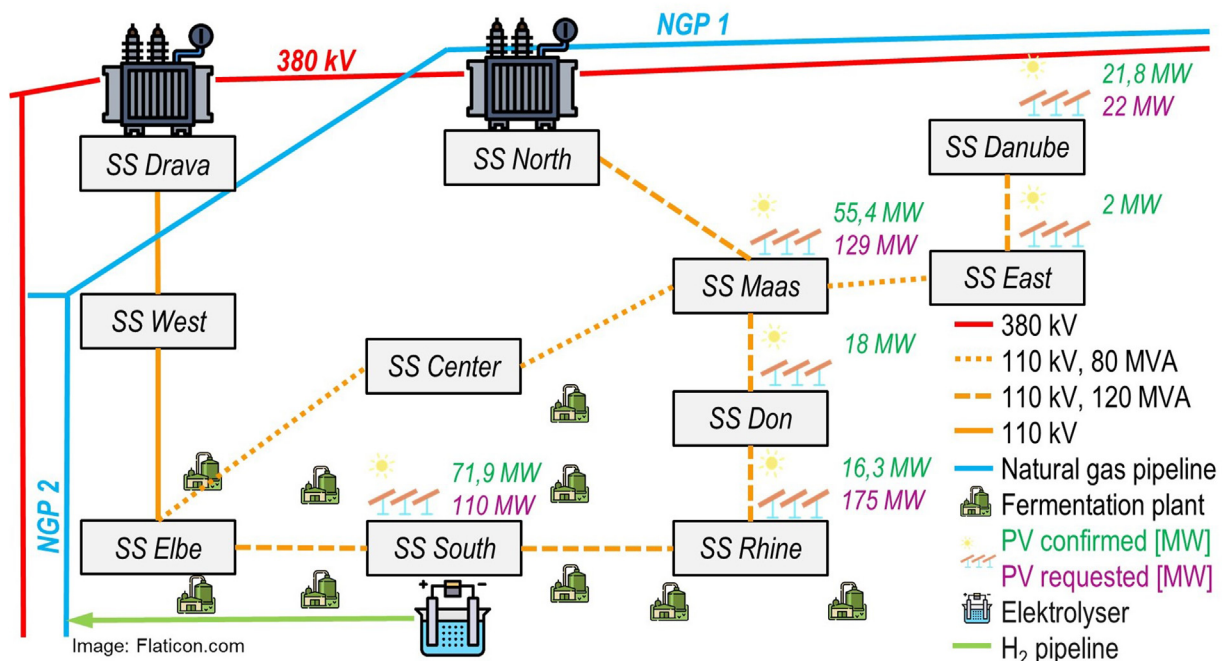


Fig. 7. Scenario 1 - hydrogen feed into NGP 2.

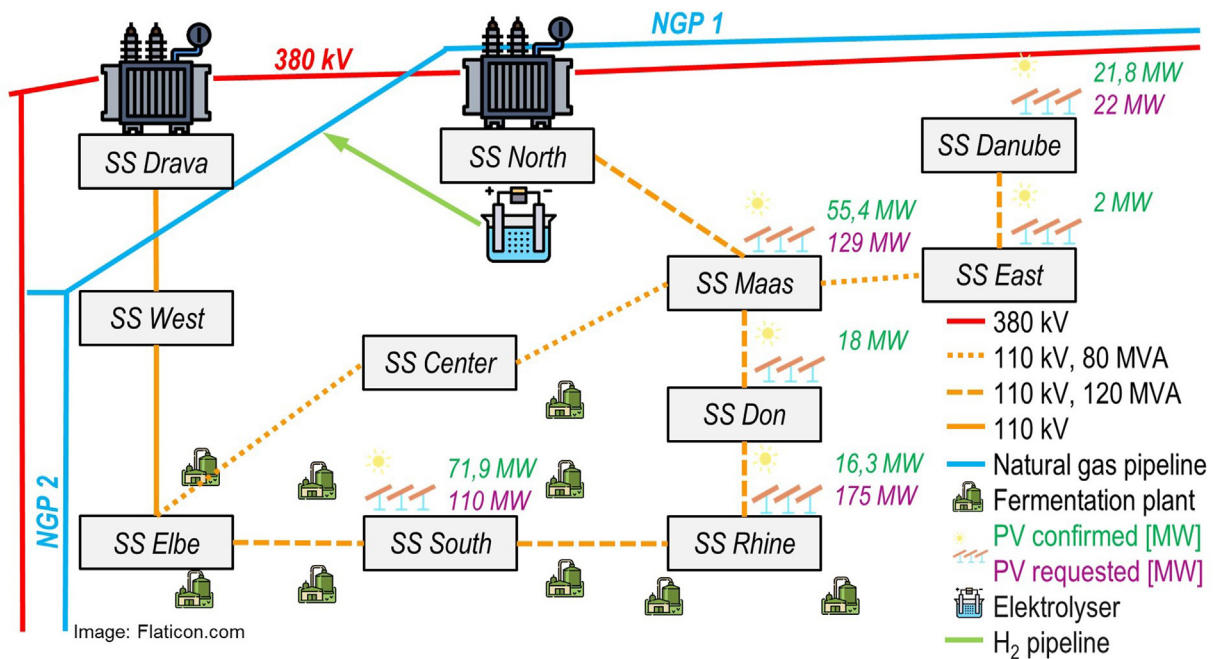


Fig. 8. Scenario 2 - hydrogen feed into NGP 1.

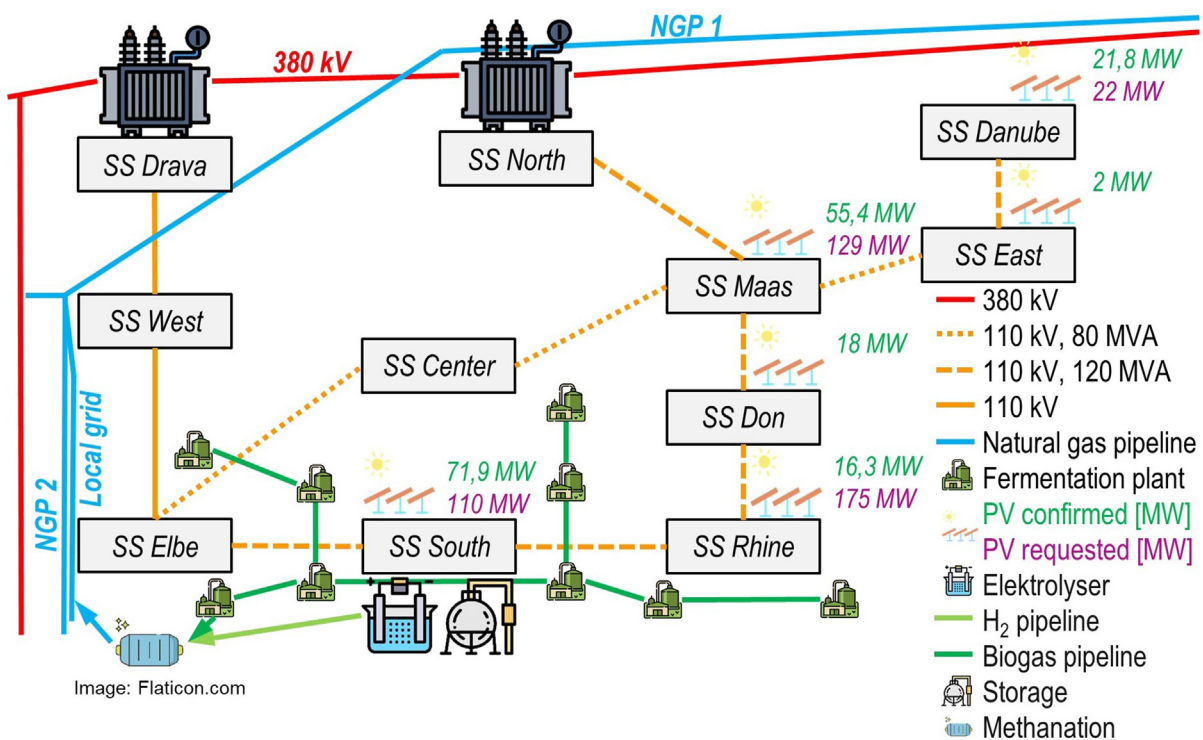


Fig. 9. Scenario 3 - Methane feed into local distribution grid.

4.1. Scenario 1: hydrogen feed into NGP 2

4.1.1. Assessment of technical results

The electrolysers mode of operation significantly impacts the achievable full-load hours, as displayed in Fig. 12, where achieved full-load hours based on installed photovoltaic and electrolyser power are shown. Operating the electrolyser based on the residual

load of substations South and Rhine (operation strategy #1) is far more advantageous compared to operating strategy #2 when considering achieved full-load hours. Substations South and Rhine have a low consumption in combination with high photovoltaic potentials. An increased utilization occurs because an over-production of electricity is achieved earlier, leading to longer electrolyser production time. Operating strategy #2 increases

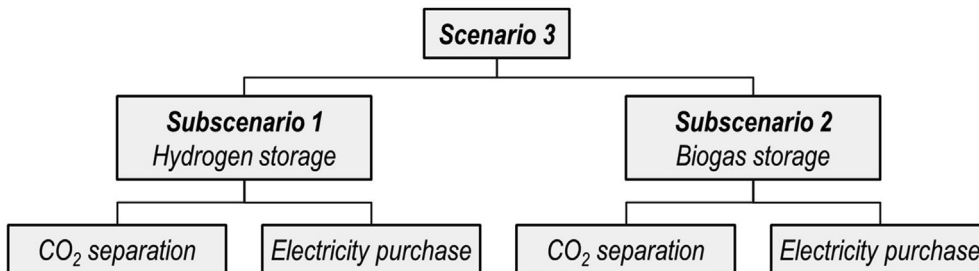


Fig. 10. Sub-scenarios in scenario 3.

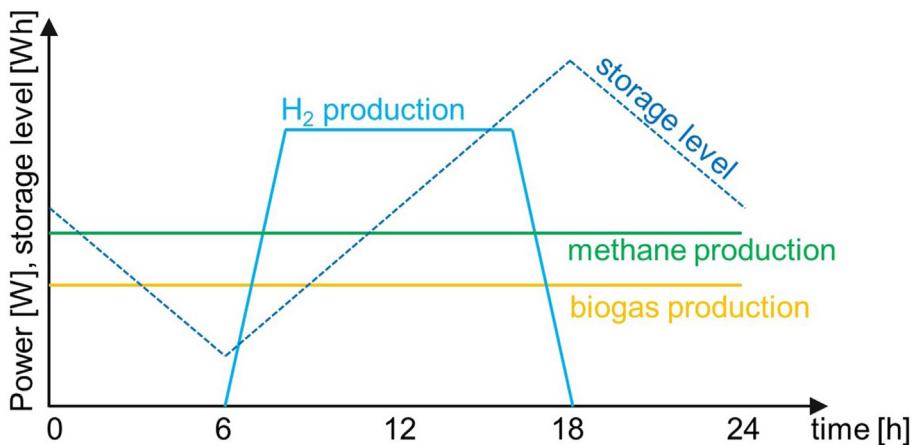


Fig. 11. Display of different production profiles and storage usage.

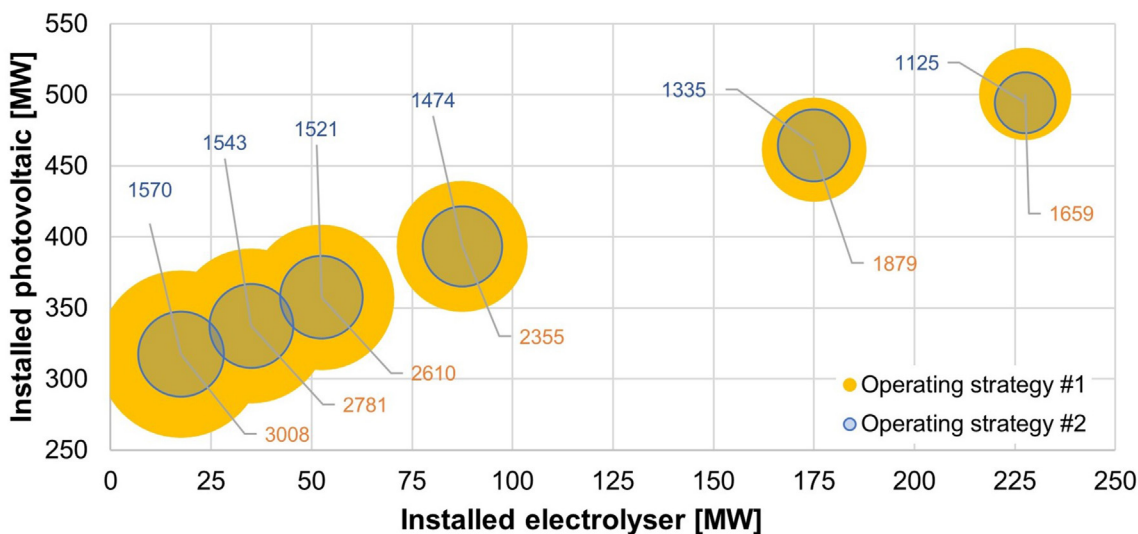


Fig. 12. Electrolyser full-load hours in dependence on operation strategy.

demand in combination with a marginal increase of photovoltaic potentials, resulting in a decreasing electrolyser utilization. Therefore, results based on operating strategy #1 will be displayed further onwards.

Fig. 13 displays the maximum photovoltaic power per substation that can be added to the electricity grid for certain electrolyser powers. “PV committed” represents the current maximum installable photovoltaic power according to distribution grid operator.

“PV inquired + committed” power contains the sum of photovoltaic power installation inquiries. Up to 500 MW of photovoltaic power could be added to the grid by installing a 227,5 MW electrolyser. A further increase of electrolyser power cannot integrate any further photovoltaic into the electricity grid due to overloads (refer to “electricity grid limitation” in Fig. 13), occurring at grid sections between SS Maas - North and South - Rhine.

However, the minimum flowrate in NGP 2 during summer is

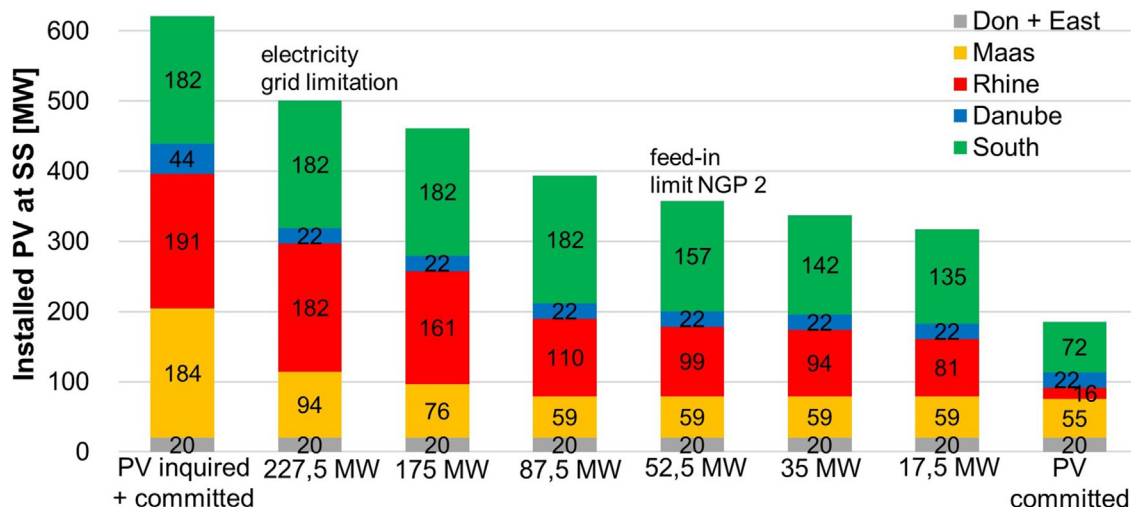


Fig. 13. Maximum installable PV per SS and electrolyser power – scenario 1.

about 65,000–100,000 Nm³/h [50], allowing a maximum electrolyser power in the range of 30–55 MW to cope with a ten percent hydrogen feed-in limit. A hydrogen storage could store excess hydrogen during daytime, and feed into NGP 2 during night time. Implementing a storage could further increase the installable electrolyser power up to approximately 100 MW (refer to “feed-in limit NGP 2” in Fig. 13). Table 4 contains technical key figures of scenario 1. It can be seen that an increase in electrolyser power results in a decrease of both full-load hours and the ratio between added photovoltaic power compared to electrolyser power ($P_{added PV} : P_{EL installed}$).

4.1.2. Assessment of economic results

The following tables display calculated CapEx (Table 5) as well as OpEx and Electricity costs (Table 6) for two different electrolyser dimensions. CapEx for electrolyser representing about 75% of total CapEx is the main CapEx driver. OpEx and electricity costs are predominantly caused by the electrolyser, therefore about 90% of specific hydrogen costs are caused by the electrolyser.

Specific hydrogen costs of 11,7 and 12,2 €/Cent/kWh_{H2} are equal to 4,4 and 4,8 €/kg_{H2}.

4.2. Scenario 2: hydrogen feed into NGP 1

4.2.1. Assessment of technical results

Fig. 14 displays the maximum photovoltaic power per substation that can be added to the electricity grid for a certain electrolyser power. It can be seen that any increase in electrolyser power doesn't correspond with an increase of installed photovoltaic. Since the electrolyser is located at a substation without any photovoltaic potentials, the electricity has to be transferred via the electricity grid to the electrolyser. This causes overloads of the electricity grid section Maas – North.

Table 4 Technical results of scenario 1.

	35 MW electrolyser	52,5 MW electrolyser
added PV Power	152 MW	172 MW
full-load hours electrolyser	2770 h	2598 h
electricity consumption	97,0 GWh	136,4 GWh
$P_{added PV} : P_{EL installed}$	4,3	3,3

Table 5 CapEx for scenario 1.

	35 MW electrolyser	52,5 MW electrolyser
Electrolyser	28 Mio. €	42 Mio. €
H ₂ storage	–	2,6 Mio. €
H ₂ pipeline	5,5 Mio. €	5,5 Mio. €
H ₂ compressor	645,000 €	967,500 €
Planning and construction	2,96 Mio. €	4,36 Mio. €
Produced H ₂	73,0 GWh	102,3 GWh
Spec. CapEx	0,050 €/kWh _{H2}	0,053 €/kWh _{H2}

Table 6 Annual OpEx and electricity costs for scenario 1.

	35 MW electrolyser	52,5 MW electrolyser
Electrolyser	840,000 €	1,26 Mio. €
H ₂ storage	–	51,600 €
H ₂ pipeline	11,000 €	11,000 €
H ₂ compressor	24,495 €	36,744 €
Spec. OpEx	0,012 €/kWh _{H2}	0,013 €/kWh _{H2}
Annual electricity costs	4,04 Mio. €	5,66 Mio. €
Spec. electricity costs	0,055 €/kWh _{H2}	0,055 €/kWh _{H2}

Due to the power grid limitation explained before, we provide technical results in Table 7, with comparable electrolyser powers as in scenario 1.

Compared to scenario 1, the added photovoltaic power doesn't increase with rising electrolyser power. Therefore the ratio $P_{added PV} : P_{EL installed}$ is lower compared to scenario 1.

4.2.2. Assessment of economic results

The following tables display calculated CapEx (Table 8) as well as annual OpEx and Electricity costs (Table 9) for two different electrolyser dimensions.

Specific hydrogen costs of 13,4 and 14,0 €/Cent/kWh_{H2} are equal to 5,3 and 5,5 €/kg_{H2}. Although the absolute CapEx values for the equipment are lower compared to scenario 1, because of fewer infrastructure requirements (H₂ pipeline and storage), the specific CapEx values are higher due to fewer electrolyser full-load hours. Lower full-load hours compared to scenario 1 are caused by including SS Maas into the control area of the electrolyser.

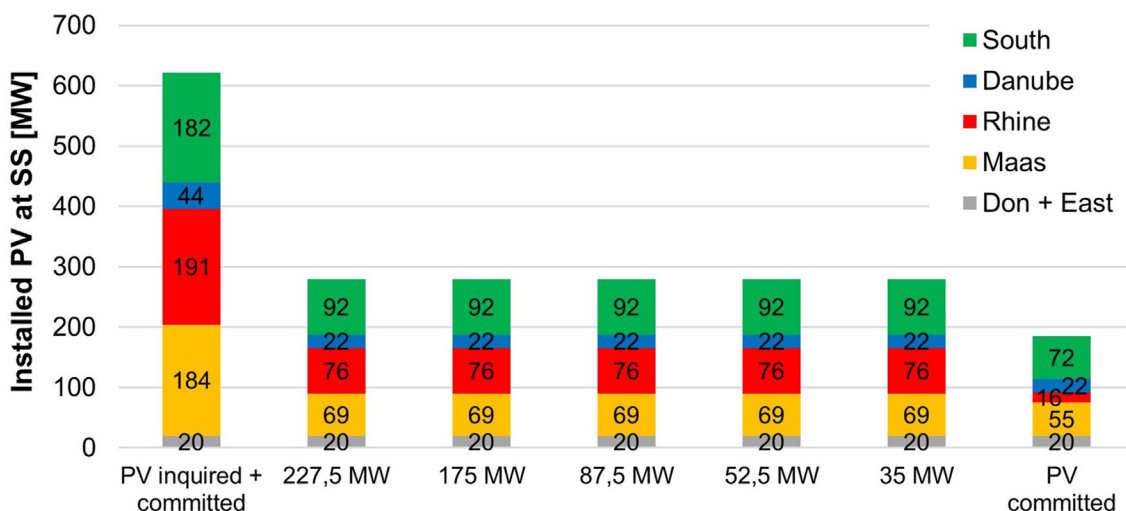


Fig. 14. Maximum installable PV per SS and electrolyser power – scenario 2.

Table 7
Technical results of scenario 2.

	35 MW electrolyser	52,5 MW electrolyser
added PV Power	94 MW	94 MW
full-load hours electrolyser	2108 h	1931 h
electricity consumption	73,8 GWh	101,4 GWh
$P_{added PV} \cdot P_{EL installed}$	2,7	1,8

Table 8
CapEx for scenario 2.

	35 MW electrolyser	52,5 MW electrolyser
Electrolyser	28 Mio. €	42 Mio. €
H ₂ pipeline	2,5 Mio. €	2,5 Mio. €
H ₂ compressor	645,000 €	967,500 €
Planning and construction	2,96 Mio. €	4,36 Mio. €
Produced H ₂	55,3 GWh	76,0 GWh
Spec. CapEx	0,063 €/kWh _{H₂}	0,068 €/kWh _{H₂}

Table 9
Annual OpEx and electricity costs for scenario 2.

	35 MW electrolyser	52,5 MW electrolyser
Electrolyser	840,000 €	1,26 Mio. €
H ₂ pipeline	5000 €	5000 €
H ₂ compressor	24,945 €	32,906 €
Spec. OpEx	0,016 €/kWh _{H₂}	0,017 €/kWh _{H₂}
Annual electricity costs	3,06 Mio. €	4,21 Mio. €
Spec. electricity costs	0,055 €/kWh _{H₂}	0,055 €/kWh _{H₂}

4.3. Scenario 3: Methane/SNG feed into local natural gas distribution grid

4.3.1. Assessment of technical results

Results for both hydrogen and biogas storage are equal in terms of purchased power, therefore, in Fig. 15 we distinguish between photovoltaic- and grid sourced electricity. In the case of the lowest considered electrolyser power of 47,5 MW, about 45% of the used electricity is sourced from the electricity grid. Compared to an electrolyser power of 65 MW, only about 25% electricity purchases from the grid. Electricity purchases are necessary only in case no

CO₂-separation is installed.

If electrolyser power is increased to 55 MW or beyond, it can be seen in Fig. 16 that even small power increases lead to large storage size growth. This can be explained by the annual production characteristics of photovoltaic. From April to September, considerably more hydrogen is produced, which is stored to be used during winter months. A declining number of storage cycles indicates a longer storage duration. There is hardly any difference between both storage technologies (hydrogen or biogas storage) in the technical assessment.

As demonstrated, if biogas or hydrogen is stored, the influence is negligible in the technical assessment. The main difference between both sub-cases of each sub-scenario (see Fig. 10) is if either electricity purchase or CO₂ separation is applied.

Fig. 17 displays electrolyser full-load hours in the range of 2500–2650 h per year if a CO₂ separation is used. In the case of electricity purchases, electrolysers reach far more full-load hours. Based on the available amount of CO₂, an electrolyser power up to 97 MW could be installed. However, in this case, annual storage of hydrogen would be necessary. If further CO₂ potentials can be tapped, an electrolyser power of 227,5 MW could be installed before electricity grid restrictions prohibit any further increase of electrolyser power. Table 10 contains technical key figures for scenario 3 for an electrolyser power similar to scenario 1 and 2.

4.3.2. Assessment of economic results

The economic assessment is split into two parts, according to sub-scenarios defined in Fig. 10. Produced methane is related to methane produced from methanation (SNG) and CO₂ separation.

Firstly, the costs of hydrogen storage are investigated (see Table 11 and Table 12).

Methane costs are 16,4 €Cent/kWh_{SNG} for CO₂ separation and 14,5 €Cent/kWh_{SNG} for electricity purchase. The price difference is caused by CO₂ separation, and different methane production.

Secondly, the costs for biogas storage are investigated (see Table 13 and Table 14).

Methane costs are 15,4 €Cent/kWh_{SNG} for CO₂ separation and 14,0 €Cent/kWh_{SNG} for electricity purchase. The price difference is caused by CO₂ separation, and different amounts of methane production.

Comparing all four displayed sub-scenarios, biogas storage in combination with electricity purchases is the most cost efficient solution for methanation.

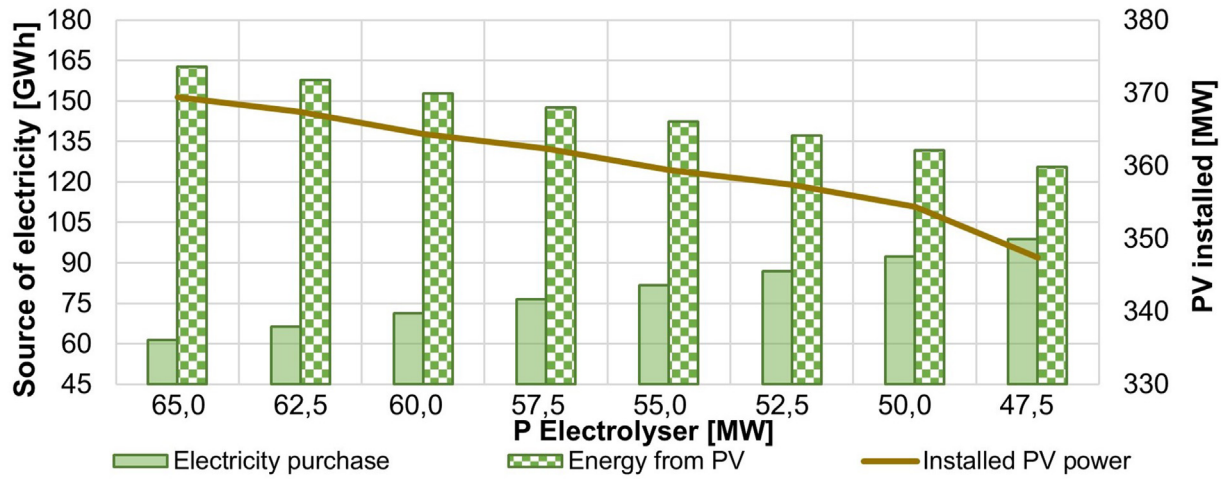


Fig. 15. Results electricity purchase for both sub-scenarios.

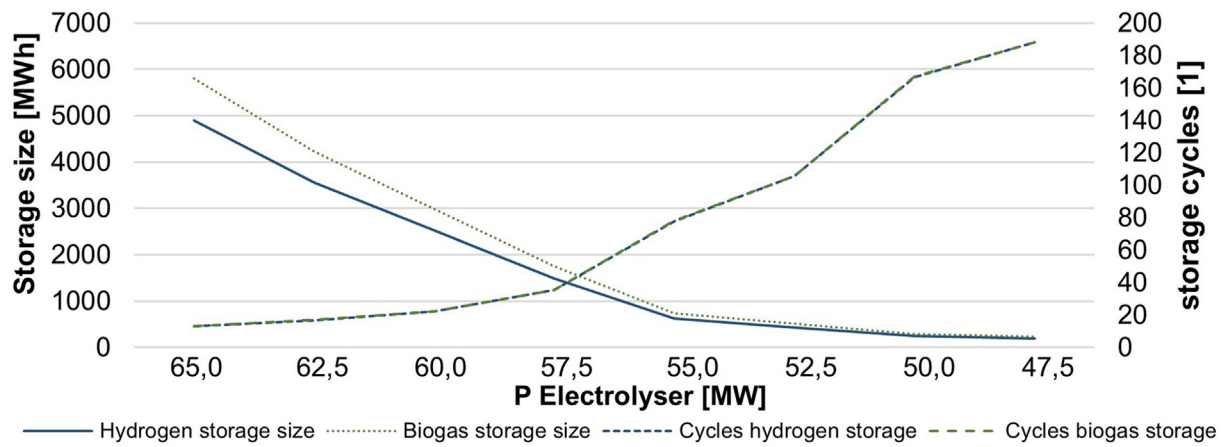


Fig. 16. Storage size and cycles.

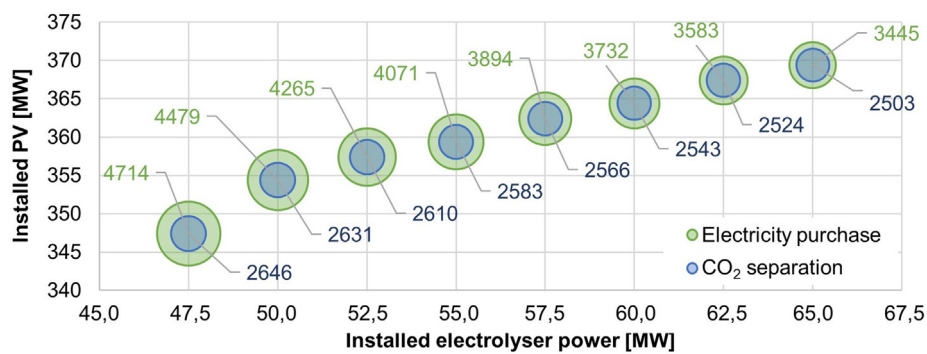


Fig. 17. Comparison of electrolyser full-load hours between CO₂ separation and electricity purchase.

Table 10
Technical results of scenario 2.

	52,5 MW electrolyser, CO ₂ separation	52,5 MW electrolyser, Electricity purchase
added PV Power	172 MW	172 MW
full-load hours electrolyser	2610 h	4265 h
electricity consumption	137,0 GWh	223,9 GWh
P _{added PV} : P _{EL} installed	3,3	3,3
Annual storage cycles	106	106

Table 11
CapEx for sub-scenario hydrogen storage.

	52,5 MW electrolyser	
	CO ₂ separation	Electricity purchase
Electrolyser	42 Mio. €	42 Mio. €
Methanation	10,5 Mio. €	10,5 Mio. €
CO ₂ separation	6,1 Mio. €	–
H ₂ pipeline	5,5 Mio. €	5,5 Mio. €
H ₂ storage	6,1 Mio. €	6,1 Mio. €
Methane compressor	3,8 Mio. €	3,8 Mio. €
Methane pipeline	9,2 Mio. €	9,2
Planning and construction	5,4 Mio. €	5,4 Mio. €
Produced methane	106,1 GWh	133,1 GWh
Spec. CapEx	0,074 €/kWh _{SNG}	0,056 €/kWh _{SNG}

Table 12
Annual OpEx and electricity costs for sub-scenario hydrogen storage.

	52,5 MW electrolyser	
	CO ₂ separation	Electricity purchase
Electrolyser	1,26 Mio. €	1,26 Mio. €
Methanation	709,261 €	814,737 €
CO ₂ separation	1,08 Mio. €	–
H ₂ pipeline	11,000 €	11,000 €
H ₂ storage	122,306 €	122,306 €
Methane compressor	222,862 €	304,238 €
Methane pipeline	61,000 €	61,000 €
Spec. OpEx	0,036 €/kWh _{SNG}	0,019 €/kWh _{SNG}
Annual electricity costs	5,70 Mio. €	9,29 Mio. €
Spec. electricity costs	0,054 €/kWh _{SNG}	0,070 €/kWh _{SNG}

Table 13
CapEx for sub-scenario biogas storage.

	52,5 MW electrolyser	
	CO ₂ separation	Electricity purchase
Electrolyser	42 Mio. €	42 Mio. €
Methanation	10,5 Mio. €	10,5 Mio. €
CO ₂ separation	6,1 Mio. €	–
H ₂ pipeline	5,5 Mio. €	5,5 Mio. €
Biogas storage	2,2 Mio. €	2,2 Mio. €
Methane compressor	3,8 Mio. €	3,8 Mio. €
Methane pipeline	9,2 Mio. €	9,2
Planning and construction	5,4 Mio. €	5,4 Mio. €
Produced methane	106,1 GWh	133,1 GWh
Spec. CapEx	0,068 €/kWh _{SNG}	0,051 €/kWh _{SNG}

Table 14
Annual OpEx and electricity costs for sub-scenario biogas storage.

	52,5 MW electrolyser	
	CO ₂ separation	Electricity purchase
Electrolyser	1,26 Mio. €	1,26 Mio. €
Methanation	709,971 €	814,737 €
CO ₂ separation	1,09 Mio. €	–
H ₂ pipeline	11,000 €	11,000 €
Biogas storage	43,775 €	43,775 €
Methane compressor	222,912 €	304,238 €
Methane pipeline	61,000 €	61,000 €
Spec. OpEx	0,032 €/kWh _{SNG}	0,019 €/kWh _{SNG}
Annual electricity costs	5,70 Mio. €	9,29 Mio. €
Spec. electricity costs	0,054 €/kWh _{SNG}	0,070 €/kWh _{SNG}

5. Discussion of results

In this section, scenario results are discussed and compared with other research.

In Fig. 18 the costs for hydrogen or SNG as well as achievable

photovoltaic power are displayed. Hydrogen generation costs range from 11,7 to 14 €/Cent/kWh_{H2}. Methane generation costs range from 14 to 16,4 €/Cent/kWh_{SNG}.

Gorre et al. [41] calculates SNG production costs between a range of 8,5 to 31 €/Cent/kWh_{SNG} in 2030. The electrolyser power is 10 MW and operates between 1000 and 6000 full-load hours per year. Electricity costs are expected to be 25 €/MWh [41]. Zauner et al. [51] expect SNG production costs of 43 €/Cent/kWh_{SNG} in 2020 and 21 €/Cent/kWh_{SNG} in 2030. A 50–100 MW electrolyser is considered, operated with energy from a 100 MW photovoltaic plant. The electrolysis achieves 1400 full-load hours if it's feed from photovoltaic and 4000 to 6000 full-load hours if additional electricity purchases are considered. Electricity purchases can reduce SNG production costs to 14 €/Cent/kWh_{SNG} in 2020 and 10 to 12 €/Cent/kWh_{SNG} 2030. Electricity prices are estimated to be 35 €/MWh in 2020 and 65 €/MWh in 2030 [51]. The calculated costs in Scenario 3 are in range with other research papers. A detailed comparison is difficult since each study has its unique scenarios. For example, our cost calculation includes necessary infrastructure investments.

Greenpeace Energy [52] published a study, concluding several papers regarding the costs of green hydrogen. Costs are expected to be 16,5 €/Cent/kWh_{H2} in 2020 and between 9 and 12 €/Cent/kWh_{H2} in 2030. Currently, hydrogen from fossil sources can be sourced for about one quarter of the electrolysers costs [52]. Kayfeci et al. [53] calculates hydrogen production costs from photovoltaic of 5,8 to 23,3 \$USD/kg, equal to 17,9 to 49,9 €/Cent/kWh_{H2} (EUR:USD = 1:1,2) [53].

The economic comparison of results shows that calculated production costs are in line with other research. However, any price deviation of the main cost drivers such as electrolyser and methanation CapEx or electricity purchase costs lead to significantly different results.

In Fig. 19, each scenarios' limitations as well as installed photovoltaic and electrolyser power are displayed. Only scenario 1 and 3 enable the installed photovoltaic power to increase beyond grid limits. If limitations such as feed-in limit and CO₂ availability can be solved, up to 227,5 MW electrolyser and 500 MW photovoltaic can be integrated into the electrical grid.

If the total inquired and committed photovoltaic potential of 621 MW should be integrated into the grid, further solutions such as a second electrolyser or electricity grid expansion are to be investigated. In contrast to our research, there are suggestions to implement large quantities of electrolysers in low- and middle voltage electricity grids [9,15].

The electrolyser's achievable full-load hours are not only influenced by the electrolysers location but also its mode of operation. As we've demonstrated, the mode of operation can be influenced by the considered area (see results of scenario 1) as well as applied technology (CO₂ separation or electricity purchases in scenario 3).

The economic efficiency of the electrolyser could potentially be further enhanced if waste heat is considered. For example, a H-TEC electrolyser can provide waste heat at a temperature of up to 65 °C [40]. However, the waste heat production corresponds with hydrogen production, therefore waste heat would mainly accrue during summer months. Further research would be necessary to assess the usability of waste heat in the examined area. Scenario 2 has shown in comparison to scenario 1 and 3 that the electrolyser's location has to be selected carefully. If the electrolyser is misplaced, no grid relief can be achieved. In order to preselect suitable locations, the framework described in Ref. [15] could be helpful for similar future research. Comparing the ratio between additionally installed photovoltaic and electrolyser's power ($P_{\text{added PV}}: P_{\text{EL installed}}$), a smaller electrolyser power is favourable because the ratio between additionally installed photovoltaic and electrolyser's

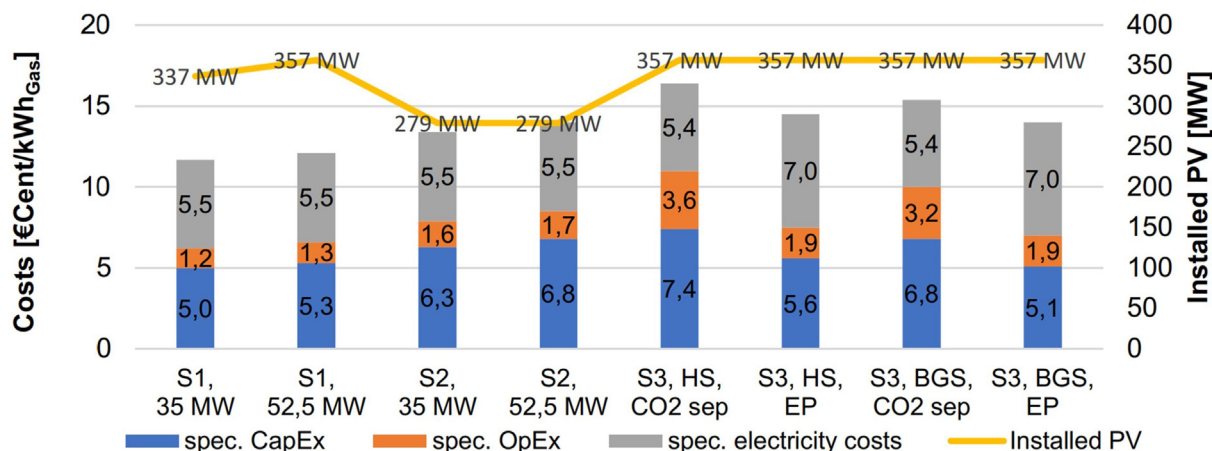


Fig. 18. Technical and economical results.

P Electrolyser	Scenario 1	Scenario 2	Scenario 3
0 MW		110 kV grid	
50 MW	NGP 2 feed-in limit PV: 337 MW	PV: 279 MW	
100 MW			CO ₂ availability PV: 411 MW
150 MW			
200 MW			
250 MW	110 kV grid PV: 500 MW		110 kV grid PV: 500 MW

Fig. 19. Technical limits comparison of each scenario.

power is greater. Additionally, a smaller electrolyser can achieve higher full-load hours, benefitting the electrolysers economic efficiency. The correlation between higher achievable full-load hours and smaller electrolyser power is also observed in Ref. [10], although electricity is sourced from wind power.

In case grid expansion is considered as an alternative to power-to-gas, the grid section from SS Elbe via Rhine and Maas to North, totaling approximately 100 km length, must be strengthened. CapEx of 600 €/m, based on an Austrian 110 kV grid construction cost analysis can be used to determine grid expansion costs [54]. Without a detailed analysis, the CapEx for grid strengthening of 60 Mio.€ is comparable to the presented power-to-gas scenarios.

6. Conclusion and future outlook

Within this work, we discuss the positive impact of power-to-gas sector-coupling in terms of increasing renewable photovoltaic electricity generation in an Austrian region. Current literature regarding power-to-gas research is mainly focused on either a regional or national level power-to-gas potential, or the operation of a single power-to-gas facility. A scientific gap was identified; both mentioned fields of research don't consider the restrictions in real-life energy grids in their assessment. To bridge between both areas of research we conducted a technical assessment of the influence of power-to-gas on an existing energy grid and used technical results to determine the production costs for renewable hydrogen or SNG.

The examined region is rural, lagging major electricity consumers but offers high renewable potentials. Due to the low

electricity demand, the local distribution grid's capacity is not designed to integrate high PV potentials. We believe the described approach of using an electrolyser as a grid relief measure can be considered in any region with a similar characteristic, provided the natural gas grid is accessible and within close proximity. A region with similar characteristics may include:

- High potential of renewable energy sources
- Low transmission capacity of electricity grids
- Low electricity demand
- Rural, sparsely populated area

In case a carbon-dioxide source (e.g. from: fermentation plants, industry) is available, produced hydrogen can be used for methanation and feed-in natural gas grids without restrictions.

The examined scenarios show that an electricity grid relief can be achieved using power-to-gas as long as the electrolyser is correctly positioned. The location as well as the mode of operation influences both the technical and economic efficiency of the electrolyser. Technically, using a 227,5 MW electrolyser, up to 500 MW of photovoltaic could be implemented into the current electricity grid. Depending on the electrolyser's rated power, between 1650 full-load hours for a 227,5 MW electrolyser up to 3000 full-load hours for a 17,5 MW electrolyser from excess photovoltaic generation can be achieved. In case electricity purchases are allowed, the electrolyser's full-load hours can be increased up to 4700 h. Smaller electrolyser powers are favourable in terms of both economic and technical efficiency. Further research should be carried out if several smaller decentralised electrolysers are favourable

compared to one centralised electrolyser in both technical and economic efficiency. Furthermore, the usage of waste heat could be investigated to increase the electrolysers economic efficiency.

Based on technical results, such as electrolyser's full-load hours and literature values for possible further cost developments, an economic assessment for each scenario was carried out. The economic assessment shows that generation costs for hydrogen (11,7 to 14 €/Cent/kWh) or SNG (14–16,4 €/Cent/kWh) in Austria are in line with literature expectations. The main cost drivers for both renewable hydrogen and SNG are CapEx for electrolyser and methanation as well as energy purchasing costs. Although costs are calculated to the best of our knowledge based on various literature sources, deviations from the assumed costs may lead to significantly different generation costs for hydrogen or SNG.

Raw materials for fermentation plants and large-scale photovoltaic consume large land areas for plantation and installation, potentially leading to land use conflicts. One further step should be a life-cycle assessment in order to examine the environmental impact of the proposed solution.

Credit author statement

Matthias Greiml: Conceptualization, Methodology, Validation, Formal analysis, Writing – original draft. Florian Fritz: Methodology, Software, Formal analysis, Visualization. Thomas Kienberger: Conceptualization, Supervision, Writing – review & editing.

Declaration of competing interest

The authors declare that they have no known competing financial interests or personal relationships that could have appeared to influence the work reported in this paper.

Acknowledgement

The authors thank E-Netze Steiermark for their kind contributions to this project.

References

- [1] Collins Seán, Deane John Paul, Poncelet Kris, Panos Evangelos, Pietzcker Robert C, Delarue Erik, Gallachóir Ó, Pádraig Brian. Integrating short term variations of the power system into integrated energy system models: a methodological review. In: Renewable and sustainable energy reviews, vol. 76; 2017. p. 839–56. <https://doi.org/10.1016/j.rser.2017.03.090>.
- [2] Hansen Kenneth, Breyer Christian, Lund Henrik. Status and perspectives on 100% renewable energy systems. Energy 2019;175:471–80. <https://doi.org/10.1016/j.energy.2019.03.092>.
- [3] Mancarella Pierluigi. MES (multi-energy systems): an overview of concepts and evaluation models. In: Energy, vol. 65; 2014. p. 1–17. <https://doi.org/10.1016/j.energy.2013.10.041>.
- [4] Kroposki Benjamin, Johnson Brian, Zhang Yingchen, Gevorgian Vahan, Denholm Paul, Hodge Bri-Mathias, Hannegan Bryan. Achieving a 100% renewable grid: operating electric power systems with extremely high levels of variable renewable energy. 2. In: IEEE power and energy magazine, vol. 15; 2017. p. 61–73. <https://doi.org/10.1109/MPPE.2016.26371122>.
- [5] #mission2030: #mission2030 : Austrian Climate and Energy Strategy. 2018. Vienna, September, https://mission2030.info/wp-content/uploads/2018/10/Klima-Energiestrategie_en.pdf.
- [6] Gruber Karl Heinz. Umsetzung der #mission2030-Ziele aus Sicht von Oesterreichs Energie. https://iewt2019.eeg.tuwien.ac.at/download/contribution/presentation/327/327_presentation_20190213_173020.pdf. Review date: 2021-01-08.
- [7] Sejkora Christoph, Kühberger Lisa, Radner Fabian, Trattner Alexander, Kienberger Thomas. Exergy as criteria for efficient energy systems—a spatially resolved comparison of the current exergy consumption, the current useful exergy demand and renewable exergy potential. 4. In: Energies, vol. 13; 2020. p. 843. <https://doi.org/10.3390/en13040843>.
- [8] Doering Michael. Assessment of storage options for reduction of yield losses in a region with 100% renewable electricity. In: Energy procedia, vol. 73; 2015. p. 218–30. <https://doi.org/10.1016/j.egypro.2015.07.675>.
- [9] Estermann T, Newborough M, Sterner M. Power-to-gas systems for absorbing excess solar power in electricity distribution networks. 32. In: International journal of hydrogen energy, vol. 41; 2016. p. 13950–9. <https://doi.org/10.1016/j.ijhydene.2016.05.278>.
- [10] Simonis B, Newborough M. Sizing and operating power-to-gas systems to absorb excess renewable electricity. In: International journal of hydrogen energy, vol. 42; 2017. p. 21635–47. <https://doi.org/10.1016/j.ijhydene.2017.07.121>.
- [11] Walker Sean B, Mukherjee Ushnik, Fowler Michael, Elkamel Ali. Benchmarking and selection of Power-to-Gas utilizing electrolytic hydrogen as an energy storage alternative. In: International journal of hydrogen energy, vol. 41; 2016. p. 7717–31. <https://doi.org/10.1016/j.ijhydene.2015.09.008>.
- [12] van Leeuwen Charlotte, Mulder Machiel. power-to-gas in electricity markets dominated by renewables. In: Applied energy, vol. 232; 2018. p. 258–72. <https://doi.org/10.1016/j.apenergy.2018.09.217>.
- [13] Hidrogeno Abengoa, Liquide Air, AkzoNobel, Alstom ECN, elementenergy, eurogas, GERG, HEDNO. Hellenic petroleum, HIA, hydrogenics, inabensa, ITM power, linde group, moixa technology, NEL hydrogen, nothern power grid, NOW, proton on site, PAE RAE OREDT, res AMERICAS, shell, SIEMENS, statkraft, staitoil, sunfire, TATA chemicals, VANADIS POWER, VATTENFALL, VOITH. In: Commercialisation of energy storage in Europe : a fact-based analysis of the implications of projected development of the European electric power system towards 2030 and beyond for the role and commercial viability of energy storage; 2015. Brussels, Match, https://www.fch.europa.eu/sites/default/files/CommercializationofEnergyStorageFinal_3.pdf.
- [14] Bellocchi Sara, Falco Marcello Sara, Gambini Marco, Manno Michele, Stilo Tommaso, Vellini Michela. Opportunities for power-to-Gas and Power-to-liquid in CO₂-reduced energy scenarios: the Italian case. In: Energy, vol. 175; 2019. p. 847–61. <https://doi.org/10.1016/j.energy.2019.03.116>.
- [15] Henni Sarah, Staudt Philipp, Kandiah Balendra, Weinhardt Christof. Infrastructural coupling of the electricity and gas distribution grid to reduce renewable energy curtailment. In: Applied energy, vol. 288; 2021. p. 116597. <https://doi.org/10.1016/j.apenergy.2021.116597>.
- [16] Kopp M, Coleman D, Stiller C, Scheffer K, Aichinger J, Scheppat B, Mainz Energiepark. Technical and economic analysis of the worldwide largest Power-to-Gas plant with PEM electrolysis. 19. In: International journal of hydrogen energy, vol. 42; 2017. p. 13311–20. <https://doi.org/10.1016/j.ijhydene.2016.12.145>.
- [17] Walker Sean B, van Lanen Daniel, Fowler Michael, Mukherjee Ushnik. Economic analysis with respect to Power-to-Gas energy storage with consideration of various market mechanisms. In: International journal of hydrogen energy, vol. 41; 2016. p. 7754–65. <https://doi.org/10.1016/j.ijhydene.2015.12.214>.
- [18] McKenna RC, Bchini Q, Weinand JM, Michaelis J, König S, Köppel W, Fichtner W. The future role of Power-to-Gas in the energy transition: regional and local techno-economic analyses in Baden-Württemberg. In: Applied energy, vol. 212; 2018. p. 386–400. <https://doi.org/10.1016/j.apenergy.2017.12.017>.
- [19] Guandalini G, Robinius M, Grube T, Campanari S, Stolten D. Long-term power-to-gas potential from wind and solar power: a country analysis for Italy. 19. In: International journal of hydrogen energy, vol. 42; 2017. p. 13389–406. <https://doi.org/10.1016/j.ijhydene.2017.03.081>.
- [20] Bailera Manuel, Lisbona Pilar. Energy storage in Spain: Forecasting electricity excess and assessment of power-to-gas potential up to 2050. Energy 2018;143: 900–10. <https://doi.org/10.1016/j.energy.2017.11.069>.
- [21] Lisbona Pilar, Frate Guido Francesco, Bailera Manuel, Desideri Umberto. Power-to-Gas: analysis of potential decarbonization of Spanish electrical system in long-term prospective. Energy 2018;159:656–68. <https://doi.org/10.1016/j.energy.2018.06.115>.
- [22] Greiml Matthias, Traupmann Anna, Sejkora Christoph, Kriechbaum Lukas, Böckl Benjamin, Pichler Patrick, Kienberger Thomas. Modelling, designing and operation of grid-based multi-energy systems. 7–24 Pages. Intl J Sustain Energy Plan manag 2020;29. <https://doi.org/10.5278/ijsepm.3598>. International Journal of Sustainable Energy Planning and Management, Vol. 29 (2020) (2020).
- [23] Clegg Stephen, Mancarella Pierluigi. Integrated modeling and assessment of the operational impact of power-to-gas (P2G) on electrical and gas transmission networks. In: IEEE transactions on sustainable energy, 6; 2015. p. 1234–44. <https://doi.org/10.1109/TSTE.2015.2424885>.
- [24] Jentsch Mareike, Trost Tobias, Höfling Holger (Mitarb), Jachmann Henning (Mitarb). Analyse von Power-to-Gas-Energiespeichern im regenerativen Energiesystem. Kassel; October 2014. https://www.researchgate.net/publication/301688145_Analyse_von_Power-to-Gas-Energiespeichern_im_regenerativen_Energiesystem.
- [25] Österreichische Vereinigung für das Gas- und Wasserfach: Regeln der ÖVGW - richtlinie G 31 : Erdgas in Österreich: Gasbeschaffenheit. 2001. Wien.
- [26] ÖVGW, Leoben Montanuniversität, Wien WU. DBI Gas- und Umwelttechnik GmbH, TU Wien, JKU Linz, ERIG: Greening the Gas : forschungsbbericht 2019. 2vol. 29; 2020. Vienna, https://www.ovgw.at/media/medialibrary/2020/03/OVGW_JB_forschung19_hi_corr2.pdf.
- [27] Gas Connect Austria. Mit Hochdruck für mehr Wasserstoff – status quo und Chancen. <https://www.gasconnect.at/aktuelles/news-presse/news/detail/News/mit-hochdruck-fuer-mehr-wasserstoff-status-quo-und-chancen>. Aktualisierungsdatum: 2021-01-11.
- [28] Austrian Gas Grid Management AG, Langfristige Planung. Für die Gas Verteilernetzinfrastruktur in Österreich für den Zeitraum 2020–2029. <https://www>.

- e-control.at/documents/1785851/1811582/LFP19_Bericht_A2_XXXBGG_inkl-Anhang.cleaned.pdf/dd1c0f44-05d4-0cc6-b951-9460e5bfaa8b? t=1574159767808; 2019. 2019.
- [29] Böckl Benjamin, Greiml Matthias, Leitner Lukas, Pichler Patrick, Kriechbaum Lukas, Kienberger Thomas. HyFlow—a hybrid load flow-modelling framework to evaluate the effects of energy storage and sector coupling on the electrical load flows. *Energies* 2019;12(5):956. <https://doi.org/10.3390/en12050956>.
- [30] Zimmerman Ray Daniel, Murillo-Sanchez, Edmundo Carlos, Thomas Robert John. MATPOWER: steady-state operations, planning, and analysis tools for power systems research and education. 1. In: *IEEE transactions on power systems*, vol. 26; 2011. p. 12–9. <https://doi.org/10.1109/TPWRS.2010.2051168>.
- [31] Konstantin Panos. *Praxisbuch Energiewirtschaft : energieumwandlung, -transport und -beschaffung, Übertragungsnetzausbau und Kernenergieausstieg*. 4., aktualisierte Auflage. Berlin: Springer Vieweg; 2017 (VDI-Buch). 978-3-662-49823-1.
- [32] Raikar Santosh, Adamson Seabron. Renewable energy finance in the international context. In: Raikar Santosh, Adamson Seabron, Hrsg, editors. *Renewable energy finance : Theory and practice*. London: Academic Press; 2020. p. 185–220.
- [33] Wulf Christina, Linßen Jochen. Zapp, Petra: *Review of power-to-gas Projects in Europe*. *Energy Procedia* 2018;155:367–78. <https://doi.org/10.1016/j.egypro.2018.11.041>.
- [34] Bertuccioli Luca, Chan Alvin, Hart David, Lehner Franz, Madden Ben, Standen Eleanor. *Study on development of water electrolysis in the EU*. 7.2. https://www.fch.europa.eu/sites/default/files/study%20electrolyser_0-Logos_0_0.pdf; 2014.
- [35] Buttler Alexander, Spliethoff Hartmut. Current status of water electrolysis for energy storage, grid balancing and sector coupling via power-to-gas and power-to-liquids: a review. In: *Renewable and sustainable energy reviews*, vol. 82; 2018. p. 2440–54. <https://doi.org/10.1016/j.rser.2017.09.003>.
- [36] Tremel Alexander. *Electricity-based fuels*. Cham: Springer International Publishing; 2018. 978-3-319-72458-4.
- [37] Thema M, Bauer F, Sterner M. Power-to-Gas: electrolysis and methanation status review. In: *Renewable and sustainable energy reviews*, vol. 112; 2019. p. 775–87. <https://doi.org/10.1016/j.rser.2019.06.030>.
- [38] Schiebahn Sebastian, Grube Thomas, Robinius Martin, Tietze Vanessa, Kumar Bhunesh, Stolten Detlef. Power to gas: technological overview, systems analysis and economic assessment for a case study in Germany. 12. In: *International journal of hydrogen energy*, vol. 40; 2015. p. 4285–94. <https://doi.org/10.1016/j.ijhydene.2015.01.123>.
- [39] SIEMENS energy. Silyzer 300 : The next paradigm of PEM electrolysis. <https://assets.siemens-energy.com/siemens/assets/api/uuid:17cdfbd8-13bd-4327-9b26-383e4754bee3/datasheet-final1.pdf>. Review date: 2021-01-08.
- [40] H-TEC SYSTEMS. PEM-Elektrolyseur – das Bindeglied für Sektorenkopplung und dezentrale H₂-Produktion. https://www.h-tec.com/fileadmin/Content/PDFs/19022019/H-TEC_SYSTEMS_Datenblatt_Elektrolyseur_ME450_1400_DE.pdf. Review date: 2021-01-08.
- [41] Gorre Jachin, Ortloff Felix, van Leeuwen Charlotte. Production costs for synthetic methane in 2030 and 2050 of an optimized Power-to-Gas plant with intermediate hydrogen storage. *Appl Energy* 2019;253:113594. <https://doi.org/10.1016/j.apenergy.2019.113594>.
- [42] Verkehrswende Agora, Energiewende Agora. *Frontier economics*; perner, jens (mitarb.);unteutsch, michaela (mitarb.); lövenich, andrea (mitarb.); deutsch, matthias (mitarb.); maier, urs (mitarb.). Berlin: Die zukünftigen Kosten strombasierter synthetischer Brennstoffe; 2018. https://www.agora-energiewende.de/fileadmin2/Projekte/2017/SynKost_2050/Agora_SynKost-Studie_WEB.pdf.
- [43] Döhler, Helmut (Hrsg.). *Faustzahlen biogas*. 3. Ausg. Darmstadt: KTBL; 2013. 978-3-941583-85-6.
- [44] van Leeuwen, Zauner Charlotte, Andreas; Gorre, Jachim (Mitarb.): *Innovative large-scale energy storage technologies and Power-to-Gas concepts after optimisation : Report on the costs involved with PtG technologies and their potentials across the EU*. 30.04. 2018. <https://ec.europa.eu/research/participants/documents/downloadPublic?documentIds=080166e5ba3ba6a8&appId=PPGMS>.
- [45] Kost Christoph, Shammugam Shivenes, Jülch Verena, Nguyen Huyen-Tran, Schlegl Thomas, Henning Hans-Martin (Mitarb.), Bett, andreas (mitarb.) : *stromgestehungskosten erneuerbare energien*. Freiburg. https://www.ise.fraunhofer.de/content/dam/ise/de/documents/publications/studies/DE2018_ISE_Studie_Stromgestehungskosten_Erneuerbare_Energien.pdf; March 2018.
- [46] European Commission. Photovoltaic geographical information system (PVGIS). <https://ec.europa.eu/jrc/en/pvgis>. Review date: 2021-01-08.
- [47] International renewable energy agency. Future of solar photovoltaic : deployment, investment, technology, grid integration and socio-economic aspects. Abu Dhabi: A Global Energy Transformation Paper; 2019. 978-992-9260-156-0.
- [48] Bundeskanzleramt. Änderung der Systemnutzungsentgelte-verordnung 2018 (SNE-V 2018 - novelle 2020) (idF v. BGBl. II nr. 424/2019 - teil 2). In: BGBl. II Nr. 424/2019; 2019.
- [49] Wko OÖ. Systemnutzungsentgelte für Strom. <https://www.wko.at/service/ooe/umwelt-energie/Die-Strom-Netzentgelte-2020-im-Detail.pdf>. Review date: 2021-03-01.
- [50] Austrian gas grid management: marktgebietsdaten. <https://platform.aggm.at/vis/visualisation/map>.
- [51] Zauner Andreas, Böhm Hans, Rosenfeld Daniel C, Tichler Robert. Innovative large-scale energy storage technologies and Power-to-Gas concepts after optimization. *Analysis on future technology options and on techno-economic optimization*; 2019. 28.02. <https://ec.europa.eu/research/participants/documents/downloadPublic?documentIds=080166e5c58ae3ff&appId=PPGMS>.
- [52] Bukold Steffen. Blauer wasserstoff : Perspektiven und Grenzen eines neuen technologiepfades. January, <https://www.greenpeace-energy.de/fileadmin/docs/publikationen/Studien/blauer-wasserstoff-studie-2020.pdf>; 2020.
- [53] Kayfeci Muhammet, Keçebaş Ali, Bayat Mutlucan. Hydrogen production. In: *Solar hydrogen production*. Elsevier; 2019. p. 45–83. <https://doi.org/10.1016/B978-0-12-814853-2.00003-5>.
- [54] Lehner Erich, Schrenk Katharina. Gutachten im Auftrag der OÖ Landesholding GmbH zum Investitions- und Kostenvergleich Freileitung–Erdkabel auf der 110 kV-Spannungsebene im ländlichen Raum. December. Linz; 2018. https://www.land-oberoesterreich.gv.at/Mediendateien/Formulare/Dokumente%20UWD%20Abt_US/4_RK_18_Gutachten_OoeLaHol_FINAL_20181221.pdf.

Article

Modelling and Simulation/Optimization of Austria's National Multi-Energy System with a High Degree of Spatial and Temporal Resolution

Matthias Greiml *, Florian Fritz, Josef Steinegger, Theresa Schlömicher, Nicholas Wolf Williams, Negar Zaghi  and Thomas Kienberger

Energy Network Technology, Montanuniversitaet of Leoben, 8700 Leoben, Austria

* Correspondence: matthias.greiml@unileoben.ac.at

Abstract: The European Union and the Austrian government have set ambitious plans to expand renewable energy sources and lower carbon dioxide emissions. However, the expansion of volatile renewable energy sources may affect today's energy system. To investigate future challenges in Austria's energy system, a suitable simulation methodology, temporal and spatially resolved generation and consumption data and energy grid depiction, is necessary. In this paper, we introduce a flexible multi-energy simulation framework with optimization capabilities that can be applied to a broad range of use cases. Furthermore, it is shown how a spatially and temporally resolved multi-energy system model can be set up on a national scale. To consider actual infrastructure properties, a detailed energy grid depiction is considered. Three scenarios assess the potential future energy system of Austria, focusing on the power grid, based on the government's renewable energy sources expansion targets in the year 2030. Results show that the overwhelming majority of line overloads accrue in Austria's power distribution grid. Furthermore, the mode of operation of flexible consumer and generation also affects the number of line overloads as well.

Keywords: 100% renewable energy sources (RESs); multi-energy system (MES) modelling; multi-energy system (MES) simulation; hybrid grid; national multi-energy system (MES)



Citation: Greiml, M.; Fritz, F.; Steinegger, J.; Schlömicher, T.; Wolf Williams, N.; Zaghi, N.; Kienberger, T. Modelling and Simulation/Optimization of Austria's National Multi-Energy System with a High Degree of Spatial and Temporal Resolution. *Energies* **2022**, *15*, 3581. <https://doi.org/10.3390/en15103581>

Academic Editors:

Zbigniew Leonowicz, Michał Jasiński and Arsalan Najafi

Received: 20 April 2022

Accepted: 10 May 2022

Published: 13 May 2022

Publisher's Note: MDPI stays neutral with regard to jurisdictional claims in published maps and institutional affiliations.



Copyright: © 2022 by the authors. Licensee MDPI, Basel, Switzerland. This article is an open access article distributed under the terms and conditions of the Creative Commons Attribution (CC BY) license (<https://creativecommons.org/licenses/by/4.0/>).

1. Introduction

Climate change is seen as a serious problem by ninety-three per cent of Europeans. According to the European Commission, the same number of Europeans have taken at least one action to tackle climate change. By setting up the ambitious “European Green Deal” program in December 2019, the European Commission aims to achieve a climate-neutral European Union by 2050 [1,2]. Concretizing the path towards achieving “European Green Deal” targets, the European Commission set up the “Fit for 55” program as an interim goal in July 2021. This program aims to reduce the European Union's carbon dioxide emissions by fifty-five per cent by the year 1990 [3].

As a member of the European Union, the Austrian government has set even more ambitious targets, aiming to achieve net CO₂ neutrality by 2040 [4]. Furthermore, the Austrian #mission2030 aims to achieve a hundred per cent renewable power generation net-balanced over one year until the year 2030. To achieve this target, renewable energy sources (RES), mainly volatile wind and photovoltaics, have to be expanded significantly [5].

The enhanced usage of RESs presents challenges for both the energy system and its operators since RESs are decentralized, hardly predictable, and introduce volatility into energy grids [6]. Achieving a hundred per cent RES might require:

- A spatial and timely compensation of energy;
- An increase in flexibility for both demand and generation in an energy system;
- The ability to cope with high instantaneous penetration of RES;

- Curtailment of RES as ultima-ratio.

In order to integrate a high share of RESs into existing energy systems and to avoid previously described issues, new approaches are necessary. In recent years, research focused on a cross-sectoral approach to consider the energy carriers' individual advantages in an energy system. This approach allows for the implementation of power, natural gas, district heating, hydrogen, and carbon dioxide grids, combined with storage and sector coupling (SC) options [7].

A need to address previously described challenges can be derived by looking at the distribution of RES in Austria. Sejkora et al. [8] provide a comprehensive overview of Austria's spatial distribution of technical exergy potentials of RES, which can be directly converted into RES energy potential [8]. Referring to Figure 1, it can be seen that renewable potentials are widely spread all over Austria, fluctuating in both the type of RES and the quantity in each district. However, it can be seen that wind potentials are mainly to be found in eastern Austria, whereas hydropower potentials are located in the western parts of Austria. Biomass and photovoltaics can be considered as more evenly distributed across Austria.

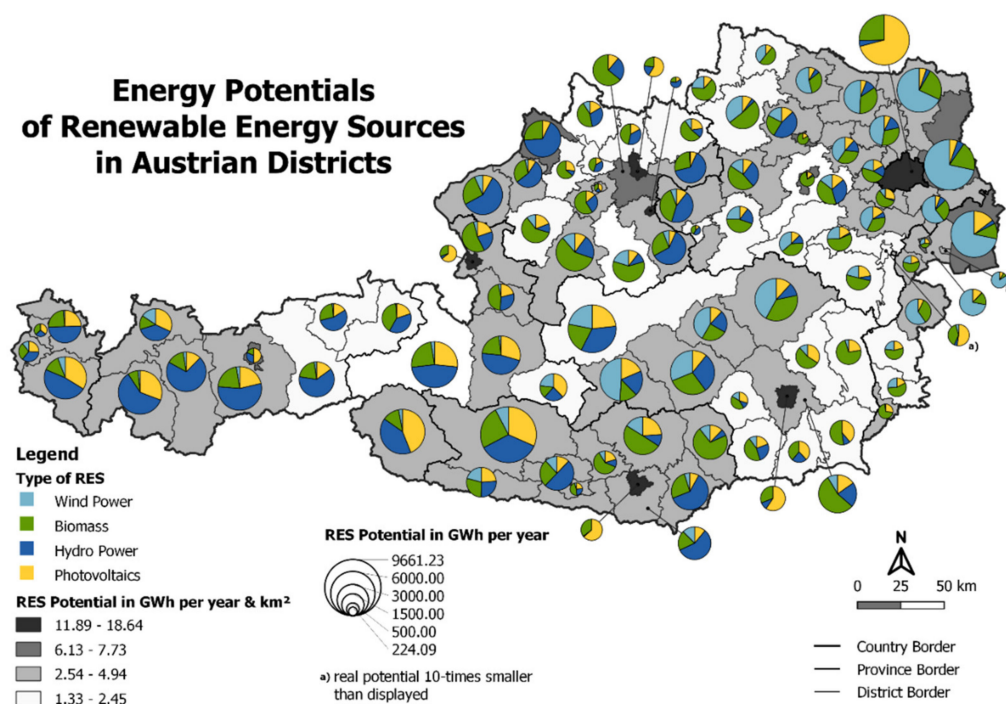


Figure 1. Technical energy potentials of RES per Austrian district, derived from [8,9].

Integrating further RES into the current energy system might lead to issues as previously disclosed. To address them, we introduce an updated multi-energy-system (MES) simulation framework, HyFlow, and discuss simulation results based on potential scenarios of the Austrian energy system in the year 2030.

1.1. Literature Overview and Research Need

As there are numerous publications on the topic of MES models, this section aims to display the current state of research regarding MES simulation and optimization approaches. Furthermore, we introduce research focusing on Austria's national multi-energy system models.

1.1.1. MES Simulation and Optimization Approaches

According to Klemm and Vennemann [10], energy system models can be methodologically categorized in optimization, forecasting/simulation, and back-casting. Depending on

the defined objective function, optimization is capable of determining an optimal solution or scenario. Forecasting or Simulation models show the system's behavior according to the selected input parameter. This scenario-based approach likely doesn't represent an optimal solution with regard to the selected boundary conditions. In back-casting models, an envisioned future state or properties are defined. Based on the future state, the back-casting model develops paths to these future conditions. Further categorization criteria could be assessment criteria, as well as analytical or mathematical approaches and challenges. The structural and technological details of MES models can include geographic coverage, spatial and temporal resolution, time horizon, sectoral coverage, and demand sectors [10].

Several pieces of research provide a comprehensive overview and comparison of existing MES assessment approaches, such as [10–14]. As can be seen in the before-mentioned sources, the predominant modelling approach for MES is optimization followed by simulation. Since the methodology described in this paper can be categorized as an MES simulation model, the following section focuses on MES simulation models. Still, it will also display differences compared to optimization models.

Bottechia et al. [12] introduce the modular, multi-energy carrier, and multi-nodal multi-energy system simulator (MESS). The framework is designed for urban areas; however, wider spatial coverage is also possible. The authors compare and investigate the cause of differences of MESS results with Calliope (MES optimization framework), based on a simple MES. The outcome of both methods tends to be similar yet different due to the individual model's target function and mode of operation. One further advantage of MESS over Calliope is a much faster computation time. A main disadvantage of MESS might be that only one grid level can be depicted [12].

A combination of Pandapower [15] and Pandapipes [13] is proposed by Lohmeier et al. [13] to create a multi-energy grid simulation framework with a focus on detailed energy grid depiction. The so-called multi-energy controller, similar to the energy hub concept, allows for the implementation of sector coupling or energy storage options. The authors demonstrate the capabilities of the MES simulation framework based on two use cases. Since detailed energy grid calculations, as well as multi-energy controllers, are computation time intensive tasks, one disadvantage of the proposed model is extensive computation time, when simulating a full year in 15 min time steps [13].

Böckl et al. [16] introduces a previous version of the MES simulation framework HyFlow, which is utilized for various research questions, such as [17–19]. By applying HyFlow, potential fields of improvements became visible, since the previous HyFlow version is not capable of addressing issues, such as:

- More than two individual network levels;
- No energy transfers across various network levels, since only step-by-step energy transfer via each network level is possible (energy must always flow via each network level without skipping network levels);
- A lack of selectable control strategies for both sector coupling and energy storage options;
- Implementation of further components of an energy system is only possible with high programming effort.

In [20,21], an MES optimization framework is proposed, consisting of individual energy hubs, interconnected with individual energy grids. Both models provide a two-stage optimization for the energy hub and the whole system. In dependence of the target function, individual research questions are addressed.

1.1.2. MES Investigations on National Level

This section aims to provide an overview of existing research on national MESs to demonstrate current research approaches.

Sejkora et al. [22] display how Austria's future energy system could be composed if exergy efficiency is defined as optimization criteria in a fully decarbonized energy system, where RES are expanded according to #mission2030 targets [5,22]. The research shows that

with restricted RES expansion in Austria, significant imports of sustainable methane and hydrogen will be necessary in the future. This research can provide guidelines for future technologies in MES, but cannot address any spatial problems [22]. In comparison, the project ONE100 from Austrian Gas Grid Management shows an energy system where RES are expanded until their maximum potential. In this case, import demand is significantly reduced to four per cent of total energy consumption. This research aims to achieve an economically optimized energy system. The model contains a rough spatial resolution of Austria, dividing Austria into 19 interconnected regions [23].

In [24], a comprehensive overview of research in the field of optimizing national energy system models is provided. However, the spatial resolution of each model shown is quite low. A lack of subnational data availability is seen as the main reason for the low spatial resolution [24].

1.1.3. Research Need

Flexible MES simulation frameworks to cover a wide range of individual problems are not available yet. Furthermore, to the best of our knowledge, it has never been attempted before to set up a national MES simulation model with detailed spatial resolution and detailed infrastructure depiction.

In this paper, we aim to close previously described scientific gaps by presenting a new version of our self-developed MES simulation framework HyFlow and demonstrate its capabilities based on Austria's energy system in 2030. The following research questions are to be investigated in this paper:

- Based on the scientific gap, how should an MES simulation framework be designed to cope with a national MES and various other research questions with a high degree of both spatial and temporal resolution?
- What steps have to be taken to model Austria's national energy system with detailed spatial and temporal resolution?
- What are the effects on power infrastructure based on #mission2030 renewable energy sources expansion, considering different modes of flexibility operation and power load flow optimization?

To answer the research questions this paper is structured as follows. The following subchapter describes considered challenges modelling the Austrian energy system. In Section 2, the methodology to set up an MES simulation framework and national MES model is described. Investigated scenarios and their corresponding results are disclosed in Sections 3 and 4, respectively. Simulation results are discussed in Section 5, followed by a conclusion and an outlook for potential further research in Section 6.

1.2. Problem Description

To address previously mentioned research questions, various obstacles need to be addressed beforehand. As demonstrated in the literature research, MES simulation frameworks that are currently available can be significantly improved to address a wide and flexible range of research questions, especially in the following fields:

- The flexible depiction of various network levels of all energy carriers (power, gas, heat), independent of spatial resolution. This should enable a large range of spatial resolution to be able to depict various areas, from single consumers up to the state level.
- The possibility to assign various flexibility options, such as sector coupling technologies, storage options, demand-side management (DSM), and operation-flexible power plants. This should include the possibility of flexibly adding any further components to expand the MES framework's functionality. Flexibilities may operate, e.g., as load following units or with various optimization-based operation strategies, such as maximizing profits or maximizing the degree of self-sufficiency in a specified area.

- State of art load flow consideration via adequate load flow calculation for all considered energy carriers. Depending on the user's selection, power flow simulation or optimal power flow load flow calculations should be selectable for the power grid.

The updated HyFlow MES simulation framework can address the previously mentioned points to develop a generic and flexible MES simulation framework.

As outlined in [24], a lack of subnational data is a major challenge when modelling a national MES. This challenge is addressed twice in this paper:

- Suitable approaches and data to be found to achieve a detailed spatial resolution. This includes consumption and generation data for all energy carriers. If data are not available in low spatial resolution, a suitable approach must be found to distribute general data towards smaller entities.
- Currently, no models of Austria's power, natural gas, and district heating energy infrastructure are openly available. To allow for the consideration of real grid properties, an energy grid model must be developed, based on available data to depict the Austrian energy infrastructure.

To demonstrate the capabilities of HyFlow, three scenarios of the Austrian energy system in the year 2030 are simulated to show the effects of RES expansion and various modes of operation of flexibilities, such as heat pumps, electric vehicles, power storage, and gas-fired power plants.

2. Methodology

This section is split into two main parts to provide a methodological overview of the HyFlow MES simulation framework and all the necessary steps to create an MES model of Austria, to be assessed with HyFlow.

2.1. HyFlow

To provide a comprehensive overview of the HyFlow MES simulation framework, the general modelling structure, the input data, the calculation procedure, and the implementation of flexibility options are discussed in the following sub-chapters.

2.1.1. General Modelling Structure

In HyFlow, the examined area can be divided into several cells. In this work, so-called substation districts are used (refer to Section 2.2.5. Spatial Data Distribution). This approach is called the cellular approach; further details can be found in [16]. All entities within one cell are aggregated into its corresponding cell. Therefore, a cell represents the smallest spatially resolved area, resulting in a node. In Figure 2, an example of a single node is displayed. To implement consumption and generation in one single term, the term "residual load" (RL) is used and defined as per Equation (1).

$$P_{RL}[t] = P_{demand}[t] - P_{Generation}[t] \quad (1)$$

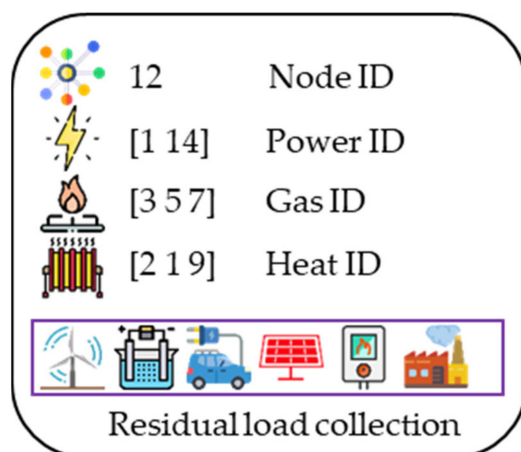


Image: Flaticon.com

Figure 2. Example of a single node.

In Table 1, an overview of the node parameters is provided. Further parameters such as maximum and minimum voltage, pressure, and temperature can also be defined.

Table 1. Overview node class parameters.

Parameter	Type	Description
Node ID	scalar	One unique number is assigned to each node.
Power ID	1 by 2 vector	Vector at [1 1] is currently a spare parameter. Vector at [1 2] indicates the node’s position in the power grid.
Gas ID	1 by 3 vector	Vector at [1 1] indicates the node’s pressure level (e.g., 2 = 70 bar). Vector at [1 2] indicates the node’s subgroup. Vector at [1 3] indicates the node’s number within the subgroup.
Heat ID	1 by 3 vector	Please refer to Gas ID.
RL collection	array	This array contains all objects, and their behavior can be expressed in active and reactive power, gas, or heat RL. Power RL is defined as per Equation (1), valid for all other energy carriers too. The RL collection in Figure 2 includes wind energy, electrolysis, electric car, photovoltaics, gas to heat (GtH), and an industrial consumer.

Nodes can be interconnected with other nodes. Depending on the availability of energy grids, a node-edge depiction is established. An example of several nodes with various connections of energy carriers (edges) is shown in Figure 3. It can be seen that all nodes are connected to the power grid. Nodes 12, 13, 14, and 327 represent one gas sub-grid. Node number 14 supplies gas to a lower pressure network (since the first vector position of gas ID is higher), consisting of nodes 26 and 27. As an example of RL collection objects, further implementable objects that can be added to a node’s RL collection, such as consumer, producer, sector coupling technology, storage options, and electric vehicles, are shown adjacent to their corresponding node.

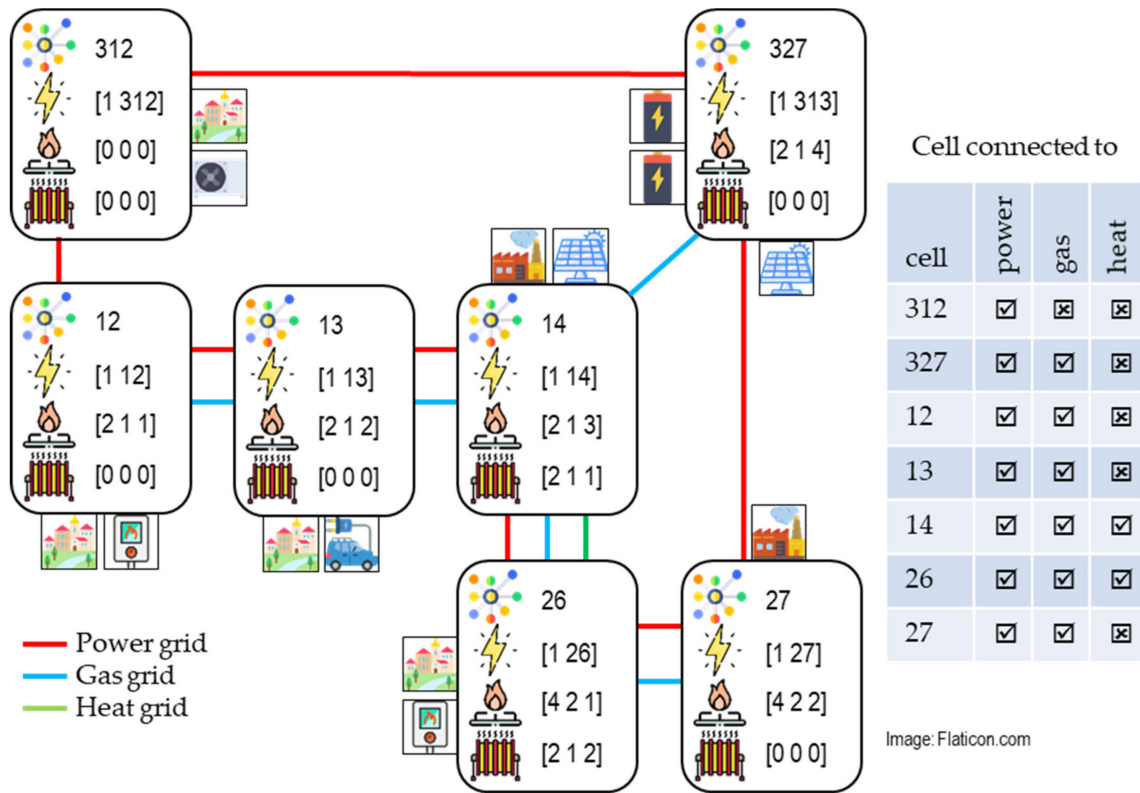


Figure 3. Energy infrastructure depiction.

To ensure that only the objects that are represented by an RL (refer to all classes hierarchically below “RL” in Figure 4) are addable to a RL collection, the programming principle of inheritance is used. A basic class “RL” is defined with simple properties (refer to Table 2 and functions). Based on the “RL” class, any derivative object can be developed and implemented by the user, with additional parameters to accommodate each object’s individual need. Figure 4 displays available derivatives of the “RL” class. In each class, individual operating strategies can be implemented, depending on the user’s need and addressed research question.

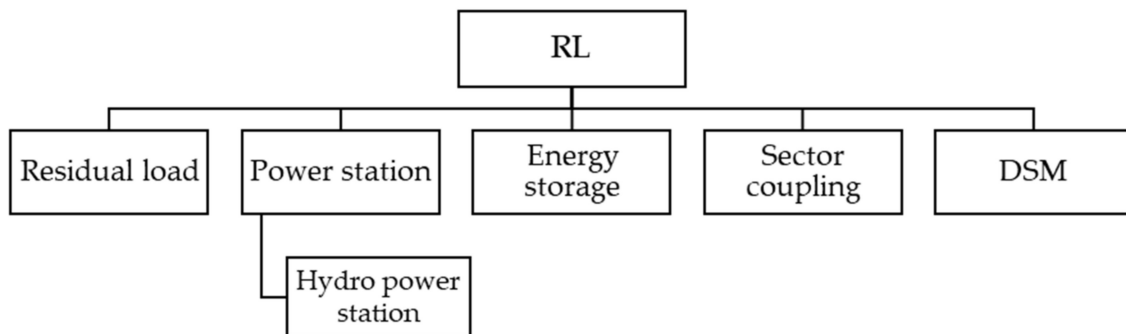


Figure 4. RL class and inherited derivatives.

Table 2. Overview of RL class properties.

Parameter	Description
<i>type</i>	<p>Defines the type of underlying object.</p> <p>Residual load or Power station 1: Pre-defined residual load profile or power station with predefined temporally resolved profiles (e.g., residual load, water flowrate).</p> <p>Sector coupling 2: Power to gas and heat (PtGH). 3: Power to heat (PtH). 4: Heat to power (HtP). 5: Gas to heat (GtH). 6: Gas to power and heat (GtPH).</p> <p>Energy storage 7: Power storage. 8: Gas storage. 9: Heat storage.</p> <p>DSM 10: Electric vehicle. 11: Demand-side management.</p>
<i>RLgas</i>	This vector contains the object's pre-set or calculated gas RL. The calculated gas RL depends on the object's operating strategy.
<i>RLheat</i>	Refer to <i>RLgas</i> .
<i>RLpower</i>	Like <i>RLgas</i> , except that active and reactive power RLs are considered.
<i>RLgasFlex</i>	These parameters contain the object's RL flexibility. The usage of these parameters depends on the object's operating strategy. The implementation of flexibility is explained in Section 2.1.4.
<i>RLheatFlex</i>	
<i>RLpowerFlex</i>	

2.1.2. Input Data

Before a simulation can be carried out in HyFlow, various input data need to be defined and read in for further processing. The input data are stored in individual objects, according to Table 2 and Figure 4. Node data must be defined, including parameters described in Table 1. Temporally resolved gas, heat, active, and reactive power RL data, including their associated node, can be defined. Properties for sector coupling options, storage, electric vehicle/DSM, and power stations (including their corresponding operating strategy) must be defined. Additionally, temporally resolved data for storage (e.g., water inflow in (pumped)-storage hydropower plant) are necessary. Properties include rated power, conversion or in-/output efficiencies, storage capacities, operating strategy, and further technology-specific properties.

Since the open-source power flow framework MATPOWER is used for power flow (PF) or optimal power flow (OPF) calculations, input data must reflect MATPOWER framework requirements. Therefore, tables for branch (=edge), bus (=node), generator, and generator cost data must be defined. The structure can be found in the MATPOWER documentation [25,26].

Gas and heat network properties follow the same principle scheme. For gas and heat, two tables need to be created. In the first sheet, connections between nodes at the same pressure level can be defined (e.g., between nodes 13 and 14 in Figure 3). The sheet number two contains connections between nodes at different pressure levels (e.g., between nodes 14 and 26 in Figure 3). Parameters are the gas or heat IDs of the connected nodes, length, diameter, roughness, and—in the case of heat—thermal conductivity of grid sections (edges).

2.1.3. Calculation Procedure and Grid Simulation

The calculation process of HyFlow is shown in Figure 5. The process of each dashed box will be explained further.

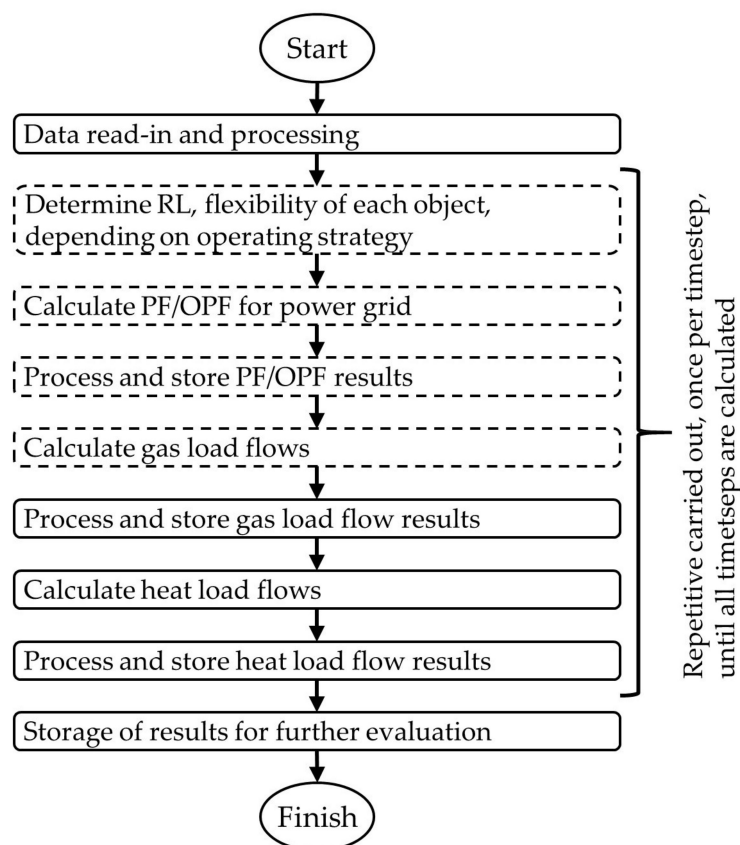


Figure 5. Overview of the calculation process.

Determination of RL

All objects in the RL collection of each specific node are assessed. Each object in the RL collection must provide an RL or flexibility based on the operating strategy of the object. The calculated summarized RLs and flexibilities of each node are transferred to the subsequent load flow calculations. The implementation and usage of flexibility are further explained in Section 2.1.4.

Power Grid PF or OPF

Depending on the users' selection MATPOWER PF or OPF, calculations can be performed for the power grid. Depending on the usage of PF or OPF, input data must be determined differently. In the case of PF simulation, all node residual loads and generator in-/outputs must be determined before a PF simulation can be performed. The PF simulation determines power load flows "as they physically are", without considering line restrictions or generation costs, for example. OPF mathematically optimizes load flows and generator dispatch, considering generation costs, line restrictions, and maximum/minimum generator power, based on the target function of minimum generation costs in the total power system [26]. Optimization restrictions, such as transmission line capacities or insufficient generation capacities, might cause an OPF to be incapable to converge. The advanced capabilities of OPF, compared to PF, come at the cost of higher complexity and increased likelihood of calculation failures. Further details regarding MATPOWER are provided in [26].

Before performing a PF or OPF calculation, bus (active and reactive power RL) and generator data (generation) must be updated in the MATPOWER data structure, based on the previous step's results (Determination of RL).

Gas and Heat Load Flow Calculation

Rüdiger adopts the node potential analysis for power grids in combination with Darcy's equation (refer to Equation (2)) to determine gas load flows [27].

$$\Delta p = \lambda \cdot \frac{8 \cdot \rho \cdot l \cdot \dot{V}^2}{d^5 \cdot \pi^2} \quad (2)$$

For heat load flows, Rüdiger's approach is extended by a second iteration loop to determine node temperatures and heat losses (refer to Equation (3) [28]) in both forward and return flow recursively.

$$T_{endnode} = (T_{startnode} - T_{ambient}) \cdot e^{\frac{-2 \cdot \pi \cdot k \cdot l}{c_p \cdot \rho \cdot \dot{V}}} + T_{ambient} \quad (3)$$

Both gas and heat load flow calculations can be characterized as steady-state load flow calculation approaches.

Process and Storage of Results

In the case of power OPF, MATPOWER determines each generator's generation based on minimum system generation costs. Therefore, the determined generation must be transferred to the corresponding object in the RL collection. The same procedure is necessary in case flexibilities are used. Depending on the energy carrier, further load flow calculation results such as load flows, voltage, angle, pressure, and temperature levels are stored.

2.1.4. Implementation and Usage of Flexibility Options

Power flexibility might generally accrue from sector coupling options, energy storage, or DSM, displayed by the yellow circles in Figure 6. Figure 6 also shows the general representation of each MES node, which is automatically adapted, depending on the properties of the node. A node optimization, similar to Chen et al. [29], is used to determine the node's flexibility band (green box in Figure 7) and usage of objects to provide flexibility (yellow box in Figure 7). Generally, node optimization aims to increase the profit of an MES (equal to minimizing costs), considering RL coverage, energy prices, technical properties of SC, and storage options [29]. This approach and its optimization target is adapted to determine the maximum/minimum power flexibility and the usage of objects providing flexibility, as explained further shortly.

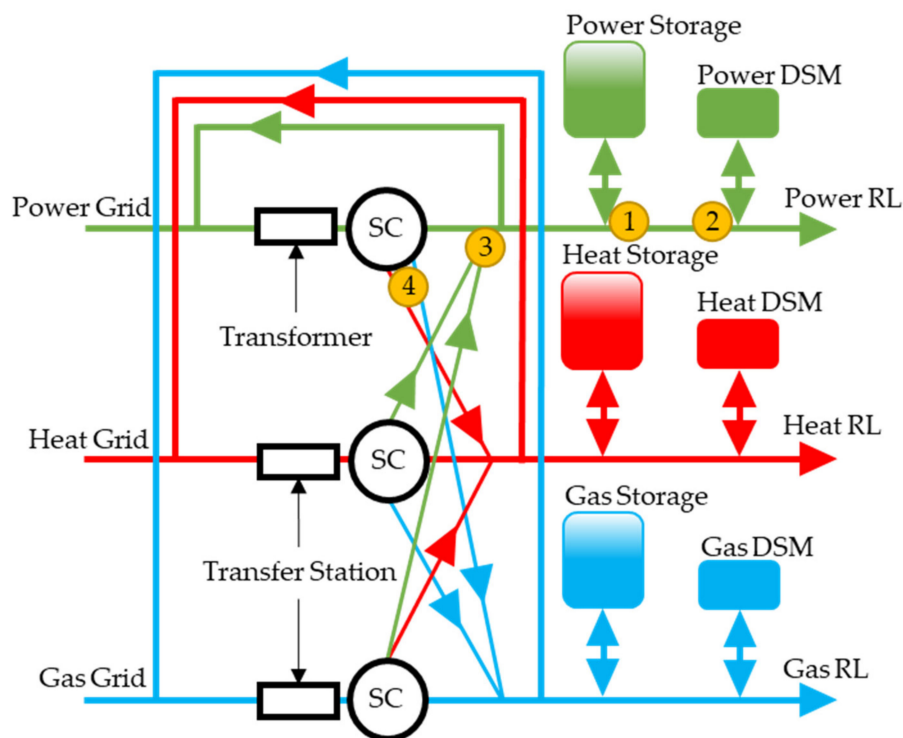


Figure 6. Generic node optimization representation.

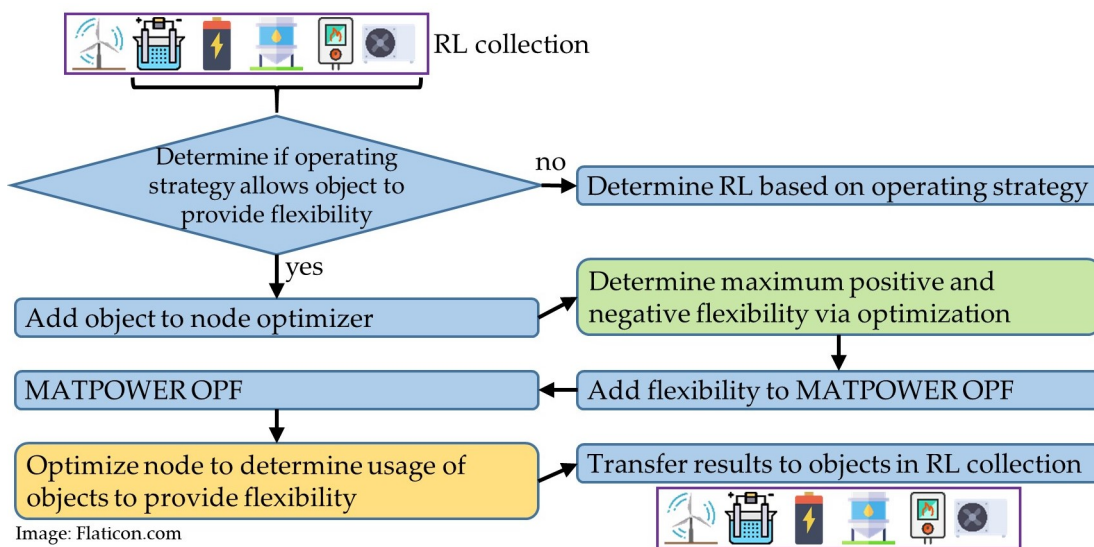


Figure 7. Process for optimized operating strategy, providing flexibility.

To consider flexibility in the HyFlow calculation process, the calculation process displayed in Figure 5 must be adapted. This adaption affects the upper three dashed boxes in Figure 5. The additional calculations to be performed are depicted in Figure 7.

If an object provides flexibility according to its operating strategy, it is considered for the following calculation procedure. If no flexibility is provided by the object, the RL is determined based on the objects operating strategy. To determine the total available flexibility per node, two optimizations are performed, aiming to determine the maximum possible positive and negative power RL (green box in Figure 7, target functions in Equations (A4) and (A5) in Appendix A), resulting in a flexibility band between both maximum and minimum power. For these optimizations, no energy prices are considered. The previously described calculation is carried out in the “Determine RL” section outlined in Figure 5.

Once a node's maximum positive and negative power flexibility is determined, it can be implemented in the MATPOWER framework as a generator at the corresponding node. The OPF, considering the whole depicted power system, determines the actual need for flexibility, ranging between the minimum and maximum possible flexibility of each node providing flexibility. So far, the need for flexibility at each node is determined; however, it is yet unknown which objects are used to what extent to provide the determined flexibility. To address this question, another node optimization is carried out (yellow box in Figure 7) to determine the actual usage of each object providing flexibility (target function in Equation (A1) in Appendix B). This optimization is carried out considering energy prices; therefore, the usage of the object is optimized economically. The determined optimal usage of each object providing flexibility is transferred to each corresponding object.

Yalmip [30] and Gurobi [31] are used to solve the optimization problems. Refer to "Appendix A. Node Optimization" for further mathematical details.

2.2. Austrian MES Modelling

The following modelling approaches are applied to develop an Austrian MES model. This includes an infrastructural depiction of power, natural gas, and heat grids, as well as timely and spatially resolved consumption and generation profiles.

2.2.1. Power Grid

The basis for the power grid model is a transmission grid plan. It shows the name of a substation's location and the transmission capacity of each line between substations for 110, 220, and 380 kV. However, the transmission grid plan only shows a past grid status. To determine a potential future power grid in 2030, potential grid expansion projects have to be included. The 220 and 380 kV transmission grid is operated by the Austrian Power Grid (APG), providing a grid development plan annually [32–37]. The 110 kV distribution grid is mainly owned and operated by nine local utilities in each federal state. Particularly for Upper Austria and Carinthia, detailed 110 kV grid expansion information is available [38,39]. Since the location of current and future substations and lines is roughly known, the geographic information system software QGIS [40], satellite images [41], and Open Street Map [42] are used to determine the exact location of substations and the course of power lines. MATPOWER requires line resistance, reactance, total line charging susceptance, and the maximum allowed apparent power flow [26]. APG provides detailed technical data for the transmission grid, which are used to parametrize the 220 and 380 kV grid [43]. The 110 kV grid is parametrized with literature values for resistance, reactance, and total line charging susceptance, as well as other already published projects [17,18,44,45], based on the maximum transmission current in the transmission grid plan.

2.2.2. Natural Gas Grid

To spatially depict Austria's natural gas infrastructure, we apply a similar approach compared to the power grid. Length and diameter for transnational pipelines and primary distribution system pipelines are available at Austrian Gas Grid Management (AGGM) [46]. The pipeline routing and length of national network level one (national transmission grid) and two (national distribution grid) can be derived from [47,48]. The diameter and pressure level are determined using statistical data [49], as well as information from utilities provided by request and previous projects [17]. Wall roughness is parameterized with the wall roughness of welded and seamless steel tubes [50].

2.2.3. Heat Grid

Currently, heat grids in Austria cover regional heat demand. Since the spatial resolution for an Austrian MES model is inadequate to depict regional heat grids, technical properties are assumed for interconnected regions, especially in urban areas. As a guideline, results from [51,52] are used to determine which areas of Austria are supplied with district heat.

2.2.4. Model of Austrian Natural Gas and Power Grid

Figure 8 displays the created model of Austria's power and natural gas infrastructure. It can be seen that the availability of Austria's energy infrastructure is much denser in urban and suburban areas in comparison to rural areas. Based on the infrastructure depiction in Figure 8 and Voronoi diagram methodology (refer to Section 2.2.5. Spatial Data Distribution), a corresponding node-edge model can be derived.

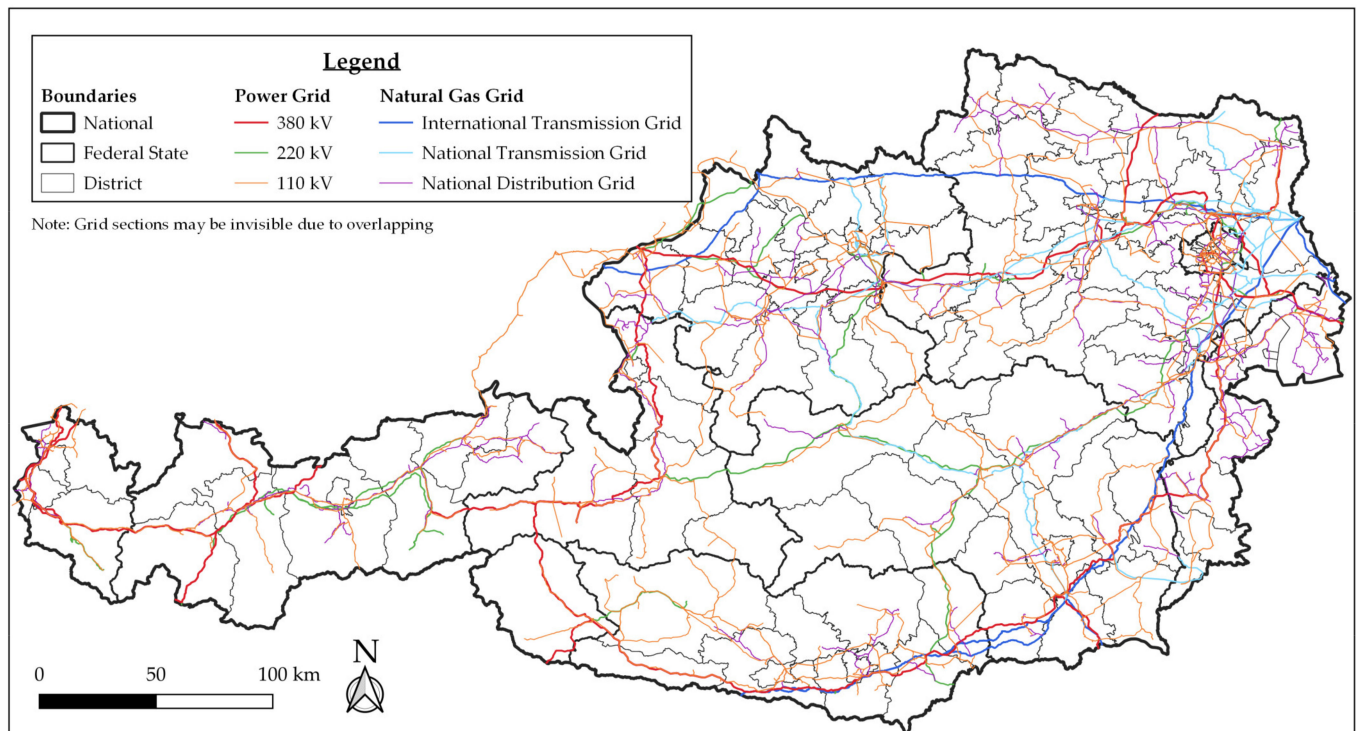


Figure 8. Model of Austria's power and natural gas infrastructure [9].

2.2.5. Spatial Data Distribution

To achieve a spatial resolution of Austria, a suitable methodology has to be selected to determine a spatial division of Austria. This is necessary to aggregate all objects (e.g., storage, power stations, RLs) within a spatial division into one node. A Voronoi diagram creates polygons starting from central points, dividing a layer into areas of equal nearest neighbors [53]. This approach is used with substations of the power grid as central points to determine single areas. The area covered by one substation is further referred to as a substation district (SSD). An example of the created SSDs within a selected area of Austria can be seen in Figure 13. In [8], the RES potentials of each Austrian community are determined. The RES potential data of each community are summed up to determine the SSD RES potential if a community is located within the boundaries of an SSD. Furthermore, power and natural gas (for both process and heating use) final energy consumption data from industrial, private, agricultural, and public and private service sectors are provided at a district level in [8]. To distribute final energy consumption data at the district level to a single community, the share of employees or households per community from *Statistik Austria*, in comparison to the district, is used [54]. Heat demand is modelled using the Austrian Heat Map [52]. Heat demand data are from 2012 but are quite stable till now [55]. Since heat demand data are available on a district level, and the same approach as for power and gas is used to distribute district demand to municipalities and then to SSDs. The useful energy analysis from *Statistik Austria* also provides information at the federal state level regarding the energy carrier used to provide heat [55].

2.2.6. Temporally Resolved Consumption Data

Annual energy consumption data of each SSD must be combined with temporally resolved load profiles to determine a temporally resolved RL profile for each SSD. For industrial power and gas demand, subsector specific load profiles are derived from [56]. For household, agriculture, and public and private service power consumption standardized load profiles (SLP) H0, L0, and G0 are used [57]. The reactive power is considered using literature and empiric values [58–60]. A $\cos(\varphi)$ of 0,98 is used. The temporal resolution of natural gas for non-heating purposes for households, agriculture, and service is determined based on the relatively steady cooking gas SigLinDe function [61]. The annual heating RL of each SSD is determined using the sectors corresponding SigLinDe function [61]. The temperature used as input data for the SigLinDe function is obtained for each SSDs substation from [62,63].

2.2.7. Temporally Resolved Generation Data

Oesterreichs Energie published a map of all power generation facilities in Austria with a power generation capacity greater than 10 MW [64,65]. In the following, we explain how each category of power station has been implemented into Austria's MES model.

Hydro Run-Off and Storage Power Station

The basic model of hydro run-off and storage power stations can be seen in Figure 9. Power generation is calculated using Equation (4) [66].

$$P = \eta \cdot \rho \cdot Q_{\text{Turbine}} \cdot g \cdot \Delta h \quad (4)$$

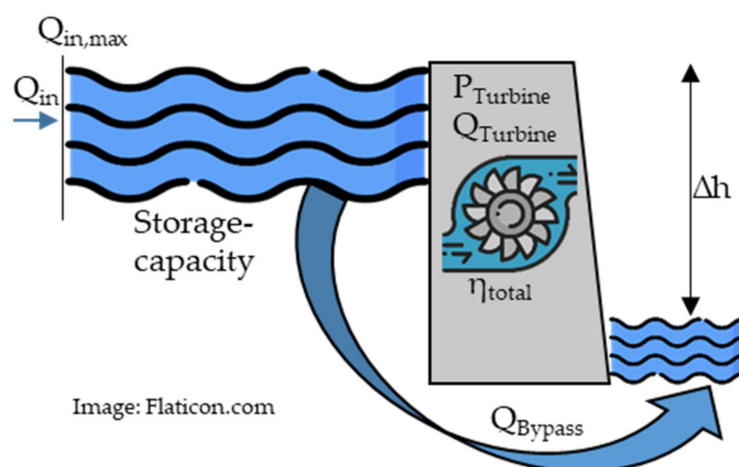


Figure 9. Hydro run-off and storage power plant model.

Each run-off and storage power station with a generation capacity greater than 10 MW is implemented into Austria's MES model in its corresponding SSD. Power station data are sourced from [67–79]. The temporally resolved generation is determined using run-off water measurements [80]. If the measurement point is different to the power station's location, interpolation is conducted between two measurement points. For hydropower stations with less than 10 MW, a different approach had to be used. *Kleinwasserkraft Österreich* [81] provides power and annual generation data for small-scale hydropower stations. These data are used together with hydropower potentials from [8] to determine small-scale hydropower in each SSD. Since no sufficient run-off measurements are available for small rivers, a standardized load profile based on measured data from small rivers (refer to Appendix B for measurement points) [80] is created, presented in Figure 10. A polynomial trend curve is used to smoothen the curve.

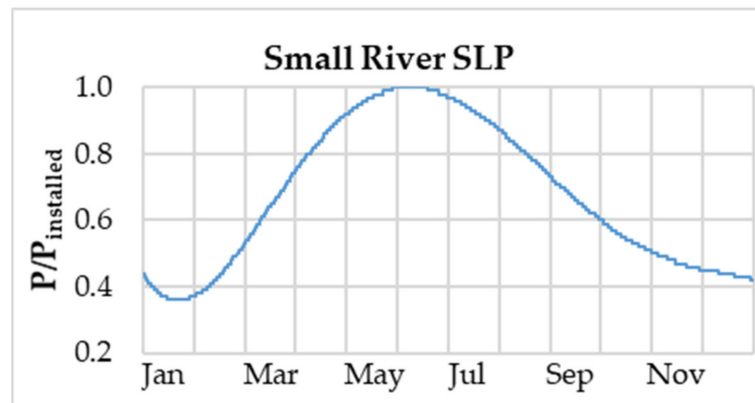


Figure 10. SLP small river, for small-scale hydro run-off power plants.

To cope with an additional 5 TWh of power, based on the government's RES expansion target [4], an increase in generation is carried out according to hydropower potentials from [82]. The small river SLP is used as a temporally resolved generation profile for these power stations.

(Pumped)-Storage Hydropower Plant

(Pumped)-storage hydropower plants are modelled as a simplified, flexible cascade of reservoirs, interconnected with pumps and turbines (refer to Figure 11).

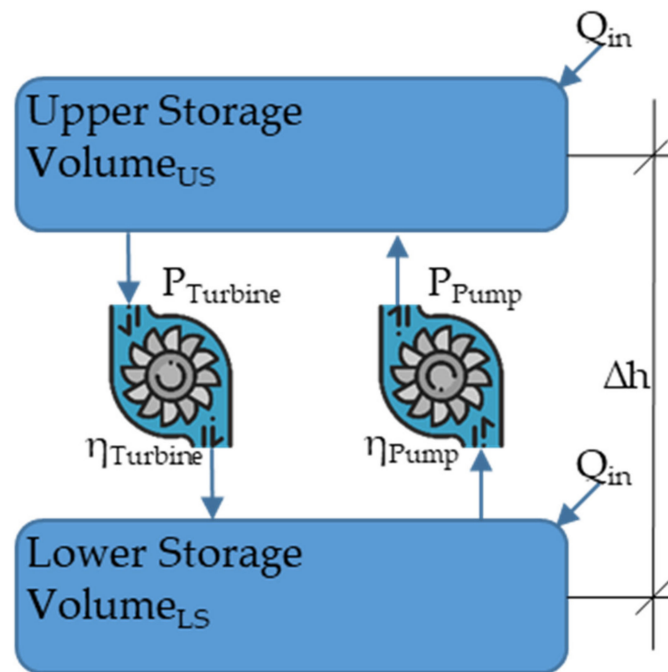


Image: Flaticon.com

Figure 11. (Pumped)-storage hydropower plant model.

Technical properties such as storage capacity (Volume), annual inflow from natural sources (Q_{in}), and pump and turbine power ($P_{Turbine}$, P_{Pump}) are sourced from [68–70,73–76,79,82–84]. Furthermore, future projects such as [85,86] are considered as well. The pump (η_{Pump}) and turbine ($\eta_{Turbine}$) efficiency is set to 0.88 [87]. Reservoirs are naturally fed by water from glacier or snow melt. To determine a temporally resolved water inflow, suitable measurement data from [80] are used to derive an annual water inflow characteristic, displayed in Figure 12 (refer to Appendix C for measurement points). It can be seen that

the majority of natural inflow occurs during the summer months; in contrast, hardly any inflow can be expected in the winter months.

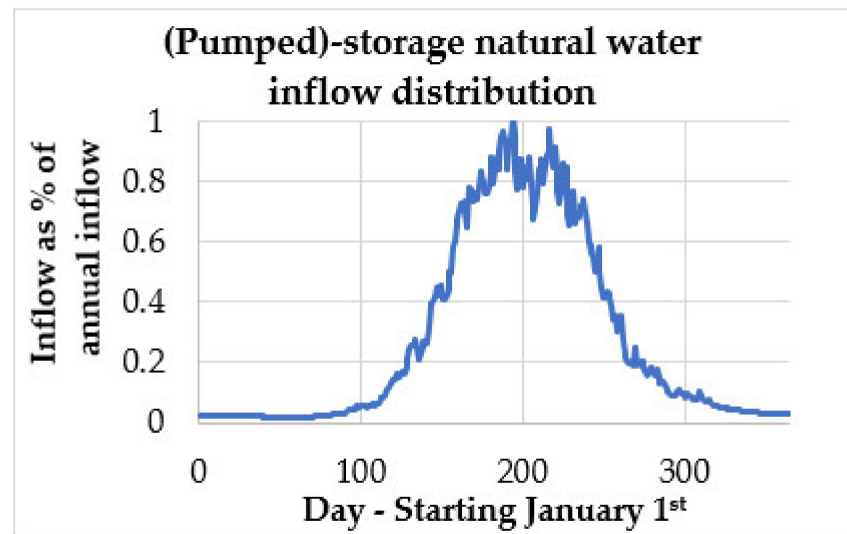


Figure 12. Annual (pumped)-storage hydropower plant natural inflow distribution.

The scenario-dependent generation and consumption profile for (pumped)-storage hydropower plants is described in the following chapter.

Biomass Combined Heat and Power (CHP) and Biogas Power Plants

Biomass CHP and biogas power plants are sourced from [88,89] and temporally resolved via SLP (E0) [57].

Photovoltaics

The installed photovoltaic power for each federal state is sourced from [90] and evenly distributed to each SSD via PV potentials from [8]. To reach the national goal of 11 TWh photovoltaics [4], photovoltaics are expanded, according to potentials in [8], by applying a split between rooftop and open area potentials of nine to one. Temporally resolved generation profiles are considered for each SSD, sourced from [62,63,91].

Wind

The locations of each wind park and their corresponding power levels are sourced from [92] and aggregated to the installed wind power of each SSD. To reach the national goal of 10 TWh wind power addition [4], the power at each SSD is evenly expanded according to potentials in [8]. Temporally resolved generation profiles are considered for each SSD, sourced from [62,63,93].

Thermal Generation

Technical data, such as power and efficiencies, of Austria's (combined cycle) gas turbine and large-scale CHP power plants are based on operators' publications [67,72,94–97]. If no efficiency data are available, an estimation based on comparable power plants is applied. The scenario-dependent generation profile is described in the following chapter.

2.2.8. Power Exchange with Neighboring Countries

Power exchange with neighboring countries of Austria is considered based on data from ENTSO-E's transparency platform for the year 2019 [98].

2.2.9. Example of Energy Infrastructure Depiction

An example of Austria's energy infrastructure and power plants can be seen in Figure 13. Exemplarily, an SSD is highlighted in yellow. The highlighted SSD contains several biogas plants and is connected to the power and natural gas grid. It can be seen that substations are concentrated in urban areas, whereas the substation density is lower in rural areas. More substations, compared to assignable municipalities, may especially occur in urban areas. In this case, suitable substations are manually selected and merged to create the Voronoi diagram. Hydropower plants are concentrated along large rivers, whereas wind, biomass CHP, and biogas are spread all over the area.

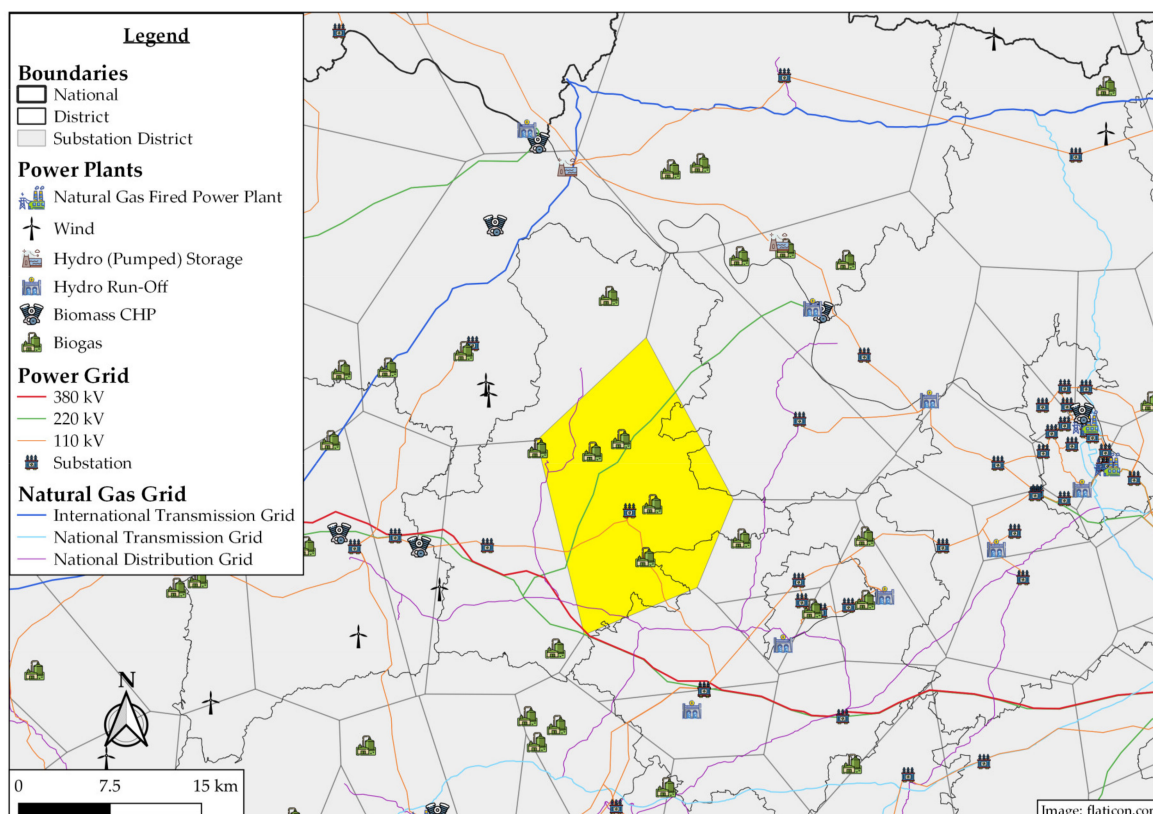


Figure 13. Example of Austria's energy infrastructure and power plants [9].

3. Scenarios

In this chapter, potential developments of the Austrian energy system are investigated based on three scenarios for the year 2030. Therefore, we apply the methodologies shown in Section 2. The following points are considered for each scenario:

- Since power, gas, and heat consumption are based on past data, sufficient studies need to be found to estimate the energy consumption in 2030. Austria's *Umweltbundesamt* (UBA) [99] estimates energy consumption in the years 2020, 2030, and 2050, based on the year 2015. Power demand is expected to remain stable between 2015 and 2020 and then increase between seven and thirty per cent, depending on the scenario. Electric vehicles, heat pumps, and electrolysis are seen as major drivers of power consumption growth. Since these consumers are additionally considered in each following scenario, we assume that the power demand will stay constant without. Depending on the scenario, a slight increase or decrease in natural gas consumption is assumed by UBA; therefore, we assume constant consumption [99]. Based on #mission2030 targets, thermal renovation of existing buildings should be doubled to two per cent per year, from current levels of around one per cent [5]. If a 50% heat demand reduction through a thermal renovation is assumed, heat demand might drop by thirteen per

cent, until 2030. The assumption of 50% heat demand reduction seems reasonable since subsidiaries are granted if more than 40% heat demand reduction is achieved [100]. The 13% heat reduction is between both *UBA* scenarios (WAM, WEM) for the final energy consumption of buildings [99].

- The number of electric vehicles in each SSD is determined based on vehicle registration data and trends in each federal state [101]. The share of electric vehicles in 2030 is expected to be 20%, based on scenarios in [102]. In Austria, a car is used for an average of 13,700 km per year. Based on the average consumption of 20 kWh/100 km, an annual electric energy demand per car of about 2750 kWh can be expected [103,104]. The temporal charging characteristic is scenario-dependent and can be explained in the following subchapters. All electric vehicles account for approximately 3 TWh of additional power consumption.
- The share of heat pumps for each SSD is determined based on the share of ambient heat usage for heating purpose divided by an assumed coefficient of performance of three [55]. Heat pump usage might increase by six-fold until 2030 based on [105]. The mode of operation depends on the scenario. All heat pumps account for approximately 1.9 TWh of additional power consumption.
- For every fourth household, battery energy storage with a storage capacity of 8 kWh, charging–discharging power of 2 kW, and an input–output efficiency of 90% [106] is implemented with a scenario-dependent mode of operation.
- Renewable energy sources are expanded according to plans of the federal government, shown in Table 3.

Table 3. Expansion of RES until 2030 [4,107].

RES	Generation 2018	Expansion Until 2030
Hydro	37.6 TWh	+5 TWh
Wind	6.0 TWh	+10 TWh
Photovoltaics	1.5 TWh	+11 TWh
Biomass	4.9 TWh	+1 TWh
Total	50 TWh	+27 TWh

Table 4 below provides an overview of the differences between each scenario. The modes of operation are explained in each scenario description.

Table 4. Scenario parameters.

	Scenario 1	Scenario 2	Scenario 3
Thermal generation and (pumped)-storage hydro	ENTSO-E	ENTSO-E	Flexibility
Electric vehicle	SLP	Optimized	Optimized
Battery storage	Greedy	Optimized	Optimized
Heat pump	Load following	Optimized with storage	Optimized with storage
Power grid calculation	PF	PF	OPF

3.1. Scenario 1—BAU

In this scenario, certain elements of the energy system are operated in the business-as-usual (BAU) mode. Electric vehicles are charged according to the SLP, derived from [108], with 3.7 kW charging power. Since the number of electric vehicles is above 1000 for the vast majority of substation districts, a low coincidence factor can be applied [108,109]. Heat pumps are operated as heat demand occurs, without a storage option. Temporal battery

storage behavior is determined as follows. The energy demand of an average household per SSD is coupled with an SLP (H0 [57]) and a 5 kW photovoltaic generation capacity, considering the SSDs' individual PV generation profile. One-quarter of households are equipped with battery storage. The battery storages operate according to the greedy algorithm to minimize the household energy demand from the power grid. Examples of the application of the greedy algorithm can be found in [110,111]. (Pumped)-storage hydropower and thermal power plants are operated according to *ENTSO-E* generation data from 2019 [98]. The resulting power RLs are added to each SSDs RL.

3.2. Scenario 2—Demand Optimization

Demand optimization is applied in this scenario to operate certain elements economically. An optimization concept similar to energy hubs is used to determine an economically optimized mode of operation of energy storage, heat pumps, and electric vehicles [29]. To enable a flexible operation of heat pumps, each heat pump is equipped with a thermal storage capacity of 50 kWh and a charging–discharging capacity of 10 kW. Electric vehicles charge their average daily consumption of about 7.5 kWh with 3.7 kW charging power. Peak demand times (6:00–9:00 and 17:00–20:00) are excluded from charging. The optimization is carried out, using power price data from 2019 [112] and each node's RL. As a result, price-optimal RLs of heat pumps, power storage, and electric vehicles are determined and added to each node's RLs.

3.3. Scenario 3—Demand Optimization and Flexibility

Heat pumps, electric vehicles, and battery power storage are operated, like in Scenario 2. Thermal power plants and (pumped)-storage hydropower plants are operated as additional flexibility (refer to Section 2.1.4). Since generation costs are considered in OPF for generator dispatch, the generation costs of each power source are set as follows:

- Subsidized forms of power generation, such as biogas, biomass CHP, wind, photovoltaics, and small-scale hydropower with 10 EUR/MWh;
- Large-scale hydropower 50 EUR/MWh;
- Flexibilities (gas turbine and CHP and (pumped)-storage hydropower) and import/export with 100 EUR/MWh.

4. Results

In all three discussed MES scenarios, natural gas and district heat grids show no critical overloads. Therefore, power grid results are discussed in detail. In Table 5, a comparison of overloaded distribution power grid (DG) and transmission power grid (TG) lines are displayed. Scenario 2 shows that the number of time steps, as well as affected power grid lines, increases compared to Scenario 1. This can be explained by the price-optimized mode of operation, since demand increases disproportionately in time steps with cheaper power, leading to RL peaks.

Table 5. Comparison of scenario results.

	Scenario 1	Scenario 2	Scenario 3
Overload time DG	182,205 time steps	206,592 time steps	81,991 time steps
Average DG line overload	38.8%	42.5%	35.5%
Count of overloaded DG lines	39/480	57/480	40/480
Overload time TG	3904 time steps	8131 time steps	144 time steps
Average TG line overload	16.0%	16.3	30.1%
Count of overloaded TG lines	5/104	7/104	6/104

To evaluate the degree of power line overloads, two different overloads are evaluated. As displayed in Figure 14, the average line overload and the top five per cent (based on the number of overloaded time steps) of line overloads are determined for each power grid line.

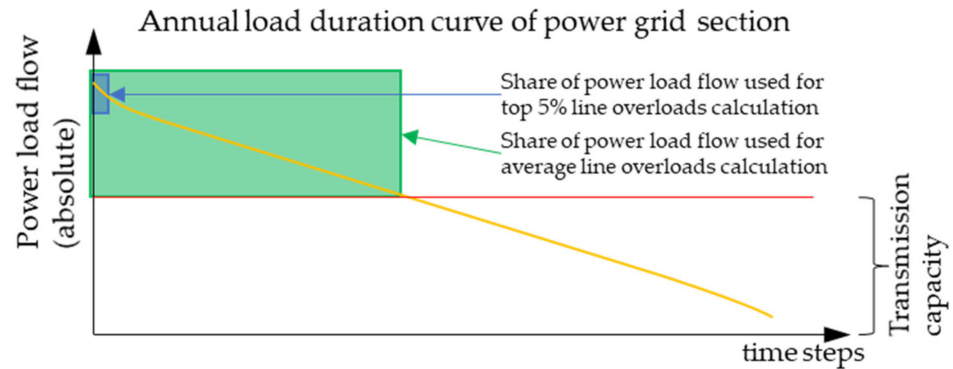


Figure 14. General determination of line overloads (an average and the top five per cent).

Subsequently, the worst (Scenario 2) and best (Scenario 3) case scenarios in terms of line overloads are displayed. In Figure 15, the average line loadings of Austria's power grid are displayed for Scenario 2. The thickness of each line qualitatively indicates the maximum transmission capacity of each line. Green lines indicate grid sections that are not affected by overloads. Orange to red lines indicate the average degree of overloads of the affected line section. Exemplarily, some grid sections are marked with a purple circle or ellipse-shaped indicators, allowing for the differentiation of the following overloads types:

- Continuous purple line—sections with low transmission capacity, e.g., single three-wire system;
- Dotted purple line—overloaded lines in urban areas;
- Dashed purple line—branch line with low transmission capacity in combination with either high potential of RES generation or demand;
- Dashed-dotted purple line—high potential of RES expansion.

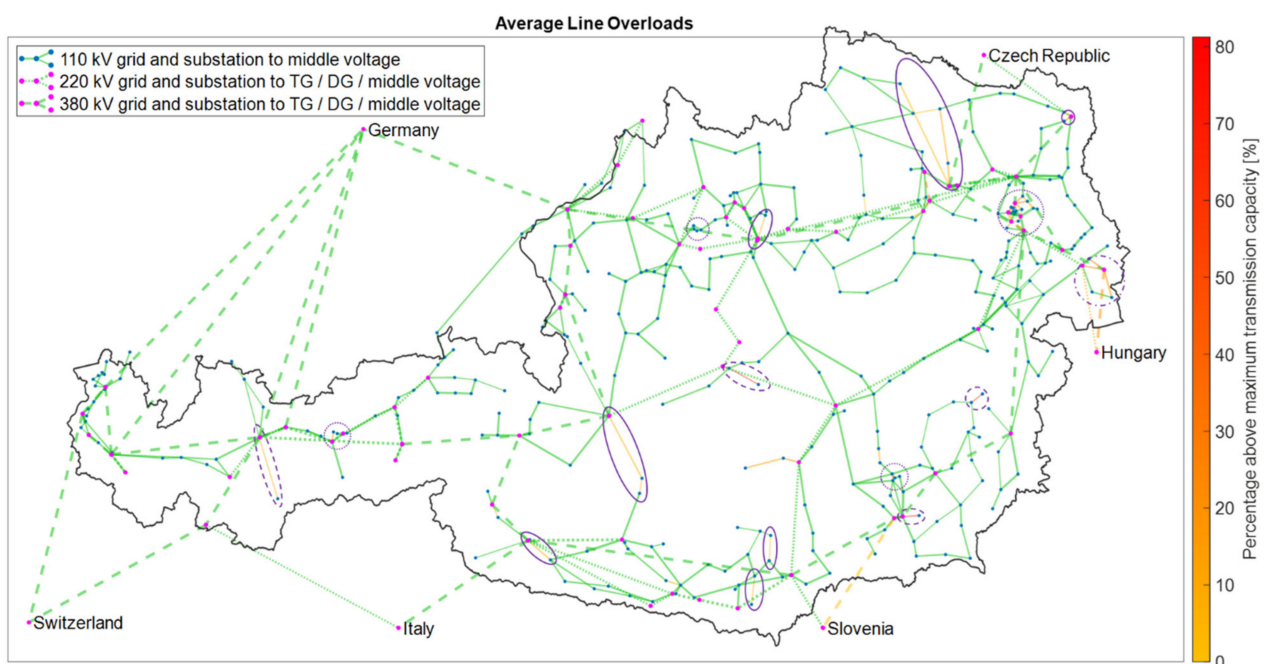


Figure 15. Average line overloads of Austria's power grid—Scenario 2.

In Figure 16, the top five per cent overloads of Austria’s electricity grid are displayed for Scenario 2. It can be seen that most overloaded transmission and distribution grid lines are overloaded by a rather small degree.

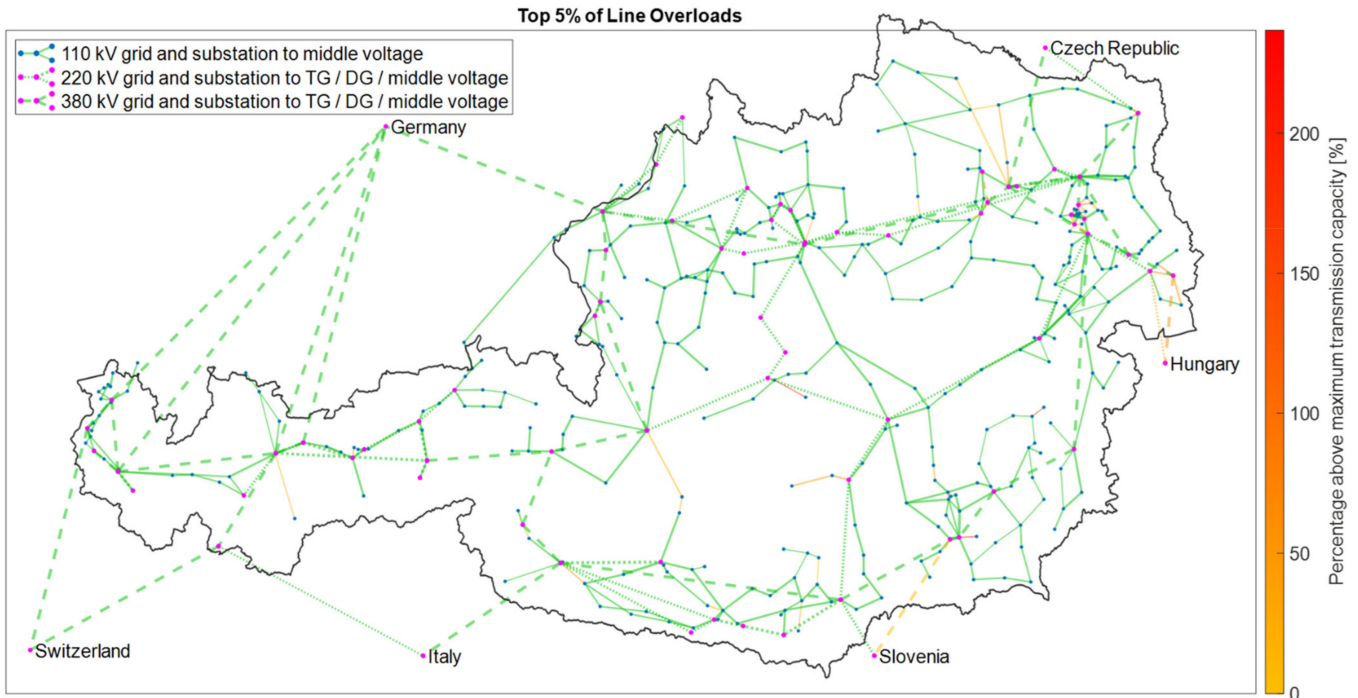


Figure 16. The top 5% line overloads of Austria’s power grid—Scenario 2.

In following Figure 17 the annual load curve for a highly overloaded power branch line is displayed. It can be seen that the maximum transmission capacity is exceeded in both positive as well as negative direction. A positive and negative sign is related to the direction of power flow. This means that branch line overloads are caused by both consumptions at the end of the branch line and excess generation flowing from the end of the branch line towards the distribution grid.

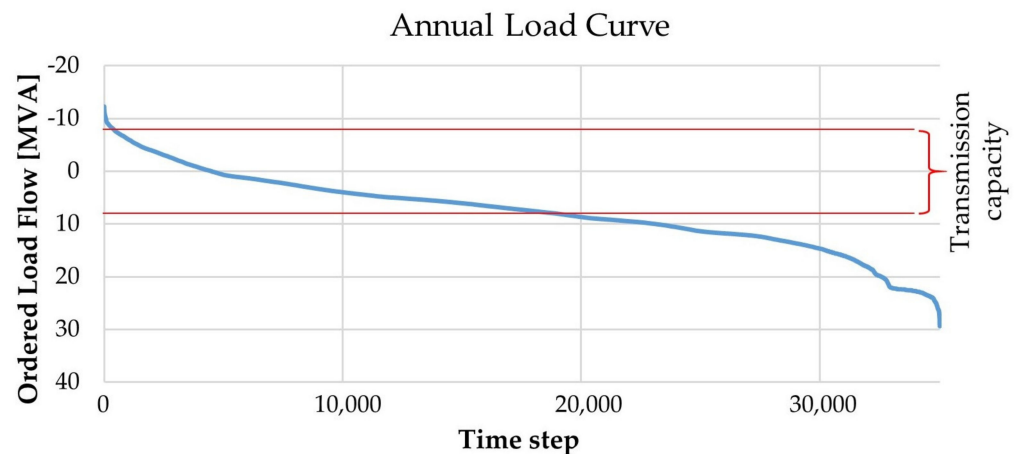


Figure 17. Annual load curve of a power branch line (ranked from min to max).

In Figure 18, the average power grid line overloads are displayed for Scenario 3. In comparison to Figure 15, the magnitude of the average overloads is significantly lower (refer to the scale magnitude). This observation is supported by line overload data displayed in Table 5, where line overloads in Scenario 3 are approximately halved in terms of

count, compared to Scenarios 1 and 2. A similar context can be observed by comparing Figures 16 and 19 where the magnitude of the top five per cent of overloads are significantly lower in Scenario 3, compared to Scenario 2.

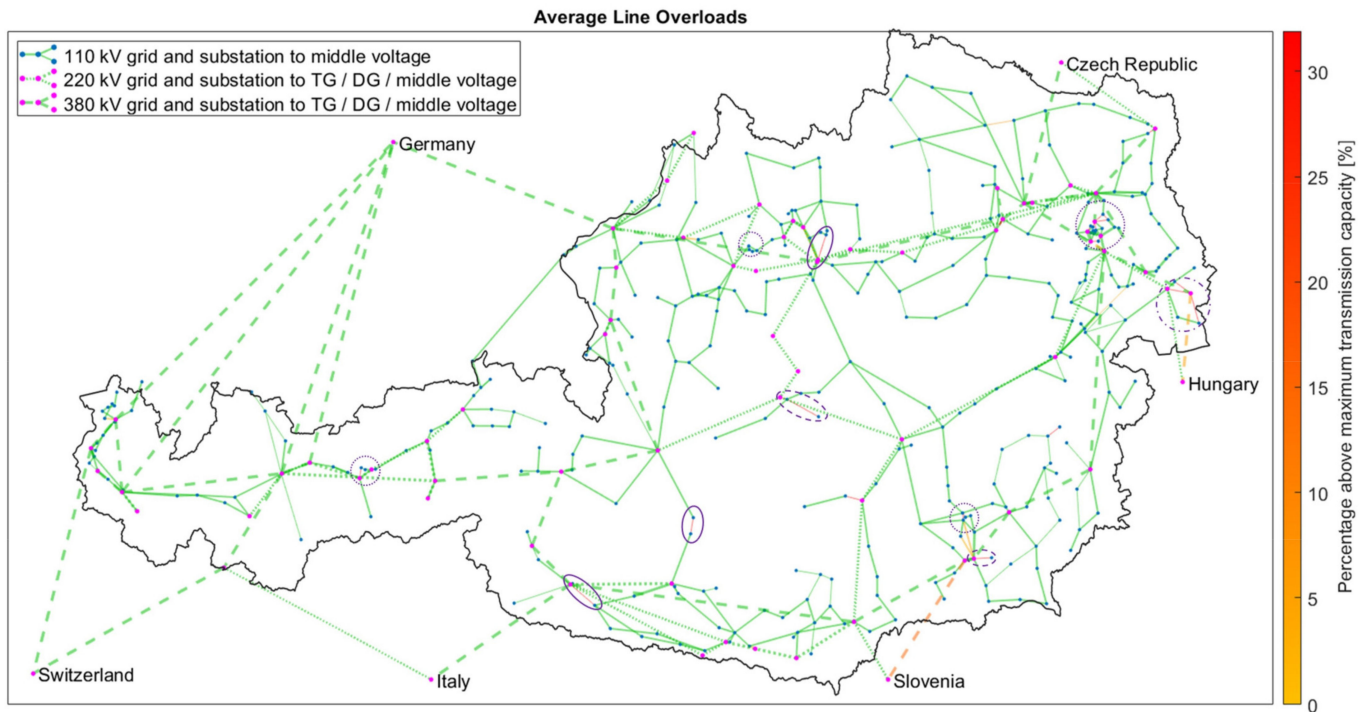


Figure 18. The average line overloads of Austria's power grid—Scenario 3.

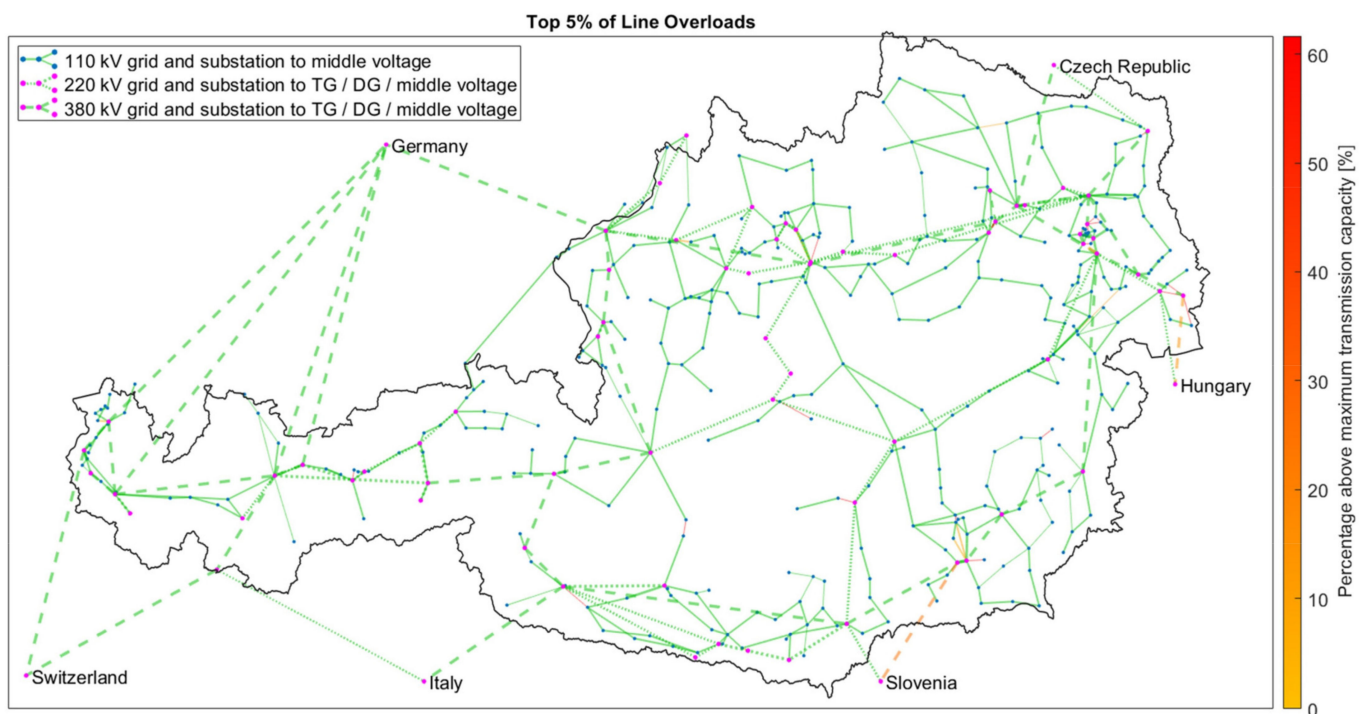


Figure 19. The top 5% line overloads of Austria's power grid—Scenario 3.

In Table 6, the power generation from each source is displayed for each scenario. It can be seen that the results for Scenarios 1 and 2 are identical, except for a small difference in imported and exported power. However, in Scenario 3, the generation from gas turbine

and CHP and (pumped)-storage hydropower is reduced by about fifty per cent compared to generations from Scenarios 1 and 2. The lower generation from both before-mentioned sources reduces power exports by about one third compared to Scenarios 1 and 2. The curtailment of generation occurs in Scenario 3 only, since OPF is used instead of PF for power load flow calculation to avoid line overloads. Imports and exports are calculated based on power line load flows connecting Austria with neighboring countries; therefore, the calculated power energy imports and exports do not consider loop flows.

Table 6. Comparison of power generation for each scenario.

	Scenario 1	Scenario 2	Scenario 3
Biomass	6.0 TWh	6.0 TWh	6.0 TWh
Photovoltaics	12.1 TWh	12.1 TWh	12.1 TWh
Wind	15.5 TWh	15.5 TWh	15.5 TWh
Gas turbine and CHP	10.8 TWh	10.8 TWh	Consumption: 0.83 TWh Generation: 8.2 TWh
(Pumped)-storage hydropower	Consumption: 1.5 TWh Generation: 8.5 TWh		
Hydropower >10 MW	27.9 TWh	27.9 TWh	27.9 TWh
Hydropower ≤10 MW	11.6 TWh	11.6 TWh	11.6 TWh
Import	8.1 TWh	10.5 TWh	3.7 TWh
Export	36.0 TWh	37.5 TWh	23.0 TWh

5. Discussion

In this section, we discuss the temporally and spatially resolved MES model of Austria, as well as the simulation results.

5.1. MES Model of Austria

Although Austria's #mission2030 aims for a net-balanced RES power supply over one year, depending on the applied scenario, significant power exports compared to imports are visible in Table 6 [5]. This gap can be explained exemplarily for Scenario 3 as follows. In Austria's MES model, power generation from company-owned CHP and power plants is not considered, since power is generated behind the meter and, therefore, company internally used. The internal generation reduces a company's power demand from the grid, as considered in the consumption data source [8]. This internal generation accounts for a total power generation of approximately 8 TWh [107]. The 7.5 TWh generation of the gas turbine and CHP has to be considered as well, since it is not a RES and therefore is not considered in the #mission2030 power generation target [5]. The remaining 3.8 TWh contain power grid losses, self-consumption of power plants, pumped-storage hydropower losses, variations of input data from [8], and others. This is in accordance with Austria's #mission2030.

The lack of subnational data available is seen as a main reason for a low spatial resolution in MES optimization projects [24]. These issues also present a main challenge within this work; however, based on experiences in [8], proven strategies are used to distribute aggregated data to more detailed granularity.

The Voronoi diagram is used because a more detailed approach may require further infrastructure data (e.g., roads) [113]. The Voronoi diagram does not take any local and geographical properties into account. Therefore, a community might be assigned to an SSD located across a mountain chain, for example. This case of misallocation is investigated manually since a small number of municipalities are affected. However, in this case, the municipalities are rather small in terms of energy consumption; therefore, the error of misallocation is considered to be negligible.

The usage of SLPs is valid if a number of several 100 consumers is aggregated [114]. This number is achieved for residential and to a smaller degree, for agricultural as well as public and private services consumers. The number of industrial consumers is significantly lower compared to the residential and service sectors. The quality of temporal consumption data can be further improved in the industrial sector, provided that more accurate industrial load profiles are available.

A temporal resolution of minutes to hours and days is common for MES frameworks which cover local levels up to regional and national levels [115]. This is important since the availability of data defines the achievable temporal resolution. For example, SLPs are available for 15 min (residential, agricultural, public, and private services) or, in the case of industrial SLPs, one-hour intervals. In comparison, wind and photovoltaic generation profiles are temporally resolved over one hour, whereas water flow rates, used to calculate hydropower plants generation, are available as daily averages. Although the simulation is carried out in 15 min interval time steps, a one-hour time step might be considered in the future to decrease computation time. Generally, simulating an MES system of the displayed size for a full year in 15 min's interval time steps takes approximately 2 days of calculation time. If node optimization is used additionally (Scenario 3), the computation time increases further.

5.2. Simulation Results

As displayed in Table 5, line overloads can be significantly reduced by more than fifty per cent in Scenario 3 compared to Scenarios 1 and 2, showing a positive effect of OPF and flexibility usage. Transmission line capacities represent a constraint using OPF applied in Scenario 3, therefore a number of zero line overloads should be expected. However, based on simulation results from Scenarios 1 and 2, the capacity of overloaded power grid sections is increased to enable the OPF to converge, since any unsolvable violation of transmission capacity would result in a termination of an OPF calculation. The count of the overload time for Scenario 3 is carried out using the original transmission capacity used in Scenario 1 and 2, considering the load flow occurring with increased line capacity.

Depending on the scenario, more than ninety-five per cent of line overloads occur in the distribution grid. Overloads can be caused by various reasons such as high RES potentials, low transmission capacity or in urban areas. No clear reason could be identified for overloads in urban areas. Potential issues might arise from the data source (consumption data) or loss of precision due to the need for grid simplification in urban areas.

In Scenario 3, the export of power is reduced significantly in comparison to Scenarios 1 and 2, since the power generation from natural gas CHP, gas turbine and especially (pumped)-storage hydropower plants is reduced. This is achieved by operating gas turbine and CHP, and (pumped)-storage hydropower plants as dispatchable flexibility. Since (pumped)-storage hydropower plants are located in western Austria and gas CHP and turbine are close to cities (=high power consumption), natural gas CHP and turbine are more likely to be activated due to lower transmission losses. This point can be further addressed through different flexibility pricing to favour (pumped)-storage hydropower usage over natural gas turbine and CHP power plants. However, this might have effects on the west-east power transmission in Austria's power grid.

6. Conclusions and Future Outlook

Within this work, we introduce a unique MES simulation framework and investigate the effects of the expansion of renewable energy sources on Austria's energy infrastructure based on a created MES model within this work.

The literature review has shown that current available multi-energy system simulation and optimization frameworks are not capable of depicting a national MES with a high degree of both high spatial and timely resolution. To overcome this scientific gap, the updated MES simulation framework HyFlow is introduced. The proposed MES simulation framework is capable of implementing the energy carrier power, natural gas and district

heat (and their corresponding energy grid infrastructure), a broad range of individual consumers and producers, as well as storage and sector coupling options. Due to the flexible MES depiction approach, a wide range of research questions can be addressed. We believe that the HyFlow framework is unique in both existing and potential expansion capabilities and should be used to address various further research questions. This may include the addition of further capabilities to be added to the existing MES framework, such as further modes of operation, new objects, or improved gas and heat load flow calculations.

To depict a national MES, three main points must be addressed. First, detailed energy infrastructure models must be available. Due to the unavailability of Austria's energy grid infrastructure models, sufficient available sources and data from existing research are used to create a detailed model of Austria's energy infrastructure. Second and third, the examined area must be fed with both spatial and time-resolved consumption and generation data. To spatially resolve Austria, Voronoi diagrams based on power grid substations are used to divide Austria into so-called substation districts. To time-resolve the energy demands and generations of each substation district, a combination of SLPs and real-measured data is used. The created MES model of Austria may serve as a foundation for any further assessments of the Austrian MES. Potential fields could be the implementation of further flexibilities (e.g., storage and sector coupling) or assessment of other energy grids (gas, heat). If detailed RES expansion plans are available, the spatial distribution of RES expansion can be updated and its effects on energy grid infrastructure can be further investigated. New energy grid projects can be added to increase the transmission capacity between SSDs. We believe that this demonstrated approach can be a useful guideline to create a spatially and temporally resolved model of any national or regional MES.

Based on the created MES model of Austria and the presented MES simulation framework HyFlow, three scenarios are examined. The scenarios investigate the effects of Austrian government targets to achieve a one hundred per cent renewable power generation, net-balanced over one year. Renewable generation is expanded (mainly volatile wind and photovoltaics) by the aimed amount of the Austrian government. Additionally, electric vehicles, battery storage, and heat pumps are implemented into the MES simulation to an expectable future degree. Each scenario considers the same renewable expansion but differentiates between modes of flexibilities operation, such as (pumped)-storage hydropower, gas-fired power plants, heat pumps, electric vehicles, and battery storage. Results show that the mode of operation of flexibilities and the power load flow calculation methodology (PF and OPF) can lead to significantly different results, in terms of power line overload counts. By optimizing the consumption and generation of electric vehicles, battery storage and heat pumps based on the power price timeline (=market oriented), short demand peaks can occur, leading to the highest count of power grid overloads of all three investigated scenarios. In contrast, using OPF in combination with the flexible dispatch of natural gas-fired and (pumped)-storage hydropower plants line overloads are reduced by more than fifty per cent. The usage of OPF is therefore advantageous in contrast to PF, in terms of flexibility usage. It can be concluded that a solely price-optimized operation (market oriented) leads to grid overloads due to the neglectance of the power grids' transmission capacities. Therefore, both market and energy grid transmission capacity should be considered. A high degree of flexibilities, in a grid-supporting operation, are favorable to mitigate power grid overloads. Potentially, the addition of further flexibilities might have further positive impacts on the power grid.

Author Contributions: Conceptualization: M.G. and T.K.; methodology, software, validation, and formal analysis: M.G., F.F., J.S., N.Z. and N.W.W.; data curation: M.G., F.F., J.S., N.W.W. and T.S.; writing—original draft preparation: M.G.; writing—review and editing: N.W.W. and T.K.; visualization, M.G. and N.W.W.; supervision, T.K. All authors have read and agreed to the published version of the manuscript.

Funding: This research received no external funding.

Conflicts of Interest: The authors declare no conflict of interest.

Abbreviations

APG	Austrian Power Grid
CHP	combined heat and power
DG	distribution grid
EC	energy carrier
GtH	gas to heat
GtPH	gas to power and heat
HtP	heat to power
MES	multi-energy system
MESS	multi-energy system simulator
OPF	optimal power flow
PF	power flow
PtGH	power to gas and heat
PtH	power to heat
RES	renewable energy source
RL	residual load
SC	sector coupling
SLP	standardized Load Profile
SSD	sub-station district
TG	transmission grid
UBA	Umweltbundesamt (Federal Environment Agency)

Appendix A. Node Optimization

The node optimization and flexibility determination can be depicted in a four-stage process, displayed in Figure A1. Main parameters are explained in the following subchapters.

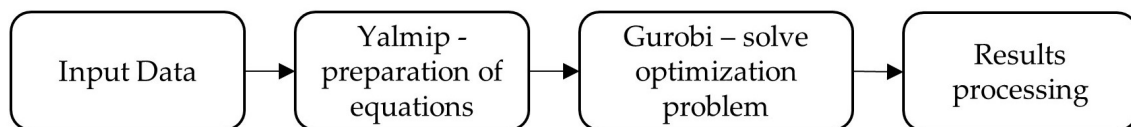


Figure A1. Optimization process.

Appendix A.1. Input Data

In Table A1, the input data for node optimization and flexibility determination are explained. Depending on the optimization problem, different input data are required. The optimization is adapted based on [29].

Table A1. Optimization input data.

Parameter	Type	Description
<i>P_{RL_Set}</i>	scalar	Residual load setting for the current time step.
<i>t</i>	scalar	Duration of one time step [h].
<i>Converter</i>	matrix	Defines properties of each converter. Each row represents one converter. [<i>FP, FH, FG, TP, TH, TG, MinP, MaxP, Ramp, PPrevPeriod</i>] <i>FP</i> —convert from power (1 or 0). <i>FH</i> —convert from heat (1 or 0). <i>FG</i> —convert from gas (1 or 0). <i>TP</i> —convert to power (η in [1]). <i>TH</i> —convert to heat (η in [1]). <i>TG</i> —convert to gas (η in [1]). <i>MinP</i> —minimum power [W]. <i>MaxP</i> —maximum power [W]. <i>Ramp</i> —ramp rate based on MaxP. <i>PPrevPeriod</i> —power of previous period [W].
<i>P_{Storage}</i> <i>H_{Storage}</i> <i>G_{Storage}</i>	matrix	Defines properties of each storage. Each row represents one storage. For power, heat, and gas, individual matrices have to be set up with the following structure. [<i>LP, MinSL, MaxSL, ISL, ηIn, MinIn, MaxIn, ηOut, MinOut, MaxOut</i>] <i>LP</i> —storage loss per period [1/h]. <i>MinSL</i> —minimum allowed storage level [Wh]. <i>MaxSL</i> —maximum allowed storage level [Wh]. <i>ISL</i> —initial storage level [Wh]. <i>ηIn</i> —input efficiency [1]. <i>MinIn</i> —minimum input power [W]. <i>MaxIn</i> —maximum input power [W]. <i>ηOut</i> —output efficiency [1]. <i>MinOut</i> —minimum output power [W]. <i>MaxOut</i> —maximum output power [W].
<i>P_{DSM}</i> <i>H_{DSM}</i> <i>G_{DSM}</i>	matrix	Defines properties of each DSM. Each row represents one DSM. For power, heat, and gas, individual matrices have to be set up with the following structure. [<i>MinP, MaxP</i>] <i>MinP</i> —minimum feed-in (demand) or maximum feed-out (generation) power. <i>MaxP</i> —maximum feed-in (demand) or minimum feed-out (generation) power.
<i>eVehicle</i>	vector	Defines parameters for electric vehicles. [<i>EC, CP, NoP, SB_1, EB_1, SB_2, EB_2</i>] <i>EC</i> —energy to be charged within <i>NoP</i> [Wh]. <i>CP</i> —charging power [W]. <i>NoP</i> —number of time steps before charging of EC must be finished (e.g., one day). <i>SB_1, SB_2</i> —the start of the charging break period. <i>EB_1, EB_2</i> —the end of the charging break period.
<i>P_{Price}</i> <i>H_{Price}</i> <i>G_{Price}</i>	vector	The number of rows is equivalent to the forecasting period. A separate vector must be defined for each energy carrier's price.
<i>P_{RL}</i> <i>H_{RL}</i> <i>G_{RL}</i>	vector	The number of rows is equivalent to the forecasting period. A separate vector must be defined for each energy carrier's residual load [W].
<i>G_{Connect}</i> <i>H_{Connect}</i>	scalar	Indicates if the node is connected (variable = 1) to gas/heat grid or not (variable = 0).
<i>ops</i>	vector	Contains settings for the Gurobi optimizer.

Appendix A.2. Node Optimization Target Function (TF)

$$TF = \min \left(\sum_{EC}^{P,H,G} \left((P_{EC} - P_{EC}^e) \cdot EP_{EC} \cdot t \right) \right) \quad (A1)$$

P_{EC} —consumed power for each energy carrier (EC).

P_{EC}^e —feed-in (sold) power for each EC.

EP_{EC} —price of EC.

Appendix A.3. Flexibility Determination Target Function

Positive and negative flexibility is determined according to (A2) and (A3).

$$TF_{Flex, neg} = \max(P_{C,out}) \quad (A2)$$

$P_{C,out}$ —power converter power output.

$$TF_{Flex, pos} = \max(P_{C,in}) \quad (A3)$$

$P_{C,in}$ —power converter power input.

To determine the total positive (A4) and negative flexibility (A5), storage and DSM options also have to be considered.

$$Flex_{pos} = TF_{Flex, pos} + \min \left(MaxIn, \frac{MaxSL - ISL}{t \cdot \eta IN} \right) + DSM_{MaxP} \quad (A4)$$

$$Flex_{neg} = TF_{Flex, neg} + \min \left(MaxOut, \frac{ISL \cdot \eta Out}{t} \right) + DSM_{MinP} \quad (A5)$$

Appendix A.4. Results

The main optimization outputs are time-resolved RLs for each converter, storage, and DSM, as well as specific results such as storage level. Furthermore, an additional parameter indicates if the optimization problem can be solved successfully.

Appendix B. Measurement Points for Small Hydropower Plant SLP

For each federal state, a random small river measurement point from [80] is used to create an SLP for small-scale hydropower plants, as displayed in Table A2.

Table A2. Measurement points used for small hydropower plant SLP [80].

Federal State	Measurement Point #	Name
Vorarlberg	200105	Garsella
Tyrol	230706	In der Au
Salzburg	203265	Schweighofbrücke
Carinthia	213389	Kaunz
Styria	211029	Anger
Upper Austria	204784	Riedau
Lower Austria	208041	Hollenstein
Burgenland	210039	Piringsdorf (Pfarrbrücke)
Vienna	None	None

Appendix C. Measurement Points for Natural Inflow Curve for (Pumped)-Storage Hydropower Plants

Natural water inflow into (pumped)-storage hydropower plants originates from water sources at high altitudes, such as snow and glacier melt. Therefore, measurement points from [80] at high elevation are selected to determine an annual inflow characteristic for (pumped)-storage hydropower plants, as displayed in Table A3.

Table A3. Measurement points used for annual (pumped)-storage hydropower plant inflow SLP [80].

Measurement Point Name	Measurement Point #	Elevation [m]
Gepatschalm	230300	1895
Vent (oberhalb Niedertalbach)	201350	1891
Obergurgl	201376	1879
Neukaser	201996	1786
Innergschlöß	212068	1686
Kees	203893	2040

References

1. European Commission. The European Green Deal, Brussels, 2019. Available online: https://eur-lex.europa.eu/resource.html?uri=cellar:b828d165-1c22-11ea-8c1f-01aa75ed71a1.0002.02/DOC_1&format=PDF (accessed on 12 January 2022).
2. European Commission. What is the European Green Deal? Brussels, 2019. Available online: https://ec.europa.eu/commission/presscorner/detail/en/fs_19_6714 (accessed on 12 November 2021).
3. European Commission. Fit for 55: Delivering the EU's 2030 Climate Target on the Way to Climate Neutrality, Brussels, 2021. Available online: <https://eur-lex.europa.eu/legal-content/EN/TXT/PDF/?uri=CELEX:52021DC0550&from=DE> (accessed on 12 November 2021).
4. Bundeskanzleramt. Aus Verantwortung für Österreich: Regierungsprogramm 2020–2024, Wien, 2020. Available online: <https://www.bundeskanzleramt.gv.at/dam/jcr:7b9e6755-2115-440c-b2ec-cbf64a931aa8/RegProgramm-lang.pdf> (accessed on 11 November 2021).
5. Bundesministerium Nachhaltigkeit und Tourismus; Bundesministerium Verkehr Innovation und Technologie. #Mission2030: Die Österreichische Klima- und Energiestrategie, Wien, 2018. Available online: https://www.bundeskanzleramt.gv.at/dam/jcr:903d5cf5-c3ac-47b6-871c-c83eae34b273/20_18_beilagen_nb.pdf (accessed on 12 January 2022).
6. Mancarella, P. MES (multi-energy systems): An overview of concepts and evaluation models. *Energy* **2014**, *65*, 1–17. [CrossRef]
7. Hansen, K.; Breyer, C.; Lund, H. Status and perspectives on 100% renewable energy systems. *Energy* **2019**, *175*, 471–480. [CrossRef]
8. Sejkora, C.; Kühberger, L.; Radner, F.; Trattner, A.; Kienberger, T. Exergy as Criteria for Efficient Energy Systems—A Spatially Resolved Comparison of the Current Exergy Consumption, the Current Useful Exergy Demand and Renewable Exergy Potential. *Energies* **2020**, *13*, 843. [CrossRef]
9. Bundesamt für Eich- und Vermessungswesen. *Katalog Verwaltungsgrenzen (VGD)—Stichtagsdaten 1:5000*; Bundesamt für Eich- und Vermessungswesen: Wien, Austria; Available online: https://www.data.gv.at/katalog/dataset/bev_verwaltungsgrenzenstichtagsdaten150000 (accessed on 15 February 2022).
10. Klemm, C.; Vennemann, P. Modeling and optimization of multi-energy systems in mixed-use districts: A review of existing methods and approaches. *Renew. Sustain. Energy Rev.* **2021**, *135*, 110206. [CrossRef]
11. Pfenninger, S.; Hawkes, A.; Keirstead, J. Energy systems modeling for twenty-first century energy challenges. *Renew. Sustain. Energy Rev.* **2014**, *33*, 74–86. [CrossRef]
12. Bottecchia, L.; Lubello, P.; Zambelli, P.; Carcasci, C.; Kranzl, L. The Potential of Simulating Energy Systems: The Multi Energy Systems Simulator Model. *Energies* **2021**, *14*, 5724. [CrossRef]
13. Lohmeier, D.; Cronbach, D.; Drauz, S.R.; Braun, M.; Kneiske, T.M. Pandapipes: An Open-Source Piping Grid Calculation Package for Multi-Energy Grid Simulations. *Sustainability* **2020**, *12*, 9899. [CrossRef]
14. Weinand, J.M.; Scheller, F.; McKenna, R. Reviewing energy system modelling of decentralized energy autonomy. *Energy* **2020**, *203*, 117817. [CrossRef]
15. Thurner, L.; Scheidler, A.; Schafer, F.; Menke, J.-H.; Dollichon, J.; Meier, F.; Meinecke, S.; Braun, M. Pandapower—An Open-Source Python Tool for Convenient Modeling, Analysis, and Optimization of Electric Power Systems. *IEEE Trans. Power Syst.* **2018**, *33*, 6510–6521. [CrossRef]
16. Böckl, B.; Greiml, M.; Leitner, L.; Pichler, P.; Kriechbaum, L.; Kienberger, T. HyFlow—A Hybrid Load Flow-Modelling Framework to Evaluate the Effects of Energy Storage and Sector Coupling on the Electrical Load Flows. *Energies* **2019**, *12*, 956. [CrossRef]
17. Kienberger, T.; Traupmann, A.; Sejkora, C.; Kriechbaum, L.; Greiml, M.; Böckl, B. Modelling, designing and operation of grid-based multi-energy systems. *Int. J. Sustain. Energy Plan. Manag.* **2020**, *29*, 7–24. [CrossRef]

18. Greiml, M.; Fritz, F.; Kienberger, T. Increasing installable photovoltaic power by implementing power-to-gas as electricity grid relief—A techno-economic assessment. *Energy* **2021**, *235*, 121307. [CrossRef]
19. FFG. SBM_Ind: Smart Business Models for Industry. Available online: <https://projekte.ffg.at/projekt/3093356> (accessed on 13 November 2021).
20. Farshidian, B.; Ghahnavieh, A.R. A comprehensive framework for optimal planning of competing energy hubs based on the game theory. *Sustain. Energy Grids Netw.* **2021**, *27*, 100513. [CrossRef]
21. Cheng, Y.; Zhang, P.; Liu, X. Collaborative Autonomous Optimization of Interconnected Multi-Energy Systems with Two-Stage Transactive Control Framework. *Energies* **2020**, *13*, 171. [CrossRef]
22. Sejkora, C.; Kühberger, L.; Radner, F.; Trattner, A.; Kienberger, T. Exergy as criteria for efficient energy systems—Maximising energy efficiency from resource to energy service, an Austrian case study. *Energy* **2022**, *239*, 122173. [CrossRef]
23. Wagner & Elbling GmbH. ONE100: Österreichs Nachhaltiges Energiesystem—100% Dekarbonisiert, Wien, 2021. Available online: https://www.aggm.at/files/get/b2327a5f19bc53c7fa0f2ae1dcd4edb1/ONE100_Kurzfassung.pdf (accessed on 14 November 2021).
24. Aryanpur, V.; O’Gallachoir, B.; Dai, H.; Chen, W.; Glynn, J. A review of spatial resolution and regionalisation in national-scale energy systems optimisation models. *Energy Strategy Rev.* **2021**, *37*, 100702. [CrossRef]
25. Zimmerman, R.D.; Murillo-Sanchez, C.E.; Thomas, R.J. MATPOWER: Steady-State Operations, Planning, and Analysis Tools for Power Systems Research and Education. *IEEE Trans. Power Syst.* **2011**, *26*, 12–19. [CrossRef]
26. Zimmerman, R.D.; Murillo-Sánchez, C.E. MATPOWER User’s Manual: Version 7.1. 2020. Available online: <https://matpower.org/docs/MATPOWER-manual.pdf> (accessed on 15 December 2021).
27. Rüdiger, J. Enhancements of the numerical simulation algorithm for natural gas networks based on node potential analysis. *IFAC-Pap.* **2020**, *53*, 13119–13124. [CrossRef]
28. Langeheinecke, K.; Jany, P.; Thieleke, G.; Langeheinecke, K.; Kaufmann, A. *Thermodynamik für Ingenieure*; Springer Fachmedien Wiesbaden: Wiesbaden, Germany, 2013; ISBN 978-3-658-03168-8.
29. Chen, Z.; Zhang, Y.; Tang, W.; Lin, X.; Li, Q. Generic modelling and optimal day-ahead dispatch of micro-energy system considering the price-based integrated demand response. *Energy* **2019**, *176*, 171–183. [CrossRef]
30. 2004 IEEE International Conference on Robotics and Automation (IEEE Cat. No.04CH37508). In Proceedings of the 2004 IEEE International Conference on Robotics and Automation (IEEE Cat. No.04CH37508), New Orleans, LA, USA, 26 April–1 May 2004.
31. Gurobi Optimization. Gurobi Optimizer Reference Manual 2021. 2021. Available online: <https://www.gurobi.com/documentation/9.5/refman/index.html> (accessed on 6 December 2021).
32. Austrian Power Grid AG. Netzentwicklungsplan 2015: Für das Übertragungsnetz der Austrian Power Grid AG (APG), Wien, 2015. Available online: <https://www.apg.at/~{}media/009493CEFD824A85962F65CEAA6521C0.pdf> (accessed on 18 November 2021).
33. Austrian Power Grid AG. Netzentwicklungsplan 2016: Für das Übertragungsnetz der Austrian Power Grid AG (APG), Wien, 2016. Available online: <https://www.apg.at/~{}media/2A8B8AC633414A359DB163BBE5104AD8.pdf> (accessed on 18 November 2021).
34. Austrian Power Grid AG. Netzentwicklungsplan 2017: Für das Übertragungsnetz der Austrian Power Grid AG (APG), Wien, 2017. Available online: <https://www.apg.at/~{}media/6B16E721BF8D45F49A907C11A7C095EC.pdf> (accessed on 18 November 2021).
35. Austrian Power Grid AG. Netzentwicklungsplan 2018: Für das Übertragungsnetz der Austrian Power Grid AG (APG), Wien, 2018. Available online: <https://www.apg.at/~{}media/B1CF20C3D97B4496AE3E06AF5B351AB7.pdf> (accessed on 18 November 2021).
36. Austrian Power Grid AG. Netzentwicklungsplan 2019: Für das Übertragungsnetz der Austrian Power Grid AG (APG), Wien, 2019. Available online: <https://www.apg.at/api/sitecore/projectmedia/download?id=bd6645e4-f83d-456a-a9d4-5757b5098a70> (accessed on 18 November 2021).
37. Austrian Power Grid AG. Netzentwicklungsplan 2020: Für das Übertragungsnetz der Austrian Power Grid AG (APG), Wien, 2020. Available online: <https://www.apg.at/de/Stromnetz/Netzentwicklung#download> (accessed on 18 November 2021).
38. Austrian Power Grid AG; LINZ NETZ GmbH; Netz Oberösterreich GmbH. Stromnetz-Masterplan Oberösterreich 2028: Ausbau des Hochspannungs-Stromnetzes (≥ 110 kV) in Oberösterreich. Planungszeitraum 2018–2028. 2018. Available online: https://www.land-oberoesterreich.gv.at/Mediendateien/Formulare/Dokumente%20UWD%20Abt_US/us-en_Stromnetz-Masterplan_Oberoesterreich_2028.pdf (accessed on 18 November 2021).
39. Land Kärnten. Energie Masterplan Kärnten, Klagenfurt. Available online: <https://www.ktn.gv.at/DE/repos/files/ktn.gv.at/A/bteilungen/Abt8/Dateien/energie/energiemasterplan%5fkärnten?exp=478252&fps=cbe8bb636710ede50d5a94df838d40cbae6a6d1> (accessed on 18 November 2021).
40. QGIS Development Team. QGIS Geographic Information System; Open Source Geospatial Foundation Project. 2021. Available online: <http://qgis.osgeo.org> (accessed on 18 November 2021).
41. Google. Map Data: Google, Terrametrics, Kartendaten (C) 2021. Available online: maps.google.at (accessed on 18 November 2021).
42. OpenStreetMap-Mitwirkende. OpenStreetMap. Available online: www.openstreetmap.org/copyright (accessed on 18 November 2021).
43. Austrian Power Grid AG. Statistische Netzdaten. Available online: <https://www.apg.at/api/sitecore/projectmedia/download?id=703efbb9-bd69-49db-b2f6-bb676cac466b> (accessed on 16 September 2020).
44. Heuck, K.; Dettmann, K.-D.; Schulz, D. (Eds.) *Elektrische Energieversorgung*; Springer Fachmedien Wiesbaden: Wiesbaden, Germany, 2013; ISBN 978-3-8348-1699-3.
45. Heuck, K.; Dettmann, K.-D.; Schulz, D. Anhang. In *Elektrische Energieversorgung*; Heuck, K., Dettmann, K.-D., Schulz, D., Eds.; Springer Fachmedien Wiesbaden: Wiesbaden, Germany, 2013; pp. 742–753.

46. AGGM Austrian Gas Grid Management AG. Unser Netz im Detail. Available online: <https://www.gasconnect.at/netzinformationen/unser-netz-im-detail> (accessed on 19 November 2021).
47. Austrian Gas Grid Management AGGM. *Erdgasinfrastruktur—Österreich: Georeferenzierte Darstellung nach Netzebenen*; Austrian Gas Grid Management AGGM: Wien, Austria, 2018.
48. Gas Connect Austria. *Erdgasleitungen & Erdgaslagerstätten in Österreich*; Gas Connect Austria: Wien, Austria, 2017.
49. E-Control. Erdgas—Bestandsstatistik: Leitungslängen zum 31. Dezember—Jahresreihen. Leitungslängen von Fern- und Verteilleitungen zum Jahresende. Available online: <https://www.e-control.at/de/statistik/gas/bestandsstatistik> (accessed on 19 November 2021).
50. Cerbe, G. *Grundlagen der Gastechnik: Gasbeschaffung, Gasverteilung, Gasverwendung*; Hanser: München, Germany, 2004; ISBN 978-3-446-22803-0.
51. Büchele, R.; Haas, R.; Hartner, M.; Hirner, R.; Hummel, M.; Kranzl, L.; Müller, A.; Ponweiser, K.; Bons, M.; Grave, K.; et al. Bewertung des Potentials für den Einsatz der hocheffizienten KWK und effizienter Fernwärme- und Fernkälteversorgung, Wien. 2015. Available online: https://ec.europa.eu/energy/sites/ener/files/documents/Austria_MNE%282016%2950514.pdf (accessed on 21 January 2021).
52. Bundesministerium Klimaschutz, Umwelt, Energie, Mobilität, Innovation und Technologie. Austrian Heat Map: Fernwärme und Kraft-Wärme-Kopplung in Österreich. Available online: <http://www.austrian-heatmap.gv.at/das-projekt/> (accessed on 19 November 2021).
53. Navarro, A.; Rudnick, H. Large-Scale Distribution Planning—Part II: Macro-Optimization With Voronoi’s Diagram and Tabu Search. *IEEE Trans. Power Syst.* **2009**, *24*, 752–758. [CrossRef]
54. Statistik Austria. STATatlas. Available online: <https://www.statistik.at/atlas/> (accessed on 20 November 2021).
55. Statistik Austria. Nutzenergieanalyse. Available online: https://www.statistik.at/web_de/statistiken/energie_umwelt_innovation_mobilitaet/energie_und_umwelt/energie/nutzenergieanalyse/index.html (accessed on 20 November 2021).
56. Gobmaier, T.; Mauch, W.; Beer, M.; von Roon, S.; Schmid, T.; Mezger, T.; Habermann, J.; Hohlenburger, S. Simulationsgestützte Prognose des elektrischen Lastverhaltens, München. 2012. Available online: <https://docplayer.org/5749688-Simulationsgestuetzte-prognose-des-elektrischen-lastverhaltens.html> (accessed on 20 November 2021).
57. Austrian Power Clearing and Settlement. Synthetische Lastprofile: Prognose von Verbrauchswerten mittels Lastprofilen, Wien. 2019. Available online: <https://www.apcs.at/de/clearing/technisches-clearing/lastprofile> (accessed on 20 November 2021).
58. Dock, J.; Janz, D.; Weiss, J.; Marschnig, A.; Kienberger, T. Time- and component-resolved energy system model of an electric steel mill. *Clean. Eng. Technol.* **2021**, *4*, 100223. [CrossRef]
59. Groiss, C.; Grubinger, D.; Schwalbe, R. Blindleistungsbilanz im Salzburger Verteilnetz. In *EnInnov 2018: 15. Symposium Energieinnovation*; Institut für Elektrizitätswirtschaft und Energieinnovation, Ed.; Verlag der Technischen Universität Graz: Graz, Austria, 2018; ISBN 978-3-85125-586-7.
60. Thormann, B.; Purgstaller, W.; Kienberger, T. Evaluating the potential of future e-mobility use cases for providing grid ancillary services. In Proceedings of the 26th International Conference and Exhibition on Electricity Distribution, Online, 20–23 September 2021.
61. BDEW; VKU; GEODE. BDEW/VKU/GEODE-Leitfaden: Abwicklung von Standardlastprofilen Gas, Berlin. 2016. Available online: https://www.bdew.de/media/documents/Leitfaden_20160630_Abwicklung-Standardlastprofile-Gas.pdf (accessed on 20 November 2021).
62. Pfenninger, S.; Staffell, I. Renewables.ninja. Available online: <https://www.renewables.ninja/> (accessed on 20 November 2021).
63. Rienecker, M.M.; Suarez, M.J.; Gelaro, R.; Todling, R.; Bacmeister, J.; Liu, E.; Bosilovich, M.G.; Schubert, S.D.; Takacs, L.; Kim, G.-K.; et al. MERRA: NASA’s Modern-Era Retrospective Analysis for Research and Applications. *J. Clim.* **2011**, *24*, 3624–3648. [CrossRef]
64. Oesterreichs Energie. Kraftwerkskarte Österreich. Available online: <https://oesterreichsenergie.at/kraftwerkskarte-1> (accessed on 21 November 2021).
65. Oesterreichs Energie. *Stromerzeugung in Österreich: Kraftwerke der Österreichischen E-Wirtschaft*; Oesterreichs Energie: Vienna, Austria, 2019.
66. Crastan, V. *Elektrische Energieversorgung 2*; Springer: Berlin/Heidelberg, Germany, 2008; ISBN 978-3-540-70877-3.
67. Verbund. Unsere Kraftwerke. Available online: <https://www.verbund.com/de-at/ueber-verbund/kraftwerke/unsere-kraftwerke> (accessed on 21 November 2021).
68. Wikipedia. Liste von Wasserkraftwerken in Österreich. Available online: https://de.wikipedia.org/wiki/Liste_von_Wasserkraftwerken_in_%C3%96sterreich (accessed on 21 November 2021).
69. KELAG AG. Kraftwerke. Available online: <https://www.kelag.at/kraftwerke> (accessed on 21 November 2021).
70. TIWAG. Kraftwerkspark: Unsere Kraftwerke im Überblick. Available online: <https://www.tiwag.at/ueber-die-tiwag/kraftwerke/bestehende-kraftwerke/kraftwerkspark/> (accessed on 21 November 2021).
71. Energie AG. Die Wasserkraftwerke der Energie AG Oberösterreich. Available online: <https://www.energieag.at/Themen/Energie-fuer-Sie/Kraftwerke/Wasserkraftwerke> (accessed on 21 November 2021).
72. Salzburg AG. Unsere Erzeugungsanlagen. Available online: <https://www.salzburg-ag.at/ueber-die-salzburg-ag/unternehmen/erzeugung/erzeugungsanlagen.html> (accessed on 21 November 2021).

73. VERBUND Hydro Power AG. *Strom aus den Hohen Tauern: Die Wasserkraftwerke in Salzburg*; VERBUND Hydro Power AG: Vienna, Austria, 2013.
74. VERBUND Hydro Power AG. *Strom aus den Zillertaler Alpen: Die Wasserkraftwerke in Tirol*; VERBUND Hydro Power AG: Vienna, Austria, 2013.
75. VERBUND Hydro Power AG. *Strom aus den Hohen Tauern und aus der Drau: Die Wasserkraftwerke in Kärnten*; VERBUND Hydro Power AG: Vienna, Austria, 2013.
76. Illwerke VKW. Kraftwerksanlagen der Illwerke VKW. Available online: https://www.illwerkevkw.at/kraftwerke_uebersicht.htm (accessed on 21 November 2021).
77. Energie Steiermark. Wasserkraft. Available online: <https://www.e-steiermark.com/ueber-uns/energieerzeugung/wasserkraft> (accessed on 21 November 2021).
78. EVN Naturkraft. Wasserkraft. Available online: <http://www.evn-naturkraft.at/Oekostrom/Wasser.aspx> (accessed on 21 November 2021).
79. Geodatenstellen des Landes Tirol. *TIRIS*; Amt der Tiroler Landesregierung: Innsbruck, Austria; Available online: <https://maps.tirol.gv.at> (accessed on 22 November 2021).
80. Bundesministerium für Landwirtschaft, Regionen und Tourismus. eHYD. Available online: <https://ehyd.gv.at/> (accessed on 16 November 2021).
81. Kleinwasserkraft Österreich. Nutzen der Kleinwasserkraft. Available online: <https://www.kleinwasserkraft.at/en/fakten/> (accessed on 21 November 2021).
82. Pöyry. Wasserkraftpotenzialstudie Österreich. 2018. Available online: https://oesterreichsenergie.at/fileadmin/user_upload/Oesterreichs_Energie/Publikationsdatenbank/Studien/2018/WasserkraftpotenzialOesterreich2018.pdf (accessed on 21 November 2021).
83. TIWAG. *Kraftwerksgruppe Sellrain-Silz*; Kraftwerksgruppe Sellrain-Silz. TIWAG: Innsbruck, Austria; Available online: <https://www.tiwag.at/unternehmen/unsere-kraftwerke/kraftwerk/kraftwerksgruppe-sellrain-silz/> (accessed on 21 November 2021).
84. KELAG AG. Pumpspeicherkraftwerke. Available online: <https://www.kelag.at/corporate/pumpspeicherkraftwerke-852.htm> (accessed on 21 November 2021).
85. TIWAG. Unsere Kraftwerksprojekte. Available online: <https://www.tiwag.at/ueber-die-tiwag/kraftwerke/wasserkraftausbau/unsere-kraftwerksprojekte/> (accessed on 21 November 2021).
86. Verbund. Pumpspeicherkraftwerk Limberg 3. Available online: <https://www.verbund.com/de-at/ueber-verbund/kraftwerke/unsere-kraftwerke/kaprun-oberstufe-limberg-3> (accessed on 21 November 2021).
87. Zahoransky, R. *Energietechnik*; Springer: Wiesbaden, Germany, 2019; ISBN 978-3-658-21846-1.
88. Österreichischer Biomasse-Verband. *Bioenergie Atlas Österreich 2019*, 2nd ed.; Österreichischer Biomasse-Verband: Wien, Austria, 2019; ISBN 978-3-9504380-3-1.
89. ÖVGW. Montanuniversität Leoben, WU Wien, DBI Gas- und Umwelttechnik GmbH, TU Wien, JKU Linz, ERIG. Greening the Gas: Forschungsbericht 2019, Vienna. 2020. Available online: https://www.ovgw.at/media/medialibrary/2020/03/OVGW_JB_forschung19_hi_corr2.pdf (accessed on 21 November 2021).
90. Photovoltaik Austria. Die österreichische Photovoltaik & Speicher-Branche in Zahlen, Wien. 2020. Available online: https://www.pvaustria.at/wp-content/uploads/2020_07_05_Fact_Sheet_PV_Branche.pdf (accessed on 22 November 2021).
91. Pfenninger, S.; Staffell, I. Long-term patterns of European PV output using 30 years of validated hourly reanalysis and satellite data. *Energy* **2016**, *114*, 1251–1265. [CrossRef]
92. The Wind Power. Windparks—Österreich. Available online: https://www.thewindpower.net/windfarms_list_de.php?country=AT (accessed on 10 December 2020).
93. Staffell, I.; Pfenninger, S. Using bias-corrected reanalysis to simulate current and future wind power output. *Energy* **2016**, *114*, 1224–1239. [CrossRef]
94. LINZ AG. Die Kraftwerke der LINZ AG: Effiziente, umweltschonende Energieerzeugung, Linz. 2018. Available online: <https://www.linzag.at/media/dokumente/linzag/folder-kraftwerke.pdf> (accessed on 22 November 2021).
95. EVN. Thermische Erzeugung. Available online: <https://www.evn.at/EVN-Group/Energie-Zukunft/Energie-aus-Niederosterreich/Gas-und-Kohle.aspx> (accessed on 22 November 2021).
96. Wien Energie. Energie ist unsere Verantwortung: Konsolidierte Umwelterklärung 2021 der Strom- und Wärmeerzeugungsanlagen der Wien Energie GmbH gemäß EMAS-Verordnung, Wien. 2021. Available online: <https://dokumente.wienenergie.at/wp-content/uploads/umwelterklaerung-2021.pdf> (accessed on 22 November 2021).
97. Energie AG. Übersicht thermische Kraftwerke. Available online: <https://www.energieag.at/Themen/Energie-fuer-Sie/Kraftwerke/Thermische-Kraftwerke> (accessed on 22 November 2021).
98. ENTSO-E. Transparency Platform. Available online: <https://transparency.entsoe.eu> (accessed on 22 November 2021).
99. Krutzler, T.; Zechmeister, A.; Stranner, G.; Wiesenberger, H.; Gallauner, T.; Gössl, M.; Heller, C.; Heinfellner, H.; Ibesich, N.; Lichtblau, G.; et al. *Energie- und Treibhausgas-Szenarien im Hinblick auf 2030 und 2050: Synthesebericht 2017*; Umweltbundesamt: Wien, Austria, 2017; ISBN 978-3-99004-445-2.
100. Österreich.gv.at. Sanierungs-offensive 2021/2022. Available online: https://www.oesterreich.gv.at/themen/bauen_wohnen_un_d_umwelt/energie_sparen/1/sanierungs-offensive.html (accessed on 23 November 2021).

101. Statistik Austria. Kraftfahrzeuge—Bestand. Available online: https://www.statistik.at/web_de/statistiken/energie_umwelt_innovation_mobilitaet/verkehr/strasse/kraftfahrzeuge_-_bestand/index.html (accessed on 23 November 2021).
102. ÖAMTC; ARBÖ. Expertenbericht Mobilität & Klimaschutz 2030, Wien. 2018. Available online: <https://www.oeamtc.at/%C3%96AMTC+Expertenbericht+Mobilit%C3%A4t+%26+Klimaschutz+2030+Web.pdf/25.789.593> (accessed on 23 November 2021).
103. Umweltbundesamt. Verkehrsmittel in Österreich. Available online: https://www.umweltbundesamt.at/fileadmin/site/themen/mobilitaet/daten/ekz_doku_verkehrsmittel.pdf (accessed on 23 November 2021).
104. ADAC. Elektroautos im Test: So hoch ist der Stromverbrauch. Available online: <https://www.adac.de/rund-ums-fahrzeug/test/s/elektromobilitaet/stromverbrauch-elektroautos-adac-test/> (accessed on 23 November 2021).
105. Hartl, M.; Biermayr, P.; Schneeberger, A.; Schöfmann, P. Österreichische Technologie-Roadmap für Wärmepumpen, Wien. 2016. Available online: https://nachhaltigwirtschaften.at/resources/nw_pdf/1608_endbericht_oesterreichische_technologieroadmap_fuer_waermepumpen.pdf?m=1469661515& (accessed on 23 November 2021).
106. Weniger, J.; Orth, N.; Lawaczeck, I.; Meissner, L.; Quaschnig, V. Energy Storage Inspection 2021, Berlin, 2021. Available online: <https://pvspeicher.htw-berlin.de/wp-content/uploads/Energy-Storage-Inspection-2021.pdf> (accessed on 23 November 2021).
107. Statistik Austria. Energiebilanzen. Available online: http://www.statistik.at/web_de/statistiken/energie_umwelt_innovation_mobilitaet/energie_und_umwelt/energie/energiebilanzen/index.html (accessed on 20 November 2021).
108. Thormann, B.; Kienberger, T. Evaluation of Grid Capacities for Integrating Future E-Mobility and Heat Pumps into Low-Voltage Grids. *Energies* **2020**, *13*, 5083. [[CrossRef](#)]
109. Thormann, B.; Kienberger, T. Estimation of Grid Reinforcement Costs Triggered by Future Grid Customers: Influence of the Quantification Method (Scaling vs. Large-Scale Simulation) and Coincidence Factors (Single vs. Multiple Application). *Energies* **2022**, *15*, 1383. [[CrossRef](#)]
110. Shi, H.; Blaauwbroek, N.; Nguyen, P.H.; Kamphuis, R. Energy management in Multi-Commodity Smart Energy Systems with a greedy approach. *Appl. Energy* **2016**, *167*, 385–396. [[CrossRef](#)]
111. Xie, Y.; Ueda, Y.; Sugiyama, M. Greedy energy management strategy and sizing method for a stand-alone microgrid with hydrogen storage. *J. Energy Storage* **2021**, *44*, 103406. [[CrossRef](#)]
112. Energy Exchange Austria. Historische Marktdaten. Available online: <https://www.exaa.at/marktdaten/historische-marktdaten/> (accessed on 15 January 2020).
113. Kays, J.; Seack, A.; Smirek, T.; Westkamp, F.; Rehtanz, C. The Generation of Distribution Grid Models on the Basis of Public Available Data. *IEEE Trans. Power Syst.* **2017**, *32*, 2346–2353. [[CrossRef](#)]
114. Esslinger, P.; Witzmann, R. Entwicklung und verifikation eines stochastischen Verbraucherlastmodells für Haushalte. In *12. Symposium Energieinnovation: Alternativen für die Energiezukunft Europas*; Elektrizitätswirtschaft und Energieinnovation, Ed.; Verlag der Technischen Universität Graz: Graz, Austria, 2012; ISBN 978-3-85125-200-2.
115. Ringkjøb, H.-K.; Haugan, P.M.; Solbrekke, I.M. A review of modelling tools for energy and electricity systems with large shares of variable renewables. *Renew. Sustain. Energy Rev.* **2018**, *96*, 440–459. [[CrossRef](#)]